Dissertation

From Morphology to Molecular Phenotyping – miRNAs as novel biomarkers

submitted by

Ines Fößl, BSc MSc

for the Academic Degree of

Doctor of Philosophy (PhD)

at the

Medical University of Graz

Department of Internal Medicine

Division of Endocrinology and Diabetology

under the Supervision of

Univ.-Prof. Dr. Barbara Obermayer-Pietsch

2022

Statutory Declaration

I hereby declare that this thesis is my own original work and that I have fully acknowledged by name all of those individuals and organizations that have contributed to the research for this thesis. The acknowledgement has been made in the text to all other materials used. Throughout this thesis and in all related publications I followed the “Guidelines of the Medical University of Graz on Good Scientific Practice”.

Graz, 29th April 2022
Ines Fößl

Disclosures

I, Ines Fößl, by myself acted as first author for all this thesis, namely the introduction and the discussion parts. The Figures 1 and 2 in the introduction are modified versions of my own figures that have been published previously, as stated. The author contributions to the publications included in this cumulative thesis are included in the respective publications.

I informed all co-authors about the publication of this thesis. All co-authors have agreed to the inclusion of their published data in the thesis and permission to reproduce illustrations and figures from own publications has been granted. Throughout this thesis and in all related publications I followed the "Guidelines of the Medical University of Graz on Good Scientific Practice".

Acknowledgements

I could not have accomplished any of this work alone. Therefore, I want to express my gratitude to the people who helped me along the way.

First, I want to thank my supervisor Univ.-Prof. Dr. Barbara Obermayer-Pietsch. Since the day she literally chased after me to recruit me as her PhD student, she has supported me wholeheartedly in every endeavour I have undertaken. Whenever I needed scientific input or support, help by any means or simply an open ear, she would give me her time. Whatever problem I had, she found a solution or knew someone who could. I could expect her to answer me within a heartbeat, even on weekends. "Impossible" is a word that does not appear in her vernacular. Almost more important for me than all the scientific support I received from her in the past years, is her big heart and her human warmth. For all that, I would like to thank her.

I also want to thank Mag. Dr. Julia Münzker and Priv.-Doz. Dipl.-Chem. Dr.rer.nat. Marcel Scheideler for their support as my thesis committee. The PhD Program DK-MOLIN and the people involved in its organization paved the way for the successful implementation of this project.

Special thanks go to Priv.-Doz. Dr.scient.med. Olivia Trummer, MSc and Ass.-Prof. Mag. Dr.rer.nat. Petra Kotzbeck, with whom I am sharing fruitful collaboration and lunchbreaks. I wouldn't have loved coming to work if I hadn't shared the lab and office with such great colleagues. Therefore, I want to thank all the people of the ENDO research group. Thank you Christoph, Vito, Ceren and Angelo for going parts of the way with me and Conny, Joakim and Kaddour for your support. Besides the people at the Medical University of Graz, I would like to thank the Laboratory of Calcium and Bone Metabolism at the Erasmus MC in Rotterdam, the Netherlands. The group accepted me as a guest researcher and Jeroen van de Peppel, PhD supported me and taught me a lot.

To all those whom I do not mention by name here, but who are or were part of my scientific and private life, my thanks are equally due.

My biggest thank, however, goes to my family and friends. You supported and encouraged me throughout my whole life. Whenever I had no time, worked late or was moody, you stood by my side. Without you, I could have never made it.

A scientist in his laboratory is not a mere technician:

He is also a child confronting natural phenomena that impress him as though they were fairy tales.

-Marie Curie

Table of Content

Abstract

Phenotyping of complex diseases is a challenging task. The exact reasons for the development of many diseases still need to be understood. Chronic diseases are becoming more of a threat to individual patients as well as an additional burden to healthcare systems in general, which are already operating at their limits. Therefore, prognostic biomarkers are desirable to identify people at risk. Biomarkers are also essential for the diagnosis of diseases, the follow-up and the monitoring of treatment successes. In the process of clinical treatment decisions, biomarker assisted workflows promise evidence-based decisions, especially in cases where a treatment regimen is difficult to assess without such decision support.

This thesis aims at trying to find solutions for new diagnostic and predictive biomarkers. The three thesis publications are dealing with different aspects of diagnostics and early detection of medical problems. The review publication by Foessl et al. can be seen as an exemplary model of how complex phenotyping is applied in today's clinical and research settings, taking bone phenotyping as an example. The research papers included in this thesis are two practical examples for different strategies of study design tailored to identify potential new miRNA biomarkers for two different types of diseases. While one publication is covering the topic of acute burn wounds the other publication deals with Hashimoto´s thyroiditis (HT), a chronic disease. Due to the different stages at which the research is currently at for both entities, the study designs were adapted for each topic. A general introduction and a discussion are framing the work for this cumulative thesis, which represents the scientific work done between October 2016 and January 2022 within the PhD programme DK-MOLIN.

Zusammenfassung

Die Phänotypisierung komplexer Erkrankungen ist anspruchsvoll. Die genauen Gründe für die Entstehung vieler Krankheiten müssen erst noch verstanden werden. Chronische Erkrankungen werden immer mehr zu einer Bedrohung für Patienten und zu einer zusätzlichen Belastung für die Gesundheitssysteme, die ohnehin schon an ihre Grenzen stoßen. Die Erforschung und Identifizierung prognostischer Biomarker ist daher wünschenswert, um Risikopersonen zu identifizieren. Biomarker sind auch für die Diagnose von Krankheiten, die Nachsorge und die Überwachung von Behandlungserfolgen von wesentlicher Bedeutung. Bei klinischen Behandlungsentscheidungen versprechen biomarkergestützte Arbeitsabläufe evidenzbasierte Entscheidungen, insbesondere in Fällen, in denen ein Behandlungsschema ohne eine solche Entscheidungshilfe schwer zu beurteilen ist.

In dieser Arbeit wird versucht, Lösungen für neue diagnostische und prädiktive Biomarker zu finden. Die drei Publikationen der Dissertation befassen sich mit verschiedenen Aspekten der Diagnostik und Früherkennung von medizinischen Problemen. Die Übersichtspublikation von Foessl et al. kann als beispielhaftes Modell dafür angesehen werden, wie komplexe Phänotypisierung in der heutigen klinischen Praxis und Forschung angewendet wird, am Beispiel von Knochenphänotypisierung. Die in dieser Arbeit enthaltenen Forschungsarbeiten sind zwei praktische Beispiele für unterschiedliche Strategien des Studiendesigns, die darauf zugeschnitten sind, potenzielle neue miRNA-Biomarker für zwei verschiedene Arten von Krankheiten zu identifizieren. Während die eine Publikation das Thema akute Brandwunden behandelt, befasst sich die andere mit der Hashimoto-Thyreoiditis (HT), einer chronischen Erkrankung. Aufgrund des unterschiedlichen Stands der Forschung für beide Entitäten wurden die Studiendesigns für jedes Thema angepasst. Eine allgemeine Einführung und eine Diskussion umrahmen die Arbeit für diese kumulative Dissertation, die die wissenschaftliche Arbeit darstellt, die zwischen Oktober 2016 und Januar 2022 im Rahmen des PhD-Programms DK-MOLIN durchgeführt wurde.

Joint Introduction

This thesis aims at trying to find solutions for new diagnostic and predictive biomarkers. The three thesis publications are dealing with different aspects of diagnostics and early detection of medical problems, which might become more relevant in the future. Rising costs for the healthcare system will necessitate intelligent, tailored diagnostic approaches.

The population in developed countries is aging. According to statista.com, in 2021 the mean age in the 10 countries with the highest median age was 47.5 years (1). In 2050, projected median ages for these countries show a mean of 53.6 years (2). Analogously, the age structure in Austria is shifting significantly towards the elderly. While 18% of the population was aged 65 and above in 2012, these data increased by around 20% in 2020 and will continue to increase to more than 25% in the longer term (after 2030). The average age of the population will rise from currently 41.8 to 47.1 years by 2060. According to Statistics Austria, Austria's population will continue to grow in the future. From 8.4 million in 2011, it will rise to 9.0 million in 2030 (+7%) and 9.4 million (+11%) in 2060 (3).

Anticipating a growing population at a higher age in Austria, it can be assumed that age-associated diseases will become more frequent in the future. Therefore, general population growth and ageing will continue to challenge the health care system beyond the "diseases of the elderly." New, effective markers could make both an early detection of diseases easier and at the same time reduce the cost of further diagnosis and treatment, while making the treatment duration for an individual patient shorter and thus potentially more efficient, better tolerated, with possibly fewer drug administration needed, and consequently more cost-effective.

The evolution of clinical genotyping and phenotyping

A deep understanding of diseases is only possible through a comprehensive knowledge of both the pathophysiological basis and phenotypic expressions. The better a disease is understood, the better a treatment strategy can be defined and, after re-analysis, potentially adapted. While physical examination and the exogenous description of the human body is almost as old as medicine itself, medical imaging technologies, such as X-rays, were introduced at the end of the 19th century. Before the evolution of molecular biology in the 1950s, medicine relied on the simple description of diseases by clinical symptoms, and other extrinsic features among others.

The advent of laboratory parameters refined diagnostics since then (4). In the past decade, the powerful tool of genomic sequencing has generated further gain in knowledge about genetic variations and disease-related mutations. The cause for several diseases could thereby be unravelled (5). Especially for monogenic disorders, where one gene mutation is responsible for the development of a disease, genotyping of an individual patient is nowadays an essential part of the diagnosis.

The exact reasons for the development of many of the complex diseases, however, still need to be decoded. Genome wide association studies (GWAS) advanced the knowledge on genetic variants associated with a number of diseases and disease states (6). Although GWAS found many genetic associations, there often remains a gap in the discovery of causality. Therefore, systematic functional associations to further resolve the complexity are necessary (7). Taking the example of skeletal diseases, Karasik et al. stress the need for new endophenotypes, meaning new diagnostic features and biomarkers, to support the validation of causal genes found by GWAS (6). Causal genes might as well simply have not been identified yet, because the corresponding endophenotype remains to be discovered.

Not only had the understanding of complex chronic diseases relied on the integration of genetic and phenotypic knowledge. It is broadly observed, that an individual's response to an injury and the following treatment can vary largely between individuals. Treatment outcomes are based on the same complex interactions between genotypic and phenotypic features (8). Therefore, deep phenotyping of the molecular processes and regulatory pathways involved is crucial for the understanding of both acute illnesses such as injuries as well as chronic diseases. The ultimate goals are prediction or early detection, course estimation and individualized treatment towards a refined, personalized medicine.

Concept of the dissertation

The three publications included in the cumulative dissertation will tell a storyline from the description of state of the art phenotyping to the two research papers, which serve as two examples to demonstrate how studies can be built to rediscover new miRNA biomarkers.

The Publication "Bone Phenotyping Approaches in Human, Mice and Zebrafish - Expert Overview of the EU Cost Action GEMSTONE ("GEnomics of MusculoSkeletal traits

TranslatiOnal NEtwork")" by Foessl et al. can be seen as an exemplary model of how complex phenotyping is applied in today's clinical and research settings. The authors give a summary of phenotyping approaches for bone phenotyping. Current, state of the art methods for phenotyping, including classical laboratory markers, imaging and physical examinations as well as standardized physiological tests and questionnaires are described. Outlooks on potential future methods and their current status are given, including new potential biomarkers such as non-coding RNAs and miRNAs. The authors aimed to summarize the current state of knowledge in one comprehensive publication.

The research papers included in this thesis are two practical examples for different strategies of study design tailored to identify potential new miRNA biomarkers for two different types of diseases. While one publication is covering acute burn wounds the other publication deals with Hashimoto´s thyroiditis (HT), a chronic disease. Due to the different stages at which the research is at for both entities, the study design was adapted for each topic to fit the circumstances.

The paper "miRNAs as Regulators of the Early Local Response to Burn Injuries" by Foessl et al. is aiming on finding new regulatory elements for a state of acute injury. Only few studies were previously available reporting on miRNAs in serum of acute burn patients, and no data existed on the local expression of miRNAs in the early phase of acute burn injury. Due to the lack of literature on which to draw from, a reverse approach starting with mRNA expression data was chosen to identify potential miRNAs targeting differential regulated mRNAs in burnt tissue.

For the second study, "Expression Profiles of miR-22-5p and miR-142-3p Indicate Hashimoto's Disease and are related to Thyroid Antibodies" by Trummer, Foessl et al. a preceding literature research was conducted to identify target miRNAs that were selected for replication in an existing cohort. In contrast to the topic of miRNAs in burn wound regulation in the skin, several publications existed, that already identified miRNAs with a potential involvement in HT. Therefore, it was decided to focus on the replication and interpretation of these pre-existing findings in a study cohort already available, the BioPersMed cohort.

Biomarkers

In biological research, the term “biological marker” was already used in the 1950s (9) and it is generally used at least since the 1980s (10). The FDA defines a biomarker as “a defined characteristic that is measured as an indicator of normal biological processes, pathogenic processes, or responses to an exposure or intervention, including therapeutic interventions.”(11) This definition is very broad and includes physiologic measures (such as blood pressure) molecular measures (such as blood glucose) as well as radiographic measures (such as bone mineral density).

The European Medicines Agency (EMA) defines biomarkers as biological molecules that can be used to follow body processes and diseases in humans and animals. Biomarkers can be found in blood, other body fluids, or tissues (12).

Until now, the definition and requirements for a molecule to become a biomarker remains under debate. Efforts such as “Biomarkers, EndpointS, and other Tools” (BEST), established by the National Institute of Health (NIH) - Food and Drug Administration (FDA) Biomarker Working Group, aim to unify the glossary and examine the definitions of biomarkers as well as to place them into context with their respective uses in clinical research, therapeutic development and patient care (11).

Biomarker classification

Biomarkers can be classified into categorical groups in several ways.

One way is to sort them by their putative application, their scientific statement. BEST defines seven categories (11):

- **Diagnostic biomarkers** are used for the diagnosis of certain conditions. As an example, C-reactive protein (CRP) is used as a diagnostic marker for acute phase response and inflammation (13).
- **Prognostic biomarkers** are identifying the likelihood of an event, disease recurrence or progression. As an example, increasing prostate-specific antigen (PSA) can be used to assess the likelihood of cancer progression in the follow-up of patients with prostate cancer (14).

- **Pharmacodynamic/response biomarkers** share overlapping features with monitoring biomarkers, as they are biomarkers changing in response to a treatment or agent. As an example, blood glucose is used to dose insulin in patients with diabetes mellitus (DM) (15).
- **Monitoring biomarkers** might be used to monitor a disease or medical condition. Often, they are used to assess whether a treatment is effective. For many drugs, dosing is dependent on a monitoring biomarker. For example, low-density lipoprotein (LDL) levels are used to monitor the effect of a treatment with statins (16).
- **Predictive biomarkers** identify individuals more likely to experience a certain event, e.g. exposure to a drug or an environmental agent. Alcohol dehydrogenase (ALDH2) deficiency is a predictive marker for head and neck cancers, since people with ALDH2-deficiency have an increased risk in developing these diseases (17).
- **Susceptibility/risk biomarkers** indicate the potential to develop a certain medical condition or disease. The key difference to prognostic biomarkers is them giving information about the likelihood of developing a disease before it is diagnosed.
- **Safety biomarkers** are measured before and/or after the exposure to an agent or medication to decrease the risk of an adverse event. For example, several drugs are only safe for patients with sufficient renal or hepatic function (18,19).

As one can see, a measured parameter can often be assigned to more than one of these groups.

Another way to classify biomarkers is by their characteristics, such as physiologic biomarkers, imaging biomarkers and molecular biomarkers. Physiological biomarkers can be determined using measurement methods from physics, as for example, heart rate and body temperature. Examples for imaging biomarkers are x-ray images, magnetic resonance imaging (MRI), computed tomography (CT) or positron emission tomography (PET) (20).

In contrast, molecular biomarkers have biophysical properties and can be measured in biological samples. Most commonly, these biomarkers are measured in samples of blood components, such as whole blood, serum or plasma (20).

Proteins and peptides are frequently measured in clinical practice. Lipids and lipid metabolites are another type as well as carbohydrates. Nucleic-acid based biomarkers are genetic features of the DNA, such as gene mutations or polymorphisms as well as quantitative gene expression

analysis measuring the mRNA levels in a sample (11). An emerging field of rather recent new biomarkers that are in focus of current research are noncoding RNA species (21).

Finding biomarkers for a specific disease or condition can be performed by candidate screening or with an unbiased approach. Candidate screening searches for biomarkers based on the current knowledge of associations with a certain disease or condition. Typically, literature is searched for candidates and their association with a certain condition is tested. In contrary, unbiased approaches scan for many possible biomarkers at the same time without the bias of a pre-existing assumption or weighting of the feature. This approach can be particularly useful when searching for new biomarkers in fields where little is known in advance, however, the huge amount of data created by screening hundreds and thousands of features makes the data processing extremely important. Bioinformatics and biostatistics need to be applied on large datasets to correctly interpret the raw data collected by big screens (22). Furthermore, if large studies are screened for biomarkers with unbiased approaches, the studies can become very expensive. Therefore, candidate screening or hybrid methods might still be useful to preselect and narrow down large datasets to a more feasible sample size.

Need for new biomarkers

As described earlier, our society ages while our healthcare systems become increasingly advanced. Infectious diseases, once a mayor cause of death until the 1950s, are nowadays better treatable and are therefore replaced by chronic and metabolic diseases as major causes of death within developed countries (23). In our aging society, risk factors for diseases are nowadays considered predictable "lifestyle factors", contrary to the rather unpredictable nature of infectious diseases and/or accidents that used to be represented at a higher rate in the first half of the 20th century (24). This view is supported by empirical research. Japan's population for example is characterized by a high life expectancy. The rate of mortality improvements recorded there does not even slow down at the age of 80 and above, meaning that an increase in life expectancy is even recorded in those older groups. In fact, death rates are declining even at ages 90 and higher. There is no agreement, however, about the developments in morbidity and disability that will accompany these remarkable improvements in life expectancy. In an ageing society, keeping the elderly healthy might not solely be in the interest of an individual. For the year 2050 it was predicted that 18% of the elderly above 64 years of age are in poor

health. Combined with the general ageing of the society, this might be a tremendous financial burden on healthcare systems as well as on treatment costs. Therefore, progress in preventing disability and preservation of health are key goals to maintain a functioning medical system within the next decades (25). On the one hand, health campaigns might become increasingly important. On the other hand, easy and cost-effective screening methods are needed for optimal diagnostics, early detection, and ideally even prediction of diseases. The aim is to "die healthy at a high age". Biomarkers for all different kinds of diseases and injuries therefore will become increasingly important.

Even though the progression of advanced trauma care and intensive care combined with the high hygienic standards made many acute diseases less threatening, optimization of care for acute patients remains desirable (26). The better the initial state of a patient is understood, the better treatment options can be tailored. Optimal outcomes for each individual patient can only be reached if treatment decisions are supported by evidence-based objective measures. But not only for the individual an optimal outcome after an acute injury or infection is desirable. Advanced healthcare and social systems might benefit as well when each patient achieves optimal recovery. Costs for prolonged duration of treatment as well as for rehabilitation and social support could be saved.

miRNAs as biomarkers

MicroRNAs (miRNAs) are non-coding, single stranded RNAs regulating the amount of gene product by binding to messenger RNAs (mRNAs). They were first described in 1993 by Lee et al. when they discovered two miRNAs in *Caenorhabditis elegans*, lin-4 RNA and let-7 RNA, being involved in the timing of larval development (27,28).

MiRNAs execute their regulatory function by binding their so -called "seed region", a sequence of 6-8 nucleotides that is energetically favorable for an interaction with a target region on the mRNA. To execute its regulatory capacity, the binding of a miRNA to the target region does not need perfect pairing. Thus, one miRNA can bind and thereby control the expression of several mRNAs by binding multiple targets. Furthermore, several miRNAs can potentially bind one mRNA. Most commonly, miRNAs bind to the 3´untranslated region (UTR) of the mRNA.

This leads to inhibition of translation or to a destabilization of the target mRNA that is followed by cleaving and degradation (29,30).

At least in humans, studies have shown that miRNA-mediated regulation of gene expression is predominantly a negative regulation. There is a discrepancy between theoretically predicted binding sites calculated by prediction algorithms and the interactions leading to biologically relevant responses. Therefore, the majority of these predicted binding sites might be irrelevant for biological processes (31,32).

miRNA biogenesis

miRNAs are either derived from transcripts that are non-protein-coding (50%), or they are encoded in intronic regions. The biogenesis of a miRNA is initiated in the nucleus, where a precursor miRNA (pri-miRNA) of a few thousand nucleotides is transcribed by RNA-polymerase II (RNAP II). This primary transcript assembles to hairpin structures and goes through several ripening steps until the mature miRNA emerges.

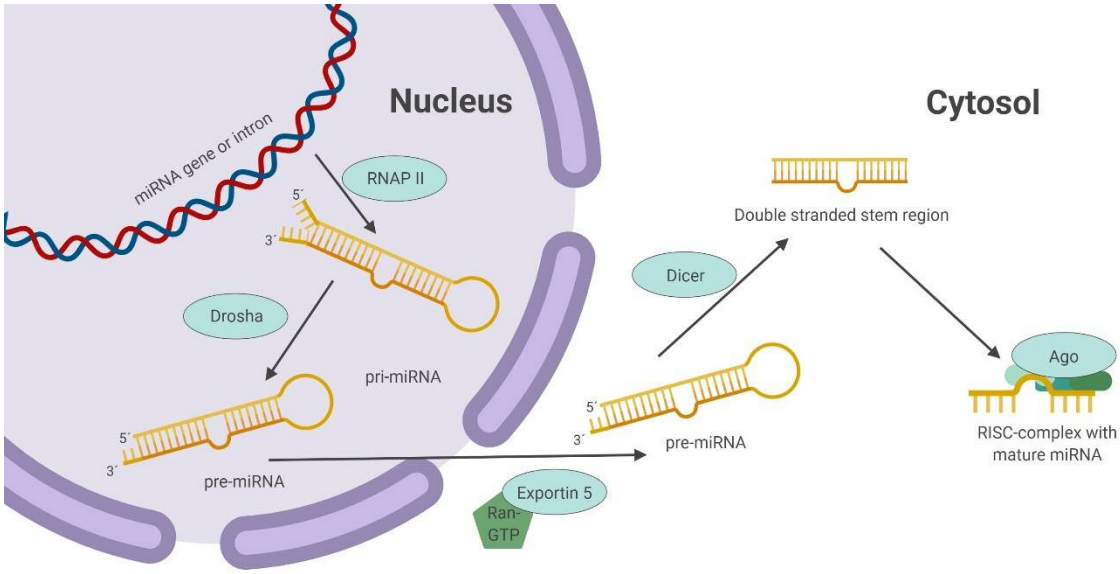

Figure 1 Biogenesis of miRNAs. Derived from miRNA genes or introns of coding genes, miRNAs are transcribed by RNA-polymerase II (RNAP II) as a precursor-miRNA (pri-miRNA) with a hairpin structure. The pri-miRNA is further processed by Drosha, an endoribonuclease. The resulting pre-miRNA is exported to the cytoplasm by Exportin 5 in a Ran-GTP (Ras-related nuclear protein-guanosine triphosphate) dependent process. Dicer binds in the cytosol and cleaves the pre-miRNA resulting in a double-stranded stem region. Finally, the RISC-complex (RNA-induced silencing complex) assembles around the mature single stranded miRNA. Adapted from Foessl et al., miRNAs as novel biomarkers for bone related diseases, JLPM 2019, Created with BioRender.com

The ribonuclease Drosha catalyzes the first step in the nucleus, leaving a hairpin structure of around 70 nucleotides which is called pre-miRNA (33). Exportin 5 forms a complex with the pre-miRNA and Ran-GTP (Ras- related nuclear protein-guanosine triphosphate).

Active transport into the cytosol is mediated from the nucleus by release of Ran-GDP and phosphate. In the cytosol Dicer, another ribonuclease, cuts the loop from the hairpin leaving a double stranded stem region (34). Binding or Argonaute (AGO)-proteins trigger the release of the so-called passenger strand. The RISC-complex (RNA-induced silencing complex) is the active unit that can complementary bind to the 3´UTR by base pairing of the nucleotides 2-8 in the 5´region of the miRNA. The binding of a miRNA can lead to one of three fates. It can hasten the degradation of the mRNA, might lead to de-adenylation and can repress translation. Some RISC-complexes are found to target chromatin directly by binding to DNA and recruiting histone methyltransferases. Thereby, heterochromatin is formed, and a target gene can be silenced directly (34).

Circulating miRNAs

Since miRNAs have first been identified in the bloodstream in 2008 (35), more and more sequences have been described in the serum and plasma of humans and animals (36). To date, circulating miRNAs are found to be associated with several diseases, where they are speculated to be “fingerprints” of a disease. The first miRNAs described in human blood could be associated with B-cell lymphoma and were already suggested as potential biomarkers. These circulating miRNAs are present in the bloodstream in several forms: The vast majority (90%) are found as protein-complexes in the bloodstream associated with AGO-proteins (37,38). The remaining 10% are bound to high density lipoprotein (HDL) (39), in exosomes (40) or apoptotic bodies (37). It is difficult to backtrack such circulating miRNAs to tissue or cells of origin. Sources can be dead blood cells, especially those miRNAs found in apoptotic bodies, but miRNAs are also actively secreted into body fluids by living cells (41). Circulating miRNAs are characterized by a high stability, which makes them very suitable as biomarkers. They are protected from degradation by their transport units, as exosomes cannot be permeated by RNases and AGO-proteins protect the miRNAs from enzymatic disruption. Of note, stability at -70°C was reported for at least one year (42,43).

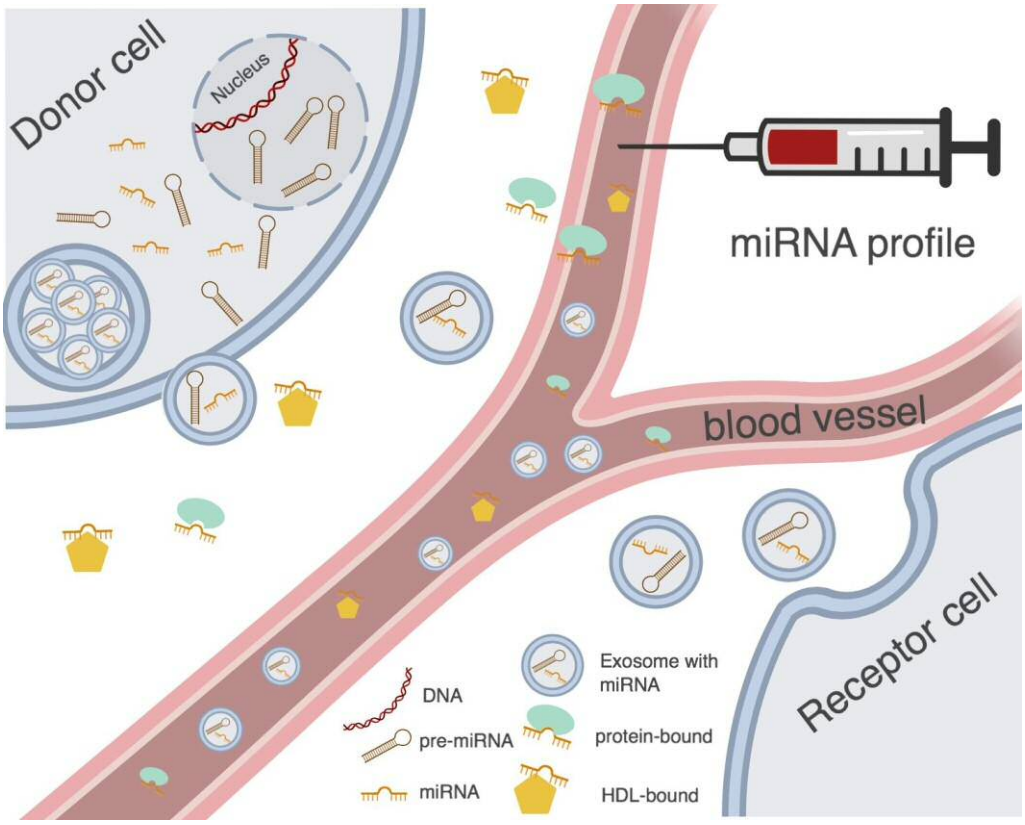

Figure 2 Circulating miRNAs as potential biomarkers. Circulating miRNAs are produced in a donor cell and either actively secreted or passively released into the bloodstream. There, they can be bound to proteins, HDL, or in exosomes and apoptotic bodies. HDL, high density lipoprotein; miRNA, microRNA. Adapted from Foessl et al., miRNAs as novel biomarkers for bone related diseases, JLPM 2019; Created with BioRender.com

More and more sequences are successfully assigned with diseases and biological functions, thereby miRNAs are presented as a novel class of potential biomarkers. Furthermore, some miRNAs have even been identified as targets for therapies already, including in the fields of metabolic diseases and wound healing (44–46).

Detection methods for miRNAs

Several methods are used to detect miRNAs in the circulation and different tissues (47,48). Here, the most common techniques are summarized as an overview.

Quantitative polymerase chain reaction (qPCR)

The most flexible technique for small-scale diverse applications to detect miRNAs is the qPCR. With high sensitivity and specificity, it allows the detection of miRNAs with established protocols. Being broadly used among different laboratories, qPCR represents the

"gold-standard" and is used for the validation of other methods (47). As the first step, miRNA extraction is performed from the biofluid or tissue. Enrichment of small RNA species can be conducted to increase the yield of miRNAs (49). Accurate primer selection further increases the specificity of the method. One has to keep in mind, that mature miRNAs are only 22 nucleotides in length, the same length as a classical qPCR primer. Therefore, most qPCR-based assays work by elongation of the sequence for amplification. A specific primer complementary to the miRNA-sequence is combined with poly(A)/stem/loop reverse primers for the elongation of the PCR product. Various providers offer both TaqMan® and SybrGreen® assays.

MiRNA detection with individual qPCR can be quite labour-intensive, which can be seen as a disadvantage. For accurate primer design the miRNA sequence has to be known, making it a biased approach (47). Selection of suitable reference genes remains challenging, especially for miRNAs that should be detected in biofluids. Classical reference genes like ribosomal proteins, glyceraldehyde 3-phosphate dehydrogenase (GAPDH), or Actin are not suitable in most of the cases, partly because of their superior length. In contrast, the use of other short RNA species as reference genes can also be problematic, since they might be transcribed by different RNA polymerases as the precursors for miRNAs. In theory, the best choice would be a reference miRNA, but a universally applicable housekeeping miRNA is yet to be described. Sometimes, miRNA candidates for normalization can be identified after a sequencing of a cohort (50). If reference genes are not available, one possibility is that no normalization is applied. If so, it has to be paid extreme attention on the equality of treatment of each sample within an experiment. To control each step of the preparation and detection process, from the RNA extraction to reverse transcription and the final PCR, Spike-In miRNAs, synthetic miRNAs with known sequence, might be added and measured. A global mean of all the detected miRNAs can be applied for experiments with at least about 50 target genes per sample. This method calculates a mean of all the miRNA content in each sample that is then used for normalization of each target (48,51).

MiRNA sequencing

miRNA sequencing is, in contrast to the biased qPCR, an unbiased approach. This makes it an ideal tool for discovering miRNAs unknown to be associated with a certain condition and can even detect previously unknown miRNA sequences. Sequencing is accurate enough to

distinguish closely related miRNAs and isoforms. It needs the most input material of the herein described techniques, and lacks sensitivity compared to qPCR. Although considered unbiased, the pre-sequencing steps and barcoding might still distort results (52). Since the amount of output data is large, data analysis can be laborious and challenging, and requires good bioinformatics knowledge. Annotation of the sequences relies on databases. Therefore, it is strongly recommended to validate and reproduce results found by sequencing with qPCR in a second experimental step (53).

MiRNA arrays

miRNA arrays are available from various distributors. They are considered less quantitative than other approaches, but are designed with easy protocols and straight forward analyses in mind. At a reasonable price, hundreds of miRNAs can be tested at once in one sample. These arrays are probed by hybridization of RNA or DNA samples that are fluorescence labelled. Measuring the brightness of individual spots, the expression can be compared between individual samples. For the discrimination of closely related sequences, miRNA arrays can be inaccurate. To partly counteract this, stringent washing and careful selection of the probes can be applied (54).

Multiplex miRNA profiling

An increasing supply of multiplex miRNA profiling methods is coming to the market in recent years (e.g., FirePlex NanoStringTM). Marketed as a user-friendly technology, it offers the possibility of analysing various miRNAs in many samples with easy protocols. Biofluids might be used directly, without preliminary steps necessary for miRNA extraction. Assays are measured by flow cytometer. Data analysis is easier if compared to sequencing of miRNAs (55,56).

Burn injuries

Burn injuries are complex injuries that can result in severe systemic effects in a patient that reverberate for years.

The initial evaluation of the burn is essential for the choice of treatment and the patient's associated chance of recovery. A complex interplay of different diagnostic decisions is crucial for this (57). Among others, the following must be evaluated:

- Burn depth is the key discriminator for the classification of burn wounds. Four stages are mostly discriminated (58):
    - Grade 1 or first degree burn wounds are confined at the superficial epidermis. Such wounds are painful but do not create blisters and they generally heal without scarring.
    - Grade 2 or second degree burn wounds affect the epidermis (superficial partial thickness) or the epidermis and the upper layers of the dermis (intermediate or deep partial thickness) and they form blisters. While the more superficial second degree burn wounds are more painful, they do not require surgery and the risk for severe scarring is low. Deep partial thickness burns are less painful but they might require surgical treatment. With increasing depth, the risk for infection and scarring increases.
    - Grade 3 or full thickness burns are affecting the deeper layers of the dermis and are characterized by a loss of pain to pricks and touch. If small, they heal with scarring and potential contracture. Larger lesions require skin grafting and are accompanied by a high risk of infections.
    - Grade 4 burns involve underlying tissue such as muscle and/or bone and they result in the loss of the severely damaged areas.
- The skin surface area occupied by the particular degree of burn is an important factor in determining the severity of the injury (58).
- The cause of the injury is another key factor for the assessment (59). All burns have in common the destruction of tissue by energy transfer. The main sources of thermic energy are fire, hot liquids or solids. Potential further origins are heat, radiation, friction, cold, electric or chemical sources among others (60). In this context, burns of different origin may show very different pathophysiologies. While flames or hot viscous liquids (like oil) (61) might cause deep immediate injuries, other agents such as hot water or steam can cause injuries that appear more superficial in the first place due to the shortened exposure time of the tissue (59).

miRNAs as biomarkers for burn

The variety of variables and their combination make it difficult in practice to accurately classify a burn injury. However, patient´s outcomes and treatment successes are often dependent on early treatment decisions. For example, early surgical treatment of severe paediatric burn wounds improved the outcome in terms of acute-phase reaction and hypermetabolic response (62). In combination with classical wound classification, biomarkers could support the decision between treatment options.

To date, there is little knowledge about miRNAs involved in the local processes of burn wounds. Therefore, we focused our study design on an initial discovery of potential regulators of genes of the early burn response, of which many are known.

Hashimoto´s thyroiditis

Hashimoto´s thyroiditis (HT) was first reported in 1912 by Hakaru Hashimoto. He described four women with enlarged thyroid glands, which appeared as if the thyroids were changed to lymphoid tissue. There are histological changes present in the disease, but the diagnosis is made by the detection of high serum titres of anti-thyroid autoantibodies(63), which were first described in the 1960s (64). Although the disease is long known and the connection with a misguided immune system, too, the exact causes of the disease are still unknown. As for many complex diseases, intrinsic as well as extrinsic factors may play a role in the development of HT.

Nowadays, HT is commonly diagnosed with a prevalence of 1-2% in iodine-replete countries. In elderly populations, the prevalence is even higher. A study conducted in the Netherlands with people between 85 and 89 years of age found that a known hypothyroidism was present in 7% of the participants (65). In contrast, in areas with known iodine-deficiency, the prevalence for hypothyroidism is much lower, however, other diseases of the thyroid such as goiter are more prominent in such areas (66,67). In Austria, iodine is supplemented through salt iodination. Since the introduction of salt iodination in 1963, the prevalence for goiter decreased successfully, especially in the population that received supplemented iodine since young age. In 2002, the goiter preference in people up to 40 years of age was below 5%, as reported by Lind et al. Whereas goiter was successfully repressed by iodine supplementation, autoimmune

diseases of the thyroid began to gain relevance since then. Although there is no data for Austria about the prevalence of thyroid autoantibodies from before the introduction of iodine supplementation, it is evident to the researchers that an increase of salt iodination from 10 mg to 20 mg in the year 1990 increased the prevalence for HT. In 2002, they further reported that the prevalence for thyroid autoantibodies was 3.2% in males and 5.2% in females, making it comparable or even higher than in studies on populations that are considered iodine-replete (68). A study in mice was able to show a correlation between the western diet and the development of HT (69). Whether this factor also plays a role in the development of the disease in humans remains unanswered. However, the influence of both nutritional factors and iodine in the environment suggests that extrinsic factors play a large role in the development of the disease.

Even though extrinsic factors seem to play an important role for the prevalence of HT, familial accumulation suggests also a genetic component underlying the development of the disease. A nation-wide study conducted in Sweden analysed the connection between HT and Graves' disease with 43 other autoimmune diseases (AIDs) registered in the study population. For HT, associations with 20 other AIDs are reported. Except of one disease, all 20 associations were also significantly associated with Graves' disease, making a inheritable, common genetic predisposition for these autoimmune thyroid diseases (AITDs) likely (70). Although Graves' disease defined by hyperthyroidism and HT defined by hypothyroidism manifest as opposite clinical pictures, they seem to be closely related entities. Patient reports document oscillations from one to the other clinical picture (71,72), and both diseases are characterized by the infiltration of B and T cells to the thyroid. The sibling recurrence risk for HT (in relation to HT and Graves' disease) is reported higher than 20 (73) and the rate of concordance in monozygotic twins is as high as 30-60% (74). Certain alleles were found to be associated with HT, as reviewed by Lee et al. There is evidence that variants in genes, that play roles in the cascade of the immune system, from the thymus to the Treg mediated immune tolerance down to disturbed events in the immunological synapse between T cells and antigen-presenting cells, all can contribute to the manifestation of HT, but these genes are commonly found associated also with other forms of AIDs (75).

Of note, patients with AITDs showed a significantly higher prevalence for thyroid cancer, which ranges from 0.5 to 30% (76). Since AITDs can be diagnosed only by the presence of thyroid autoantibodies together with a clinical examination of a patient´s thyroid gland, early

detection is impossible. The treatment is solely reactive, and consists of supplementation of thyroid hormones. Prognostic markers could not only prevent patients from getting AITDs, but also make early treatment possible, potentially preventing the thyroid gland from being attacked by the immune system in the first place.

miRNAs as biomarkers for Hashimoto´s thyroiditis

Since dysregulation of the immune system is the cause for AITDs including HT, it is obvious that miRNAs potentially regulating factors involved in the underlying immune responses are the main focus when searching for potential biomarkers. Therefore, we focused on such miRNAs in our studies. A review published in January of 2022, the same time as our paper was published, sums up miRNAs as potential regulators of immune responses (77). Taheri et al. also recently reviewed the current state of literature regarding non-coding RNAs, including miRNAs, and AITDs. To sum up, most of the few studies existing are conducted on a limited number of samples and the miRNAs that pop up as differentially regulated in these studies are only partly overlapping. Nevertheless, results indicate that there might be a miRNA – immune regulatory axis involved in the development of AITDs. Therefore, such regulatory miRNAs could potentially also serve as biomarkers at the early onset or even before the onset of the disease.

Recently, an interesting new potential mechanism by which miRNAs might act as contributors to the development of AITDs was reported. Martínez-Hernández et al. published results of an integrated miRNA and mRNA profiling. They identified miRNAs miR-21-5p, miR-146b-3p, miR-5571-3p and miR-6503-3p as upregulated in AITD. Furthermore, they suggest that these miRNAs might regulate genes involved in the formation of primary cilia in thyroid tissue and speculate this might be a potential mechanism of pathogenesis (78).

This thesis aims to span a bow from the description of biomarkers and how they are used in the clinical practice as well as in a preclinical setting to describing two examples on how novel biomarkers can be discovered. The two research papers included in this cumulative thesis aim at finding novel miRNA biomarkers. They are describing different approaches adjusting to the existing knowledge of the disease states of acute burn injuries and Hashimoto´s thyroiditis.

Joint Discussion

This chapter of the dissertation will focus on summarizing the strengths, weaknesses, opportunities and threats of the three publications included in the cumulative thesis. While each individual publication includes the specific discussion directly, this joint discussion addresses the more general considerations and discussion points. Furthermore, this chapter includes a critical review on miRNAs as biomarkers in general, reflections on the topic of appropriate study design to identify miRNA biomarkers, which are fundamental to any scientific study, and a section discussing general outlooks and future perspectives.

Discussion on the review "Bone Phenotyping Approaches in Human, Mice and Zebrafish - Expert Overview of the EU Cost Action GEMSTONE"

The review article "Bone Phenotyping Approaches in Human, Mice and Zebrafish - Expert Overview of the EU Cost Action GEMSTONE" was created as one of the deliverables of a COST Action of the European Cooperation in Science and Technology (79). Designed as a networking opportunity for interdisciplinary research, the GEMSTONE project aims at bringing musculoskeletal researchers from different fields together to join forces in order to form a breeding ground for new ideas and research projects. In working group 2, led by Barbara Obermayer-Pietsch and Ines Foessl, the idea was born to write a publication summarizing current state-of-the-art techniques. This has resulted in the review article "Bone Phenotyping Approaches in Human, Mice and Zebrafish - Expert Overview of the EU Cost Action GEMSTONE", presenting a collection of the most common phenotyping methods in humans and comparing them with methods to assess bone properties in mice and zebrafish.

Although certain aspects and some of the methods are described in more depth by other publications, a synoptic collection of the state-of-the-art methods had not been published before and was yet to be written. It is of value that the manuscript represents one compressive collection to sum up not only the knowledge of the GEMSTONE consortium, but shows a broad cross-section of the methods and techniques currently used for clinical phenotyping of the human skeletal system. The emphasis on comparability of the techniques with currently used methodology in animal modelling characterizes the paper as valid reference collection for the

preclinical researcher who wants to get a basic overview about the equivalence of certain techniques. As leads for working group 2, “Phenotyping”, Barbara Obermayer-Pietsch and Ines Foessl coordinated the writing team. The group of 34 authors was composed of international experts from various disciplines, ranging from clinical researchers to animal model specialists, medical doctors, molecular biologists and others from all-over Europe and beyond. The close collaboration between clinical, translational and basic researchers highlights this joint work. Dedicated experts wrote the individual passages of the paper, so the quality of the paragraphs should be rated highly. However, the large number of contributors also brought difficulties. The coordination of such a large number of authors proved to be challenging, as several authors sometimes showed delayed action times. The final touches of unifying the manuscript into a complete work took quite a bit of effort, which was ultimately accomplished by the coordinating team.

The fact that the narrative overview article is mainly a collection of state-of-the-art techniques might be seen as a weakness of the manuscript. However, due to the already considerable scope of the work, it was necessary to refrain from including a comprehensive discussion of the individual techniques in the work. Although the limitations and strengths of each technique are discussed in each chapter, this discussion is not the main focus of the article. The limitations and strengths are merely shortly indicated and thus serve more as a basis and food for thoughts than as a discussion claiming to be complete.

The paper describes in detail clinical phenotyping and preclinical applications with a humanocentric focus. It can be seen as a criticism that the techniques for characterization of animal models are rather short. Again, the authors were well aware of this point and it is one of the compromises made to achieve a manageable length for the document. The work aimed precisely at the compressive complete summary of the most common techniques used in humans. It was already of considerable length even without the detailed reference to methods for the characterization of animal models, and therefore, a more detailed elaboration of these topics was refrained from. Thus, the cross-references to techniques for animal models cannot insist on completeness but also represent the starting point for further research.

The animal models mouse and zebrafish were selected for the inclusion in the article based on the expertise available in GEMSTONE. However, this meant that other animal models like rats,

sheep and horses, which are quite commonly used in musculoskeletal research (80), were not included. This represents another limitation of the article.

Discussion on the publication "miRNAs as Regulators of the Early Local Response to Burn Injuries"

The publication "miRNAs as Regulators of the Early Local Response to Burn Injuries" has a pioneering scientific status. At the date the publication was released, no comparable publications could be recorded that investigated the regulatory role of miRNAs in the early local processes of deep partial thickness burns in human tissue. Additionally, in this publication for the first time miRNAs were described in interstitial fluid of the skin sampled with dermal open flow microperfusion. The fact that these miRNAs may also play a regulatory role, is a new approach in the development of biomarkers for burns and might even lead to their further investigation as potential pharmacological targets.

The publication is based on a solid experimental setting using an *in vitro* human skin model, that allowed to cover and model the first hours after a burn at three time points. The use of the specialized method of dermal open flow microperfusion on a human *ex vivo* model for skin-burn injuries allowed for a detailed time resolution, which had previously not been possible in an *in vivo* setting.

The authors decided on this experimental setup, and against the use of an animal model, because the common animal models assemble the morphological characteristics of human skin only moderately. For example, if compared to the skin of rodents, some important points are different. First, the absence of fur, and therefore the lack of follicles, differentiates human skin from most mammals. Although the layers of skin are the same, human skin is about four times thicker with 100µm. While human skin is firm and well connected to the underlying tissue, rodents have a much looser skin, which can be easily shifted from the underlying layers (81). Swine skin resembles human skin much more than rodent skin in these parameters. However, even in the porcine animal model, longitudinal sampling over several timepoints *in vivo* is difficult. Therefore, we consider the human skin model ideal to study the complex factors happening in human skin after a partial thickness burn (82).

For the publication on miRNAs in burns, a preceding literature research was performed. Several studies reported the involvement of miRNAs in the process of skin wound healing through different mechanisms (83–86). However, the only study we found prior to our publication that analysed miRNAs in tissue of burn patients was published by Liang et al. However, they used samples of denatured dermis at the 4th day post burn, so the samples were from severe injured skin parts at later time points.

The decision towards the semi-biased approach for this publication on miRNA biomarkers was based on several presumptions. No reports on miRNAs in dermal interstitial fluid or serum of patients within the first few hours/days after the injury could be found at the time of the literature research. On the other hand, several studies reported differential expressed genes in burnt tissue. The sequencing and array data of some of these studies were publicly available. Therefore, we decided to use an existing dataset as a starting point for a bioinformatics approach in order to identify miRNAs involved in the regulation of these genes of the early local burn response. The bioinformatics analysis was designed to scan for miRNAs potentially targeting these described differentially regulated genes. We thereby could integrate existing knowledge on gene expression in the subject area of burns for our miRNA study, even though no pre-existing miRNA-expression data were reported for partial thickness burn wounds.

To what extent the miRNAs, that were found differentially regulated, are also biologically relevant for burn wound management needs further investigation. Furthermore, if they indeed play a regulatory role in the local processes, they might even be considered druggable targets for local or systemic therapy.

Discussion on the publication "Expression Profiles of miR-22-5p and miR-142-3p Indicate Hashimoto's Disease and Are Related to Thyroid Antibodies"

The publication "Expression Profiles of miR-22-5p and miR-142-3p Indicate Hashimoto's Disease and Are Related to Thyroid Antibodies" describes miRNAs that are differentially regulated in patients with HT. A major strength of the publication is the used cohort: The BioPersMed Cohort (87). It is a single centre, prospective cohort that included participants with one cardiovascular risk factor. Due to the good cohort specifically built to identify biomarkers

in different entities, and the careful selection of both the Hashimoto and the control group from the cohort, the present study has special relevance, although the number of subjects per group is rather small.

In consideration of the factors described in the chapter “Selecting the appropriate study design for finding miRNA biomarkers”, we chose an existing cohort for our HT study. As before mentioned, the BioPersMed cohort (87) is a highly controlled cohort where a lot of background information on each individual participant exists. Designed as an observational study with initiation in 2010, a total of 1022 study subjects were included in the study, where clinical and anthropometric data of each study subject are recorded over up to a decade. The follow-up is still ongoing. The premises for the enrolment were that a person brings one classical cardiovascular risk factor in the absence of any primary cardiovascular events. Such risk factors included family history of cardiovascular disease, dyslipidaemia or hypertension. Patients enrolled in the study are closely evaluated and followed. Study subjects with severe illness or serious co-morbidities were excluded, minimizing concomitant factors, since the patients' entire medical history is very well known. The control group is as well studied as the patients who entered the study as the Hashimoto group. Of the total study population, study subjects with previously diagnosed HT were selected (n=27). As controls, healthy age and sex matched controls (n=22) were selected. Given the importance of well controlled study populations especially for miRNA studies, this unique cohort gave us the opportunity to investigate miRNA biomarkers with an optimal exclusion of concomitant factors.

Our decision towards a literature-based approach to select the miRNAs to be studied was based on some preconditions. A literature research was conducted that found several publications reporting miRNAs differentially regulated in the serum/plasma of HT patients. Based on the literature findings, miRNAs of interest were selected. The expression of these miRNAs was analysed in the selected subpopulation of the BioPersMed Cohort.

An observation arises from the general tendency to overexpression of the measured miRNAs in HT, which could indicate a systemic measurement error. However, in accordance to our findings, in thyroid tissue of HT a global tendency towards the upregulation of genes is reported also in other studies, with 88% of differentially regulated genes showing an upregulation in an expression profiling by microarray (88). In this context, the observed upregulation of most miRNAs in our study of HT is conclusive.

Taking this one step further, the study attempted to theoretically assign the identified miRNAs to the immunological process of HT development. The miRNAs identified as indicators of HT were classified only on the basis of their potential function in regulating immunological processes. Other effects, that these miRNAs might also have, were not highlighted in this work. This creates a biased picture, as many miRNAs are known to target hundreds of potential mRNAs. Further cellular processes that might be also regulated by the miRNAs described as differentially regulated in the study are still to be discovered. However, since the immunological processes are exceedingly important for the development of the disease, this aspect of potential regulation was mainly highlighted in the first step.

General discussion points on the topic of miRNAs as biomarkers

A high risk for biomarkers in general, but for miRNA biomarkers in particular, is inter- and intra-individual variation (89). Although we were aware of the fact, we could not address this question in the present studies, as this would have exceeded their capacities. Wu et al. assessed these intra-individual variations in plasma samples and came to the conclusion, that several miRNAs remain stably expressed over a relatively long period of time and are therefore suitable as markers (90). However, another group of miRNAs showed high fluctuations. Similarly, Otsu et al. found an alike picture in samples of patients with AITDs. Some miRNAs, like miR-155 and miR-125a, are reported relatively stable throughout the day whilst others seem to fluctuate in a circadian rhythm. Further studies are needed to determine the intra-individual stability of our biomarker candidates or to address a potential circadian fluctuation through a homogeneity in sampling, e.g. by a blood draw at the same time of the day. This was partly addressed by the well-defined blood sampling from the BioPersMed cohort. In contrary, no consideration could be given to timing in the burn study. Since sampling relied on the delivery of the removed human skins from surgery, neither the tissue biopsies nor the interstitial fluid samples could be collected at fully controlled times. Nevertheless, most human skin flaps for the study arrived during the morning or early afternoon, and the sample preparation took place immediately thereafter. Skin flaps collected in the later afternoon were not included in the study, which achieved a certain temporal containment.

A weakness of both research publications included in this dissertation is a rather small sample size. For biomarker studies, this could result in a reduced transferability of the resulting data to

the general population. However, for both studies we chose “quality before quantity”. Our approach was to find potential biomarkers in rather small subgroups, where the framework conditions could be tightly controlled. We are aware that more data will be needed to confirm our findings. For this purpose, the proposed miRNA markers for both burn injuries and Hashimoto´s thyroiditis need to be confirmed in larger cohorts in the future.

Selecting the appropriate study design for finding miRNA biomarkers

In translational research, biomarker studies are mostly designed as cohort studies that can be either prospectively or retrospectively designed. A tailored, prospective study design is best suited for many of the applications. Ideally, study design starts with a research question. Thereafter, a study is designed and samples are collected to answer that specific research question. Study populations should be carefully selected by setting the inclusion and exclusion criteria in a way that concomitant factors can be widely excluded. The study should be designed appropriately with careful attention to the evaluations and examinations needed and the suitable quality and quantity of sample material.

This ideal aim is often impossible to achieve under clinical circumstances and, in many cases, researchers have to find compromises between an ideal situation and reality. In practice, often a more pragmatic approach needs to be taken for several reasons. One reason why setting up a prospective study might not be the go-to is the factor time. In some cases, especially when the disease or condition is rather rare, prospective collection of samples might simply be a lengthy task (91). Sample collections for rare conditions are often conducted by specialized departments in clinical centres and such samples are precious and highly desired. Therefore, collaboration with such study centres and the use of existing data and samples might sometimes be the only way for researchers to get their hands on rare patient samples.

Another factor that might influence the method of choice is, of course, financial resources. Prospective studies are time- and labour intense, making it sometimes unaffordable to conduct prospective sample collection with the often limited resources available. In such cases, the usage of existing cohorts can be an efficient way to overcome these limitations. By collaboration with study groups that already have suitable cohorts and samples available, costs can be often dramatically reduced.

Resource-saving approaches might also be needed for the welfare of the patients. From an ethical and philosophical point of view, research should not bother patients when there is a simpler way. Especially if the study design is complex and means troublesome visits, long examinations and maybe even painful or potentially dangerous interventions, it might be the best approach to reuse material from existing cohorts for several research projects.

The two different approaches of study design described in the two research papers included in this cumulative doctoral thesis show how a tailored study design can successfully use pre-existing data and knowledge to create novel insights into the biomarker landscape of two distinct diseases, without the need of costly and labour-intense sequencing.

General outlook and future perspective

In this work, several aspects of phenotyping were shown in three independent publications. The two research papers show different approaches to study design. While the burn study used an *ex vivo* model to identify potential biomarkers, the HT study used an existing cohort. These two approaches allowed for both studies to identify miRNAs that can be considered as good candidates for new biomarkers in the respective entity. We are aware that despite the large number of publications suggesting miRNAs as potential biomarkers within the last years, no miRNA-based test is yet successfully implicated as clinically approved standard (92,93) due to a number of reasons. The general lack of reproducibility in independent studies and a lack of miRNAs specific for certain diseases are among them. Jacquet et al. suggest a lack of standardized experimental methodology and clinical protocols, expression heterogeneity at the interindividual level and the limited number of patients as some other reasons (94). In the present research publications, we tried to address these topics. Careful attention was paid to the selection of the study cohort for the HT paper, as discussed further above. For the burns paper, special care was taken to maximize reproducibility by choosing an *ex vivo* model without departing from the human setting. This limited number of patients and specimens is also present in our studies. However, the strict selection of patients and the attention paid to the experimental design of the *ex vivo* trials counteract the low number of samples. We chose quality before quantity.

Joint efforts such as multicentre collaborations and consortia need to be implemented in the field of miRNA biomarker research to overcome the struggles of lacking reproducibility. The Extracellular RNA Communication Consortium might be such an initiative (95). The success of genome-wide association study-(GWAS) consortia such as GEFOS (GEnetic Factors for OSteoporosis Consortium) (96), and the GEMSTONE consortium (Genomics of MusculoSkeletal traits Translational Network) (97) are examples from other fields on how such joint efforts can lead to success. Collaborative efforts are needed for biomarker research in general, to unify methodology as well as for the collaborative integration of data. Such efforts already exist, for example in the field of neurodegenerative diseases (98). For other disciplines, however, such joint projects are yet to be initiated. The GEMSTONE initiative in the field of musculoskeletal research might be one step in the right direction to form such an integrational platform.

Among the opportunities of miRNA-based methods are the combinability of several miRNAs into one panel. With the potential to screen several miRNA markers in one go this brings the opportunity to screen for multiple markers in a multiplexed step. Therefore, cost-effective screens could be performed easily.

If miRNAs could be successfully implemented as biomarkers into clinical practice, they could provide large benefits. Besides a general gain of knowledge for another facette of diseases, the implementation of miRNAs could add another layer of laboratory-diagnostic fine-tuning. If not as stand-alone biomarkers, miRNAs could be adding depth to existing risk assessment tools such as FRAX® (Fracture risk assessment tool). They could be implemented as a miRNA panel alone or in combination with other biomarkers to new, algorithm based assessment tools for early diagnostics of chronic diseases such as HT as well as for outcome assessment for acute injuries such as burns.

The co-evolution of bioinformatics algorithms to integrate different individual indicators opens up new opportunities even for markers that do not provide a sufficient yes/no information on their own. As in many topics, the pioneer in this field is cancer research. For example, a test is currently being developed for ovarian cancer in which microRNAs and proteins are being combined (99). In addition, the combination of different RNA-entities into one classifier might hold new, promising insights. It is reported that a combined miRNA, lncRNA and mRNA signature is a predictor for identifying colorectal cancer patients at high risk to progression (100). Such integrated markers are being found more and more frequently, and their potential clinical applicability is also increasing as the evolution of computational algorithms happens more rapidly (101).

Bibliography

1. Countries with the highest median age 2021 | Statista [Internet]. [cited 2022 Apr 3]. Available from: https://www.statista.com/statistics/264727/median-age-of-the-population-in-selected-countries/

2. Countries with the highest median age 2050 | Statista [Internet]. [cited 2022 Apr 3]. Available from: https://www.statista.com/statistics/673014/top-ten-countries-with-highest-projected-median-age/

3. Demographische Prognosen [Internet]. [cited 2022 Apr 3]. Available from: http://www.statistik.at/web_de/statistiken/menschen_und_gesellschaft/bevoelkerung/demographische_prognosen/067546.html

4. Danese E, Montagnana M. An historical approach to the diagnostic biomarkers of acute coronary syndrome. Ann Transl Med. 2016 May 1;4(10):8–8.

5. Apgar TL, Sanders CR. Compendium of causative genes and their encoded proteins for common monogenic disorders. Protein Sci. 2022 Jan 1;31(1):75–91.

6. Rauner M, Foessl I, Formosa MM, Kague E, Prijatelj V, Lopez NA, et al. Perspective of the GEMSTONE Consortium on Current and Future Approaches to Functional Validation for Skeletal Genetic Disease Using Cellular, Molecular and Animal-Modeling Techniques. Front Endocrinol (Lausanne). 2021 Nov 30;12.

7. Visscher PM, Wray NR, Zhang Q, Sklar P, McCarthy MI, Brown MA, et al. 10 Years of GWAS Discovery: Biology, Function, and Translation. Am J Hum Genet. 2017 Jul 6;101(1):5–22.

8. Baldan D, Negash M, Ouyang JQ. Are individuals consistent? Endocrine reaction norms under different ecological challenges. J Exp Biol. 2021 Jun 1;224(12).

9. Porter KA. Effect of homologous bone marrow injections in x-irradiated rabbits. Br J Exp Pathol. 1957 Aug;38(4):401–12.

10. Aronson JK. Biomarkers and surrogate endpoints. Br J Clin Pharmacol. 2005 May;59(5):491.

11. Silver Spring (MD): Food and Drug Administration (US); Bethesda (MD): National Institutes of Health (US). BEST (Biomarkers, EndpointS, and other Tools) Resource. BEST (Biomarkers , EndpointS , and other Tools) Resource Food and Drug Administration (US); 2016.

12. ema.europa.eu. Biomarker [Internet]. 2022 [cited 2022 Feb 9]. Available from: https://www.ema.europa.eu/en/glossary/biomarker

13. Pepys MB. The acute phase response and C-reactive protein. In: Oxford Textbook of Medicine. 2020.

14. Roberts SG, Blute ML, Bergstralh EJ, Slezak JM, Zincke H. PSA doubling time as a predictor of clinical progression after biochemical failure following radical prostatectomy for prostate cancer. Mayo Clin Proc. 2001;76(6):576–81.

15. Long J, Yang Z, Wang L, Han Y, Peng C, Yan C, et al. Metabolite biomarkers of type 2

diabetes mellitus and pre-diabetes: a systematic review and meta-analysis. BMC Endocr Disord. 2020 Dec 1;20(1):1–17.

16. Harley CR, Gandhi S, Blasetto J, Heien H, Sasane R, Nelson SP. Low-density lipoprotein cholesterol (LDL-C) levels and LDL-C goal attainment among elderly patients treated with rosuvastatin compared with other statins in routine clinical practice. Am J Geriatr Pharmacother. 2007 Sep;5(3):185–94.

17. Crabb DW, Matsumoto M, Chang D, You M. Overview of the role of alcohol dehydrogenase and aldehyde dehydrogenase and their variants in the genesis of alcohol-related pathology. Proc Nutr Soc. 2004 Feb;63(1):49–63.

18. Weersink RA, Bouma M, Burger DM, Drenth JPH, Harkes-Idzinga SF, Hunfeld NGM, et al. Evidence-Based Recommendations to Improve the Safe Use of Drugs in Patients with Liver Cirrhosis. Drug Saf. 2018 Jun 1;41(6):603–13.

19. Whittaker CF, Miklich MA, Patel RS, Fink JC. Medication Safety Principles and Practice in CKD. Clin J Am Soc Nephrol. 2018;13(11):1738.

20. Foessl I, Bassett JHD, Bjørnerem Å, Busse B, Calado Â, Chavassieux P, et al. Bone Phenotyping Approaches in Human, Mice and Zebrafish – Expert Overview of the EU Cost Action GEMSTONE ("GEnomics of MusculoSkeletal traits TranslatiOnal NEtwork"). Front Endocrinol (Lausanne). 2021 Dec 1;12:1476.

21. Stepien E, Costa MC, Kurc S, Drozdz A, Cortez-Dias N, Enguita FJ. The circulating non-coding RNA landscape for biomarker research: lessons and prospects from cardiovascular diseases. Acta Pharmacol Sin 2018 397. 2018 Jun 7;39(7):1085–99.

22. Chen-Plotkin AS. Unbiased approaches to biomarker discovery in neurodegenerative diseases. Vol. 84, Neuron. 2014. p. 594–607.

23. Klenk J, Keil U, Jaensch A, Christiansen MC, Nagel G. Changes in life expectancy 1950-2010: Contributions from age- and disease-specific mortality in selected countries. Popul Health Metr. 2016 May 23;14(1):1–11.

24. Urbas E, Statistik Österreich. Österreichischer Todesursachen Atlas 1998/2004 = Atlas of mortality in Austria by cause of death 1998/2004. :260.

25. Muszyńska MM, Rau R, Muszyńska MM, Rau R. The Old-Age Healthy Dependency Ratio in Europe. J Popul Ageing 2012 53. 2012 Jul 7;5(3):151–62.

26. Hietbrink F, Houwert RM, van Wessem KJP, Simmermacher RKJ, Govaert GAM, de Jong MB, et al. The evolution of trauma care in the Netherlands over 20 years. Eur J Trauma Emerg Surg. 2020 Apr 1;46(2):329–35.

27. Reinhart BJ, Slack FJ, Basson M, Pasquinelll AE, Bettlnger JC, Rougvle AE, et al. The 21-nucleotide let-7 RNA regulates developmental timing in Caenorhabditis elegans. Nature. 2000 Feb 24;403(6772):901–6.

28. Lee RC, Feinbaum RL, Ambros V. The C. elegans heterochronic gene lin-4 encodes small RNAs with antisense complementarity to lin-14. Cell. 1993 Dec 3;75(5):843–54.

29. Dweep H, Sticht C, Pandey P, Gretz N. miRWalk--database: prediction of possible miRNA binding sites by "walking" the genes of three genomes. J Biomed Inform. 2011

Oct;44(5):839–47.

30. Lewis BP, Shih IH, Jones-Rhoades MW, Bartel DP, Burge CB. Prediction of mammalian microRNA targets. Cell. 2003 Dec 26;115(7):787–98.

31. Zhang L, Hammell M, Kudlow BA, Ambros V, Han M. Systematic analysis of dynamic miRNA-target interactions during C. elegans development. Development. 2009;136(18):3043.

32. Liu B, Li J, Cairns MJ. Identifying miRNAs, targets and functions. Brief Bioinform. 2014 Jan;15(1):1–19.

33. Lee Y, Ahn C, Han J, Choi H, Kim J, Yim J, et al. The nuclear RNase III Drosha initiates microRNA processing. Nat 2003 4256956. 2003 Sep 25;425(6956):415–9.

34. Hutvágner G, Zamore PD. A microRNA in a multiple-turnover RNAi enzyme complex. Science (80-). 2002 Sep 20;297(5589):2056–60.

35. Gilad S, Meiri E, Yogev Y, Benjamin S, Lebanony D, Yerushalmi N, et al. Serum MicroRNAs Are Promising Novel Biomarkers. PLoS One. 2008 Sep 5;3(9):e3148.

36. Chen X, Ba Y, Ma L, Cai X, Yin Y, Wang K, et al. Characterization of microRNAs in serum: a novel class of biomarkers for diagnosis of cancer and other diseases. Cell Res 2008 1810. 2008 Sep 2;18(10):997–1006.

37. Turchinovich A, Weiz L, Langheinz A, Burwinkel B. Characterization of extracellular circulating microRNA. Nucleic Acids Res. 2011 Sep;39(16):7223–33.

38. Arroyo JD, Chevillet JR, Kroh EM, Ruf IK, Pritchard CC, Gibson DF, et al. Argonaute2 complexes carry a population of circulating microRNAs independent of vesicles in human plasma. Proc Natl Acad Sci U S A. 2011 Mar 22;108(12):5003–8.

39. Vickers KC, Palmisano BT, Shoucri BM, Shamburek RD, Remaley AT. MicroRNAs are transported in plasma and delivered to recipient cells by high-density lipoproteins. Nat Cell Biol. 2011 Apr;13(4):423–35.

40. Valadi H, Ekström K, Bossios A, Sjöstrand M, Lee JJ, Lötvall JO. Exosome-mediated transfer of mRNAs and microRNAs is a novel mechanism of genetic exchange between cells. Nat Cell Biol. 2007 Jun;9(6):654–9.

41. Sohel MH. Extracellular/Circulating MicroRNAs: Release Mechanisms, Functions and Challenges. Achiev Life Sci. 2016 Dec 1;10(2):175–86.

42. Li Y, Jiang Z, Xu L, Yao H, Guo J, Ding X. Stability analysis of liver cancer-related microRNAs. Acta Biochim Biophys Sin (Shanghai). 2011 Jan;43(1):69–78.

43. Sourvinou IS, Markou A, Lianidou ES. Quantification of circulating miRNAs in plasma: effect of preanalytical and analytical parameters on their isolation and stability. J Mol Diagn. 2013 Nov;15(6):827–34.

44. Dangwal S, Stratmann B, Bang C, Lorenzen JM, Kumarswamy R, Fiedler J, et al. Impairment of Wound Healing in Patients With Type 2 Diabetes Mellitus Influences Circulating MicroRNA Patterns via Inflammatory Cytokines. Arterioscler Thromb Vasc Biol. 2015 Jun 27;35(6):1480–8.

45. Gupta SK, Bang C, Thum T. Circulating microRNAs as biomarkers and potential paracrine mediators of cardiovascular disease. Circ Cardiovasc Genet. 2010 Oct;3(5):484–8.

46. Benz F, Roy S, Trautwein C, Roderburg C, Luedde T. Circulating MicroRNAs as Biomarkers for Sepsis. Int J Mol Sci. 2016 Jan 9;17(1).

47. Van Rooij E. The art of microRNA research. Circ Res. 2011 Jan 21;108(2):219–34.

48. Baker M. MicroRNA profiling: separating signal from noise. Nat Methods. 2010 Sep;7(9):687–92.

49. McDonald JS, Milosevic D, Reddi H V., Grebe SK, Algeciras-Schimnich A. Analysis of circulating microRNA: preanalytical and analytical challenges. Clin Chem. 2011 Jun;57(6):833–40.

50. Chugh P, Dittmer DP. Potential pitfalls in microRNA profiling. Wiley Interdiscip Rev RNA. 2012 Sep;3(5):601–16.

51. Bockmeyer CL, Säuberlich K, Wittig J, Eßer M, Roeder SS, Vester U, et al. Comparison of different normalization strategies for the analysis of glomerular microRNAs in IgA nephropathy. Sci Reports 2016 61. 2016 Aug 24;6(1):1–14.

52. Alon S, Vigneault F, Eminaga S, Christodoulou DC, Seidman JG, Church GM, et al. Barcoding bias in high-throughput multiplex sequencing of miRNA. Genome Res. 2011 Sep 1;21(9):1506–11.

53. Pritchard CC, Cheng HH, Tewari M. MicroRNA profiling: approaches and considerations. Nat Rev Genet. 2012 May;13(5):358–69.

54. Li W, Ruan K. MicroRNA detection by microarray. Anal Bioanal Chem. 2009 Jun;394(4):1117–24.

55. Tackett MR, Diwan I. Using FirePlex ™ Particle Technology for Multiplex MicroRNA Profiling Without RNA Purification. Methods Mol Biol. 2017;1654:209–19.

56. Mestdagh P, Hartmann N, Baeriswyl L, Andreasen D, Bernard N, Chen C, et al. Evaluation of quantitative miRNA expression platforms in the microRNA quality control (miRQC) study. Nat Methods. 2014;11(8):809–15.

57. Boissin C, Laflamme L. Accuracy of Image-Based Automated Diagnosis in the Identification and Classification of Acute Burn Injuries. A Systematic Review. Eur Burn J 2021, Vol 2, Pages 281-292. 2021 Nov 30;2(4):281–92.

58. Alharbi Z, Piatkowski A, Dembinski R, Reckort S, Grieb G, Kauczok J, et al. Treatment of burns in the first 24 hours: simple and practical guide by answering 10 questions in a step-by-step form. World J Emerg Surg. 2012 May 14;7(1):1–10.

59. Jeschke MG, van Baar ME, Choudhry MA, Chung KK, Gibran NS, Logsetty S. Burn injury. Nat Rev Dis Prim. 2020 Feb 13;6(1):1–25.

60. Al-Qattan MM, Al-Zahrani K, Al-Shanawani B, Al-Arfaj N. Friction burn injuries to the dorsum of the hand after car and industrial accidents: classification, management, and functional recovery. J Burn Care Res. 2010 Jul;31(4):610–5.

61. Klein MB, Gibran NS, Emerson D, Sullivan SR, Honari S, Engrav LH, et al. Patterns of grease burn injury: Development of a classification system. Burns. 2005;31(6):765–7.

62. Barret JP, Herndon DN. Modulation of inflammatory and catabolic responses in severely burned children by early burn wound excision in the first 24 hours. Arch Surg. 2003 Feb 1;138(2):127–32.

63. Dayan CM, Daniels GH. Chronic Autoimmune Thyroiditis. http://dx.doi.org/101056/NEJM199607113350206. 2009 Aug 20;335(2):99–107.

64. Roitt IM, Doniach D, Campbell PN, Vaughan Hudson R. Auto-antibodies in Hashimoto's disease (lymphadenoid goitre). Lancet (London, England). 1956 Oct 20;271(6947):820–1.

65. Gussekloo J, Van Exel E, De Craen AJM, Meinders AE, Frölich M, Westendorp RGJ. Thyroid status, disability and cognitive function, and survival in old age. JAMA. 2004 Dec 1;292(21):2591–9.

66. Knudsen N, Jørgensen T, Rasmussen S, Christiansen E, Perrild H. The prevalence of thyroid dysfunction in a population with borderline iodine deficiency. Clin Endocrinol (Oxf). 1999;51(3):361–7.

67. Aghini-Lombardi F, Antonangeli L, Martino E, Vitti P, Maccherini D, Leoli F, et al. The spectrum of thyroid disorders in an iodine-deficient community: the Pescopagano survey. J Clin Endocrinol Metab. 1999 Feb;84(2):561–6.

68. Lind P, Aigner H, Kumnig G, Heinisch M, Igerc I, Mikosch P, et al. Iodine supplementation in Austria: Methods and results. Thyroid. 2002;12(10):903–7.

69. Christ A, Günther P, Lauterbach MAR, Duewell P, Biswas D, Pelka K, et al. Western Diet Triggers NLRP3-Dependent Innate Immune Reprogramming. Cell. 2018 Jan 11;172(1–2):162-175.e14.

70. Thomsen H, Li X, Sundquist K, Sundquist J, Försti A, Hemminki K. Familial risks between Graves disease and Hashimoto thyroiditis and other autoimmune diseases in the population of Sweden. J Transl Autoimmun. 2020 Jan 1;3:100058.

71. Tamai H, Ohsako N, Takeno K, Fukino O, Takahashi H, Kuma K, et al. Changes in Thyroid Function in Euthyroid Subjects with a Family History of Graves' Disease: A Foliow-Up Study of 69 Patients. J Clin Endocrinol Metab. 1980 Nov 1;51(5):1123–7.

72. Kralem Z, Baron E, Kahana L, Sadeh O, Shelnfeld M. Changes in stimulating and blocking TSH receptor antibodies in a patient undergoing three cycles of transition from hypo to hyper-thyroidism and back to hypothyroidism. Clin Endocrinol (Oxf). 1992 Feb 1;36(2):211–4.

73. Villanueva R, Greenberg DA, Davies TF, Tomer Y. Sibling recurrence risk in autoimmune thyroid disease. Thyroid. 2003 Aug 1;13(8):761–4.

74. Brix TH, Kyvik KO, Hegedüs L. A population-based study of chronic autoimmune hypothyroidism in Danish twins. J Clin Endocrinol Metab. 2000 Feb;85(2):536–9.

75. Lee HJ, Li CW, Hammerstad SS, Stefan M, Tomer Y. Immunogenetics of autoimmune thyroid diseases: A comprehensive review. J Autoimmun. 2015 Nov 1;64:82–90.

76. Caturegli P, De Remigis A, Rose NR. Hashimoto thyroiditis: Clinical and diagnostic criteria. Autoimmun Rev. 2014;13(4–5):391–7.

77. Bogusławska J, Godlewska M, Gajda E, Piekiełko-Witkowska A. Cellular and molecular basis of thyroid autoimmunity. Eur Thyroid J. 2022 Feb 1;11(1).

78. Martínez-Hernández R, Serrano-Somavilla A, Ramos-Leví A, Sampedro-Nuñez M, Lens-Pardo A, Muñoz De Nova JL, et al. Integrated miRNA and mRNA expression profiling identifies novel targets and pathological mechanisms in autoimmune thyroid diseases. EBioMedicine. 2019 Dec 1;50:329–42.

79. COST | European Cooperation in Science and Technology [Internet]. [cited 2022 Apr 3]. Available from: https://www.cost.eu/

80. van Weeren PR, Tryfonidou MA. Musculoskeletal health from the "One Medicine" perspective – what can we learn from large and small animal models (with emphasis on articular cartilage)? BMC Musculoskelet Disord 2015 161. 2015 Dec 1;16(1):1–2.

81. Zomer HD, Trentin AG. Skin wound healing in humans and mice: Challenges in translational research. J Dermatol Sci. 2018 Apr 1;90(1):3–12.

82. Andersson M, Madsen LB, Schmidtchen A, Puthia M. Development of an Experimental Ex Vivo Wound Model to Evaluate Antimicrobial Efficacy of Topical Formulations. Int J Mol Sci 2021, Vol 22, Page 5045. 2021 May 10;22(9):5045.

83. Shukla SK, Sharma AK, Gupta V, Yashavarddhan MH. Pharmacological control of inflammation in wound healing. J Tissue Viability. 2019 Nov 1;28(4):218–22.

84. Wu SG, Li HT, Wang LL, Yan L. Lidocaine promotes fibroblast proliferation after thermal injury via up-regulating the expression of miR-663 and miR-486. Kaohsiung J Med Sci. 2020 Apr 1;36(4):274–80.

85. Wang T, Feng Y, Sun H, Zhang L, Hao L, Shi C, et al. miR-21 Regulates Skin Wound Healing by Targeting Multiple Aspects of the Healing Process. Am J Pathol. 2012 Dec 1;181(6):1911–20.

86. Yan Y, Wu R, Bo Y, Zhang M, Chen Y, Wang X, et al. Induced pluripotent stem cells-derived microvesicles accelerate deep second-degree burn wound healing in mice through miR-16-5p-mediated promotion of keratinocytes migration. Theranostics. 2020;10(22):9970–83.

87. Haudum CW, Kolesnik E, Colantonio C, Mursic I, Url-Michitsch M, Tomaschitz A, et al. Cohort profile: 'Biomarkers of Personalised Medicine' (BioPersMed): a single-centre prospective observational cohort study in Graz/Austria to evaluate novel biomarkers in cardiovascular and metabolic diseases. BMJ Open. 2022 Apr 1;12(4):e058890.

88. Qiu K, Li K, Zeng T, Liao Y, Min J, Zhang N, et al. Integrative Analyses of Genes Associated with Hashimoto's Thyroiditis. J Immunol Res. 2021;2021.

89. Otsu H, Watanabe M, Inoue N, Masutani R, Iwatani Y. Intraindividual variation of microRNA expression levels in plasma and peripheral blood mononuclear cells and the associations of these levels with the pathogenesis of autoimmune thyroid diseases. Clin Chem Lab Med. 2017 May 1;55(5):626–35.

90. Wu J, Cai H, Xiang YB, Matthews CE, Ye F, Zheng W, et al. Intra-individual Variation of miRNA Expression Levels in Human Plasma Samples. Biomarkers. 2018 May 19;23(4):339.

91. Euser AM, Zoccali C, Jager KJ, Dekker FW. Cohort Studies: Prospective versus Retrospective. Nephron Clin Pract. 2009 Oct;113(3):c214–7.

92. Jenike AE, Halushka MK. miR-21: a non-specific biomarker of all maladies. Biomark Res. 2021 Dec 1;9(1).

93. Jarry J, Schadendorf D, Greenwood C, Spatz A, van Kempen LC. The validity of circulating microRNAs in oncology: five years of challenges and contradictions. Mol Oncol. 2014 Jun 1;8(4):819–29.

94. Jacquet K, Vidal-Cruchez O, Rezzonico R, Nicolini VJ, Mograbi B, Hofman P, et al. New technologies for improved relevance in miRNA research. Trends Genet. 2021 Dec 1;37(12):1060–3.

95. Das S, Abdel-Mageed AB, Adamidi C, Adelson PD, Akat KM, Alsop E, et al. The Extracellular RNA Communication Consortium: Establishing Foundational Knowledge and Technologies for Extracellular RNA Research. Cell. 2019 Apr 4;177(2):231–42.

96. Gregson CL, Newell F, Leo PJ, Clark GR, Paternoster L, Marshall M, et al. Genome-wide association study of extreme high bone mass: Contribution of common genetic variation to extreme BMD phenotypes and potential novel BMD-associated genes. Bone. 2018 Sep 1;114:62–71.

97. Koromani F, Alonso N, Alves I, Brandi ML, Foessl I, Formosa MM, et al. The "GEnomics of Musculo Skeletal Traits TranslatiOnal NEtwork": Origins, Rationale, Organization, and Prospects. Front Endocrinol (Lausanne). 2021 Aug 16;12:928.

98. New European initiative will build a collaborative platform for data and sample sharing, to accelerate the discovery and validation of biomarkers for neurodegenerative diseases - BBMRI-ERIC: Making New Treatments Possible [Internet]. [cited 2022 Apr 3]. Available from: https://www.bbmri-eric.eu/news-events/new-european-initiative-will-build-a-collaborative-platform-for-data-and-sample-sharing-to-accelerate-the-discovery-and-validation-of-biomarkers-for-neurodegenerative-diseases/

99. Cirillo PDR, Margiotti K, Fabiani M, Barros-Filho MC, Sparacino D, Cima A, et al. Multi-analytical test based on serum miRNAs and proteins quantification for ovarian cancer early detection. PLoS One. 2021 Aug 1;16(8):e0255804.

100. Xiong Y, Wang R, Peng L, You W, Wei J, Zhang S, et al. An integrated lncRNA, microRNA and mRNA signature to improve prognosis prediction of colorectal cancer. Oncotarget. 2017 Oct 17;8(49):85463.

101. Kaul V, Enslin S, Gross SA. History of artificial intelligence in medicine. Gastrointest Endosc. 2020 Oct 1;92(4):807–12.

List of publications produced in the course of the PhD, including details on the contributions

Research Papers as first author:

Foessl I, Haudum CW, Vidakovic I, Prassl R, Franz J, Mautner SI, Kainz S, Hofmann E, Obermayer-Pietsch B, Birngruber T, Kotzbeck P, miRNAs as Regulators of the Early Local Response to Burn Injuries. *Int J Mol Sci*. 2021;22(17):9209.

Trummer, O.*; **Foessl, I**.*; Schweighofer, N.; Arifi, E.; Haudum, C.W.; Reintar, S.; Pilz, S.; Theiler-Schwetz, V.; Trummer, C.; Zirlik, A.; et al. Expression Profiles of miR-22-5p and miR-142-3p Indicate Hashimoto's Disease and Are related to Thyroid Antibodies. Genes 2022, 13, 171.

*These authors contributed equally to this study.

Research papers as co-author:

Nevola KT, Kiel DP, Zullo AR, Weiss S, Homuth G, **Foessl I**, Obermayer-Pietsch B, Motyl KJ, Lary CW. miRNA Mechanisms Underlying the Association of Beta Blocker Use and Bone Mineral Density. J Bone Miner Res. 2021 Jan;36(1):110-122.

Reviews as first author:

Foessl I, Bassett JHD, Bjørnerem Å, Busse B, Calado Â, Chavassieux P, Christou M, Douni E, Fiedler IAK, Fonseca JE, Hassler E, Högler W, Kague E, Karasik D, Khashayar P, Langdahl BL, Leitch VD, Lopes P, Markozannes G, McGuigan FEA, Medina-Gomez C, Ntzani E, Oei L, Ohlsson C, Szulc P, Tobias JH, Trajanoska K, Tuzun Ş, Valjevac A, van Rietbergen B, Williams GR, Zekic T, Rivadeneira F, Obermayer-Pietsch B. Bone Phenotyping Approaches in Human, Mice and Zebrafish - Expert Overview of the EU Cost Action GEMSTONE ("GEnomics of MusculoSkeletal traits TranslatiOnal NEtwork"). Front Endocrinol. 2021 Dec 1;12:720728.

Foessl I, Kotzbeck P, Obermayer-Pietsch B. miRNAs as novel biomarkers for bone related diseases. Journal of Laboratory and Precision Medicine. 2019;4(2)

Rauner M*, **Foessl I***, Formosa MM*, Kague E*, Prijatelj V*, Lopez NA, Banerjee B, Bergen D, Busse B, Calado Â, Douni E, Gabet Y, Giralt NG, Grinberg D, Lovsin NM, Solan XN, Ostanek B, Pavlos NJ, Rivadeneira F, Soldatovic I, van de Peppel J, van der Eerden B, van Hul W, Balcells S, Marc J, Reppe S, Søe K, Karasik D. Perspective of the GEMSTONE Consortium on Current and Future Approaches to Functional Validation for Skeletal Genetic Disease Using Cellular, Molecular and Animal-Modeling Techniques. Front Endocrinol. 2021 Nov 30;12:731217.

* These authors share first authorship.

Reviews as co-author:

Koromani F, Alonso N, Alves I, Brandi ML, **Foessl I**, Formosa MM, Morgenstern MF, Karasik D, Kolev M, Makitie O, Ntzani E, Pietsch BO, Ohlsson C, Rauner M, Soe K, Soldatovic I, Teti A, Valjevac A, Rivadeneira F. The "GEnomics of Musculo Skeletal Traits TranslatiOnal NEtwork": Origins, Rationale, Organization, and Prospects. Front Endocrinol (Lausanne). 2021 Aug 16;12:709815.

Obermayer-Pietsch, B; **Fössl, I**; Dimai, HP. Long-term treatment concepts for osteoporosis. INTERNIST. 2021; 62(5): 474-485.

Obermayer-Pietsch, B; Francic, V; Haudum, C; Borzan, V; Schweighofer, N; Ascani, A; **Foessl, I**. Diabetoporosity—diabetes and the bone. Journal of Laboratory and Precision Medicine. 2018;3(98)

Other publications:

Herrmann, M., Barth, B., **Foessl, I**., Genest, F., Linhart, C., Stein, M., Schwab, A., Boeker K. O., Schmidt, F. Netzwerke Junger Muskuloskelettaler Forscher* Innen. *Osteologie,* 2021, *30*(02), 157-162.

Under revision:

Kotzbeck, P., Taschler,Haudum CW., **Foessl, I.,** Schoiswohl, G., Boulgaropoulos, B., Bounab, K., Einsiedler, J., Pajed, L., Eichmann, TO., Obermayer-Pietsch, B., Giordano, A., Cinti, S., Zechner, R., Pieber, TR. ER stress and white adipose tissue inflammation in HSL knock-out mice. Journal of Lipid Research

Published abstracts:

Fößl, I., Haudum, C., Trummer, O., Dobnig, H., Fahrleitner-Pammer, A., Kassem, M., Obermayer-Pietsch, B. (2020, August). Inactivation of diabetoporosity-associated miRNAs in human mesenchymal stem cells. In *Endocrine Abstracts* (Vol. 70). Bioscientifica.

Foessl, I., Groselj-Strele, A., Piswanger-Sölkner, J. C., Dobnig, H., Fahrleitner-Pammer, A., Kassem, M., Obermayer-Pietsch, B., van de Peppel, J. (2020). Generation of human mesenchymal stem cells lacking diabetoporosity-associated miRNAs using CRISPR/Cas9. *Osteologie*, *29*(01), V-5.

Foessl, I., Kotzbeck, P., Francic, V., Haudum, C., Groselj-Strehle, A., Piswanger-Solkner, J. C., ... & Obermayer-Pietsch, B. (2018, May). MicroRNA profiles in diabetic octogenarians with and without historical and prospective hip fractures. In *Endocrine Abstracts* (Vol. 56). Bioscientifica.

Nevola, K. T., Kiel, D. P., Zullo, A. R., **Foessl, I**., Obermayer-Pietsch, B., Motyl, K., & Lary, C. W. (2020). Pharmacogenetic and MicroRNA Effects of Beta Blocker Association with Increased Bone Mineral Density in Humans.

Biasin, V., Kotzbeck, P., **Foessl, I**., Birnhuber, A., Marsh, L. M., Olschewski, A., Obermayer-Pietsch, B., Kwapiszewska, G. (2020, August). Steroid hormones influence systemic sclerosis prevalence. In *Endocrine Abstracts* (Vol. 70). Bioscientifica.

Printed copies of selected publications

frontiers in Endocrinology

REVIEW
published: 01 December 2021
doi: 10.3389/fendo.2021.720728

Bone Phenotyping Approaches in Human, Mice and Zebrafish – Expert Overview of the EU Cost Action GEMSTONE ("GEnomics of MusculoSkeletal traits TranslatiOnal NEtwork")

*Ines Foessl[1], J. H. Duncan Bassett[2], Åshild Bjørnerem[3,4], Björn Busse[5], Ângelo Calado[6], Pascale Chavassieux[7], Maria Christou[8], Eleni Douni[9,10], Imke A. K. Fiedler[5], João Eurico Fonseca[6,11], Eva Hassler[12], Wolfgang Högler[13], Erika Kague[14], David Karasik[15], Patricia Khashayar[16], Bente L. Langdahl[17], Victoria D. Leitch[18], Philippe Lopes[20], Georgios Markozannes[8], Fiona E. A. McGuigan[20], Carolina Medina-Gomez[21], Evangelia Ntzani[8,22], Ling Oei[23], Claes Ohlsson[23,24], Pawel Szulc[7], Jonathan H. Tobias[25,26], Katerina Trajanoska[21], Şansın Tuzun[27], Amina Valjevac[28], Bert van Rietbergen[29], Graham R. Williams[2], Tatjana Zekic[30], Fernando Rivadeneira[21] and Barbara Obermayer-Pietsch[1]**

[1] Department of Internal Medicine, Division of Endocrinology and Diabetology, Endocrine Lab Platform, Medical University of Graz, Graz, Austria, [2] Molecular Endocrinology Laboratory, Department of Metabolism, Digestion and Reproduction, Imperial College London, London, United Kingdom, [3] Department of Clinical Medicine, UiT The Arctic University of Norway, Tromsø, Norway, [4] Norwegian Research Centre for Women's Health, Oslo University Hospital, Oslo, Norway, [5] Department of Osteology and Biomechanics, University Medical Center, Hamburg-Eppendorf, Hamburg, Germany, [6] Instituto de Medicina Molecular João Lobo Antunes, Faculdade de Medicina, Universidade de Lisboa, Centro Académico de Medicina de Lisboa, Lisboa, Portugal, [7] INSERM UMR 1033, University of Lyon, Lyon, France, [8] Department of Hygiene and Epidemiology, Medical School, University of Ioannina, Ioannina, Greece, [9] Institute for Bioinnovation, Biomedical Sciences Research Center "Alexander Fleming", Vari, Greece, [10] Department of Biotechnology, Agricultural University of Athens, Athens, Greece, [11] Rheumatology Department, Hospital de Santa Maria, Centro Hospitalar Universitário Lisboa Norte (CHULN), Lisbon Academic Medical Centre, Lisbon, Portugal, [12] Division of Neuroradiology, Vascular and Interventional Radiology, Department of Radiology, Medical University Graz, Graz, Austria, [13] Department of Paediatrics and Adolescent Medicine, Johannes Kepler University Linz, Linz, Austria, [14] The School of Physiology, Pharmacology and Neuroscience, Biomedical Sciences, University of Bristol, Bristol, United Kingdom, [15] Azrieli Faculty of Medicine, Bar-Ilan University, Ramat Gan, Israel, [16] Center for Microsystems Technology, Imec and Ghent University, Ghent, Belgium, [17] Department of Endocrinology and Internal Medicine, Aarhus University Hospital, Aarhus, Denmark, [18] Innovative Manufacturing Cooperative Research Centre, Royal Melbourne Institute of Technology, School of Engineering, Carlton, VIC, Australia, [19] Laboratoire de Biologie de l'Exercice pour la Performance et la Santé (LBEPS), Univ Evry, Université Paris Saclay, Evry, France, [20] Department of Clinical Sciences, Lund University, Malmö, Sweden, [21] Department of Internal Medicine, Erasmus MC Rotterdam, Rotterdam, Netherlands, [22] Department of Health Services, Policy and Practice, Center for Research Synthesis in Health, School of Public Health, Brown University, Providence, RI, United States, [23] Centre for Bone and Arthritis Research, Institute of Medicine, Sahlgrenska Academy at University of Gothenburg, Gothenburg, Sweden, [24] Department of Drug Treatment, Sahlgrenska University Hospital, Gothenburg, Sweden, [25] Musculoskeletal Research Unit, Translational Health Sciences, Bristol Medical School, University of Bristol, Bristol, United Kingdom, [26] MRC Integrative Epidemiology Unit, Bristol Medical School, Bristol, University of Bristol, Bristol, United Kingdom, [27] Physical Medicine & Rehabilitation Department, Cerrahpasa Medical Faculty, Istanbul University-Cerrahpaşa, Istanbul, Turkey, [28] Department of Human Physiology, School of Medicine, University of Sarajevo, Sarajevo, Bosnia and Herzegovina, [29] Department of Biomedical Engineering, Eindhoven University of Technology, Eindhoven, Netherlands, [30] Department of Rheumatology and Clinical Immunology, Faculty of Medicine, Clinical Hospital Center Rijeka, Rijeka, Croatia*

OPEN ACCESS

Edited by:
Geert Carmeliet, KU Leuven, Belgium

Reviewed by:
Lilian Irene Plotkin, Indiana University Bloomington, United States
David B. Burr, Indiana University Bloomington, United States

***Correspondence:**
Barbara Obermayer-Pietsch
barbara.obermayer@medunigraz.at

Specialty section:
This article was submitted to Bone Research, a section of the journal Frontiers in Endocrinology

Received: *04 June 2021*
Accepted: *21 October 2021*
Published: *01 December 2021*

Citation:
Foessl I, Bassett JHD, Bjørnerem Å, Busse B, Calado Â, Chavassieux P, Christou M, Douni E, Fiedler IAK, Fonseca JE, Hassler E, Högler W, Kague E, Karasik D, Khashayar P, Langdahl BL, Leitch VD, Lopes P, Markozannes G, McGuigan FEA, Medina-Gomez C, Ntzani E, Oei L, Ohlsson C, Szulc P, Tobias JH, Trajanoska K, Tuzun Ş, Valjevac A, van Rietbergen B, Williams GR, Zekic T, Rivadeneira F and Obermayer-Pietsch B (2021) Bone Phenotyping Approaches in Human, Mice and Zebrafish – Expert Overview of the EU Cost Action GEMSTONE ("GEnomics of MusculoSkeletal traits TranslatiOnal NEtwork"). Front. Endocrinol. 12:720728. doi: 10.3389/fendo.2021.720728

A synoptic overview of scientific methods applied in bone and associated research fields across species has yet to be published. Experts from the EU Cost Action GEMSTONE ("GEnomics of MusculoSkeletal Traits translational Network") Working Group 2 present an overview of the routine techniques as well as clinical and research approaches employed to characterize bone phenotypes in humans and selected animal models (mice and zebrafish) of health and disease. The goal is consolidation of knowledge and a map for future research. This expert paper provides a comprehensive overview of state-of-the-art technologies to investigate bone properties in humans and animals – including their strengths and weaknesses. New research methodologies are outlined and future strategies are discussed to combine phenotypic with rapidly developing –omics data in order to advance musculoskeletal research and move towards "personalised medicine".

Keywords: bone and skeletal diseases, phenotyping, imaging, animal models, GEMSTONE, COST

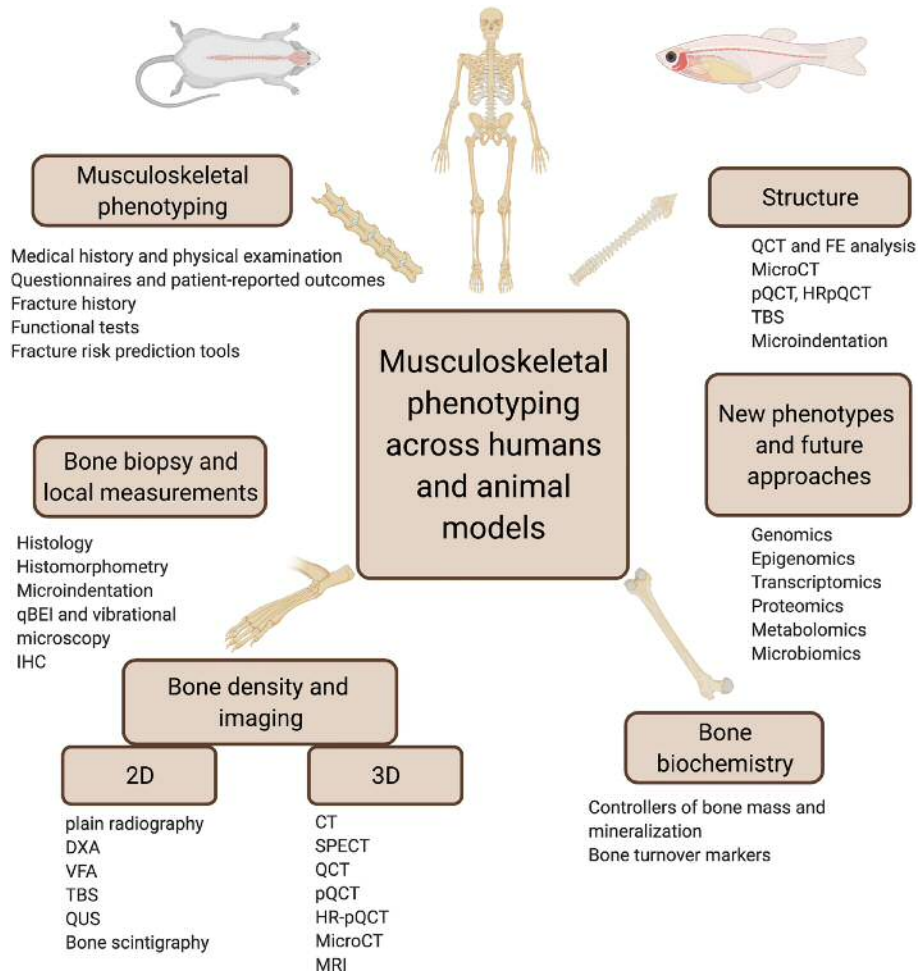

GRAPHICAL ABSTRACT |

INTRODUCTION

Bone metabolism and its regulation involves complex interactions and crosstalk across multiple tissues, physiological systems and pathways from fat and muscle to the immune system and gut-bone axis (1–3). With this knowledge and based on the recent advances in our understanding of genetics and genomics, this narrative overview of technological evidence

intends a practical information for young researchers and/or scientists outside the respective bone areas to enable crosstalk between the disciplines.

The ultimate goal is to translate between clinical and preclinical research and aim for mutual interaction and development of future diagnostic and therapeutic approaches, drug development and risk assessment. This task is being undertaken by experts from the EU Cost Action GEMSTONE ("Genomics of MusculoSkeletal traits Translational Network"). One remit is to facilitate interaction between researchers in animal and human bone science and establish common phenotypic terminology across different spheres of expertise, thus enabling translational comparability of phenotypic signatures. The first step in this process, undertaken by GEMSTONE working group 2, Phenotyping, is to curate a comprehensive catalogue of bone phenotyping methods used within GEMSTONE in human and give a compressed overview on comparable methodology used in mice and zebrafish studies.

In this publication, we summarise the current state of the art, identify gaps in knowledge and suggest future directions/needs to be addressed. We provide insights in how the presented animal models can be used to model bone disease and complement human studies in order to advance bone phenotyping. Integrating the aims of this working group and the larger GEMSTONE action, we briefly outline how –omics technologies can contribute to the phenotypic dissection of skeletal traits. Finally, we offer our perspective on triangulation of the diagnostic evidence and lay out strengths and limitations of the respective techniques.

Discrepancies in the translation of clinical and preclinical research results are an important issue that complicates the understanding and progress in the care for patients with bone disease but also in associated disciplines in the bone field. Bone diseases are complex and multifactorial and require more than the just traditional methods to aim for new horizons with future diagnostic and therapeutic approaches.

Phenotyping and endophenotyping can be mechanistically oriented towards drug development, targeted treatment or prognostically oriented towards treatment stratification and treatment decisions. With this expert view on phenotyping methods across species, we aim for building bridges between animal and human bone science to establish common phenotypic terminology including growth-specific aspects, enabling translational comparability of phenotypic signatures for all researchers involved.

There are many open questions and unmet needs in the field of bone diseases in humans, such as the achievement of an optimal peak bone mass, robust evaluations of bone strength in clinical practice, including cross-validation between measurement methods and more holistic approaches in diagnosis as well as personalized, tailored treatment (4). An increased understanding of perspectives in animal models might help to solve a number of these open questions, as they are important issues for millions of people, e.g., diagnosis and treatment in children, adolescents or young adults, questions of the ideal use of current imaging techniques including new technologies to measure bone quality and strength, the interaction of epigenetic factors and the microbiome with bone quantities and qualities and future treatment options. Many new aspects might be answered by specific animal models, which are described in more detail.

Mice models are popular in studies of skeletal physiology due to their relatively low cost, high rates of reproduction, and ease of handling and care (5). They also provide the opportunity to collect phenotype data not available from humans, and to study the effect of single, specific interventions that are not possible in patients such as changes to diet, age, or genetics (6).

A number of features of bone biology are shared between the mouse and human skeleton. Like humans, mice experience age-related bone loss (5). They also undergo similar patterns of bone turnover and bone healing to humans (7, 8). However, there are differences that should be considered such as the lack of Haversian organisation and non-closure of growth plates at skeletal maturity (6).

Mice have a high homology to the human genome, making them suitable models for many human genetic disorders (6, 7). Manipulation of the mouse genome has allowed for the creation of models for numerous human musculoskeletal diseases. Transgenic and gene-targeted mice have allowed for studies of global overexpression or deletion of genes of interest for decades, but more recent technologies are making more specific genetic manipulation possible. The Cre-lox system applies for cell-specific and temporal deletion of target genes. In this system, LoxP sites are inserted on either side of the target gene or sequence, and when bred to a mouse expressing the Cre recombinase the relevant segment of DNA is excised in the desired cell type or developmental stage (9). CRISPR/Cas9 is the most recently developed technology and uses adapted bacterial proteins which cleave double stranded DNA at specific sites, offering a quick and accurate option for gene editing (10).

An additional model for bone research are small teleost fish such as zebrafish (*Danio rerio*) and medaka (*Oryzias latipes*). This model has been increasingly used to interrogate the biology of human skeletal conditions. Here, we will focus on zebrafish as an emerging and alternative model system used for the study of molecular mechanisms and gene function associated with human skeletal diseases. Zebrafish show conserved physiology compared to mammals and display advantages as animal model, such as the generation of a high number of embryos per cross (over 150), their rapid and transparent embryonic development that combined with the availability of a number of bone specific transgenic lines, allow *in vivo* cell trackability (11, 12). Moreover, genetic manipulation in zebrafish is relatively simple and highly efficient. Evaluation of the first bones in larval stages and adult whole skeleton can be performed in high-resolution with reasonably high throughput (13, 14). Zebrafish have been used for genetic and drug screening, and they pose an attractive model system to accelerate functional validation of human-omics findings.

Despite being evolutionarily more distant from humans than mice, zebrafish share key bone similarities, showing the same bone cell types (osteoblasts, osteocytes osteoclasts and

chondrocytes) and types of ossification (intramembranous and endochondral) as those found in mammals, with the advantage that the first bones and cartilage are available for studies from the 3rd day of development (11). During ageing, zebrafish show bone macro and microstructure reminiscent of osteoporosis (15) and osteoarthritis (16). Furthermore, non-invasive bone fracture experiments in zebrafish allow investigation of bone healing and fracture repair (17, 18). At the molecular scale, zebrafish bone is reminiscent of mammalian bone up to the level of aligned mineralized collagen fibrils (19). Zebrafish also show some differences that should be considered. Unlike in humans, zebrafish bones do only show few bones with trabeculae, whereas long bones are absent. The bone marrow in zebrafish is fatty and does not harbour a site for haematopoiesis, but blood vessels invade the bone marrow similar to mammals (20). Zebrafish have growth plates, but the main source of longitudinal growth relies on cartilage proliferation and not from accumulation of hypertrophic chondrocytes, as only a small portion of chondrocytes become hypertrophic (21).

For further information and details, see also the GEMSTONE WG3 publication on "Gene & Therapeutic Discoveries in Bone Mass Disorders".

Insights into mouse and zebrafish biology and pathophysiology will allow for a better understanding for human investigations and open clinical questions. There are substantial differences between the views of experts in human disease on various aspects of bone. Therefore, a translational approach for new research reducing the discrepancy between the animal and human models is highly warranted. Even in case, techniques cannot be directly compared, they may be tailored to specific research questions in the future.

Many links liaise this publication to those of Working Group 3 and 4 of the GEMSTONE COST Action with important details to many topics mentioned in this manuscript. This comprehensive overview allows us to better classify and detect bone diseases, predict disease progression using radiographic and clinical scores, clustering (identification of different groups/phenotypes of patients with bone diseases), pinpoint the most important characteristics that could affect disease progression and identify patients who will be rapid progressors for the development of late sequelae, e.g. multiple fractures. This paper aims to link the knowledge and understanding of different aspects of bone disease from various expert viewpoints, contributing to a solid basis for further and more effective cooperation between various specialities to enable a personalized care in this field in the future.

1 MUSCULOSKELETAL PHENOTYPING OF BONE CONDITIONS

Musculoskeletal phenotyping is a broad and multi-faceted process that provides essential information for establishing a diagnosis of bone conditions, with or without bone fragility and muscle weakness. For all common or rare forms of musculoskeletal disorders, a comprehensive evaluation of clinical and functional aspects is required since fragility depends on much more than bone mineral density (BMD) alone (**Figure 1**).

1.1 Medical History and Physical Examination

A fragility fracture in children or adults is often the first sign of an underlying primary or secondary disease. A detailed medical history and thorough clinical examination can provide valuable insights into the overall state of musculoskeletal health. The content of the medical history depends on a patient's age. In a child, family history of bone fragility, joint laxity or hearing loss gives essential clues towards the presence of genetic disorder, such as osteogenesis imperfecta. For humans of all ages, a history of back pain can relate to the presence of low-impact vertebral fractures, which may in turn increase the risk for future fractures. In addition, chronic or acute underlying conditions such as rheumatoid arthritis, diabetes, malabsorption, hypogonadism or premature menopause and stroke and neural damage may cause cytokine-, glucocorticoid- or immobility-induced metabolic disease that in turn can affect skeletal and muscular strength. The physical examination includes anthropometry, inspection of limbs and spine for deformities, assessing sclerae and teeth, palpation of spine and extremities along with observing the patient's posture, limb length, muscle tone and mass, balance, joint mobility and gait. The spine is assessed for tenderness, and deformities (such as scoliosis, hyperkyphosis, or hyperlordosis). Decreased mobility and low lean mass predict low bone mass in humans according to the mechanostat theory (22). Sarcopenia, pain, presence of gait, balance and vision disturbances therefore provide important information on the risk of falling and future fractures. These parameters may be summarized in the concept of Patient Reported Outcome Measures from Questionnaires (PROMs) or Clinician Reported Outcome Measures (CROMs), respectively (see **Figure 1**) and may include a large number of additional terms, including psychological and social approaches. For more detailed phenotyping in genetic musculoskeletal diseases, see also, "Careful patient phenotyping is key to disease discovery" in the publication by GEMSTONE WG3.

Limitations: Taking a thorough medical history and assessing a deep clinical phenotype is time consuming and requires profound expertise of an experienced examiner. Studies may not even employ sufficient clinical phenotyping or time into this important investigation. An additional limiting factor may be a lack of knowledge and patients´ recall bias as well as the non-availability of x-rays or other clinical imaging for the clinician to confirm a patient's fracture history and assess the radiological bone phenotype.

Strengths: Medical history and careful physical examination provide essential hints for the further diagnostic workup and avoid unnecessary or repetitive testing.

In mice models, detailed records and breeding charts should be kept for all mouse colonies, and these can and should be used as a proxy for medical history. These detailed colony records allow tracing of recurring skeletal problems or fractures. Physical examination is equally important in mice as in humans, and should include inspection of their condition, behaviour and environment. In regard to the skeleton and muscle tonus, this inspection should include examination of the incisors, gait

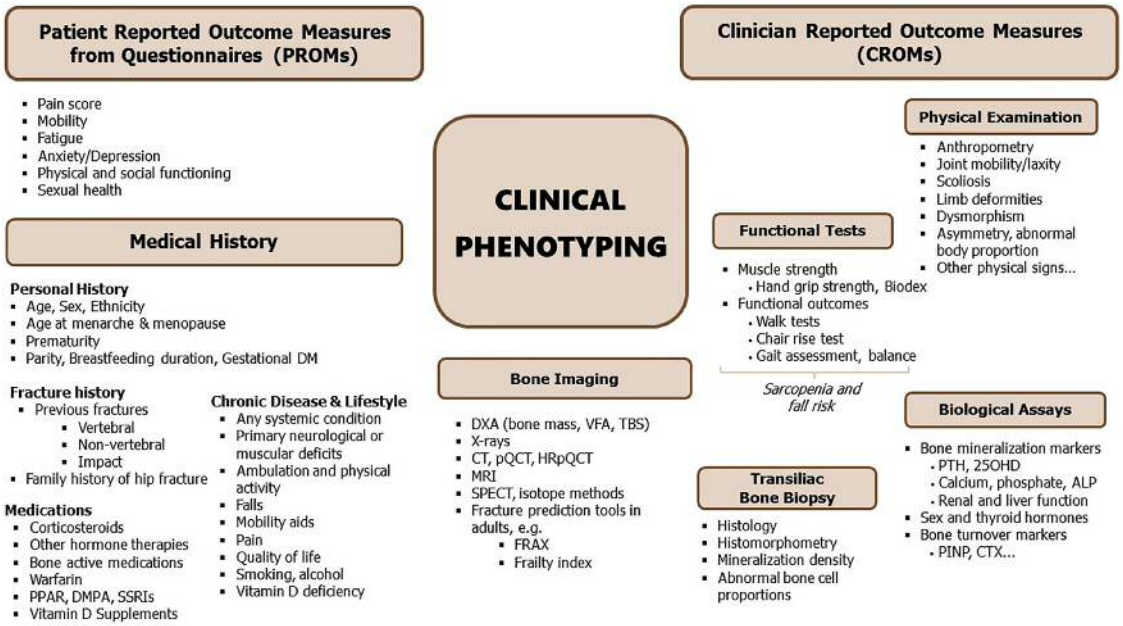

FIGURE 1 | Synopsis of clinical phenotyping. ALP, alkaline phosphatase; Biodex, muscle strength by isodynamic dynamometer; CT, computed tomography; CTX, serum crosslaps; DM, diabetes mellitus; DXA, dual energy x-ray absorptiometry; FRAX, fracture risk assessment tool (https://www.sheffield.ac.uk/FRAX/); HGS, handgrip strength; HRpQCT, high-resolution peripheral quantitative CT; PINP, N-terminal propeptide of type I procollagen; PPAR, peroxisome proliferator-activated receptor agonists; pQCT, peripheral quantitative CT; QUS, quantitative bone ultrasound; SPECT, single photon emission computed tomography; SSRI, selective serotonin reuptake inhibitors; TBS, trabecular bone score; VFA, vertebral fracture assessment; biochemical parameters include 25OHD, 25-hydroxy-vitamin D; PTH, parathyroid hormone; [see also *Bone Turnover Markers (BTMs)*].

abnormalities or lameness, and manually manipulating of the limbs (23).

In zebrafish, the skeleton can be regionalized into functional groups including the craniofacial skeleton and the vertebral column (together with the tail fin, being parts of the axial skeleton), and fins (pectoral, dorsal, anal fins). Since different genetic mutations often affect several skeletal compartments, it is common to perform skeletal phenotyping as a whole (13). Gross skeletal deformities such as scoliosis, hyperkyphosis, hyperlordosis, emaciation, as well as peculiar swimming patterns, are readily visible (16). Severe abnormal spinal curvature can be detected as the fish swim in the tank. It can be argued that "family history" is as relevant for the genetically-modified fish as for the mice of inbred lines; although the exact parents are usually not known for every specific fish, parental pairs usually come from well-documented strains/established mutants. Although there may be a lack of one-to-one relationship with the fish musculoskeletal phenotype during aging, the latter is measurable (24).

1.2 Questionnaires and Patient-Reported Outcome Measures

Patient-reported outcome measures (PROMs), which are collected using questionnaires are essential to comprehend the full extent of how musculoskeletal diseases influence the quality of life. In adults, questionnaires are often used to systematically collect information on self-reported socio-demography, medical conditions, family and fracture history, medication use, lifestyle such as dietary intake, smoking habits, alcohol consumption, physical activity and quality of life. Such information is important given that environmental factors, in combination with genetic susceptibility contribute to general frailty and risk for fracture.

In premenopausal women, there might be special attention to pregnancy and lactation based on hormonal changes and challenged calcium metabolism, due to the nutritional demands of the foetus and neonate (25–27). Female specific questions may address age at menarche, cycle abnormalities and conditions such as gestational diabetes (28) and preeclampsia, also for the child (29). In men, hypogonadism and other endocrine disturbances, but also exogenous toxins might be asked for. In children and adolescents, where heritable forms of osteoporosis are mostly diagnosed, questionnaires are not commonly used and emphasis is put on family history and physical examination.

A wide variety of patient-reported outcomes (pain, mobility, anxiety/depression, fatigue, peer relationship, physical function, sexual function) are available and can be collected as part of the European Registry for Rare Bone and Mineral conditions (https://eurr-bone.com). This EU initiative will provide extended phenotype information and increase knowledge about rare bone disorders.

Limitations: The quality of the patient interview is critical for the successful diagnostic support. Many PROMs questionnaires

are validated and tested in a population-based setting and they are preferable over non-validated questionnaires. However, regular, systematic collection and assessment of PROMs in a clinical setting takes time and resources, which may not be available to doctors and patients alike. Self-reported information may not be well formulated to provide sufficient levels of detail, therefore, recall bias and other uncertainties have to be taken into consideration.

Strengths: PROMs questionnaires are widely available and at relatively low costs, and they are easy to administer, allow for repeated assessments and may use different formats (in person, postal, telephone, or electronic).

1.3 Fracture History

Family and personal fracture history are strong risk factors for fragility fractures in humans of all ages and can give hints to frailty in the elderly and genetic disorders and abnormalities in children. This reflects the genetic component of risk for fracture, particularly for hip fragility fracture (30).

Predicting the 'first fracture' is still challenging, since the majority who fracture do not have osteoporosis (31). A first fracture of any type doubles the risk of a new fracture (32). The timeframe for a new fracture is partially dependent on age and type; for a first fracture in young adulthood, the next may be 20 years ahead, but for an octogenarian, 2-3 years. Stress fractures – including both fatigue fractures (from abnormal, or repetitive loading on normal bone) and insufficiency fractures by normal loading on abnormal bone (33) - are important events in a patient's history and should be an additional indication for a thorough clinical exploration for potential secondary causes (34). Fracture type and location are of particular relevance. Lower limb and vertebral fractures are typical for young children with osteogenesis imperfecta, vertebral fractures associated with back pain in acute lymphoblastic leukaemia and distal femur fractures in immobilized persons.

Limitations: Recall of elderly patients fracture history may be poor. Silent vertebral fractures can also come with little or no symptoms or they may be non-specific and therefore prone to be misinterpreted or overlooked (35).

Strengths: Information is easily ascertained in a healthcare setting and the well-established link with family history and previous fracture should be sufficient to merit bone characterization and potential pharmacological and/or non-pharmacological musculoskeletal management *via* a Fracture Liaison Service (FLS) (36).

In mouse models, most studies describe changes in material properties and histology at a certain timepoint (37). Therefore, fracture history for an individual mouse will not be evaluated. However, in the context of mouse strains, probability and time until a fragility fracture occurs might provide important information.

In the zebrafish skeleton, ribs and fins should be given attention when analysing fractures. Zebrafish models for osteogenesis imperfecta e.g. show recurrent fractures in the ribs and fins (38–40). Rib fractures can be evaluated through life using radiographs, as well as analysing the fins under a transmitted light microscope. Fracture recurrence can be annotated longitudinally.

1.4 Functional Tests

The functional assessment of an increased risk of fall *via* the muscle-bone unit involves evaluation of a) muscle force using tools such as dynamometer, leg press and chest press; and b) physical performance using tools such as 30sec or 6min walk test (gait speed test), chair rise test, short physical performance battery (SPPB) and timed-up-and-go test (TUG) (reviewed in detail elsewhere) (41).

In children, the chair rise test, the 30sec or 6min walk test or the BOT™-2 (Bruininks-Oseretsky-Test of Motor Proficiency, second edition) test are commonly used.

Limitations: The results of the functional tests are largely influenced by the presence of chronic diseases and the patient's cooperation as well as trained health care personnel.

Strengths: The dynamometer and the gait speed tests can be of greatest utility given the fact they can be used in research settings, in specialist clinical settings and in primary care settings at very low expenditures. These techniques provide valuable information on muscle mass and function, important determinants of falls and fragility fracture risk.

In mice, gait analysis can be used to detect abnormalities in speed, stride length, and limb-force profile (42). This technique has been used to measure altered stride length, velocity and limb angle after fracture fixation in mice (43). For muscle mass and strength assessment, multiple methods such as grip strength test (44), wire hang test (45), treadmill test (46), vertical pole test (47) and swimming endurance (48). Additionally, invasive methods include *in vitro* and *in situ* muscle force measurement (49).

Adult swimming behaviour analysis in the fish provides information on how the skeletal system is functioning as a whole (bone and muscles), with potential measurements of angle achieved during the swim, velocity achieved after tail propulsion, as well the time that it takes for exhaustion and induction of fractures (50).

1.5 Fracture Risk Prediction Tools

For a potential prediction of future fragility fractures, information gathered from the above described tools can be used with risk calculators that combine several risk factors, with or without BMD testing, e.g. the Fracture Risk Assessment Tool (FRAX®) algorithm[1], the Garvan Fracture Risk Calculator[2] and QFracture®[3]. These tools provide a valuable risk stratification for the screening and management of osteoporotic patients (51). As an example, the FRAX®-based community screening in the elderly is increasingly used to provide individualized 10-year probability estimates of hip and major osteoporotic fractures (52). However, to date, there is no consensus on the discriminative ability of these tools to predict fragility fracture risk, except FRAX® with BMD, Garvan with BMD and QFracture® (53). Furthermore, the holistic approach of data collection together with physical and clinical measurements could help the construction of frailty index scores (54, 55) to

[1] https://www.sheffield.ac.uk/FRAX/.
[2] https://www.garvan.org.au/bone-fracture-risk.
[3] https://qfracture.org/.

identify subjects at higher risk of fragility fractures (56), and mortality (57).

In children, such prediction programs have not been developed since the underlying conditions vary in nature; osteoporosis can be transient (e.g., acute leukaemia) or permanent (genetic). For example, vertebral fractures may spontaneously reshape in a leukemic child if the remaining growth potential suffices but this would be highly unlikely in a child with osteogenesis imperfecta (58).

Limitations: Some tools might be less representative for a number of important factors, such as probably an individual bone turnover. A lack of medical history data or the number of prior fractures might result in over- or underestimating a person's personal risk.

Strengths: Community screening is more easily feasible and patients may be more adherent to bone-active treatment options in view of numeral risk estimation.

In a quadrupedal mouse model, studying bipedal fracture risk and the link between muscle mass/strength and falls is difficult. However genetically modified models, as well as induced fracture models, allow for the study of changes in motion and function of the muscle bone unit which may provide insight into human cases.

Zebrafish fractures, their numbers and recurrence can be easily evaluated *in vivo* and longitudinally. As in mammals, fractures that happen early in life would indicate higher risks of fracture recurrence in zebrafish. Nevertheless, there are no estimates available, yet, for fracture risk predictions in zebrafish.

2 BONE DENSITY AND IMAGING - 2D

Many different imaging modalities have been used to quantify bone density, strength, fracture risk and remodelling (**Table 1**). Some of these methods are specific for the human, but many can be used as well (in modified form) for animals (**Figure 2**). Essentially, imaging methods can be 2D (slices or projections) or 3D. In this section we focus on the 2D imaging methods while the next section deals with 3D methods.

Different options are available for 2D bone assessment based on imaging in humans, which include plain radiography, bone densitometry by dual energy x-ray absorptiometry (DXA), bone scintigraphy, as well as vertebral fracture assessment (VFA) and trabecular bone score (TBS) based on lumbar spine DXA. The different imaging modalities have specificities in their local availabilities, as well as varying advantages and disadvantages depending on the technology, like radiation exposure, spatial resolution and the information that can be obtained.

2.1 Plain Radiography

Conventional and digital x-rays are widely available and are frequently used as the first-line overview for imaging almost all pathological changes in the bone e.g. to assess bone structure and morphology in case of a suspected vertebral fracture. The main feature of osteoporosis in radiographs is increased radiolucency of the trabecular bone and cortical thinning, though this is mostly subjective and with low specificity, found at advanced stages of osteoporosis when bone mass is substantially reduced or bone mass accrual was insufficient as in osteogenesis imperfecta (OI) (59), and shows other mechanical or inflammatory changes of the vertebrae.

The Genant classification of vertebral fractures has been implemented using a semi quantitative technique (60) in five subtypes (OF1-5) (61) based on lateral vertebral imaging with a relatively low interobserver variation [see *Vertebral Fracture Assessment* (*VFA*)].

Limitations: The biggest disadvantage of plain radiography for assessing changes in the bone structure is the 2D nature, resulting in superposition of three-dimensional structures consisting of soft tissue and hard tissue onto a 2D plane. Thus, the interpretation can be difficult due to the superposition of shadows (62, 63). Another drawback is the limited resolution (order 200 microns) and the inability to discriminate between low bone mass and mineralization defects. As for all the techniques involving x-rays, there should be careful consideration between examination outcome and radiation dosage.

Strengths: Nevertheless, plain radiographs are widely available and some additional software techniques for bone density estimation from radiographs are under development. Generally, radiography is the first assessment due to the wide availability of the equipment, and the low cost (64). Radiographs may also provide an initial differential diagnosis covering also scoliosis assessment and other diseases of the spine presenting with back pain.

In mouse, 2D radiography is a highly sensitive method to study bone properties. The x-ray microradiography imaging is a useful tool for phenotyping. With this technique an X-ray tube with a small spot size (around 10 microns) is used that enables magnified projections of bone details. It can be used to assess changes in bone size and cortical thickness, and if used with appropriate standards, it can also provide a quantitative measure of mineral content (65). It also has the ability to detect cortical thinning and bone loss as seen in humans suffering osteoporosis (66). Lateral x-ray imaging has been applied in high-throughput format to identify bones with altered length and mineral content (66). It has the benefit of being fast and non-destructive, but drawbacks include that it only provides a two-dimensional image and may be affected by poor or inconsistent positioning of the animal or bone.

In zebrafish, radiographs are useful for rapid evaluation of skeletal deformities and bone density. As an example for the power of the technique, Fisher et al. have identified the zebrafish mutant Chihuahua (chi) (mutation in the α1 chain of collagen type I) through a zebrafish forward genetic screening in which the authors leveraged from radiographies to screen a high number of adult zebrafish for skeletal abnormalities (67). Radiographs allow longitudinal studies of the zebrafish spine. Imaging takes a few seconds, allowing anesthetized zebrafish to be imaged without water, and followed by full recovery. However, due to the small size of the zebrafish bones, many aspects of bone morphology, microarchitecture, and mineralization, are limited in radiographic analysis, while μCT captures all these metrics.

TABLE 1 | Comparison of 2D imaging and bone density techniques between species.

Imaging technique	Human		Mouse/rat models		Zebrafish models	
	Strengths	**Limitations**	**Strengths**	**Limitations**	**Strengths**	**Limitations**
Plain radiographs	Widely available	2D analyses	availability	2D image	Longitudinal skeletal assessment	Detailed aspects of bone morphology and density are not captured due to the imaging resolution, overlay with soft tissues, and small bones in zebrafish
	Additional density estimation in development	Potential superposition		Poor or inconsistent positioning of the animal or bone.	Relative bone density estimation	
	Low cost				Low cost and rapid imaging for high-throughput screenings	
	Moderate radiation dose				Full fish recovery after imaging	
DXA	Low radiation	Artefacts from bone (fractures), osteophytes, vascular calcifications and other superpositions	Most suitable method for BMD measurement in small animals	General anaesthesia needed	N.A.	N.A.
	Fast and highly reproducible measurements	2D information only		Poor edge detection and accuracy for very small animals (<50 gr)		
	Widely available and full automatization	No differentiation of trabecular vs cortical compartments		Accurate positioning of the animals and placement of the region of interest can be challenging		
	WHO/ISCD definition for osteoporosis/ osteopenia Individual longitudinal monitoring possible	No correction for bone size or skeletal maturity (e.g. in children)		Measurements affected by size and weight of the animal		
TBS	Non-invasive	No direct relation to fracture risk published	N.A.	N.A.	N.A.	N.A.
	Tool for trabecular bone structure	Improvement of risk prediction *via* FRAX				
	Discrimination in secondary osteoporosis e.g. in diabetes mellitus	Potential artefacts				
VFA	Information on vertebral fractures	Lateral positioning of patient sometimes difficult	N.A.	N.A.	N.A.	N.A.
	Low radiation exposure					
QUS	Transportable	No WHO definitions of osteoporosis/ osteopenia	N.A.	N.A.	N.A.	N.A.
	Quick	Many different devices – no standardization				
	Non-invasive	Individual monitoring difficult				
	radiation free	No direct translation to bone structure				
	Inexpensive					
	It can be used apart from specialised centres					
Bone scintigraphy	Widely available	Potential false positive results	Mainly use of SPECT (see *Single-Photon Emission Computed Tomography (SPECT)*)	Mainly use of SPECT (see *Single-Photon Emission Computed Tomography (SPECT)*)	N.A.	N.A.
		Inferior to SPECT in 3D questions				

DXA, dual energy x-ray absorptiometry; FRAX, fracture risk assessment tool; QUS, quantitative ultrasound; SPECT, Single-photon emission computed tomography; TBS, trabecular bone score; VFA, vertebral fracture assessment.
N.A., not applicable.

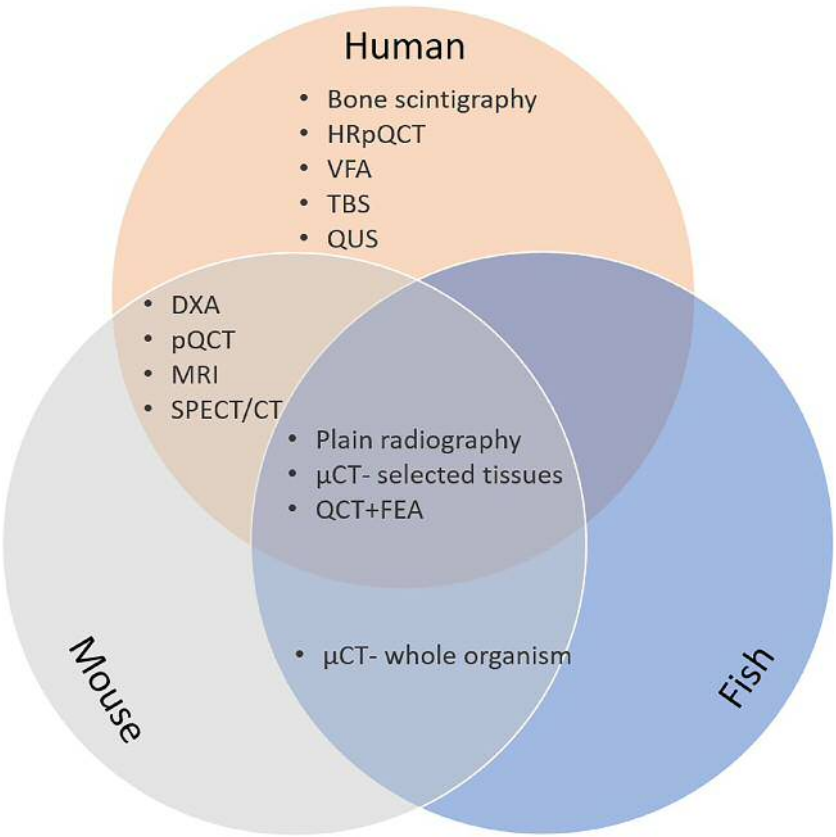

FIGURE 2 | Bone imaging techniques in humans; mice and fish. CT, computed tomography; µCT, microCT; DXA, dual energy x-ray absorptiometry; FE, finite element analysis; HRpQCT, high resolution peripheral quantitative computed tomography; MRI, magnetic resonance imaging; pQCT, peripheral quantitative CT; QCT, quantitative CT; QUS, quantitative bone ultrasound; SPECT, single-photon emission computed tomography.

2.2 Dual Energy X-Ray Absorptiometry (DXA)

DXA provides a two-dimensional (2D) representation of bone, but also information about body composition including lean and fat mass. Measurement sites include the lumbar spine, hip, radius and whole body. Though anterior-posterior scans are generally obtained, lateral spine scanning is also performed to assess vertebral morphology and fractures (see *Vertebral Fracture Assessment* (*VFA*). The DXA image comprises a series of pixels containing information about mineral content. Total mineral content within a region of interest is defined, from which bone mineral density [BMD, in g/cm^2, also often noted as areal BMD (aBMD)] is obtained after dividing bone mass by bone area. aBMD measured by DXA predicts fracture risk in adults (68), for which this method is widely used for clinical and research purposes. In clinical settings, aBMD is compared to a young reference cohort of the same ethnic background and sex, generating a T-score. The International Society of Clinical densitometry (ISCD) defines osteoporosis in adults as a T score ≤2.5, representing 2.5 standard deviations below the young reference mean value (69). Another score reported from DXA measurements is the Z-score. This score quantifies the number of SDs above/below the mean value of an age and sex matched population. This score is not used for the diagnosis of osteoporosis but provides information about an individual's fracture risk compared to peers (70). Volumetric bone mineral density (mass per volume, (vBMD)) also noted as bone mineral apparent density (BMAD) is strongly correlated with bone strength in experimental studies (71). Although DXA just provides an 'areal' density, this remains the most common technique of assessing bone strength clinically. BMD thresholds also contribute, but less than in adults, to the diagnosis of osteoporosis in children (58, 72). In children, aBMD data require adjustment for body size to avoid misinterpretation from size artefacts, by using lumbar spine BMAD and total body less head (73). The ISCD definitions of osteoporosis in children are mainly based on the presence of fractures (74). Hip structural analysis (HSA) (75, 76), has been developed to derive other parameters related to bone strength, for example by calculating femoral neck width (77). Finite element analysis has also been applied to hip DXA images, which may provide additional information on fracture risk (78). In addition, current DXA devices enable specific morphological features to be assessed such as vertebral

fractures and osteophytes. Due to the strong relationships with fat and particularly lean mass, DXA scans provide regional body composition measures which are particularly useful in evaluating android and gynoid fat distribution (79). In fact, DXA is considered the gold standard method for body composition assessment in clinical practice due to its advantages of high accuracy and precision, low cost, low radiation dose and short scan time. It has a variety of clinical applications, such as diagnosis and follow-up of lipodystrophy and sarcopenia, as well as being widely used in research studies of body composition. Further technologies based on DXA are analyses of fractures by Vertebral Fracture Assessment (VFA), and the trabecular bone score (TBS) described in section *Vertebral Fracture Assessment (VFA)* and *Trabecular Bone Score (TBS)*.

Limitations: BMD can be artificially elevated by collapsed vertebrae or mineral deposits at sites that do not contribute to bone strength, such as osteophytes and aortic calcification. In addition, due to its 2D nature, DXA is unable to capture the complex 3D morphological characteristics of skeletal elements. For instance, the trabecular vs cortical compartments cannot be differentiated and DXA gives no information on the bone microarchitecture (80). Moreover, DXA measurements are not corrected for skeletal size, hence DXA underestimates BMD in humans and animals with short stature, and overestimates BMD in those with tall stature. Such artefacts are not generally corrected for in adult medicine and in many animal studies. In children or growing animals alike, interpretation of DXA results requires adjustment not just for age and sex but also for body or bone size, and skeletal maturity (bone age or pubertal status).

Strengths: DXA scans use very low radiation doses and a fast-scanning mode, making this method suitable for research as well as clinical use. Derivation of commonly used measures such as BMD is fully automated and highly reproducible, enabling small changes to be detected in longitudinal studies.

In mice, as in humans, DXA is the most commonly used method for measuring BMD (81). DXA has been demonstrated to be accurate and precise in measuring total bone and bone mineral content in mice (82). It has been used to characterise the bone loss in multiple models of post-menopausal osteoporosis in mice (83). Benefits in animal characterization include the ability for live imaging, its low cost, relatively fast speed, and low-radiation emission. Limitations of the application of DXA in animal models are the low resolution of the technique, and the need for correct (sometimes repeated) positioning.

For zebrafish, techniques of bone density measurements are reflected in section *MicroCT (μCT)*.

2.3 Vertebral Fracture Assessment (VFA)

VFA uses lateral DXA imaging of the thoracic and lumbar spine for the presence of vertebral fractures (VF). Images can be obtained at the same time as areal (aBMD) measurement. The radiation exposure is lower than in plain radiographs of the spine (84). According to the ISCD, Genant's semi-quantitative fracture assessment is the method of reference for the diagnosis of VF on VFA or other lateral spine imaging (74, 85–87).

Limitations: In some devices, the analysis requires a lateral positioning of the patient, which is sometimes not feasible. This limitation can be solved by the use of a "C-arm", allowing supine lateral spine imaging. The upper thoracic vertebrae (Th4 to Th7) might be poorly visible.

Strengths: The low radiation exposure of VFA is an advantage in all, but especially in paediatric patients (according to the latest ISCD paediatric recommendations (74, 88), as well as the combination of both aBMD and VFA in one session.

In mouse, VFA is not used in the mouse skeletal phenotyping.

In zebrafish, vertebral fractures can be assessed longitudinally through radiographs and post-mortem through μCT and whole mount staining (Alizarin Red S staining). Although vertebral fractures in zebrafish are not commonly observed, compressive forces applied *ex vivo*, anteroposterior at the vertebral column and visualized using μCT, have demonstrated points of stress in the vertebrae where it is subjected to fracture in zebrafish (89). Recently, a non-invasive method to induce fractures in zebrafish has been established. By using physical pressure applied to the fin rays of the anaesthetized fish, one can easily cause fin fractures (90). This allows the assessment and the study of fractures from the initial moment that they happened.

2.4 Trabecular Bone Score (TBS)

Trabecular bone score (TBS) is a texture-based index that provides an indirect assessment of trabecular bone microarchitecture. It is calculated based on the pixel gray-level variations in lumbar spine DXA images (78, 91). While this index is increasingly used in adult human patients, there are no animal studies to date, except *ex vivo* comparisons with porcine vertebrae (92). TBS provides additional information on fracture risk and is mainly used in secondary osteoporosis, e.g. in diabetes (93) and ankylosing spondylitis (94). However, the proportion of risk prediction in a more general osteoporosis approach warrants further studies, and also depends on the software used (TBS iNsight®, Version 4.0) with a 54% (OR 1.54; 95% CI, 1.18 to 2.00) increase of having a major osteoporotic fracture (MOF) for each standard deviation decline in TBSv4.0 values (95). Chronological age and TBS are related; significant age-related changes seem to occur with a turning point to higher TBS values at age 8 in girls and age 10 in boys (96). The use of the TBS has not yet been sufficiently explored or recommended for clinical use in children, (see the current ISCD position at iscd.org/learn/official-positions, last access Dec 2020). Assessment of TBS at other bone sites than the lumbar spine might be an interesting development (97), also in view of comparisons with animal measurements and high-resolution (peripheral) quantitative computed tomography HR(p)QCT or bone biopsies including state-of-the-art histomorphometry.

Limitations: TBS is used as an add-on tool to DXA-scans; patterns for specific osteoporosis risk prediction are warranted. An independent contribution of TBS to fracture prediction seems to be small (98), and potential artefacts can be due to collapsed vertebrae.

Strengths: The respective software is a widely used non-invasive tool for indirect assessment of trabecular bone structure based on already existing compatible DXA scans. TBS might allow for a discrimination of patients at risk, e.g. in secondary osteoporosis, where DXA alone does not.

The inclusion of TBS into the Fracture Risk Assessment Tool (FRAX®) may improve the fracture prediction beyond FRAX® without TBS.

In mice and zebrafish, TBS or similar scores are not currently used.

2.5 Quantitative Ultrasound (QUS)

QUS provides a measure of bone quality and quantity (99). Broadband ultrasound attenuation (BUA, dB/MHz) reflects anisotropic characteristics of trabecular bone, and speed of sound (SOS, m/s) refers to the division of sound waves by the length of the bone and transmission time. Some devices combine BUA and SOS values to provide a quantitative ultrasound index (QUI) or stiffness index (STI). Though providing a distinct measure to DXA-evaluated BMD, QUS and DXA have similar predictive value for hip fracture risk in elderly populations (100). QUS is used to assess easily accessible bones like the calcaneus, which is the most widely used measurement site, and patella, tibia, metatarsal bone at weight-bearing sites, as well as phalanges and radius (101). Clinically, QUS is used as a screening tool for osteoporosis. QUS has also provided major insights for genetic discovery, through its incorporation in UK Biobank, based on estimated bone mineral density (eBMD, g/cm^2) derived as a linear combination of SOS and BUA (102). The device is not recommended for routine use in children and adolescents.

Fracture sonography is a special field of application of medical ultrasound diagnostics (sonography) for the detection of bone fractures. In addition, there are other applications of bone sonography, such as osteoporosis diagnostics and for the representation of callus. In patients younger than 12, proximal humerus or clavicle fractures can be visualized by ultrasound due to the changes at the bone surface (103).

Limitations: As WHO definitions of osteoporosis and osteopenia require DXA measurements (104), confirmation of QUS findings by DXA measurement is needed. A lack of standardization hampers result comparison, in view of the many different QUS devices available and of the influence of environmental conditions (temperature etc.). Furthermore, in contrast to DXA, the precision of QUS is insufficient for monitoring individual patients (101). QUS cannot assess bone structure.

Strengths: Advantages of QUS include being transportable, quick, non-invasive, radiation free, inexpensive, and useful for large population screening studies even apart from health care centres.

In mice and zebrafish QUS is not used.

2.6 Bone Scintigraphy

Bone scintigraphy detects an increase in osteoblastic activity or vascularization, which may be associated with osteoporotic fracture or localized bone lesions. Radionuclides such as technetium-99m [99m Tc], often linked to a bone-avid tracer molecule such as bisphosphonates, e.g. 99mTc-methylene diphosphonate (MDP) emit gamma-radiation in proportion to their attachment to a target structure. This technology may supplement radiographs with additional information about recent/old fractures or may identify radiographically occult injuries and differential diagnoses such as metastatic disease (63).

Limitations: Bone scans are a sensitive technique, but may produce false positive results and cannot determine the extension of a fracture, whereas SPECT is superior in the detection of vertebral fractures (see section *CT-Based Techniques*).

Strengths: Bone scintigraphy is widely available in specialized nuclear medicine departments and may be used to address clinical questions not only for oncological diagnosis. It can discriminate recent from healed spinal fractures and demonstrate evidence for radiographically difficult to assess fractures, e.g. atypical femoral fractures (105). Furthermore, positive tracer uptake is reported in areas that subsequently develop osteonecrosis of the jaw (ONJ) (106).

In mice, radioactive methods are widely used, but mainly in context with SPECT (see section *CT-Based Techniques*).

In zebrafish, scintigraphy is nor used mainly due to the water-based environment.

3 BONE DENSITY AND IMAGING - 3D

Development of three-dimensional (3D) methods for bone imaging allowed for new approaches in bone phenotyping, such as computed tomography (CT), single-photon emission computed tomography (SPECT) and magnetic resonance imaging (MRI) (**Table 2**). Implementation in clinical use and research protocols depend on local availability and technical knowledge. For scientific purposes, international cooperation of researchers might be an additional benefit by bringing bone scientists together.

3.1 CT-Based Techniques

3.1.1 Computed Tomography (CT)

Computed tomography is a sectional imaging method that allows a representation of soft tissues, bones and vessels. Thanks to the spiral technology (except QCT), clinical CTs produce small isotropic voxels, which enables a high spatial resolution in any spatial direction. The multiplanar slicing also allows sagittal and coronal representations of high quality and 3D visualization provides structural and morphological information. The x-ray-based imaging technique is widely used for characterization of degenerative changes, vascular and soft tissue calcifications (84). The voxel size varies according to the method, e.g., 250 - 1000 µm for clinical whole-body CTs, 50 - 80 µm for HR-pQCT [see *High Resolution Peripheral Quantitative Computed Tomography (HR-pQCT)*] and 10 - 30 µm for microCT (see *MicroCT*, used for instance for microscopic bone structure analysis on bone biopsies) (107).

Quantitative CT enables the measurement of volumetric BMD (vBMD) at the spine and any bone, and allows separate evaluation of cortical and trabecular bone. Further details are available in *Quantitative CT*.

Limitations: CT scans involve high radiation exposure. A direct comparison with DXA is not possible.

Strengths: CT scans are widely available and can be used for the characterization of morphological changes and differential diagnoses.

In mice and zebrafish, clinical CT scanners are not used due to the low resolution (See µCT section *MicroCT*).

TABLE 2 | Comparison of 3D imaging techniques between species.

Imaging technique	Human		Mouse/rat models		Zebrafish models	
	Strengths	Limitations	Strengths	Limitations	Strengths	Limitations
CT	Widely available Morphological use Concomitant differential diagnosis	High radiation exposure No direct comparison to 2D methods (e.g. DXA)	See µCT below	See µCT below	N.A	Low resolution
SPECT/CT	Correlation of skeletal standardized uptake values (SUVs) and BMD possible	Not useful in children due to radiation and inflammation concerns radiation exposure	Good spatial resolution Useful for bone growth and repair Non-invasive and longitudinal tracking of changes	Radiation	N.A.	N.A.
QCT	Volumetric bone density information Can be used for continuum FE models	Considerable costs Higher radiation dosage Long operational time	See µCT below	See µCT below	See µCT below	See µCT below
pQCT	Evaluation of cortical and trabecular bone density, structure and strength Relatively low radiation dose	Thresholding and difficulties with standardisation at distal sites Size artefacts by partial volume effect Needs adjustment for bone length	See µCT below	See µCT below	See µCT below	See µCT below
HR-pQCT	Only existing non-invasive imaging method obtaining bone microarchitecture Fast and safe Low radiation dose 3 µSv/scan Good reproducibility No side effects	Only for distal extremities Movement artefacts Manual analysis required due to potential inaccurate estimates	See µCT below	See µCT below	See µCT below	See µCT below
MicroCT (µCT)	In bone specimen, fast and non-destructive assessment Excellent reproducibility and accuracy	*Ex vivo* use in humans only Lack of specificity for soft tissues	Most suitable method for skeletal measurement	Time-consuming Stabilization required Radiation exposure	Most suitable method for skeletal measurements as well as assessment of individual bone morphologies	High radiation allows only *ex vivo* bone assessment
MRI	No radiation exposure Widely available Well-defined morphological tools	No direct comparison to 2D methods (DXA)	Longitudinal assessment	Long scanning time Low resolution due to small sample	Bones and muscles can be visualized	Aquatic flow cell system is needed for *in vivo* scanning Low resolution Difficult in use

CT, computed tomography; µCT, microCT; FE, finite element analysis; HRpQCT, high resolution peripheral computed tomography; MRI, magnetic resonance imaging; pQCT, peripheral quantitative CT; QCT, quantitative CT; SPECT, Single-photon emission computed tomography.
N.A., not applicable.

3.1.2 Single-Photon Emission Computed Tomography (SPECT)

Non-quantitative bone scintigraphy using 99mTc-MDP may be combined with CTs for Single-photon emission computed tomography SPECT)/CTs. Standardized uptake volume (SUV) is also used for bone metabolism measurements. The range of SUV in normal lumbar spine is roughly coherent with 18F-fluoride in positron emission tomography (PET). In addition, it correlates positively with Hounsfield units (HU) of the lumbar spine and negatively with age (108). As a fusion method SPECT/CT has been shown to be superior to SPECT alone in the identification of vertebral lesions especially in distinguishing acute fractures in a multiple fracture setting (109) and is consistent with MRI in patients with osteoporotic vertebral compression fractures (109).

Limitations: SPECT should be avoided in children unless oncologic or inflammatory conditions are suspected (110).

Strengths: The correlation of skeletal standardized uptake values (SUVs) and BMD suggests its use for clinical and research purposes (108).

In mice, SPECT scanners designed for pre-clinical models, can have a spatial resolution of <0.5mm due to pinhole and multi-pinhole collimators (111). This is useful when used in combination with CT scanning (SPECT/CT) which allows co-registration of the area of activity, and the skeleton, hence areas of new bone formation or high bone turnover (112). Multi-pinhole SPECT has successfully been used to track bone growth and repair in a mouse model for 12 weeks – specifically to track the temporal and spatial positioning of hydroxyapatite deposition in a bone defect mouse model (113). Benefits of this technique in mice are the non-invasive character allowing longitudinal tracking of changes in individual animals, which may reduce cost, animal numbers and inter-animal variability. Fast scan times (minutes) require less time under anaesthetic. However, exposure to radiation is required and this may be significant if repeated scans are taken.

In zebrafish, as for other radioactivity-based measurements, no special scintigraphy technology is available due to the water-based environment.

3.1.3 Quantitative CT

Quantitative CT (QCT) enables 3D imaging of bone *in vivo* while providing quantitative information about the spatial bone density distribution at a resolution of around 0.5 mm (114, 115). The possibility to calculate vBMD provides a true density measure of the whole bone cross-section, in contrast to areal BMD obtained from DXA. QCT images can also be used as the basis for Finite Element (FE) models (116, 117). With such models, the bone geometry is represented by a large number of sub-volumes (the 'elements'), typically one or a few mm^3 in size. As the QCT resolution is not enough to resolve the trabecular or cortical microstructure, these models represent bone as a 'continuum' in which the bone microstructure is homogenized and represented by its density only (116, 118). Using such models, it is possible to calculate the bone stiffness, the stresses in the bone and the bone strength for a specified set of forces ('boundary conditions') (116, 119, 120). Such loading conditions can represent physiological loading (e.g. vertebral forces in the spine, or hip joint forces) to calculate physiological stress values in the bone tissue, or can represent loading conditions that typically lead to fracture (e.g. a fall) to calculate bone strength. QCT can be used in clinical trials aiming at quantifying the effects of drugs or other treatments on bone strength or in research studies correlating e.g. nutrition, lifestyle or genetic factors with bone strength. In addition, images can be analysed as an "add-on" screening tool in cases where QCT images are made for other reasons, e.g. during virtual colonoscopy or cardiovascular research focus, in which vertebrae are in the field of view (116, 121, 122). In both human and animal, FE modelling of bone in young versus older ages may differ. In particular, the growth plate can lead to artefacts, as these may appear as gap regions. In addition, the tissue mineralization in young versus old bone can differ, which may require using different empirical relationships to translate density to material properties.

Limitations: QCT images involve considerable costs, radiation dose and operational time. QCT based FE is not suitable as a screening tool (120). It is not possible to account for bone microstructure (other than its mere density), and thus empirical relationships between bone density and material properties are needed. Routine use of QCT in children is not established.

Strengths: A particular strength of QCT-based continuum FE models is that the technique is based on well-validated mechanical principles. This is in contrast to stochastic relationships that predict bone strength from bone density and structural parameters, for which no underlying theoretical relationship exists.

QCT based continuum FE is less suitable for small animals because of the smaller size of their bones (123). Thereby, the assumption that the bone microstructure can be homogenized to a continuum becomes less accurate. The resolution is not enough to resolve thin cortices. For small animals, the use of high-resolution micro-finite element analysis (micro-FE) therefore is more appropriate.

See section 3.1.6 MicroCT (μCt).

3.1.4 Peripheral Quantitative CT (pQCT)

Peripheral quantitative CT (pQCT) is used to image the radius and tibia. The spatial distribution of fat, muscle and bone within the cross section is obtained after applying density thresholds for each of these tissues. At diaphyseal sites, cortical bone indices are obtained including cortical vBMD, periosteal circumference and cortical thickness, as well as muscle and fat cross-sectional area (124). In addition, estimates of cortical bone strength can be generated, such as cross-sectional moments of inertia. At the distal radius (i.e. metaphysis), trabecular vBMD is obtained at a pre-defined central region of the medullary space.

Limitations: A disadvantage is the poor standardisation at distal sites (positioning of reference line relative to the growth plate), which in children and growing animals limits reproducibility. In addition, in humans and animals alike, the partial volume effects (the situation where a voxel volume is only partially filled by bone tissue) lead to size artefacts, i.e. cortical vBMD is artificially reduced in individuals with reduced cortical thickness as a larger part of the voxel is not within the bone tissue. Adjustment for bone length may be required for subjects with tall or small stature, to correct for bone size.

Strengths: The ability of pQCT to evaluate cortical and trabecular vBMD, structure and strength variables separately represents an important advantage compared to DXA scans, and has provided the basis for separate genetic studies of cortical vBMD (125), trabecular vBMD (126) and cortical thickness (127). This may be even more important for the assessment of bone conditions where the relations between cortical and trabecular bone are shifted (128). Furthermore, pQCT scans are associated with a relatively low radiation dose, making this method suitable for clinical studies.

In mouse models, pQCT is useful to accurately measure both trabecular and cortical vBMD, as well as predicting bone strength (129). pQCT has been shown to be accurate and precise in mouse models, confirmed by both μCT and histology (130). It can be

used *in vivo* on live animals. There is however the potential for errors in vBMD measurements based on specimen thickness and positioning (129, 131).

See section 3.1.6 MicroCT (μCt).

3.1.5 High Resolution Peripheral Quantitative Computed Tomography (HR-pQCT)

Like the classical pQCT, HR-pQCT assesses bone microarchitecture in the cortical and trabecular compartments, but with higher resolutions of 82 μm for the first-generation devices and 61 μm for the second-generation devices (132, 133). Depending on technical developments, the clinically standardized volume of interest (VOI) is to be set to 9.5 mm in length for the first generation and 10.2 mm for the second-generation of devices. In adults, the beginning of the VOI is situated at a fixed distance proximally from a reference line through the joint at the distal cortex of radius and tibia (134). Thus, in taller individuals, the VOI is relatively more distal and has greater cross-sectional and trabecular areas as well as thinner cortices. For HR-pQCT imaging, the participant's extremity is placed in a cast, which reduces motion. The cast is then inserted into the device and is fixed in position, while the x-ray source rotates around the extremity. The scanning time is around 2.5 min for these standard measurements. Cortical and trabecular vBMD, cortical and medullary cross-sectional area, cortical thickness, cortical porosity, trabecular spacing (Tb.Sp), trabecular number (Tb.N = 1/Tb.Sp) and Tb.Sp standard deviation are typically reported and satisfactorily accurate (135). For the first generation HR-pQCT only Tb.N was directly measured, while other parameters were derived from Tb.N and BV/TV using standard methods adapted from histomorphometry (134). For the second generation all parameters were measured directly. HR-pQCT is used for longitudinal assessment of changes in bone microarchitecture, e.g., of age-related bone loss (136). However, bone loss at the endocortical bone surface results in trabecularisation of the inner cortex and errors in estimation of cortical and trabecular bone loss (137). More recent software permits to transfer the initial endocortical contour on the follow-up scans and assess bone loss in the cortical and trabecular compartment. HR-pQCT scans may be used for micro-FE analysis to estimate bone strength (138, 139). In addition, vascular and tissue calcifications are targets of HR-pQCT measurements and currently under development.

Limitations: For now, HR-pQCT is available only for distal extremities, although with the second generation scanning of areas up to the knee and elbow has become possible as well (140, 141). As HR-pQCT is sensitive to movements, some scans have to be excluded due to poor quality. The occurrences of movement artefacts are higher for radius than for tibia scans, probably because the sitting position is less comfortable. Furthermore, the necessity to stay in a resting position without any movement of the scanned limb might be challenging especially in the elderly patient with tremor and people with pain in joints may have trouble being positioned. Any x-ray based method is not conclusive in areas with metallic or other implants (133).

In the structural analysis, identification of the endocortical limit between cortical and trabecular compartments by software is challenging (142). Thus, estimates of cortical thickness and area and that of trabecular area may be inaccurate. Manual analysis is time-consuming and has only moderate-to-good reproducibility. However, the endocortical limit on the HR-pQCT scan is not always evident even for experts and the manual analysis does not improve its identification. Several algorithms assess cortical porosity, but they are based on unverified assumptions (143–145).

Strengths: HR-pQCT is the only existing non-invasive imaging method obtaining bone microarchitecture in clinical studies. It is fast and safe (low radiation dose 3 μSv/scan), has good reproducibility (<1% for vBMD, <4% for structural variables) and gives no side effects (146).

HR-pQCT permits to assess the structural basis of the effects of the risk factors of osteoporosis (e.g., sex steroid deficit), predict fragility fracture and the effect of anti-osteoporotic treatments on bone (147–149). The biomechanical parameters assessed by micro-FE can improve fracture prediction (148). Scanning protocols for children are being developed.

For mouse and zebrafish context see section 3.1.6 MicroCT (μCt).

3.1.6 MicroCT (μCT)

Micro-computed tomography (MicroCT or μCT) is a high-resolution imaging modality that offers quantitative analysis of trabecular and cortical bone morphology in animals and human specimens. First introduced in the late 1980s (150), μCT now has become the gold standard for the evaluation of bone microarchitecture throughout species.

The method, such as the other CT-methods, is based on the use of x-rays to create cross-sections of an object. For μCT voxel sizes lower than 10 μm can be obtained (151). The degree of x-ray beam absorption is recorded, so that the 3D structure of the object can be visualized and numerous bone structural parameters can be quantified with a high degree of accuracy, such as cortical and trabecular vBMD, cortical thickness, and if used at high enough resolution/voxel size, cortical porosity.

As an *ex vivo* imaging modality in humans, μCT enables 3D characterization of small bone specimens acquired from bone biopsies, or of larger cadaveric specimens such as vertebrae (152, 153). Studies have shown that μCT can reproducibly quantify 3D microarchitecture of the trabecular and cortical bone in iliac crest biopsies, demonstrating significant changes in 3D trabecular structural parameters in postmenopausal samples, including a decrease in BV/TV, an increase in trabecular separation and a shift from platelike to rodlike structure (154). μCT quantification of bone structure from iliac crest biopsies is an important end point in longitudinal drug efficacy studies (155). Assessment of 3D trabecular and cortical structural characteristics may improve our ability to understand the pathophysiology of osteoporosis, to test the efficacy of pharmaceutical intervention, and to predict bone biomechanical properties.

Limitations: Due to the high radiation exposure, the use in humans is restricted to *ex vivo* measurements and thereby limits the clinical application of μCT. High-resolution scans produce

large amounts of data that require support for data acquisition, processing and management. Even though a considerable limitation of the μCT technology is the lack of specificity for soft tissues, it can be combined with contrast agents for the visualization and quantification of soft tissues like vascular structures and bone marrow adiposity within the bone specimens (156, 157).

Strengths: Compared with histology, μCT has many advantages as larger volumes are analysed, 3D-measurements can be performed faster with higher resolution, excellent reproducibility and accuracy. The assessment of bone morphology is non-destructive and does not require fixating agents, enabling subsequent analyses of specimens for histology, mechanical testing and biochemical analysis.

In mice, μCT is a widely used method for analysing bones of small animal models *in vivo* and *ex vivo*, due to its high resolution, with the ability to achieve resolutions as small as 1-micron (158) and identifying body composition. Guidelines for μCT assessment of rodent bone specimens have been recommended including sample preparation, image acquisition, processing and analysis (159).

Ex vivo μCT can be used to measure cortical and trabecular vBMD, cortical thickness, and if used at high enough resolution/voxel size, cortical porosity (160). It has been used at high-throughput format to identify bones with altered BV/TV, trabecular thickness (Tb.Th) and trabecular number (Tb.N) (66) and can be used for longitudinal assessment of the same animal over time due to the non-destructive character. It can be performed on living animals, although long scan times do require large doses of anaesthetics and radiation (above 400 mGy/scan) can affect osteoblasts and subsequent evaluation of bone formation (161, 162).

In adult zebrafish, μCT is a well-established and widely used tool for the detection of skeletal abnormalities (13, 40, 163–165). Due to the small size of the bones in zebrafish, the visualisation of the skeleton through standard μCT has been mostly limited to skeletally mature animals. The use of contrast agents, such as AgNO3, has been shown useful for the visualisation of earlier ages of the zebrafish skeleton, as well as for soft tissue [28]. 3D tissue mineral density (TMD) reflects the amount of mineral per unit volume of bone tissue and is used to measure cortical TMD in zebrafish. TMD values of 450-600 mg HA/cm^3 have been reported in the vertebrae of adult zebrafish (13) which is noticeably less than the TMD values of 800-1000 mg HA/cm3 in the cortical bone of adult mice (166) or human cancellous bone (167). These differences in TMD have been attributed to differences from human bone in material properties and mineralization dynamics (12) and as a possible reflection of adaptation to mechanical loading and bi- or quadrupedalism in terrestrial mammals (168). In parallel with TMD, values of the vertebrae length, area, volume, thickness and other measurements of shape are often used for phenotypic characterisation of the zebrafish vertebral column (13, 164, 169). The vertebral column, as a major skeletal structure of the zebrafish adult skeleton, is most commonly studied by μCT. However, it is also used for the analysis of other parts, such as the zebrafish craniofacial skeleton (11, 164, 170, 171). Semi- to full automation of bone segmentation from μCT imaging data would allow rapid and robust analysis. In this line, a supervised segmentation algorithm (Fish-μCT) enables segmentation of each vertebrae and profiling of phenotypic measures (13, 39).

3.2 Magnetic Resonance Imaging of Bone (MRI)

Magnetic resonance imaging is an intersectional imaging method. It technically uses a combination of a strong magnetic field (1.5-9T) and stimulation of protons by radiofrequency pulses. MRI provides high contrast resolution and better soft tissue display than computed tomography. Due to different imaging techniques, like fat suppression, it provides a high sensitivity for findings like periosteal edema and bone marrow changes as well as intracortical signal abnormalities (172). Frequent findings in acute and subacute vertebral fractures are vertebral edemas with a low signal on T1-weighted images (WI, using basic pulse sequences in MRI) and a high signal on T2-WI, and high signals on STIR (Short tau inversion recovery), while old fractures show the opposite (109). MRI has been analysed for "M-scores", deviated from signal to noise ratios (SNR) in the vertebrae L1-L4 as compared to T-scores using DXA. The SNR in L1–L4 is negatively related to BMD, but the cut-off value for M-scores is still under debate (173). Some of the novel MRI imaging techniques are able to quantify bone composition and may generate precise phenotypes of bone changes related to age (174). Future developments should define calibration phantoms for routine imaging. Artificial intelligence (AI) algorithms may be used for existing images to identify patients at risk for bone fractures.

Limitations: MRI requires expensive equipment and training. A direct comparison to 2D DXA is not possible, and limited resolution is often not sufficient for morphological analysis. Especially high field MR scanners (over 7T) are not widely available and costly, therefore only accessible in well-equipped institutions. In general, this equipment is exclusively used for research purposes. MR examinations are time-consuming due to the longer scanning time and therefore more susceptible to motion artefacts, which can affect the accuracy of evaluations. Furthermore, MR is very susceptible to artefacts caused by metallic implants, for example postoperatively in the case of spondylodesis, which in turn reduces image quality and makes partial evaluations impossible.

Strengths: MR technologies are widely available, at least in developed countries. There is no radiation exposure, therefore repeated and large areal scans are possible. Well-defined morphological tools may help to characterize significant changes in clinical work-up. A powerful strength of magnetic resonance is the excellent soft tissue imaging. It is superior for imaging muscle pathologies and, through special techniques such as the Dixon technique (175), for quantifying adipose tissue and muscle mass in a reasonable time frame, which might also add important information in connection with osseous pathologies. Furthermore, cartilage damage and degenerative as well as inflammatory changes in articular cartilage and intervertebral disc tissue can be identified and

quantified, which is not technically possible to the same extent using computer tomography.

MRI is a useful tool in mouse phenotyping as it allows concurrent imaging of soft tissue (cartilage, bone marrow, muscle, fat) and bone with good spatial resolution. MRI has been used to image bone injuries in mice with good distinction between the bone, soft tissue and injury sites, with a good signal-noise ratio (176). MRI is particularly useful for monitoring endochondral fracture healing, which involves a cartilaginous tissue callus (177). MRI has the benefit of providing 3D images, and allowing longitudinal assessment of single animals. Disadvantages include a long scanning time (up to hours), the potential for artefacts at the bone-soft tissue interfaces, and low resolution due to the size of the sample (176, 178).

MRI has not been widely used in zebrafish. However, recent studies demonstrated the use of the imaging technology for longitudinal and non-invasive studies. 3D scans covering the thoracic region of the same adult zebrafish at an isotropic voxel resolution of 31 μm allowed longitudinal studies of the zebrafish heart. Bone and muscles were observed with MRI (179). To overcome the limitations of the aquatic system, a flow cell system has been developed for MRI imaging, allowing to monitor the zebrafish during the scan and to fully recover the animal (180). However, the methodology needs to be further improved to establish it as a routine bone assessment in zebrafish.

4 BONE BIOPSY AND LOCAL MEASUREMENTS

Investigations at the tissue level have a long tradition for histology and several microscopic technologies which are important in clinical practice for the differential diagnosis of disease entities. However, new approaches will help to expand our understanding of bone properties using microindentation (see *Microindentation*) or compositional bone matrix analyses *via* quantitative backscattered electron microscopy imaging (qBEI) and vibrational spectroscopy (see *Compositional Bone Matrix Analysis Using Quantitative Backscattered Electron Microscopy Imaging (qBEI) and Vibrational Spectroscopy*) – these new approaches and their use in human and animal bone research is of increasing importance.

4.1 Histology

Histology of bone biopsies provide qualitative information about bone cells, matrix (e.g. the orientation of collagen fibres), mineralization and bone marrow. Evaluation of bone biopsy should comprise its histological (visual, qualitative) and histomorphometric (quantitative) assessment (181). The biopsy should be examined for the presence of mast cells and cancer cells infiltrating the bone marrow or the bone. It should be noted if the bone has the normal lamellar texture or if woven bone is present (182).

Limitations: Histology only provides information on the 2D structure of tissues and cells which can lead to an over- or underestimation of morphological features. However, the stacking of layers can be applied to regain 3D-information. It is a destructive method, and only the remaining parts of an embedded sample can be analysed with other techniques than the histological assessment.

Strengths: Histology is one of the most established and versatile methods to identify different types of tissues, and osseous cell components at high resolution. Various staining protocols are readily available for the detection of bone matrix alterations due to diseases or treatment.

In mouse and zebrafish studies, histology is widely used. As with human studies, it can provide information on cell type and number, bone matrix and mineralisation and help to characterize specific disease models.

4.2 Histomorphometry (Static and Dynamic)

In addition to specific histology, a histomorphometric evaluation of bone modelling and remodelling can provide quantitative information about mineralization disorders, metabolic bone diseases, and secondary bone diseases including cancer. "Static" bone histomorphometry (HM) consists in counting cells and measuring bone tissue components. For "dynamic" purposes, oral tetracyclines are administered separated by 10-12 days. Tetracycline is incorporated into new bone at the "mineralization front", and its fluorescence allows for the assessment of bone turnover (183–185).

Histomorphometry from patients requires bone biopsies obtained standardly from the iliac crest under local or (in children) general anaesthesia.

Bone samples are processed without prior decalcification according to published protocols. The stains should allow the differentiation between mineralized bone tissue and osteoid, and the identification of bone and marrow cells by using several methods, with Goldner's trichrome and toluidine blue being most widely used. Solochrome cyanine R allows the observation of bone texture under polarized light. Unstained sections are prepared for the observation of the tetracycline labels by fluorescence microscopy. May-Grünwald-Giemsa or toluidine blue are used for the analysis of bone marrow and especially for the identification of mast cells and TRAP-staining is common to assess osteoclast parameters.

Quantitative analysis is performed on complete and unbroken samples. Measurements are performed by using automatic or semi-automatic image analysers. Parameters can be measured separately on periosteal, cortical, endocortical and cancellous bone. The bone histomorphometric parameters with abbreviations have been standardized by the American Society for Bone and Mineral Research (ASBMR) Histomorphometric Nomenclature Committee (186, 187).

For some specific diagnoses histomorphometric examination is required. For example, osteomalacia shows an accumulation of osteoid i.e. non-mineralised bone. While the experienced examinator can give the diagnosis of osteomalacia without quantification, the degree of the delay of mineralization requires HM. Hyperparathyroidism (HPTH) is associated with high bone turnover and an increased amount of immature bone showing a diverged picture from the usual lamellar structure

referred to as woven bone, as well as marrow fibrosis. An important indication for bone biopsies is chronic kidney disease (CKD) with potential high or low turnover conditions. In mild CKD, changes may be similar to HPTH with woven bone and peri-trabecular marrow fibrosis, referred to as osteitis fibrosa. Osteomalacia and adynamic bone disease are showing with low turnover features in bone histomorphometry. Both conditions require careful therapy adaptation. Bone fragility disorders such as osteogenesis imperfecta are associated with typical static and dynamic HM. Reference values of healthy children and adolescents (188), adult osteoporosis (183) as well as patients with OI type 1 (189) are used for interpretation of HM results.

Limitations: This invasive method depends on established procedures and trained personnel. Localised bone diseases like Paget's disease of bone and fibrous dysplasia are usually not seen in iliac biopsies. Analysis is performed on an iliac bone sample, an unloading site not prone to fracture in contrast to vertebra, forearm or femoral neck. Despite differences in microarchitecture and turnover between iliac crest and the other skeletal sites, significant correlations were found (190).

Strengths: Bone HM remains the only method allowing the study of bone at the tissue and cell levels to enable measurements at intermediary levels of organization of bone i.e., the osteon. It also remains the only established method to diagnose osteomalacia.

In the study of mouse bone, both static and dynamic histomorphometry are widely used mostly on sections of the distal femoral metaphysis and, for cancellous bone, in the appendicular skeleton. Several staining methods are used to measure osteoblast parameters, such as Toluidine blue or Von Kossa and McNeal stain (191). Osteoclast parameters additionally are measured using the TRAP staining (192). In dynamic histomorphometry, bone formation and apposition rates are calculated using a timed fluorescent agent which is incorporated into newly formed bone, much like described for human studies. Fluorochromes such as calcein, tetracycline and alizarine red (193), can even be combined for double labelling that has demonstrated both increased and reduced bone formation and mineral apposition rates in cortical and trabecular bone (160, 192).

As in human and mice, static and dynamic histomorphometry are used in zebrafish. Vertebral endplates are active sites of bone formation, providing a suitable region for typical static bone histomorphometry (50). Number of osteoblasts per bone perimeter (N.Ob/B.Pm), osteoid thickness (O.Th), osteoid surface per bone surface (OS/BS) and osteocyte density (N.Ot/B.Ar) can be assessed (40). As zebrafish are transparent during skeletogenesis and through juvenile stages, bone staining are often readily observed in whole-mount, alleviating the time and resources required for tissue sectioning. Alizarin Red and Calcein staining are used to label mineralizing tissues (194), which can be monitored *in vivo* in bones that are optically accessible, such as early developing vertebrae, growing vertebrae, scales and adult fin rays. Pulse labelling with Alizarin and Calcein can demarcate bone formation between labelling periods (50, 195–197), similar to dynamic histomorphometric approaches in mammals. Mineralised bone can also be assessed by Von-Kossa staining and activity of alkaline phosphatase (ALP) (198). Cartilage is frequently visualized using Alcian Blue (199–201). Moreover, the use of transgenic lines also allows *in vivo* assessment of specific cell types, including osteoblasts (202, 203), osteocytes (203) and osteoclasts (204, 205). Osteoclast activity can be observed in whole-mount or histological sections using TRAP staining (206).

4.3 Microindentation

Micro- and nano- indentation have been used in many studies to quantify the modulus (stiffness) and hardness (resistance to yielding) of bone tissue (207, 208). A limitation of these techniques is that they can be applied only to extracted bone samples or biopsies. Reference Point Indentation (RPI) estimates the resistance of the cortical bone to fracture (209, 210). It is based on the hypothesis that the microindentation of the bone surface induces the separation of mineralized collagen microfibers and the initiation of micro-cracks (211). Whereas this measure is related to the resistance of bone tissue to fracture, it is incompletely understood which mechanical properties of bone are captured by RPI. For this reason, measurements typically quantify a parameter called Bone Material Strength index (BMSi) units representing the ratio between the penetration of the probe into the bone and its penetration in a methyl methacrylate reference phantom (209, 210). In RPI, a probe is applied to the outer surface of the cortical bone of the tibia under local anaesthesia to produce a microindentation (of a size similar to a resorption lacuna), and thus, to measure the distance the probe can penetrate the bone. The higher this distance, the less the bone is able to resist the formation and propagation of micro-cracks, and thus the weaker it is (210).

Two distinct RPI techniques exist (208). The first to be developed was the cyclic reference point microindentation (CMI) using the BioDent^{TM} device (211). CMI was used in the first human clinical studies and is currently the most used technique in animal studies (209). The second technique called impact microindentation (IMI) is conducted with the Osteoprobe R device (212). IMI was developed for *in vivo* use in clinical studies exclusively from 2013 on (210), and in larger animals (209). As the two techniques differ in mechanical challenges, and do not exactly measure the same mechanical properties, the preclinical results from CMI cannot be extrapolated to clinical results from IMI (209).

Limitations: The use of IMI in the clinical practice is still hampered by methodological and technical limitations and the lack of reference values validated according to ethnicity, sex and geographical regions. The development of standardized procedure (213) and future prospective multicentre studies will clarify the benefit of the methods for the assessment of the pathophysiology and the response to treatment interventions (208–210).

Strengths: This technique holds great promise as it provides clinicians a minimally invasive, simple and safe tool for assessing the material properties of bones *in vivo* (209). Existing data support IMI as a valuable technique for the assessment of bone

fragility in research studies and possibly for its follow-up (209, 210). Importantly, IMI has been proposed as an additional tool to assess and comprehend bone quality, instead of replacing the existing techniques (208–210).

In mice, micro- and nanoindentation is not a commonly used technique, but has been used to assess bone homeostasis and bone repair following micro-damage (214, 215). Among the techniques, RPI is used most frequently. Benefits are the capacity for longitudinal, *in vivo* assessment of the mechanical properties of bone. However, during *ex vivo* technique validation, it has been shown that RPI testing data is poorly correlated with fracture data from traditional biomechanical testing, and has relatively large variability (216, 217).

In zebrafish, nano-indentation is used instead of micro-indentation due to the small size of the zebrafish bones (vertebral length ~ 500 μm, and width ~ 50 μm). It allows the determination of local mechanical properties in sagittal or transverse planes of individual zebrafish bone (40, 218–220). Specifically, the modulus of elasticity, hardness, and modulus-to-hardness ratio (E/H; used as a surrogate measure bone fracture toughness (221) can be extracted and correlated to compositional parameters. In this context, an increase in mineralization under physiological conditions, e.g. with aging, results in an increasing elasticity of zebrafish vertebrae, homologous to human and mammalian bone in general. However, in case of a more disoriented bone matrix, e.g. due to collagen pathologies, an altered organization of the mineral has been correlated with a decrease in mechanical performance. Given the high resolution of nano-indentation experiments, i.e. penetration depth of several 100 nm with a Bercovic tip, heterogeneities in mechanical performance can be assessed, e.g. vertebral end plate region vs. vertebral centrum.

4.4 Compositional Bone Matrix Analysis Using Quantitative Backscattered Electron Microscopy Imaging (qBEI) and Vibrational Spectroscopy

Blocks from bone biopsies can be analysed using quantitative backscattered electron microscopy imaging (qBEI). For qBEI, specimens are commonly embedded, polished coplanar and coated with carbon to provide stable electron conductivity. Assessed is bone mineralization density distribution (BMDD), reflecting the calcium content of cortical and trabecular bone matrix (222–224). With qBEI, the phenotype of several conditions can be further delineated, for example the typically elevated bone tissue density in osteogenesis imperfecta (223). Using a backscattered electron (BSE) detector, variations of intensity of the BSE-signal are measured. Backscattered electrons interact mainly with the sample surface, whereby the intensity is dependent on the local mean atomic number of the sample. Calcium, being the heaviest element in bone, is used to quantify the degree of mineralization based on a linear correlation between the calcium content and the grey value of the BSE image. With the help of reference materials, the brightness and contrast of the image are calibrated and the mean calcium weight percent distribution can be determined based on the grey value histograms of the BSE image, which allow to assess the average calcium content in the mineralized bone tissue area (Ca_{mean}), the heterogeneity of mineralization (Ca_{width}), as well as areas of high and low mineralization (Ca_{high} and Ca_{low}, respectively).

Whereas qBEI provides compositional information mainly on the inorganic component of bone, vibrational spectroscopy can be used for the simultaneous analysis of mineral- and protein-related parameters in bone. The identification of molecular components based on their energy-specific vibrations is used in both Fourier-Transform Infrared spectroscopy and Raman spectroscopy (225). In the context of bone quality assessment, vibrational spectroscopy is a specialized tool to evaluate the "structural fingerprint" for the identification of molecular bonding involved. During vibrational spectroscopy, the sample is irradiated with a specific wavelength, which leads to changes in the vibrational modes of specific molecules, allowing to detect mineral-related components in a spectrum (peaks of phosphate, carbonate) and protein-related components (peaks of amide I and II, phenylalanine, hydroxyproline and proline). Typical Raman and FTIR parameters of bone quality include the mineral-to-matrix-ratio (e.g. phosphate-to-amide I, indicative of the degree of mineralization), the carbonate-to-phosphate ratio (indicative of carbonate substitution in the crystal lattice), and crystallinity (full-width-at-half-maximum of the phosphate peak, related to crystal size), e.g. with different reactions of bound-water compartments for collagen and mineral-bound water. Certain aspects of collagen are also assessable (226). For a more in-depth view also on strengths and limitations, please see e.g (227).

Limitations: Electron microscopy is a complex method, depending on specific clinical/research questions and requires established highly specialized procedures and trained personnel. Moreover, both qBEI and vibrational spectroscopy are generally limited to 2D information.

Strengths: True bone density distribution at the tissue level is measured. Additional information on molecular components and mineralisation enables for new approaches in the interpretation of bone metabolism and structure.

For studying mouse bone, backscattered electron scanning electron microscopy is particularly useful. Resin embedded samples have been used to determine local tissue level mineralisation of bone and the high resolution allows for the investigation of lacunar properties, such as their size and appearance of their surface. Osteoblasts and osteocytes bound to the surface of the specimen can be assessed for their various phenotypic stages. Macerated, non-embedded samples can be used to identify changes in microarchitecture and surface values (192, 227).

Similar to performing qBEI and vibrational spectroscopy in humans, zebrafish bones can be investigated in terms of calcium content and heterogeneity of mineralization as well as Raman spectral parameters. For instance, an increased calcium content has been observed after exercise of zebrafish, as well as in zebrafish OI models (40). Raman and Fourier-transform infrared (FTIR) spectroscopy (19) imaging in zebrafish have shown that zebrafish bone contains carbonated hydroxyapatite as well as other mineral phases, similar to mammalian bone. Moreover, in a zebrafish model of OI, lower matrix maturity is

confirmed through reduced collagen maturity and altered carbonate-to-phosphate ratio using FTIR (40).

4.5 Immunohistochemistry of Bone (IHC)

Immunohistochemistry (IHC) allows to determine the cellular localization of proteins and their expression within tissues (228). This technique requires two phases: 1) specimen fixation and tissue processing and 2) interpretation and quantification of the obtained expression (229). Tissue properties can be analysed in depth, making it possible to study not only bone but also the surrounding tissues like cartilage, muscle and tendons. There are different approaches in immunohistochemistry analysis and reporting and for some IHC markers like bone morphogenic proteins (BMP), osteocalcin (OCN), osteopontin (OPN), and few others scoring systems are available (230), which may include IHC markers of the surrounding tissue. Sequential antibody immunostaining for quantification is used to detect antigens of interest. This is a complementary method to *in situ* hybridization histochemistry (ISHH) which detects cellular nucleic acids based on the formation of double-stranded hybrids between a nucleic acid fragment (the probe) and a DNA or RNA sequence present within bone cells (231).

Limitations: Decalcified bone samples are widely used for IHC. However, during the decalcification process, the integrity of the trabecular network is lost, which can cause changes in the overall appearance of the bone morphology. Careful specimen preparation and analysis by experienced researchers should be applied. As an alternative, methyl methacrylate embedding retains the mineral fraction of the bone tissue. However, the hard embedding makes sectioning more difficult and epitope retrieval complex (228). The process of optimization of the method for each target can be relatively time-consuming, costly and labour intense.

Strengths: For humans, a great variety of antibodies are available and established for IHC. On its own and in combination with different antibodies and other staining techniques, this enables a multitude of possibilities to visualize complex interactions.

In mouse studies, IHC can provide useful information on the temporo-spatial expression of key factors important for musculoskeletal development and function. However, careful and experienced specimen handling of the small mouse samples is needed due to the tendency for samples to detach from slides. IHC has been used to locate many important antigens in bone such as SOX9, OSX and sclerostin (232, 233). As in humans, decalcified bone specimens are most commonly used.

Immunohistochemistry is applied in histological sections (234) and whole-mount zebrafish samples, often performed in larval stages and dissected adult tissues (171, 235–237). While a plethora of antibodies are available for human and mice proteins, only few are available for zebrafish. Antibody tests and protocol optimization need to be performed in zebrafish as for mice and human samples.

5 BIOCHEMISTRY FOR BONE PHENOTYPING

In patients, a number of general laboratory analyses are necessary to assess a patient's general health and potential causes of secondary bone disease (238, 239). These include a full blood count, erythrocyte sedimentation rate (ESR) or C-reactive protein (CRP), markers of liver and kidney function and markers of calcium/phosphate metabolism. Further, optional tests include serum proteins (including electrophoresis; to exclude multiple myeloma), markers of thyroid function (to exclude thyrotoxicosis), sex hormones (to exclude hypogonadism) and measurement of free cortisol in 24-hour urine for screening for Cushing's syndrome. Some additional tests might be useful to exclude other pathologies, e.g. celiac disease *via* transglutaminase antibodies or systemic mastocytosis *via* serum tryptase and/or urine methyl histamine.

Limitations: Optional laboratory parameters require a diagnostic plan for the individual patient to be useful and may be more expensive.

Strengths: Differential diagnoses are frequently based on the knowledge about general health conditions and should be available in acceptable quality.

In mice, most studies use a defined mouse model for distinct research questions. Therefore, it is not necessary to perform biochemistry for the diagnosis of a disease in this context. However, biochemistry can be performed on blood and plasma samples. Other than in humans, the amount of blood obtained from the living animal can be a limiting factor for such tests. They are therefore mostly performed with terminal blood collection in mice.

In zebrafish, although neither pregnancy nor lactation exist, the sex-hormonal changes and sexual-development milestones (analogous to "puberty" or "post-reproductive" age) are well characterized. Sex in zebrafish (as well as amphibians and reptiles) is not determined by a particular chromosome, but by the interaction between gene and environment. Sex hormones are well studied, hypogonadism could be easily obtained and well as orchid- and ovariectomy. Catecholamines, mineralocorticoids and microelements are measured similarly to mammals, as well as thyroid stimulating hormone and its receptor (13). Blood can be collected from the adult zebrafish through the aorta and decapitation. Recently, it has been shown that repeated blood collection can be performed from the same adult zebrafish longitudinally for the measurements of triglycerides and glucose (240). Due to the small size of zebrafish, a limitation of the method is the total blood sample volume that can be collected at time, ≤0.4% of body weight per week for repeated measurements.

5.1 Controllers of Bone Mass and Mineralisation

Many factors are involved in the regulation of bone mineralization, among them calcium, phosphate, calcitriol, fibroblast growth factor 23 (FGF23) and parathyroid hormone (PTH). A major clinical problem worldwide is vitamin D deficiency, which has attracted considerable interest over the last two decades (241). Active Vitamin D is the main supplier of bone minerals to bone tissue. In patients with sufficient vitamin D levels, additional supplementation has no effect on bone (242). Hence, recent studies in osteoporosis have seriously questioned the routine use of vitamin D supplementation for the purpose of preventing osteoporotic fractures (243). Bone mineralization disorders in general (osteomalacia/rickets) can easily be excluded, diagnosed

and treated - there is global consensus for what constitutes sufficient vitamin D levels and calcium intake for the prevention of osteomalacia and rickets (244).

The calcium sensing receptor senses decreased dietary calcium supply and increases PTH secretion. Hence, PTH levels are inversely correlated with 25-hydroxycholecalciferol [25(OH)D] levels and dietary calcium supply. However, while PTH is generally known as an indicator of vitamin D status, there is no consensus regarding the accuracy of measuring PTH to determine vitamin D depletion (245). Dietary calcium supply is the likely reason for this (245). Through an unknown phosphate sensing mechanism, FGF23 controls renal phosphate reabsorption. Bone hypo-mineralisation (osteomalacia, rickets) only develops when serum phosphate is low (246) and is accompanied by elevated (bone) alkaline phosphatase and PTH concentrations.

Laboratory analysis of calciotropic hormones, mainly 25-hydroxycholecalciferol (25(OH)D) as a surrogate for the individual pool of vitamin D and several metabolites including the active 1,25-dihydroxycalciferol (1,25(OH2)D) have gradually undergone worldwide standardization with European and U.S. quality and accuracy methods including reference samples used as gold standards for both mass spectrometry and enzyme-linked assays (247). PTH measurements have undergone considerable development over the years, discriminating between the entire molecule and distinct fragments. Currently used assays identify intact PTH and assays for subforms are still available for specific questions.

Limitations: There is an urgent need to define non-invasive diagnostic criteria for osteomalacia (248). There is some discussion about the analytical approaches and the conversion of units used e.g. in 25(OH)D measurements. There is no single biochemical marker that represents normal bone mineralization.

Strengths: Bone mineralization disorders can be excluced by simple blood tests.

In mice, assays are available for testing serum levels of vitamin D and PTH in mice. Although these tests have been used in the study of dietary intervention and bone health, they are not regularly used in the routine monitoring of bone health in mice (249). On the other hand, a particular benefit of mouse models for studying skeletal disease is that they have less natural variation than humans. Identical diets, environments and genetics mean that mice should have minimal variation in vitamin D or PTH levels.

In zebrafish, measurements have not yet been performed *in vivo* in longitudinal studies. Upon fish decapitation, blood and serum readings could be potentially performed for levels of PTH, calcium phosphate (dependent on food intake), FGF23 levels and vitamin D. It would be interesting to test if such assays could be performed using small volumes of blood/serum that can be collected from zebrafish allowing longitudinal studies.

5.2 Bone Turnover Markers (BTMs)

Systemic markers of bone turnover (BTMs) reflect bone remodelling in adults (250), but also a combination of bone remodelling, modelling and 3-dimensional bone growth in children (251) (**Figure 3**).

Bone formation markers such as osteocalcin (OC), and N-terminal and C-terminal propeptides of type I procollagen (PINP, PICP) are proteins secreted by osteoblasts and represent the activity of bone formation. PINP is also expressed in other tissues (e.g., skin) and during fibrotic processes. Therefore, its concentration may be elevated in skin diseases and in case of active fibrosis (e.g., liver, lungs, heart) (252). Bone alkaline phosphatase (bone ALP) is an ectoenzyme present on the outer surface of osteoblasts. Their serum levels are correlated positively with histomorphometric measures of bone formation (e.g., osteoid surface, appositional rate, mineralization) (253).

The markers of bone resorption activity comprise C-terminal and N-terminal telopeptides of type I collagen (CTX, NTX), deoxypyridinoline (DPD) and hydroxyproline (HPro). They are products of bone collagen degradation. Blood and urinary levels of bone resorption markers reflect the activity of bone resorption. They are correlated positively with histomorphometric measures of bone resorption and decrease rapidly after administration of an anti-resorptive agent (254). Among bone resorption markers, CTX is the most specific for bone. Tartrate-resistant acid phosphatase 5b (TRAP5b) is an enzyme expressed by osteoclasts. It is an indicator of the presence (number) of osteoclasts, but not necessarily of their resorptive activity. Therefore, in some situations (osteopetrosis, treatment with cathepsin K inhibitors), discrepancy between the TRAP5b concentration and the levels of collagen degradation products may be observed (255, 256).

Serum PINP and CTX are defined as the reference markers of bone formation and bone resorption (257).

Limitations: Their specific technical and analytical limitations are categorized in two main groups (258):

Analytical variability: Despite the reduced analytical coefficient of variation (CV) of the techniques used to measure these markers, lack of a uniform standardization technique has resulted in difficulties in comparing values obtained by dissimilar methods in different laboratories. The intra-individual biological variability of BTMs is still of concern, especially when therapeutic approaches should be chosen based on a single measurement.

Pre-analytical variability: The BTMs' preanalytical variability due to uncontrollable and controllable factors should be considered during their clinical interpretation. Uncontrollable factors are for instance age, sex, renal function, growth rate, pubertal or menopausal status, comorbidities or recent fracture. The use of appropriate reference ranges, in particular in children, and suitable adjustments can help overcome this variability to some extent. Controllable factors are for instance food intake/fasting status, circadian and menstrual cycle or exercise. The effects of these factors can be minimized by standardizing the timing and conditions of sample collection.

Measurements of BTMs are not helpful for diagnosis of osteoporosis, bone fragility or skeletal dysplasia. For instance, only 20% of osteoporotic women had serum CTX-I concentration exceeding the upper limit of the reference values in premenopausal women (259). However, elevated BTM levels (especially urinary bone resorption markers and bone ALP) may point to more rapid bone loss and higher risk of hip fracture in adults, mainly in postmenopausal women (260, 261). On an individual level, BTMs may be helpful for monitoring

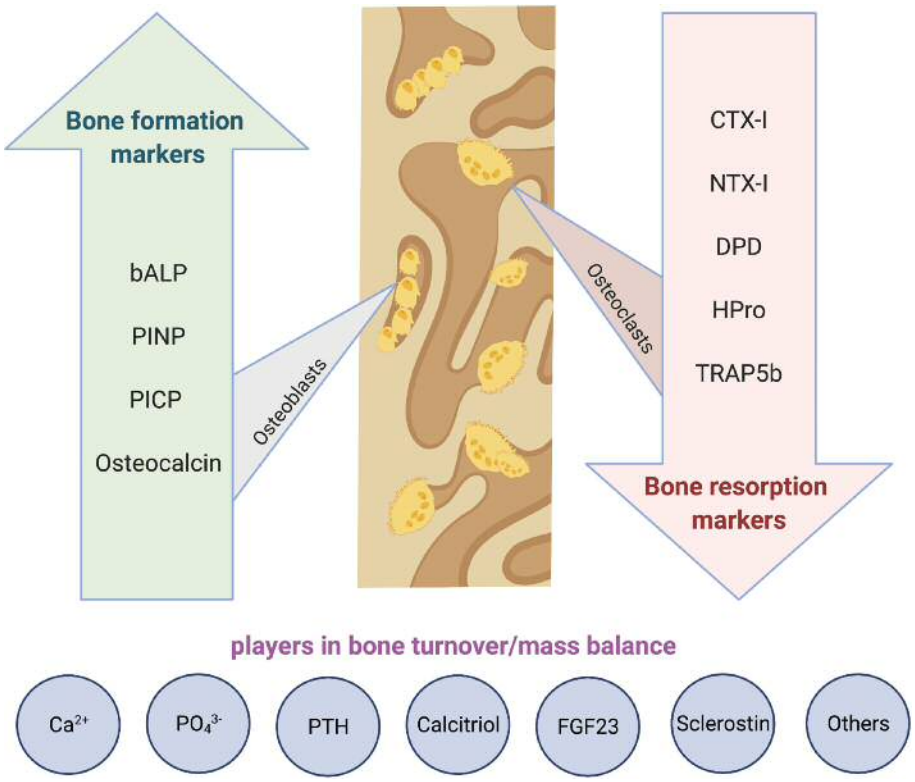

FIGURE 3 | Bone turnover markers and players in bone turnover/mass balance. bALP; bone alkaline phosphatase, Ca^{2+}; calcium/ionised calcium, CTX; C-terminal telopeptide of type I collagen, DPD; deoxypyridinoline, FGF23; fibroblast growth factor 23, HPro. hydroxyproline, PINP and PICP; N-terminal and C-terminal propeptides of type I procollagen, PO_4^{2+}; phosphate, PTH; parathyroid hormone, TRAP5b; tartrate-specific acid phosphatase type 5b.

anti-osteoporotic treatments in adults (262) and children (263). Circadian rhythms and fasting are important factors in the clinical validation - blood samples for PINP can be collected at any time of the day due to only a slight circadian variation comparable to the measurement error of the assay (264). By contrast, blood CTX decreases rapidly after breakfast (265) and blood for CTX assay must be collected in the fasting status in the morning before 10 am.

In children, specific age- and development-associated reference ranges are used for most of the markers but the diagnostic value is limited (266).

Strengths: BTMs are non-invasive to bone. They closely monitor systemic bone turnover and are increasingly established and accessible. Standardization of the analytes is ongoing, but assay results may differ between providers.

BTMs are easily measured in mice using ELISA or commercially available assays. In an ovariectomized mouse (as a model of osteoporosis) OC and CTX provided conclusive outcomes on bone turnover when compared to µCT imaging (267, 268). Although serum BTMs hold the benefit of allowing multiple tests to be taken from one animal over a time course, it should be considered when planning an experiment whether more useful data can be gained by qPCR or western blot of bone tissue post mortem.

Bone formation (osteocalcin, alkaline phosphatase) and resorption markers (TRAP) are measured *ex vivo* through immunoassays in whole-mount, dissected tissues and on histological sections. For *in vivo* studies Alizarin Red and Calcein can be used to measure bone formation as well as the use of transgenic lines for osteocalcin, and TRAP line labelling osteoclasts (205, 269). *In vivo* longitudinal studies for such markers through blood and serum collection have not yet been performed in zebrafish.

6 NEW PHENOTYPING AND FUTURE ASPECTS

For the purpose of personalized medicine and to avoid a "one size fits all" approach, a differentiated pattern of patients' characteristics might be a goal for future investigations based on age, sex and ethnicity and other background information, which should be taken into consideration. Duration of exposure to any harmful agent or environmental condition is important during the life course and of great interest from the epigenetic perspective. In the young, damaging environmental exposures have not yet accumulated. One example is obesity, where

duration of exposure in relation to bone health is something comparatively little is known, but which could be explored in animal models.

There are numerous important new angles, e.g. the view on bone health early in life, shown by the recent insights in the paediatric field. Children with severe illness or skeletal disorders often have short stature, scoliosis, joint contractures and bone deformities. Hence, despite size adjustment, DXA data can be falsely low or unobtainable. Therefore, clinical assessment of bone health and research studies focus on defining bone phenotypes from bone biopsy, x-rays and vertebral fractures and less on DXA. This is improving our understanding of bone physiology of rare diseases. For example, skeletal effects associated with transgender pharmacotherapy have not yet been widely studied. Issues include start-time for treatment, particularly with regard to puberty, and the short- and long-term effects from cross-sex therapies on mineral metabolism.

Looking to the future, a more holistic approach to musculoskeletal health is needed given the multifactorial, polygenic nature of osteoporosis, to facilitate healthy aging/frailty prevention.

6.1 Future Developments in 2D and 3D Imaging

To date, bone mass measured by DXA is the most widely used bone phenotypic measure for genetic population studies of osteoporosis, in large part due to the ubiquitous presence of DXA scanners, which are widely used clinically and in large scale population studies. More recent genetic studies have examined other related phenotypes including hip geometry and shape (270). Looking to the future, DXA scans are likely to contribute to genetic studies of other age-related musculoskeletal conditions. For example, a range of other phenotypes, more closely related to osteoarthritis, are currently being generated in hip and knee DXA scans from approximately 100,000 individuals from UK Biobank[4]. However, a broad number of new technical approaches are under development.

For mammalian and fish studies, an optical coherence tomography (OCT) and synchrotron radiation microcomputed tomography (SR-μCT) may be developed for future use. OCT provides non-invasive high-resolution three-dimensional (3D) images of biological tissue and quantification of chromophores in tissues (271). Fish and human bones contain hydroxyapatite crystals so it can be compared and quantification of BMD is possible to obtain by comparison to sample with known hydroxyapatite levels. Better resolution (100 nm) can be achieved with synchrotron equipped μCT technologies (SR-μCT) with better assessing of bone micro-architecture (11).

Among recently developed MRI techniques is ultrashort echo time (UTE) MRI. Clinical MRI cannot detect water bound to organic matrix, or the free water in the pores of the Haversian system of cortical bone due to the very short apparent transverse relaxation times (T2 *). Therefore, a new class of sequences, ultrashort-TE (UTE) sequences have been developed recently, with TEs of less than 100 μs. This is much shorter than TEs of conventional sequences. These sequences can be used to detect water signals from within cortical bone (272, 273).

PET scanning can be used for some analyses in bone, and has been used in animal models to assess changes in e.g. bone vascularity or stress fractures (274). However, the reduction of radiation and dose exposures are critical in medical and research imaging, since high doses of radiation are associated with DNA damage. Multiple researchers are actively engaged in the development of clinical total-body PET hardware, promising improvements in dose reductions, reduced scan times, and quantitative kinetic modelling capabilities (275).

Artificial intelligence as new methods for automatic image segmentation, and prediction of fracture risk shows promising clinical value (276). Advances in artificial intelligence (deep learning) also perform well in classifying skeletal radiographs (277). Drug and genetic screening as well as longitudinal studies in zebrafish would benefit from AI, towards implementing novel platforms for gene functional validation through rapid skeletal phenotypic assessment.

6.2 Contribution of -omics Technologies to the Phenotypic Dissection of Musculoskeletal Traits

Historically, genome-wide association studies (GWAS) and next generation sequencing have revolutionized genetic diagnostic services and our understanding of common and rare bone diseases. For example, there are now 20+ genes identified that cause osteogenesis imperfecta through whole genome, exome and RNA sequencing and thousands of genetic variants arising from meta-analyses of the Genetic Factors of Osteoporosis (GEFOS) consortium, and the UK Biobank.

Nevertheless, several steps are needed before GWAS discoveries can be translated to biologic processes underlying the genotype-phenotype relationship. First, variants identified by GWAS need to be linked to the gene(s) in the region. Second, such target genes [identified through GWAS or whole exome sequencing (WES)] need to be placed in the context of pathways affected by the genetic variation. Third, functional, mechanistic studies need to establish how the given alteration of the biologic pathway(s) results in a phenotype.

It is here, where the confluence of a roadmap of gene functional evaluations and a detailed assessment of the laboratory and musculoskeletal phenotype can provide mechanistic insight into the relevant biological processes underlying disease. Multi-omics approaches are used to identify laboratory, phenotypic, disease-specific signatures.

Here we provide a succinct overview of multi-omics layers and their importance for bone phenotyping:

Genomics and Epigenomics: Gene coding regions (underlying most Mendelian disorders) make up less than 3% of the human genome while, approximately 90% of the single-nucleotide polymorphisms (SNPs) that are associated with human disease lie within intergenic or intronic regions. As such, genetic variation (polymorphisms, insertion/deletions and mutations) in intergenic regions, such as enhancers, can strongly affect gene expression, demonstrating a tight regulatory network between the coding and noncoding parts of the genome.

[4] https://www.ukbiobank.ac.uk/.

Epigenetic changes at DNA level include methylation, where methyl groups are added to the DNA molecule and change DNA activity, e.g. the repression of gene transcription without change of the DNA sequence. Important examples for these effects include genomic imprinting, X-chromosome inactivation, or repression of transposable elements. Effects on bone have been described in ageing (278) and oncology (279), but also increasingly during metabolic challenges, such as chronic kidney disease (280).

Another important epigenetic modification among others is considered histone tail modifications, where covalent post-translational modification (PTM) of nuclear histone proteins occur *via* methylation, phosphorylation, acetylation, ubiquitination, crotonisation, or sumoylation processes. These changes are currently addressed in a number of bone fields, such as bone and cancer as well as inflammation and rheumatic diseases (281). As an example, for bone/vasculature calcification interactions, a crosstalk between osteogenic transcription factors and histone deacetylases has been described. The inhibition/activation of histone deacetylases might help to develop potential therapeutic interventions in future (282).

For more specific information, see also the publication of GEMSTONE WG3 "Gene & Therapeutic Discoveries in Bone Mass Disorders".

Transcriptomics: RNA Sequencing, gene expression, eQTLs, Non-coding RNAs (lncRNA and miRNA)

Non-coding RNAs (ncRNAs) are recent candidates to become future diagnostic bone biomarkers (283). ncRNA transcripts vary in length from around 22 nucleotides for microRNAs (miRNAs) to more than 200 nucleotides for long non-coding RNAs (lncRNAs). They are found in tissues, but importantly also in body fluids, where they are easier accessible for detection (283, 284).

Different types of ncRNAs are involved in several processes like DNA replication (285, 286), translation (287), RNA splicing (288) and transcriptional regulation (289). Especially miRNAs and lncRNAs are in focus as biomarkers for many conditions, including osteoporosis with some commercially available assays (290–292). They are stable in the bloodstream and protected from RNAse digestion. In the exosomal fraction of body fluids, both miRNAs and lncRNAs are enriched, indicating potentially active secretion of these RNA species from their cells of origin (293, 294).

miRNAs are best studied for their involvement in the control of bone formation and homeostasis through their regulatory functions in osteoblast and osteoclast development (295), not only in metabolic bone diseases, but also in case of cancer and bone metastases. Currently, ncRNA assays are not routinely used and require in most cases a dedicated lab with established PCR procedures. However, ncRNAs may help in the multi-omics phenotype characterization of rare bone diseases and defining disease state in common bone diseases.

Proteomics and metabolomics: The protein contents, i.e. the proteomes, of tissues and cells logically occupy a central position within the biologic processes underlying genotype-phenotype relationships. Proteomes can be studied qualitatively and/or quantitatively at a large scale by proteomics (296). Nowadays, mostly based on the use of liquid chromatography and mass spectroscopy methodologies, proteomic approaches can be employed for protein identification and quantification in samples as diverse as tissues, blood and cells, to provide a comprehensive and quantitative information on their proteomes (296). Therefore, a closer inspection of the bone proteome by proteomics is surely a fundamental tool to put in place towards the phenotypic dissection of musculoskeletal traits. For instance, proteomic approaches can help detect changes in the signal transduction of bone cells, in the regulatory mechanisms that govern bone cell differentiation, among other cellular and tissue processes enrolled in bone metabolism in both physiologic and pathological contexts (297). Accordingly up to now, several studies have made important contributions to our knowledge of the bone proteome, as well as, of the proteomes of individual bone cells (reviewed in (297–299). A special emphasis has been given to identify proteomic changes in osteoporosis (300).

Modern metabolomic analysis (analytical chemistry and bioinformatics) is capable of detecting hundreds of metabolites in human serum and hence identify novel biomarkers and biochemical signatures of disease. These topics are further described in the publication of GEMSTONE WG4.

Microbiomics: Animal studies using germ free mice, antibiotics, probiotics (i.e., microorganisms which confer a health benefit on the host) or prebiotics (i.e., nutrients capable to modify the gut microbiota) have shown that the complex community of microbes colonizing the gastrointestinal tract may regulate bone mass (301, 302). The impact of major alterations of the gut microbiota has been evaluated using either germ-free mice raised in sterile isolators and completely devoid of microbiota, or rodents depleted of gut microbiota by antibiotic use. These rodent models may be inoculated with specific microbes or communities of microbes to examine the effects they trigger on the skeleton in their host. All these studies using germ free mice or antibiotic treated mice exemplify extreme situations and it might be more physiological to look at the bone effects of treatments resulting in minor but specific changes of an already present gut microbiota. Probiotics and prebiotics given to rodents with an already present gut microbiota have been used to demonstrate that specific changes in the gut microbiota may protect against ovariectomy-induced and inflammation-induced bone loss (303). To characterize the skeletal phenotypes in these rodent bone loss models, standard analyses including DXA of areal BMD, MicroCT of cortical and trabecular bone parameters in the axial and appendicular skeleton, static and dynamic bone histomorphometry, bone strength estimates using three-point bending tests of long bones, *in vitro* studies of primary cultures of osteoblasts and osteoclasts precursors as well as analyses of circulating BTMs can be used (304).

The first promising findings of two randomized clinical probiotic treatment trials recently revealed that certain probiotic

treatments had some bone sparing effects on DXA measurements of areal BMD at the lumbar spine (305) or by CT measurements of volumetric BMD of the distal tibia in humans (306).

The results from the first human cross-sectional association studies between the gut microbiota composition and bone related parameters have yielded conflicting results, most likely as some of the studies were underpowered and not adjusted for major confounders affecting the gut microbiota composition. Large-scale population-based studies assessing the association between the gut microbiome composition, as assessed by cost efficient 16S rRNA sequencing, and DXA-derived phenotypes adjusting for relevant confounders including lifestyle factors, diet and medications are underway. Furthermore, meta-genome wide association studies using state of the art sequence methodology in combination with other -omics platforms should be performed to characterize functional gut microbiota signatures associated with human bone health in detail. In addition, these analyses should not be restricted to DXA-derived areal BMD but include bone architecture and dimensions, specific cortical and trabecular bone parameters and incident fracture risk.

CONCLUSION AND THE TRIANGULATION OF [DIAGNOSTIC] EVIDENCE: THE PATH TO PERSONALIZED MEDICINE

Understanding complex systems such as the skeleton requires the integration of multiple layers of evidence arising from a combination of analytical methods, in humans and animals, as outlined in this publication. Integration across many disciplines is required to solve outstanding questions and create a "deep phenotype" which accurately captures disease signatures. Key to this is translatability – whether across methodologies or species – and synchronization of efforts. The 'triangulation of evidence' (307) can overcome logistical and ethical constraints related to experimental design and speed the rate at which the reality of personalized medicine is attained. Looking to the future, there are several areas where the utility of animal models is obvious. For example, skeletal effects associated with transgender pharmacotherapy have not yet been widely studied. Issues include start-time for treatment, particularly with regard to puberty, and the short- and long-term effects from cross-sex therapies on mineral metabolism. Further, on a broader scale 'duration of exposure' to a given risk factor during the life course is of interest for skeletal health from an epigenetic perspective. In the young, damaging exposures have not yet accumulated, while with age, these contribute to accelerated biological aging. In conclusion, the idea of triangulation of evidence emerges as a solid way to weigh the robustness of each layer of evidence, but most importantly to gain insight from the integrated systems perspective. Similarly, the triangulation approach helps to overcome severe logistical and ethical constraints on experimental design potentially arising at each level. Once etiologic validity has been satisfactorily established across the different dimensions, the next challenge is to amalgamate these into a "deep phenotype". This assembled deep phenotype will pave the road to find drug targets and clinical applications, ultimately charting the course toward personalized medicine approaches, for each of us.

AUTHOR CONTRIBUTIONS

IF and BO-P initiated and organised the manuscript. IF, FM, WH, and BO-P generated the figures for the manuscript. All authors contributed to the article and approved the submitted version.

FUNDING

Funding was obtained from the GEMSTONE COST Action (CA18139). The Origins of Bone and Cartilage Disease Programme analysed the skeletal phenotypes of knockout mice generated by the International Mouse Phenotyping Consortium (IMPC) and was funded by a Welcome Trust Strategic Award (101123) to GRW and JHDB. IF is enrolled in the PhD program MOLIN at the Medical University of Graz, funded by the Austrian Science Fund (FWF). FM is funded by the Swedish Research Council (2018-02981), Greta and Johan Kock Foundation, the A. Påhlsson, A. Osterlund Foundation and H Järnhardt Foundations, King Gustav V 80 year fund, Swedish Rheumatism foundation, Skåne University Hospital Research Fund, Research and Development Council of Region Skåne.

ACKNOWLEDGMENTS

This publication is based upon work from COST Action GEMSTONE (CA18139), supported by COST (European Cooperation in Science and Technology). COST is a funding agency for research and innovation networks. Our Actions help connect research initiatives across Europe and enable scientists to grow their ideas by sharing them with their peers. This boosts their research, career and innovation. (www.cost.eu).
The Graphical Abstract and **Figure 3** are created with BioRender (www.BioRender.com).

REFERENCES

1. Sobacchi C, Menale C, Villa A. The RANKL-RANK Axis: A Bone to Thymus Round Trip. *Front Immunol* (2019) 10. doi: 10.3389/fimmu.2019.00629
2. Zaiss MM, Jones RM, Schett G, Pacifici R. The Gut-Bone Axis: How Bacterial Metabolites Bridge the Distance. *J Clin Invest* (2019) 129:3018–28. doi: 10.1172/JCI128521
3. Behera J, Ison J, Tyagi SC, Tyagi N. The Role of Gut Microbiota in Bone Homeostasis. *Bone* (2020) 135. doi: 10.1016/j.bone.2020.115317
4. Lems WF, Raterman HG. Critical Issues and Current Challenges in Osteoporosis and Fracture Prevention. An Overview of Unmet Needs. *Ther Adv Musculoskelet Dis* (2017) 9(12):299–316. doi: 10.1177/1759720X17732562
5. Kan L. Animal Models of Bone Diseases-A. In: *Animal Models for the Study of Human Disease*. Elsevier Inc (2013). p. 353–90.

6. Maynard RD, Ackert-Bicknell CL. Mouse Models and Online Resources for Functional Analysis of Osteoporosis Genome-Wide Association Studies. *Front Endocrinol* (2019) 10:277. doi: 10.3389/fendo.2019.00277
7. Haffner-Luntzer M, Kovtun A, Rapp AE, Ignatius A. Mouse Models in Bone Fracture Healing Research. *Curr Mol Biol Rep* (2016) 2(2):101–11. doi: 10.1007/s40610-016-0037-3
8. Jilka RL. The Relevance of Mouse Models for Investigating Age-Related Bone Loss in Humans. *Biol Sci Cite J as J Gerontol A Biol Sci Med Sci* (2013) 68(10):1209–17. doi: 10.1093/gerona/glt046
9. Song AJ, Palmiter RD. Detecting and Avoiding Problems When Using the Cre–lox System. *Trends Genet* (2018) 34:333–40. doi: 10.1016/j.tig.2017.12.008
10. Hsu PD, Lander ES, Zhang F. Development and Applications of CRISPR-Cas9 for Genome Engineering. *Cell* (2014) 157:1262–78. doi: 10.1016/j.cell.2014.05.010
11. Bergen DJM, Kague E, Hammond CL. Zebrafish as an Emerging Model for Osteoporosis: A Primary Testing Platform for Screening New Osteo-Active Compounds. *Front Endocrinol* (2019) 10:6. doi: 10.3389/fendo.2019.00006
12. Kwon RY, Watson CJ, Karasik D. Using Zebrafish to Study Skeletal Genomics. *Bone* (2019) 126:37–50. doi: 10.1016/j.bone.2019.02.009
13. Hur M, Gistelinck CA, Huber P, Lee J, Thompson MH, Monstad-Rios AT, et al. MicroCT-Based Phenomics in the Zebrafish Skeleton Reveals Virtues of Deep Phenotyping in a Distributed Organ System. *Elife* (2017) 6:e26014. doi: 10.7554/eLife.26014
14. Pardo-Martin C, Allalou A, Medina J, Eimon PM, Wahlby C, Yanik MF. High-Throughput Hyperdimensional Vertebrate Phenotyping. *Nat Commun* (2013) 4(1):1–9. doi: 10.1038/ncomms2475
15. Monma Y, Shimada Y, Nakayama H, Zang L, Nishimura N, Tanaka T. Aging-Associated Microstructural Deterioration of Vertebra in Zebrafish. *Bone Rep* (2019) 11:100215. doi: 10.1016/j.bonr.2019.100215
16. Hayes AJ, Reynolds S, Nowell MA, Meakin LB, Habicher J, Ledin J, et al. Spinal Deformity in Aged Zebrafish Is Accompanied by Degenerative Changes to Their Vertebrae That Resemble Osteoarthritis. Heymann D, Editor. *PloS One* (2013) 8(9):e75787. doi: 10.1371/journal.pone.0075787
17. Gilad S, Meiri E, Yogev Y, Benjamin S, Lebanony D, Yerushalmi N, et al. Serum MicroRNAs Are Promising Novel Biomarkers. Williams S, Editor. *PloS One* (2008) 3(9):e3148. doi: 10.1371/journal.pone.0003148
18. Tomecka MJ, Ethiraj LP, Sánchez LM, Roehl HH, Carney TJ. Clinical Pathologies of Bone Fracture Modelled in Zebrafish. *Dis Model Mech* (2019) 12(9):dmm037630. doi: 10.1242/dmm.037630
19. Mahamid J, Sharir A, Addadi L, Weiner S. Amorphous Calcium Phosphate is a Major Component of the Forming Fin Bones of Zebrafish: Indications for an Amorphous Precursor Phase. *Proc Natl Acad Sci USA* (2008) 105 (35):12748–53. doi: 10.1073/pnas.0803354105
20. Giovannone D, Paul S, Schindler S, Arata C, Farmer DT, Patel P, et al. Programmed Conversion of Hypertrophic Chondrocytes Into Osteoblasts and Marrow Adipocytes Within Zebrafish Bones. *Elife* (2019) 8:e42736. doi: 10.7554/eLife.42736
21. Heubel BP, Bredesen CA, Schilling TF, Le Pabic P. Endochondral Growth Zone Pattern and Activity in the Zebrafish Pharyngeal Skeleton. *Dev Dyn* (2021) 250(1):74–87. doi: 10.1002/dvdy.241
22. Frost HM. Bone "Mass" and the "Mechanostat": A Proposal. *Anat Rec* (1987) 219(1):1–9. doi: 10.1002/ar.1092190104
23. Burkholder T, Foltz C, Karlsson E, Linton CG, Smith JM. Health Evaluation of Experimental Laboratory Mice. *Curr Protoc Mouse Biol* (2012) 2(2):145–65. doi: 10.1002/9780470942390.mo110217
24. Kishi S, Slack BE, Uchiyama J, Zhdanova IV. Zebrafish as a Genetic Model in Biological and Behavioral Gerontology: Where Development Meets Aging in Vertebrates - A Mini-Review. *Gerontology* (2009) 55:430–41. doi: 10.1159/000228892
25. Salles JP. Bone Metabolism During Pregnancy. *Ann Endocrinol (Paris)* (2016) 77(2):163–8. doi: 10.1016/j.ando.2016.04.004
26. Salari P, Abdollahi M. The Influence of Pregnancy and Lactation on Maternal Bone Health: A Systematic Review. *J Fam Reprod Heal* (2014) 8 (4):135–48.
27. Ireland A, Crozier SR, Heazell AEP, Ward KA, Godfrey KM, Inskip HM, et al. Breech Presentation is Associated With Lower Bone Mass and Area: Findings From the Southampton Women's Survey. *Osteoporos Int* (2018) 29 (10):2275–81. doi: 10.1007/s00198-018-4626-2
28. Engberg E, Koivusalo SB, Huvinen E, Viljakainen H. Bone Health in Women With a History of Gestational Diabetes or Obesity. *Acta Obstet Gynecol Scand* (2020) 99(4):477–87. doi: 10.1111/aogs.13778
29. Hannam K, Lawlor DA, Tobias JH. Maternal Preeclampsia Is Associated With Reduced Adolescent Offspring Hip BMD in a UK Population-Based Birth Cohort. *J Bone Miner Res* (2015) 30(9):1684–91. doi: 10.1002/jbmr.2506
30. Cummings SR, Nevitt MC, Browner WS, Stone K, Fox KM, Ensrud KE, et al. Risk Factors for Hip Fracture in White Women. *N Engl J Med* (1995) 332 (12):767–73. doi: 10.1056/NEJM199503233321202
31. Siris ES, Chen YT, Abbott TA, Barrett-Connor E, Miller PD, Wehren LE, et al. Bone Mineral Density Thresholds for Pharmacological Intervention to Prevent Fractures. *Arch Intern Med* (2004) 164(10):1108–12. doi: 10.1001/archinte.164.10.1108
32. Kanis JA, Johnell O, De Laet C, Johansson H, Oden A, Delmas P, et al. A Meta-Analysis of Previous Fracture and Subsequent Fracture Risk. *Bone* (2004) 35(2):375–82. doi: 10.1016/j.bone.2004.03.024
33. Matcuk GR, Mahanty SR, Skalski MR, Patel DB, White EA, Gottsegen CJ. Stress Fractures: Pathophysiology, Clinical Presentation, Imaging Features, and Treatment Options. *Emergency Radiol* (2016) 23:365–75. doi: 10.1007/s10140-016-1390-5
34. Saunier J, Chapurlat R. Stress Fracture in Athletes. *Joint Bone Spine* (2018) 85:307–10. doi: 10.1016/j.jbspin.2017.04.013
35. Jager PL, Jonkman S, Koolhaas W, Stiekema A, Wolffenbuttel BHR, Slart RHJA. Combined Vertebral Fracture Assessment and Bone Mineral Density Measurement: A New Standard in the Diagnosis of Osteoporosis in Academic Populations. *Osteoporos Int* (2011) 22(4):1059–68. doi: 10.1007/s00198-010-1293-3
36. Ganda K, Puech M, Chen JS, Speerin R, Bleasel J, Center JR, et al. Models of Care for the Secondary Prevention of Osteoporotic Fractures: A Systematic Review and Meta-Analysis. *Osteoporosis Int* (2013) 24:393–406. doi: 10.1007/s00198-012-2090-y
37. Nilsson KH, Henning P, Shahawy M, Nethander M, Andersen TL, Ejersted C, et al. RSPO3 Is Important for Trabecular Bone and Fracture Risk in Mice and Humans. *Nat Commun* (2021) 12(1):4923. doi: 10.1038/s41467-021-25124-2
38. Kague E, Roy P, Asselin G, Hu G, Simonet J, Stanley A, et al. Osterix/Sp7 Limits Cranial Bone Initiation Sites and is Required for Formation of Sutures. *Dev Biol* (2016) 413(2):160–72. doi: 10.1016/j.ydbio.2016.03.011
39. Gistelinck C, Kwon RY, Malfait F, Symoens S, Harris MP, Henke K, et al. Zebrafish Type I Collagen Mutants Faithfully Recapitulate Human Type I Collagenopathies. *Proc Natl Acad Sci USA* (2018) 115(34):E8037–46. doi: 10.1073/pnas.1722200115
40. Fiedler IAK, Schmidt FN, Wölfel EM, Plumeyer C, Milovanovic P, Gioia R, et al. Severely Impaired Bone Material Quality in Chihuahua Zebrafish Resembles Classical Dominant Human Osteogenesis Imperfecta. *J Bone Miner Res* (2018) 33(8):1489–99. doi: 10.1002/jbmr.3445
41. Bergquist R, Weber M, Schwenk M, Ulseth S, Helbostad JL, Vereijken B, et al. Performance-Based Clinical Tests of Balance and Muscle Strength Used in Young Seniors: A Systematic Literature Review. *BMC Geriatr* (2019) 19 (1):9. doi: 10.1186/s12877-018-1011-0
42. Clarke KA, Still J. Gait Analysis in the Mouse. *Physiol Behav* (1999) 66 (5):723–9. doi: 10.1016/S0031-9384(98)00343-6
43. Histing T, Kristen A, Roth C, Holstein JH, Garcia P, Matthys R, et al. *In Vivo* Gait Analysis in a Mouse Femur Fracture Model. *J Biomech* (2010) 43 (16):3240–3. doi: 10.1016/j.jbiomech.2010.07.019
44. Takeshita H, Yamamoto K, Nozato S, Inagaki T, Tsuchimochi H, Shirai M, et al. Modified Forelimb Grip Strength Test Detects Aging-Associated Physiological Decline in Skeletal Muscle Function in Male Mice. *Sci Rep* (2017) 7(1):1–9. doi: 10.1038/srep42323
45. Connolly AM, Keeling RM, Mehta S, Pestronk A, Sanes JR. Three Mouse Models of Muscular Dystrophy: The Natural History of Strength and Fatigue in Dystrophin-, Dystrophin/Utrophin-, and Laminin α2-Deficient Mice. *Neuromuscul Disord* (2001) 11(8):703–12. doi: 10.1016/S0960-8966(01)00232-2

46. Justice JN, Carter CS, Beck HJ, Gioscia-Ryan RA, McQueen M, Enoka RM, et al. Battery of Behavioral Tests in Mice That Models Age-Associated Changes in Human Motor Function. *Age (Omaha)* (2014) 36(2):583–95. doi: 10.1007/s11357-013-9589-9
47. Brooks SP, Dunnett SB. Tests to Assess Motor Phenotype in Mice: A User's Guide. *Nat Rev Neurosci* (2009) 10:519–29. doi: 10.1038/nrn2652
48. Matsumoto K, Ishihara K, Tanaka K, Inoue K, Fushiki T. An Adjustable-Current Swimming Pool for the Evaluation of Endurance Capacity of Mice. *J Appl Physiol* (1996) 81(4):1843–9. doi: 10.1152/jappl.1996.81.4.1843
49. Nelson CE, Hakim CH, Ousterout DG, Thakore PI, Moreb EA, Castellanos Rivera RM, et al. *In Vivo* Genome Editing Improves Muscle Function in a Mouse Model of Duchenne Muscular Dystrophy. *Science* (2016) 351 (6271):403–7. doi: 10.1126/science.aad5143
50. Suniaga S, Rolvien T, Vom Scheidt A, Fiedler IAK, Bale HA, Huysseune A, et al. Increased Mechanical Loading Through Controlled Swimming Exercise Induces Bone Formation and Mineralization in Adult Zebrafish. *Sci Rep* (2018) 8(1):3646. doi: 10.1038/s41598-018-21776-1
51. Leslie WD, Morin SN. New Developments in Fracture Risk Assessment for Current Osteoporosis Reports. *Curr Osteoporosis Rep* (2020) 18:115–29. doi: 10.1007/s11914-020-00590-7
52. Kanis JA, Harvey NC, Johansson H, Liu E, Vandenput L, Lorentzon M, et al. A Decade of FRAX: How has it Changed the Management of Osteoporosis? *Aging Clin Exp Res* (2020) 32:187–96. doi: 10.1007/s40520-019-01432-y
53. Beaudoin C, Moore L, Gagné M, Bessette L, Ste-Marie LG, Brown JP, et al. Performance of Predictive Tools to Identify Individuals at Risk of non-Traumatic Fracture: A Systematic Review, Meta-Analysis, and Meta-Regression. *Osteoporosis Int* (2019) 30:721–40. doi: 10.1007/s00198-019-04919-6
54. Searle SD, Mitnitski A, Gahbauer EA, Gill TM, Rockwood K. A Standard Procedure for Creating a Frailty Index. *BMC Geriatr* (2008) 8(1):24. doi: 10.1186/1471-2318-8-24
55. Rockwood K, Howlett SE. Age-Related Deficit Accumulation and the Diseases of Ageing. *Mech Ageing Dev* (2019) 180:107–16. doi: 10.1016/j.mad.2019.04.005
56. Kennedy CC, Ioannidis G, Rockwood K, Thabane L, Adachi JD, Kirkland S, et al. A Frailty Index Predicts 10-Year Fracture Risk in Adults Age 25 Years and Older: Results From the Canadian Multicentre Osteoporosis Study (CaMos). *Osteoporos Int* (2014) 25(12):2825–32. doi: 10.1007/s00198-014-2828-9
57. Bartosch P, McGuigan FE, Akesson KE. Progression of Frailty and Prevalence of Osteoporosis in a Community Cohort of Older Women—a 10-Year Longitudinal Study. *Osteoporos Int* (2018) 29(10):2191–9. doi: 10.1007/s00198-018-4593-7
58. Ward LM, Weber DR, Munns CF, Högler W, Zemel BS. A Contemporary View of the Definition and Diagnosis of Osteoporosis in Children and Adolescents. *J Clin Endocrinol Metab* (2020) 105:e2088–97. doi: 10.1210/clinem/dgz294
59. Messina C, Maffi G, Vitale JA, Ulivieri FM, Guglielmi G, Sconfenza LM. Diagnostic Imaging of Osteoporosis and Sarcopenia: A Narrative Review. *Quantitative Imaging Med Surgery* (2018) 8:86–99. doi: 10.21037/qims.2018.01.01
60. Genant HK, Wu CY, van Kuijk C, Nevitt MC. Vertebral Fracture Assessment Using a Semiquantitative Technique. *J Bone Miner Res* (1993) 8(9):1137–48. doi: 10.1002/jbmr.5650080915
61. Schnake KJ, Blattert TR, Hahn P, Franck A, Hartmann F, Ullrich B, et al. Classification of Osteoporotic Thoracolumbar Spine Fractures: Recommendations of the Spine Section of the German Society for Orthopaedics and Trauma (DGOU). *Glob Spine J* (2018) 8(2 Suppl):46S–9S. doi: 10.1177/2192568217717972
62. Szulc P. Vertebral Fracture: Diagnostic Difficulties of a Major Medical Problem. *J Bone Mineral Res* (2018) 33:553–9. doi: 10.1002/jbmr.3404
63. Fan YL, Peh WCG. Radiology of Osteoporosis: Old and New Findings. *Semin Musculoskelet Radiol* (2016) 20(3):235–45. doi: 10.1055/s-0036-1592371
64. Monsour PA, Dudhia R. Implant Radiography and Radiology. *Aust Dental J* (2008) 53(Suppl 1):S11–25. doi: 10.1111/j.1834-7819.2008.00037.x
65. Butterfield NC, Logan JG, Waung J, Williams GR, Bassett JHD. Quantitative X-Ray Imaging of Mouse Bone by Faxitron. *Methods Mol Biol* (2019) 1914:559–69. doi: 10.1007/978-1-4939-8997-3_30
66. Bassett JHD, Gogakos A, White JK, Evans H, Jacques RM, van der Spek AH, et al. Rapid-Throughput Skeletal Phenotyping of 100 Knockout Mice Identifies 9 New Genes That Determine Bone Strength. *PloS Genet* (2012) 8(8):e1002858. doi: 10.1371/journal.pgen.1002858
67. Fisher S, Jagadeeswaran P, Halpern ME. Radiographic Analysis of Zebrafish Skeletal Defects. *Dev Biol* (2003) 264(1):64–76. doi: 10.1016/S0012-1606(03)00399-3
68. Cummings SR, Browner W, Cummings SR, Black DM, Nevitt MC, Browner W, et al. Bone Density at Various Sites for Prediction of Hip Fractures. *Lancet* (1993) 341(8837):72–5. doi: 10.1016/0140-6736(93)92555-8
69. Xi Z, Mummaneni PV, Wang M, Ruan H, Burch S, Deviren V, et al. The Association Between Lower Hounsfield Units on Computed Tomography and Cage Subsidence After Lateral Lumbar Interbody Fusion. *Neurosurg Focus* (2020) 49(2):1–8. doi: 10.3171/2020.5.FOCUS20169
70. Dimai HP. Use of Dual-Energy X-Ray Absorptiometry (DXA) for Diagnosis and Fracture Risk Assessment; WHO-Criteria, T- and Z-Score, and Reference Databases. *Bone* (2017) 104:39–43. doi: 10.1016/j.bone.2016.12.016
71. Johannesdottir F, Thrall E, Muller J, Keaveny TM, Kopperdahl DL, Bouxsein ML. Comparison of non-Invasive Assessments of Strength of the Proximal Femur. *Bone* (2017) 105:93–102. doi: 10.1016/j.bone.2017.07.023
72. Bishop N, Arundel P, Clark E, Dimitri P, Farr J, Jones G, et al. Fracture Prediction and the Definition of Osteoporosis in Children and Adolescents: The ISCD 2013 Pediatric Official Positions. *J Clin Densitom* (2014) 17 (2):275–80. doi: 10.1016/j.jocd.2014.01.004
73. Crabtree NJ, Shaw NJ, Bishop NJ, Adams JE, Mughal MZ, Arundel P, et al. Amalgamated Reference Data for Size-Adjusted Bone Densitometry Measurements in 3598 Children and Young Adults-The ALPHABET Study. *J Bone Miner Res* (2017) 32(1):172–80. doi: 10.1002/jbmr.2935
74. Weber DR, Boyce A, Gordon C, Högler W, Kecskemethy HH, Misra M, et al. The Utility of DXA Assessment at the Forearm, Proximal Femur, and Lateral Distal Femur, and Vertebral Fracture Assessment in the Pediatric Population: 2019 ISCD Official Position. *J Clin Densitometry* (2019) 22:567–89. doi: 10.1016/j.jocd.2019.07.002
75. Bonnick SL. HSA: Beyond BMD With DXA. *Bone* (2007) 41(1 SUPPL):S9–12. doi: 10.1016/j.bone.2007.03.007
76. Cha YH, Yoo J. Comparison of Hip Structure Analysis and Grip Strength Between Femoral Neck and Basicervical Fractures. *BMC Musculoskelet Disord* (2021) 22(1):461. doi: 10.1186/s12891-021-04363-w
77. Kaptoge S, Beck TJ, Reeve J, Stone KL, Hillier TA, Cauley JA, et al. Prediction of Incident Hip Fracture Risk by Femur Geometry Variables Measured by Hip Structural Analysis in the Study of Osteoporotic Fractures. *J Bone Miner Res* (2008) 23(12):1892–904. doi: 10.1359/jbmr.080802
78. Leslie WD, Luo Y, Yang S, Goertzen AL, Ahmed S, Delubac I, et al. Fracture Risk Indices From DXA-Based Finite Element Analysis Predict Incident Fractures Independently From FRAX: The Manitoba BMD Registry. *J Clin Densitom* (2019) 22(3):338–45. doi: 10.1016/j.jocd.2019.02.001
79. Ponti F, Santoro A, Mercatelli D, Gasperini C, Conte M, Martucci M, et al. Aging and Imaging Assessment of Body Composition: From Fat to Facts. *Front Endocrinol* (2020) 10:861. doi: 10.3389/fendo.2019.00861
80. Busse B, Hahn M, Soltau M, Zustin J, Püschel K, Duda GN, et al. Increased Calcium Content and Inhomogeneity of Mineralization Render Bone Toughness in Osteoporosis: Mineralization, Morphology and Biomechanics of Human Single Trabeculae. *Bone* (2009) 45(6):1034–43. doi: 10.1016/j.bone.2009.08.002
81. Shi J, Lee S, Uyeda M, Tanjaya J, Kim JK, Pan HC, et al. Guidelines for Dual Energy X-Ray Absorptiometry Analysis of Trabecular Bone-Rich Regions in Mice: Improved Precision, Accuracy, and Sensitivity for Assessing Longitudinal Bone Changes. *Tissue Eng Part C Methods* (2016) 22(5):451–63. doi: 10.1089/ten.tec.2015.0383
82. Nagy TR, Clair AL. Precision and Accuracy of Dual-Energy X-Ray Absorptiometry for Determining *In Vivo* Body Composition of Mice. *Obes Res* (2000) 8(5):392–8. doi: 10.1038/oby.2000.47
83. Wright LE, Christian PJ, Rivera Z, Van Alstine WG, L Funk J, L Bouxsein M, et al. Comparison of Skeletal Effects of Ovariectomy Versus Chemically Induced Ovarian Failure in Mice. *J Bone Miner Res* (2008) 23(8):1296–303. doi: 10.1359/jbmr.080309

84. Chou SH, LeBoff MS. Vertebral Imaging in the Diagnosis of Osteoporosis: A Clinician's Perspective. *Curr Osteoporosis Rep* (2017) 15:509–20. doi: 10.1007/s11914-017-0404-x
85. Adult Positions - ISCD. Available at: https://iscd.org/learn/official-positions/adult-positions/.
86. Lewiecki EM, Gordon CM, Baim S, Binkley N, Bilezikian JP, Kendler DL, et al. Special Report on the 2007 Adult and Pediatric Position Development Conferences of the International Society for Clinical Densitometry. *Osteoporos Int* (2008) 19(10):1369–78. doi: 10.1007/s00198-008-0689-9
87. Cosman F, de Beur SJ, LeBoff MS, Lewiecki EM, Tanner B, Randall S, et al. Clinician's Guide to Prevention and Treatment of Osteoporosis. *Osteoporos Int* (2014) 25(10):2359–81. doi: 10.1007/s00198-014-2794-2
88. Pediatric Positions - ISCD. Available at: https://iscd.org/learn/official-positions/pediatric-positions/.
89. Newham E, Kague E, Aggleton JA, Fernee C, Brown KR, Hammond CL. Finite Element and Deformation Analyses Predict Pattern of Bone Failure in Loaded Zebrafish Spines. *J R Soc Interface* (2019) 16(160):20190430. doi: 10.1098/rsif.2019.0430
90. Sousa S, Valerio F, Jacinto A. A New Zebrafish Bone Crush Injury Model. *Biol Open* (2012) 1(9):915–21. doi: 10.1242/bio.2012877
91. Lerchbaum E, Trummer C, Theiler-Schwetz V, Kollmann M, Wölfler M, Pilz S, et al. Effects of Vitamin D Supplementation on Bone Turnover and Bone Mineral Density in Healthy Men: A Post-Hoc Analysis of a Randomized Controlled Trial. *Nutrients* (2019) 11(4):731. doi: 10.3390/nu11040731
92. Mirzaali MJ, Libonati F, Ferrario D, Rinaudo L, Messina C, Ulivieri FM, et al. Determinants of Bone Damage: An Ex-Vivo Study on Porcine Vertebrae. Vashishth D, Editor. *PloS One* (2018) 13(8):e0202210. doi: 10.1371/journal.pone.0202210
93. Leslie WD, Aubry-Rozier B, Lamy O, Hans D. TBS (Trabecular Bone Score) and Diabetes-Related Fracture Risk. *J Clin Endocrinol Metab* (2013) 98 (2):602–9. doi: 10.1210/jc.2012-3118
94. Richards C, Hans D, Leslie WD. Trabecular Bone Score (TBS) Predicts Fracture in Ankylosing Spondylitis: The Manitoba BMD Registry. *J Clin Densitom* (2020) 23(4):543–8. doi: 10.1016/j.jocd.2020.01.003
95. Shevroja E, Aubry-Rozier B, Hans G, Gonzalez-Rodriguez E, Stoll D, Lamy O, et al. Clinical Performance of the Updated Trabecular Bone Score (TBS) Algorithm, Which Accounts for the Soft Tissue Thickness: The OsteoLaus Study. *J Bone Miner Res* (2019) 34(12):2229–37. doi: 10.1002/jbmr.3851
96. Guagnelli MA, Winzenrieth R, Lopez-Gonzalez D, McClung MR, Del Rio L, Clark P. Bone Age as a Correction Factor for the Analysis of Trabecular Bone Score (TBS) in Children. *Arch Osteoporos* (2019) 14(1):1–7. doi: 10.1007/s11657-019-0573-6
97. Jazinizadeh F, Quenneville CE. Enhancing Hip Fracture Risk Prediction by Statistical Modeling and Texture Analysis on DXA Images. *Med Eng Phys* (2020) 78:14–20. doi: 10.1016/j.medengphy.2020.01.015
98. vom Scheidt A, Grisolia Seifert EF, Pokrant C, Püschel K, Amling M, Busse B, et al. Subregional Areal Bone Mineral Density (aBMD) is a Better Predictor of Heterogeneity in Trabecular Microstructure of Vertebrae in Young and Aged Women Than Subregional Trabecular Bone Score (TBS). *Bone* (2019) 122:156–65. doi: 10.1016/j.bone.2019.02.014
99. Glüer CC. Quantitative Ultrasound Techniques for the Assessment of Osteoporosis: Expert Agreement on Current Status. *J Bone Miner Res* (1997) 12(8):1280–8. doi: 10.1359/jbmr.1997.12.8.1280
100. Hans D, Dargent-Molina P, Schott AM, Sebert JL, Cormier C, Kotzki PO, et al. Ulrasonographic Heel Measurements to Predict Hip Fracture in Elderly Women: The EPIDOS Prospective Study. *Lancet* (1996) 348(9026):511–4. doi: 10.1016/S0140-6736(95)11456-4
101. Knapp KM. Quantitative Ultrasound and Bone Health. *Salud Publica Mex* (2009) 51(SUPPL.1):S18–24. doi: 10.1590/S0036-36342009000700005
102. Kemp JP, Morris JA, Medina-Gomez C, Forgetta V, Warrington NM, Youlten SE, et al. Identification of 153 New Loci Associated With Heel Bone Mineral Density and Functional Involvement of GPC6 in Osteoporosis. *Nat Genet* (2017) 49(10):1468–75. doi: 10.1038/ng.3949
103. Ackermann O, Simanowski J, Eckert K. Fracture Ultrasound of the Extremities. *Ultraschall der Medizin* (2020) 41(1):12–28. doi: 10.1055/a-1023-1782
104. Kanis JA, Melton LJ, Christiansen C, Johnston CC, Khaltaev N. The Diagnosis of Osteoporosis. *J Bone Miner Res* (1994) 9(8):1137–41. doi: 10.1002/jbmr.5650090802
105. Lentle BC, Hammond I, Firth GB, Sutton RAL. Imaging of Osteoporotic Fractures on XR, CT, and MR. *Curr Radiol Rep* (2014) 2:1–9. doi: 10.1007/s40134-013-0032-x
106. O'Ryan FS, Khoury S, Liao W, Han MM, Hui RL, Baer D, et al. Intravenous Bisphosphonate-Related Osteonecrosis of the Jaw: Bone Scintigraphy as an Early Indicator. *J Oral Maxillofac Surg* (2009) 67(7):1363–72. doi: 10.1016/j.joms.2009.03.005
107. Grüneboom A, Kling L, Christiansen S, Mill L, Maier A, Engelke K, et al. Next-Generation Imaging of the Skeletal System and its Blood Supply. *Nat Rev Rheumatol* (2019) 15:533–49. doi: 10.1038/s41584-019-0274-y
108. Huang K, Feng Y, Liu D, Liang W, Li L. Quantification Evaluation of 99mtc-MDP Concentration in the Lumbar Spine With SPECT/CT: Compare With Bone Mineral Density. *Ann Nucl Med* (2020) 34(2):136–43. doi: 10.1007/s12149-019-01425-x
109. Li YB, Zheng X, Wang R, Wu H, Han S, Deng ZY, et al. SPECT-CT Versus MRI in Localizing Active Lesions in Patients With Osteoporotic Vertebral Compression Fractures. *Nucl Med Commun* (2018) 39(7):610–7. doi: 10.1097/MNM.0000000000000857
110. Butterfield NC, Logan JG, Waung J, Williams GR, Bassett JHD. Quantitative X-Ray Imaging of Mouse Bone by Faxitron. In: *Methods in Molecular Biology*. New York, NY: Humana Press (2019). p. 559–69.
111. Khalil MM, Tremoleda JL, Bayomy TB, Gsell W. Molecular SPECT Imaging: An Overview. *Int J Mol Imaging* (2011) 2011:1–15. doi: 10.1155/2011/796025
112. Tremoleda JL, Khalil M, Gompels LL, Wylezinska-Arridge M, Vincent T, Gsell W. Imaging Technologies for Preclinical Models of Bone and Joint Disorders. *EJNMMI Res* (2011) 1(1):1–14. doi: 10.1186/2191-219X-1-11
113. Lienemann PS, Metzger S, Kiveliö AS, Blanc A, Papageorgiou P, Astolfo A, et al. Longitudinal *In Vivo* Evaluation of Bone Regeneration by Combined Measurement of Multi-Pinhole SPECT and Micro-CT for Tissue Engineering. *Sci Rep* (2015) 5:10238. doi: 10.1038/srep10238
114. Adams JE. Quantitative Computed Tomography. *Eur J Radiol* (2009) 71 (3):415–24. doi: 10.1016/j.ejrad.2009.04.074
115. Lang TF. Quantitative Computed Tomography. *Radiologic Clinics North America* (2010) 48:589–600. doi: 10.1016/j.rcl.2010.03.001
116. Engelke K, van Rietbergen B, Zysset P. FEA to Measure Bone Strength: A Review. *Clin Rev Bone Mineral Metab* (2016) 14:26–37. doi: 10.1007/s12018-015-9201-1
117. Johannesdottir F, Allaire B, Bouxsein ML. Fracture Prediction by Computed Tomography and Finite Element Analysis: Current and Future Perspectives. *Curr Osteoporosis Rep* (2018) 16(4):411–22. doi: 10.1007/s11914-018-0450-z
118. Lengsfeld M, Schmitt J, Alter P, Kaminsky J, Leppek R. Comparison of Geometry-Based and CT Voxel-Based Finite Element Modelling and Experimental Validation. *Med Eng Phys* (1998) 20(7):515–22. doi: 10.1016/S1350-4533(98)00054-X
119. Zysset PK, Dall'Ara E, Varga P, Pahr DH. Finite Element Analysis for Prediction of Bone Strength. *Bonekey Rep* (2013) 2:386. doi: 10.1038/bonekey.2013.120
120. Viceconti M. Predicting Bone Strength From CT Data: Clinical Applications. *Morphologie* (2019) 103(343):180–6. doi: 10.1016/j.morpho.2019.09.007
121. Keaveny TM. Biomechanical Computed Tomography-Noninvasive Bone Strength Analysis Using Clinical Computed Tomography Scans. *Ann N Y Acad Sci* (2010) 1192(1):57–65. doi: 10.1111/j.1749-6632.2009.05348.x
122. Hoffmann U, Massaro JM, D'Agostino RB Sr, Kathiresan S, Fox CS, O'Donnell CJ. Cardiovascular Event Prediction and Risk Reclassification by Coronary, Aortic, and Valvular Calcification in the Framingham Heart Study. *J Am Heart Assoc* (2016) 5(2):e003144. doi: 10.1161/JAHA.115.003144
123. Ryan TM, Shaw CN. Trabecular Bone Microstructure Scales Allometrically in the Primate Humerus and Femur. *Proc R Soc B Biol Sci* (2013) 280 (1758):20130172. doi: 10.1098/rspb.2013.0172
124. Stagi S, Cavalli L, Cavalli T, De Martino M, Brandi ML. Peripheral Quantitative Computed Tomography (pQCT) for the Assessment of Bone Strength in Most of Bone Affecting Conditions in Developmental Age: A Review. *Ital J Pediatrics* (2016) 42:1–20. doi: 10.1186/s13052-016-0297-9
125. Paternoster L, Lorentzon M, Vandenput L, Karlsson MK, Ljunggren Ö, Kindmark A, et al. Genome-Wide Association Meta-Analysis of Cortical Bone Mineral Density Unravels Allelic Heterogeneity at the RANKL Locus

and Potential Pleiotropic Effects on Bone. Gibson G, Editor. *PloS Genet* (2010) 6(11):e1001217. doi: 10.1371/journal.pgen.1001217
126. Paternoster L, Lorentzon M, Lehtimäki T, Eriksson J, Kähönen M, Raitakari O, et al. Genetic Determinants of Trabecular and Cortical Volumetric Bone Mineral Densities and Bone Microstructure. Richards JB, Editor. *PloS Genet* (2013) 9(2):e1003247. doi: 10.1371/journal.pgen.1003247
127. Zheng H-F, Tobias JH, Duncan E, Evans DM, Eriksson J, Paternoster L, et al. WNT16 Influences Bone Mineral Density, Cortical Bone Thickness, Bone Strength, and Osteoporotic Fracture Risk. Gibson G, Editor. *PloS Genet* (2012) 8(7):e1002745. doi: 10.1371/journal.pgen.1002745
128. Compston J. Type 2 Diabetes Mellitus and Bone. *J Intern Med* (2018) 283 (2):140–53. doi: 10.1111/joim.12725
129. Gasser JA, Willnecker J. Bone Measurements by Peripheral Quantitative Computed Tomography in Rodents. *Methods Mol Biol* (2019) 1914:533–58. doi: 10.1007/978-1-4939-8997-3_29
130. Schmidt C, Priemel M, Kohler T, Weusten A, Müller R, Amling M, et al. Precision and Accuracy of Peripheral Quantitative Computed Tomography (pQCT) in the Mouse Skeleton Compared With Histology and Microcomputed Tomography (μct). *J Bone Miner Res* (2003) 18(8):1486–96. doi: 10.1359/jbmr.2003.18.8.1486
131. Brodt MD, Pelz GB, Taniguchi J, Silva MJ. Accuracy of Peripheral Quantitative Computed Tomography (pQCT) for Assessing Area and Density of Mouse Cortical Bone. *Calcif Tissue Int* (2003) 73(4):411–8. doi: 10.1007/s00223-002-0006-0
132. Manske SL, Zhu Y, Sandino C, Boyd SK. Human Trabecular Bone Microarchitecture can be Assessed Independently of Density With Second Generation HR-pQCT. *Bone* (2015) 79:213–21. doi: 10.1016/j.bone.2015.06.006
133. Whittier DE, Boyd SK, Burghardt AJ, Paccou J, Ghasem-Zadeh A, Chapurlat R, et al. Guidelines for the Assessment of Bone Density and Microarchitecture *In Vivo* Using High-Resolution Peripheral Quantitative Computed Tomography. *Osteoporos Int* (2020) 31(9):1607–27. doi: 10.1007/s00198-020-05438-5
134. Boutroy S, Bouxsein ML, Munoz F, Delmas PD. *In Vivo* Assessment of Trabecular Bone Microarchitecture by High-Resolution Peripheral Quantitative Computed Tomography. *J Clin Endocrinol Metab* (2005) 90 (12):6508–15. doi: 10.1210/jc.2005-1258
135. Laib A, Hauselmann HJ, Ruegsegger P. *In Vivo* High Resolution 3D-QCT of the Human Forearm. *Technol Heal Care* (1998) 6(5–6):329–37. doi: 10.3233/THC-1998-65-606
136. Shanbhogue VV, Brixen K, Hansen S. Age- and Sex-Related Changes in Bone Microarchitecture and Estimated Strength: A Three-Year Prospective Study Using HRpQCT. *J Bone Miner Res* (2016) 31(8):1541–9. doi: 10.1002/jbmr.2817
137. Hamilton EJ, Ghasem-Zadeh A, Gianatti E, Lim-Joon D, Bolton D, Zebaze R, et al. Structural Decay of Bone Microarchitecture in Men With Prostate Cancer Treated With Androgen Deprivation Therapy. *J Clin Endocrinol Metab* (2010) 95(12):E456–63. doi: 10.1210/jc.2010-0902
138. van Rietbergen B, Ito K. A Survey of Micro-Finite Element Analysis for Clinical Assessment of Bone Strength: The First Decade. *J Biomech* (2015) 48 (5):832–41. doi: 10.1016/j.jbiomech.2014.12.024
139. Whittier DE, Manske SL, Kiel DP, Bouxsein M, Boyd SK. Harmonizing Finite Element Modelling for non-Invasive Strength Estimation by High-Resolution Peripheral Quantitative Computed Tomography. *J Biomech* (2018) 80:63–71. doi: 10.1016/j.jbiomech.2018.08.030
140. Kroker A, Zhu Y, Manske SL, Barber R, Mohtadi N, Boyd SK. Quantitative *In Vivo* Assessment of Bone Microarchitecture in the Human Knee Using HR-pQCT. *Bone* (2017) 97:43–8. doi: 10.1016/j.bone.2016.12.015
141. Sada K, Chiba K, Kajiyama S, Okazaki N, Yonekura A, Tomita M, et al. Bone Mineral Density and Microstructure of the Elbow in Baseball Pitchers: An Analysis by Second-Generation HR-pQCT. *J Clin Densitom* (2020) 23 (2):322–8. doi: 10.1016/j.jocd.2019.03.001
142. Zebaze R, Seeman E. Cortical Bone: A Challenging Geography. *J Bone Miner Res* (2015) 30(1):24–9. doi: 10.1002/jbmr.2419
143. Nishiyama KK, Macdonald HM, Buie HR, Hanley DA, Boyd SK. Postmenopausal Women With Osteopenia Have Higher Cortical Porosity and Thinner Cortices at the Distal Radius and Tibia Than Women With Normal aBMD: An *In Vivo* HR-pQCT Study. *J Bone Miner Res* (2009) 25 (4):091019190442039–30. doi: 10.1359/jbmr.091020
144. Burghardt AJ, Buie HR, Laib A, Majumdar S, Boyd SK. Reproducibility of Direct Quantitative Measures of Cortical Bone Microarchitecture of the Distal Radius and Tibia by HR-pQCT. *Bone* (2010) 47(3):519–28. doi: 10.1016/j.bone.2010.05.034
145. Zebaze R, Ghasem-Zadeh A, Mbala A, Seeman E. A New Method of Segmentation of Compact-Appearing, Transitional and Trabecular Compartments and Quantification of Cortical Porosity From High Resolution Peripheral Quantitative Computed Tomographic Images. *Bone* (2013) 54(1):8–20. doi: 10.1016/j.bone.2013.01.007
146. Burghardt AJ, Pialat JB, Kazakia GJ, Boutroy S, Engelke K, Patsch JM, et al. Multicenter Precision of Cortical and Trabecular Bone Quality Measures Assessed by High-Resolution Peripheral Quantitative Computed Tomography. *J Bone Miner Res* (2013) 28(3):524–36. doi: 10.1002/jbmr.1795
147. Piot A, Chapurlat RD, Claustrat B, Szulc P. Relationship Between Sex Steroids and Deterioration of Bone Microarchitecture in Older Men: The Prospective STRAMBO Study. *J Bone Miner Res* (2019) 34(9):1562–73. doi: 10.1002/jbmr.3746
148. Samelson EJ, Broe KE, Xu H, Yang L, Boyd S, Biver E, et al. Cortical and Trabecular Bone Microarchitecture as an Independent Predictor of Incident Fracture Risk in Older Women and Men in the Bone Microarchitecture International Consortium (BoMIC): A Prospective Study. *Lancet Diabetes Endocrinol* (2019) 7(1):34–43. doi: 10.1016/S2213-8587(18)30308-5
149. Tsai JN, Uihlein AV, Burnett-Bowie SM, Neer RM, Derrico NP, Lee H, et al. Effects of Two Years of Teriparatide, Denosumab, or Both on Bone Microarchitecture and Strength (DATA-HRpQCT Study). *J Clin Endocrinol Metab* (2016) 101(5):2023–30. doi: 10.1210/jc.2016-1160
150. Feldkamp LA, Goldstein SA, Parfitt MA, Jesion G, Kleerekoper M. The Direct Examination of Three-Dimensional Bone Architecture *In Vitro* by Computed Tomography. *J Bone Miner Res* (1989) 4(1):3–11. doi: 10.1002/jbmr.5650040103
151. Campbell GM, Sophocleous A. Quantitative Analysis of Bone and Soft Tissue by Micro-Computed Tomography: Applications to Ex Vivo and In Vivo Studies. *Bonekey Rep* (2014) 3:564. doi: 10.1038/bonekey.2014.59
152. Ozan F, Pekedis M, Koyuncu Ş, Altay T, Yıldız H, Kayalı C. Micro-Computed Tomography and Mechanical Evaluation of Trabecular Bone Structure in Osteopenic and Osteoporotic Fractures. *J Orthop Surg* (2017) 25 (1):2309499017692718. doi: 10.1177/2309499017692718
153. Perilli E, Parkinson IH, Reynolds KJ. Micro-CT Examination of Human Bone: From Biopsies Towards the Entire Organ. *Ann Ist Super Sanita* (2012) 48(1):75–82. doi: 10.4415/ANN_12_01_13
154. Jiang Y, Zhao J, Liao EY, Dai RC, Wu XP, Genant HK. Application of Micro-Ct Assessment of 3-D Bone Microstructure in Preclinical and Clinical Studies. *J Bone Mineral Metab* (2005) 23:122–31. doi: 10.1007/BF03026336
155. Burghardt AJ, Link TM, Majumdar S. High-Resolution Computed Tomography for Clinical Imaging of Bone Microarchitecture. *Clin Orthopaedics Related Res* (2011) 469(8):2179–93. doi: 10.1007/s11999-010-1766-x
156. De Bournonville S, Vangrunderbeeck S, Kerckhofs G. Contrast-Enhanced microCT for Virtual 3D Anatomical Pathology of Biological Tissues: A Literature Review. *Contrast Media Mol Imaging* (2019) 2019:8617406. doi: 10.1155/2019/8617406
157. Tratwal J, Labella R, Bravenboer N, Kerckhofs G, Douni E, Scheller EL, et al. Reporting Guidelines, Review of Methodological Standards, and Challenges Toward Harmonization in Bone Marrow Adiposity Research. Report of the Methodologies Working Group of the International Bone Marrow Adiposity Society. *Front Endocrinol* (2020) 11:65. doi: 10.3389/fendo.2020.00065
158. Dall'Ara E, Boudiffa M, Taylor C, Schug D, Fiegle E, Kennerley AJ, et al. Longitudinal Imaging of the Ageing Mouse. *Mech Ageing Dev* (2016) 160:93–116. doi: 10.1016/j.mad.2016.08.001
159. Bouxsein ML, Boyd SK, Christiansen BA, Guldberg RE, Jepsen KJ, Müller R. Guidelines for Assessment of Bone Microstructure in Rodents Using Micro-Computed Tomography. *J Bone Mineral Res* (2010) 25:1468–86. doi: 10.1002/jbmr.141
160. Leitch VD, Brassill MJ, Rahman S, Butterfield NC, Ma P, Logan JG, et al. PYY is a Negative Regulator of Bone Mass and Strength. *Bone* (2019) 127:427–35. doi: 10.1016/j.bone.2019.07.011

161. Oliviero S, Giorgi M, Laud PJ, Dall'Ara E. Effect of Repeated *In Vivo* microCT Imaging on the Properties of the Mouse Tibia. *PloS One* (2019) 14(11):e0225127. doi: 10.1371/journal.pone.0225127
162. Nadel HR. SPECT/CT in Pediatric Patient Management. *Eur J Nucl Med Mol Imaging* (2014) 41(Suppl 1):S104–14. doi: 10.1007/s00259-014-2697-7
163. Almeida M, Laurent MR, Dubois V, Claessens F, O'Brien CA, Bouillon R, et al. Estrogens and Androgens in Skeletal Physiology and Pathophysiology. *Physiol Rev* (2017) 97(1):135–87. doi: 10.1152/physrev.00033.2015
164. Charles JF, Sury M, Tsang K, Urso K, Henke K, Huang Y, et al. Utility of Quantitative Micro-Computed Tomographic Analysis in Zebrafish to Define Gene Function During Skeletogenesis. *Bone* (2017) 101:162–71. doi: 10.1016/j.bone.2017.05.001
165. Khajuria DK, Kumar VB, Gigi D, Gedanken A, Karasik D. Accelerated Bone Regeneration by Nitrogen-Doped Carbon Dots Functionalized With Hydroxyapatite Nanoparticles. *ACS Appl Mater Interfaces* (2018) 10 (23):19373–85. doi: 10.1021/acsami.8b02792
166. Main RP, Lynch ME, van der Meulen MCH. Load-Induced Changes in Bone Stiffness and Cancellous and Cortical Bone Mass Following Tibial Compression Diminish With Age in Female Mice. *J Exp Biol* (2014) 217 (10):1775–83. doi: 10.1242/jeb.085522
167. Wang J, Kazakia GJ, Zhou B, Shi XT, Guo XE. Distinct Tissue Mineral Density in Plate- and Rod-Like Trabeculae of Human Trabecular Bone. *J Bone Miner Res* (2015) 30(9):1641–50. doi: 10.1002/jbmr.2498
168. Doherty AH, Ghalambor CK, Donahue SW. Evolutionary Physiology of Bone: Bone Metabolism in Changing Environments. *Physiology* (2015) 30 (1):17–29. doi: 10.1152/physiol.00022.2014
169. Gistelinck C, Witten PE, Huysseune A, Symoens S, Malfait F, Larionova D, et al. Loss of Type I Collagen Telopeptide Lysyl Hydroxylation Causes Musculoskeletal Abnormalities in a Zebrafish Model of Bruck Syndrome. *J Bone Miner Res* (2016) 31(11):1930–42. doi: 10.1002/jbmr.2977
170. Kague E, Witten PE, Soenens M, Campos CL, Lubiana T, Fisher S, et al. Zebrafish Sp7 Mutants Show Tooth Cycling Independent of Attachment, Eruption and Poor Differentiation of Teeth. *Dev Biol* (2018) 435(2):176–84. doi: 10.1016/j.ydbio.2018.01.021
171. Lawrence EA, Kague E, Aggleton JA, Harniman RL, Roddy KA, Hammond CL. The Mechanical Impact of *Col11a2* Loss on Joints; *Col11a2* Mutant Zebrafish Show Changes to Joint Development and Function, Which Leads to Early-Onset Osteoarthritis. *Philos Trans R Soc B Biol Sci* (2018) 373 (1759):20170335. doi: 10.1098/rstb.2017.0335
172. Adams JE. Advances in Bone Imaging for Osteoporosis. *Nat Rev Endocrinol* (2013) 9(1):28–42. doi: 10.1038/nrendo.2012.217
173. Shayganfar A, Khodayi M, Ebrahimian S, Tabrizi Z. Quantitative Diagnosis of Osteoporosis Using Lumbar Spine Signal Intensity in Magnetic Resonance Imaging. *Br J Radiol* (2019) 92(1097):20180774. doi: 10.1259/bjr.20180774
174. Abbasi-Rad S, Saligheh Rad H. Quantification of Human Cortical Bone Bound and Free Water in Vivo With Ultrashort Echo Time MR Imaging: A Model-Based Approach. *Radiology* (2017) 283(3):862–72. doi: 10.1148/radiol.2016160780
175. Dixon WT. Simple Proton Spectroscopic Imaging. *Radiology* (1984) 153 (1):189–94. doi: 10.1148/radiology.153.1.6089263
176. Taha MA, Manske SL, Kristensen E, Taiani JT, Krawetz R, Wu Y, et al. Assessment of the Efficacy of MRI for Detection of Changes in Bone Morphology in a Mouse Model of Bone Injury. *J Magn Reson Imaging* (2013) 38(1):231–7. doi: 10.1002/jmri.23876
177. Haffner-Luntzer M, Müller-Graf F, Matthys R, Hägele Y, Fischer V, Jonas R, et al. Evaluation of High-Resolution *In Vivo* MRI for Longitudinal Analysis of Endochondral Fracture Healing in Mice. Garcia Aznar JM, Editor. *PloS One* (2017) 12(3):e0174283. doi: 10.1371/journal.pone.0174283
178. Turnbull DH, Mori S. MRI in Mouse Developmental Biology. *NMR Biomed* (2007) 20(3):265–74. doi: 10.1002/nbm.1146
179. Koth J, Maguire ML, McClymont D, Diffley L, Thornton VL, Beech J, et al. High-Resolution Magnetic Resonance Imaging of the Regenerating Adult Zebrafish Heart. *Sci Rep* (2017) 7(1):2917. doi: 10.1038/s41598-017-03050-y
180. Merrifield GD, Mullin J, Gallagher L, Tucker C, Jansen MA, Denvir M, et al. Rapid and Recoverable *In Vivo* Magnetic Resonance Imaging of the Adult Zebrafish at 7T. *Magn Reson Imaging* (2017) 37:9–15. doi: 10.1016/j.mri.2016.10.013
181. Recker RR, Moreira CA. *Bone Histomorphometry in Clinical Practice*. (2018). pp. 310–318. doi: 10.1002/9781119266594.ch39
182. Chappard D, Baslé MF, Legrand E, Audran M. New Laboratory Tools in the Assessment of Bone Quality. *Osteoporosis Int* (2011) 22:2225–40. doi: 10.1007/s00198-011-1573-6
183. Compston J. Bone Histomorphometry. In: *Methods in Bone Biology*. Boston, MA: Springer (2007). p. 177–97.
184. Slyfield CR, Tkachenko EV, Wilson DL, Hernandez CJ. Three-Dimensional Dynamic Bone Histomorphometry. *J Bone Miner Res* (2012) 27(2):486–95. doi: 10.1002/jbmr.553
185. Malhan D, Muelke M, Rosch S, Schaefer AB, Merboth F, Weisweiler D, et al. An Optimized Approach to Perform Bone Histomorphometry. *Front Endocrinol (Lausanne)* (2018) 9:666. doi: 10.3389/fendo.2018.00666
186. Dempster DW, Compston JE, Drezner MK, Glorieux FH, Kanis JA, Malluche H, et al. Standardized Nomenclature, Symbols, and Units for Bone Histomorphometry: A 2012 Update of the Report of the ASBMR Histomorphometry Nomenclature Committee. *J Bone Mineral Res* (2013) 28:2–17. doi: 10.1002/jbmr.1805
187. Parfitt AM, Drezner MK, Glorieux FH, Kanis JA, Malluche H, Meunier PJ, et al. Bone Histomorphometry: Standardization of Nomenclature, Symbols, and Units: Report of the Asbmr Histomorphometry Nomenclature Committee. *J Bone Miner Res* (1987) 2(6):595–610. doi: 10.1002/jbmr.5650020617
188. Glorieux FH, Travers R, Taylor A, Bowen JR, Rauch F, Norman M, et al. Normative Data for Iliac Bone Histomorphometry in Growing Children. *Bone* (2000) 26(2):103–9. doi: 10.1016/S8756-3282(99)00257-4
189. Rauch F, Travers R, Parfitt A, Glorieux F. Static and Dynamic Bone Histomorphometry in Children With Osteogenesis Imperfecta. *Bone* (2000) 26(6):581–9. doi: 10.1016/S8756-3282(00)00269-6
190. Amling M, Pösl M, Ritzel H, Hahn M, Vogel M, Wening VJ, et al. Architecture and Distribution of Cancellous Bone Yield Vertebral Fracture Clues. A Histomorphometric Analysis of the Complete Spinal Column From 40 Autopsy Specimens. *Arch Orthop Trauma Surg* (1996) 115(5):262–9. doi: 10.1007/BF00439050
191. Erben RG, Glösmann M. Histomorphometry in Rodents. *Methods Mol Biol* (2019) 1914:411–35. doi: 10.1007/978-1-4939-8997-3_24
192. Bassett JHD, Boyde A, Howell PGT, Bassett RH, Galliford TM, Archanco M, et al. Optimal Bone Strength and Mineralization Requires the Type 2 Iodothyronine Deiodinase in Osteoblasts. *Proc Natl Acad Sci USA* (2010) 107(16):7604–9. doi: 10.1073/pnas.0911346107
193. Dion N, Fortin A, Ste-Marie L-G. Methods in Bone Histomorphometry for Animal Models. *Osteoporos Res* (2011) 37–43. doi: 10.1007/978-0-85729-293-3_4
194. Jun Du S, Frenkel V, Zohar Y, Kindschi G. Visualizing Normal and Defective Bone Development in Zebrafish Embryos Using the Fluorescent Chromophore Calcein. *Dev Biol* (2001) 238(2):239–46. doi: 10.1006/dbio.2001.0390
195. Kimmel CB, DeLaurier A, Ullmann B, Dowd J, McFadden M. Modes of Developmental Outgrowth and Shaping of a Craniofacial Bone in Zebrafish. *PloS One* (2010) 5(3):e9475. doi: 10.1371/journal.pone.0009475
196. Recidoro AM, Roof AC, Schmitt M, Worton LE, Petrie T, Strand N, et al. Botulinum Toxin Induces Muscle Paralysis and Inhibits Bone Regeneration in Zebrafish. *J Bone Miner Res* (2014) 29(11):2346–56. doi: 10.1002/jbmr.2274
197. Inohaya K, Takano Y, Kudo A. The Teleost Intervertebral Region Acts as a Growth Center of the Centrum: *In Vivo* Visualization of Osteoblasts and Their Progenitors in Transgenic Fish. *Dev Dyn* (2007) 236(11):3031–46. doi: 10.1002/dvdy.21329
198. Edsall SC, Franz-Odendaal TA. A Quick Whole-Mount Staining Protocol for Bone Deposition and Resorption. *Zebrafish* (2010) 7(3):275–80. doi: 10.1089/zeb.2009.0641
199. Tang P, Xiong Q, Ge W, Zhang L. The Role of MicroRNAs in Osteoclasts and Osteoporosis. *RNA Biol* (2014) 11(11):1355–63. doi: 10.1080/15476286.2014.996462
200. Schilling TF, Piotrowski T, Grandel H, Brand M, Heisenberg CP, Jiang YJ, et al. Jaw and Branchial Arch Mutants in Zebrafish I: Branchial Arches. *Development* (1996) 123:329–44. doi: 10.1242/dev.123.1.329
201. Piotrowski T, Schilling TF, Brand M, Jiang YJ, Heisenberg CP, Beuchle D, et al. Jaw and Branchial Arch Mutants in Zebrafish II: Anterior Arches and

Cartilage Differentiation. *Development* (1996) 123:345–56. doi: 10.1242/dev.123.1.345
202. DeLaurier A, Frank Eames B, Blanco-Sánchez B, Peng G, He X, Swartz ME, et al. Zebrafish Sp7:EGFP: A Transgenic for Studying Otic Vesicle Formation, Skeletogenesis, and Bone Regeneration. *Genesis* (2010) 48 (8):505–11. doi: 10.1002/dvg.20639
203. Singh SP, Holdway JE, Poss KD. Regeneration of Amputated Zebrafish Fin Rays From *De Novo* Osteoblasts. *Dev Cell* (2012) 22(4):879–86. doi: 10.1016/j.devcel.2012.03.006
204. Sharif F, De Bakker MA, Richardson MK. Osteoclast-Like Cells in Early Zebrafish Embryos. *Cell J* (2014) 16(2):211–24.
205. Kobayashi-Sun J, Yamamori S, Kondo M, Kuroda J, Ikegame M, Suzuki N, et al. Uptake of Osteoblast-Derived Extracellular Vesicles Promotes the Differentiation of Osteoclasts in the Zebrafish Scale. *Commun Biol* (2020) 3(1):190. doi: 10.1038/s42003-020-0925-1
206. Witten PE, Hansen A, Hall BK. Features of Mono- and Multinucleated Bone Resorbing Cells of the Zebrafish Danio Rerio and Their Contribution to Skeletal Development, Remodeling, and Growth. *J Morphol* (2001) 250 (3):197–207. doi: 10.1002/jmor.1065
207. Nyman JS, Granke M, Singleton RC, Pharr GM. Tissue-Level Mechanical Properties of Bone Contributing to Fracture Risk. *Curr Osteoporosis Rep* (2016) 14:138–50. doi: 10.1007/s11914-016-0314-3
208. Allen MR, McNerny EMB, Organ JM, Wallace JM. True Gold or Pyrite: A Review of Reference Point Indentation for Assessing Bone Mechanical Properties In Vivo. *J Bone Miner Res* (2015) 30:1539–50. doi: 10.1002/jbmr.2603
209. Herrera S, Diez-Perez A. Clinical Experience With Microindentation *In Vivo* in Humans. *Bone* (2017) 95:175–82. doi: 10.1016/j.bone.2016.11.003
210. Schoeb M, Hamdy NAT, Malgo F, Winter EM, Appelman-Dijkstra NM. Added Value of Impact Microindentation in the Evaluation of Bone Fragility: A Systematic Review of the Literature. *Front Endocrinol* (2020) 11. doi: 10.3389/fendo.2020.00015
211. Diez-Perez A, Güerri R, Nogues X, Cáceres E, Peñ MJ, Mellibovsky L, et al. Microindentation for *In Vivo* Measurement of Bone Tissue Mechanical Properties in Humans. *J Bone Miner Res* (2010) 25(8):1877–85. doi: 10.1002/jbmr.73
212. Bridges D, Randall C, Hansma PK. A New Device for Performing Reference Point Indentation Without a Reference Probe. *Rev Sci Instrum* (2012) 83 (4):044301. doi: 10.1063/1.3693085
213. Diez-Perez A, Bouxsein ML, Eriksen EF, Khosla S, Nyman JS, Papapoulos S, et al. Technical Note: Recommendations for a Standard Procedure to Assess Cortical Bone at the Tissue-Level *In Vivo* Using Impact Microindentation. *Bone Rep* (2016) 5:181–5. doi: 10.1016/j.bonr.2016.07.004
214. Kennedy OD, Lendhey M, Mauer P, Philip A, Basta-Pljakic J, Schaffler MB. Microdamage Induced by *In Vivo* Reference Point Indentation in Mice is Repaired by Osteocyte-Apoptosis Mediated Remodeling. *Bone* (2017) 95:192–8. doi: 10.1016/j.bone.2016.11.029
215. Williamson L, Hayes A, Hanson ED, Pivonka P, Sims NA, Gooi JH. High Dose Dietary Vitamin D3 Increases Bone Mass and Strength in Mice. *Bone Rep* (2017) 6:44–50. doi: 10.1016/j.bonr.2017.02.001
216. Carriero A, Bruse JL, Oldknow KJ, Millán JL, Farquharson C, Shefelbine SJ. Reference Point Indentation is Not Indicative of Whole Mouse Bone Measures of Stress Intensity Fracture Toughness. *Bone* (2014) 69:174–9. doi: 10.1016/j.bone.2014.09.020
217. Srisuwananukorn A, Allen MR, Brown DM, Wallace JM, Organ JM. *In Vivo* Reference Point Indentation Measurement Variability in Skeletally Mature Inbred Mice. *Bonekey Rep* (2015) 4:712. doi: 10.1038/bonekey.2015.81
218. Wang XM, Cui FZ, Ge J, Zhang Y, Ma C. Variation of Nanomechanical Properties of Bone by Gene Mutation in the Zebrafish. *Biomaterials* (2002) 23(23):4557–63. doi: 10.1016/S0142-9612(02)00201-6
219. Zhang Y, Cui FZ, Wang XM, Feng QL, Zhu XD. Mechanical Properties of Skeletal Bone in Gene-Mutated Stöpseldtl28d and Wild-Type Zebrafish (Danio Rerio) Measured by Atomic Force Microscopy-Based Nanoindentation. *Bone* (2002) 30(4):541–6. doi: 10.1016/S8756-3282(02)00676-2
220. Chang Z, Chen PY, Chuang YJ, Akhtar R. Zebrafish as a Model to Study Bone Maturation: Nanoscale Structural and Mechanical Characterization of Age-Related Changes in the Zebrafish Vertebral Column. *J Mech Behav BioMed Mater* (2018) 84:54–63. doi: 10.1016/j.jmbbm.2018.05.004
221. Fan ZF, Smith P, Rauch F, Harris GF. Nanoindentation as a Means for Distinguishing Clinical Type of Osteogenesis Imperfecta. *Compos Part B Eng* (2007) 38(3):411–5. doi: 10.1016/j.compositesb.2006.08.006
222. Roschger P, Fratzl P, Eschberger J, Klaushofer K. Validation of Quantitative Backscattered Electron Imaging for the Measurement of Mineral Density Distribution in Human Bone Biopsies. *Bone* (1998) 23(4):319–26. doi: 10.1016/S8756-3282(98)00112-4
223. Roschger P, Paschalis EP, Fratzl P, Klaushofer K. Bone Mineralization Density Distribution in Health and Disease. *Bone* (2008) 42(3):456–66. doi: 10.1016/j.bone.2007.10.021
224. Fratzl-Zelman N, Roschger P, Misof BM, Pfeffer S, Glorieux FH, Klaushofer K, et al. Normative Data on Mineralization Density Distribution in Iliac Bone Biopsies of Children, Adolescents and Young Adults. *Bone* (2009) 44 (6):1043–8. doi: 10.1016/j.bone.2009.02.021
225. Carden A, Morris MD. Application of Vibrational Spectroscopy to the Study of Mineralized Tissues (Review). *J BioMed Opt* (2000) 5(3):259. doi: 10.1117/1.429994
226. Unal M, Akkus O. Raman Spectral Classification of Mineral- and Collagen-Bound Water's Associations to Elastic and Post-Yield Mechanical Properties of Cortical Bone. *Bone* (2015) 81:315–26. doi: 10.1016/j.bone.2015.07.024
227. Shah FA, Ruscsák K, Palmquist A. 50 Years of Scanning Electron Microscopy of Bone—a Comprehensive Overview of the Important Discoveries Made and Insights Gained Into Bone Material Properties in Health, Disease, and Taphonomy. *Bone Res* (2019) 7:1–15. doi: 10.1038/s41413-019-0053-z
228. Akkiraju H, Bonor J, Nohe A. An Improved Immunostaining and Imaging Methodology to Determine Cell and Protein Distributions Within the Bone Environment. *J Histochem Cytochem* (2016) 64(3):168–78. doi: 10.1369/0022155415626765
229. Matos LL, Trufelli DC, de Matos MGL, da Silva Pinhal S. Immunohistochemistry as an Important Tool in Biomarkers Detection and Clinical Practice. *Biomark Insights* (2010) 5:9–20. doi: 10.4137/BMI.S2185
230. Fedchenko N, Reifenrath J. Different Approaches for Interpretation and Reporting of Immunohistochemistry Analysis Results in the Bone Tissue - A Review. *Diagn Pathol* (2014) 9:221. doi: 10.1186/s13000-014-0221-9
231. Malluche HH, Mawad H, Monier-Faugere MC. Bone Biopsy in Patients With Osteoporosis. *Curr Osteoporosis Rep* (2007) 5:146–52. doi: 10.1007/s11914-007-0009-x
232. Yang J, Pan H, Mishina Y. Tissue Preparation and Immunostaining of Mouse Craniofacial Tissues and Undecalcified Bone. *J Vis Exp* (2019) 2019 (147):e59113. doi: 10.3791/59113
233. McDonald MM, Reagan MR, Youlten SE, Mohanty ST, Seckinger A, Terry RL, et al. Inhibiting the Osteocyte-Specific Protein Sclerostin Increases Bone Mass and Fracture Resistance in Multiple Myeloma. *Blood* (2017) 129 (26):3452–64. doi: 10.1182/blood-2017-03-773341
234. Oralová V, Rosa JT, Soenens M, Bek JW, Willaert A, Witten PE, et al. Beyond the Whole-Mount Phenotype: High-Resolution Imaging in Fluorescence-Based Applications on Zebrafish. *Biol Open* (2019) 8(5):bio042374. doi: 10.1242/bio.042374
235. Kague E, Hughes SM, Lawrence EA, Cross S, Martin-Silverstone E, Hammond CL, et al. Scleraxis Genes are Required for Normal Musculoskeletal Development and for Rib Growth and Mineralization in Zebrafish. *FASEB J* (2019) 33(8):9116–30. doi: 10.1096/fj.201802654RR
236. Brunt LH, Begg K, Kague E, Cross S, Hammond CL. Wnt Signalling Controls the Response to Mechanical Loading During Zebrafish Joint Development. *Dev* (2017) 144(15):2798–809. doi: 10.1242/dev.153528
237. Paul S, Schindler S, Giovannone D, de Millo Terrazzani A, Mariani FV, Crump JG. Ihha Induces Hybrid Cartilage-Bone Cells During Zebrafish Jawbone Regeneration. *Dev* (2016) 143(12):2066–76. doi: 10.1242/dev.131292
238. Lee J, Vasikaran S. Current Recommendations for Laboratory Testing and Use of Bone Turnover Markers in Management of Osteoporosis. *Ann Lab Med* (2012) 32:105–12. doi: 10.3343/alm.2012.32.2.105
239. Fink HA, Litwack-Harrison S, Taylor BC, Bauer DC, Orwoll ES, Lee CG, et al. Clinical Utility of Routine Laboratory Testing to Identify Possible Secondary Causes in Older Men With Osteoporosis: The Osteoporotic

Fractures in Men (MrOS) Study. *Osteoporos Int* (2016) 27(1):331–8. doi: 10.1007/s00198-015-3356-y
240. Zang L, Shimada Y, Nishimura Y, Tanaka T, Nishimura N, Novel A. Reliable Method for Repeated Blood Collection From Aquarium Fish. *Zebrafish* (2013) 10(3):425–32. doi: 10.1089/zeb.2012.0862
241. Holick MF. The Vitamin D Deficiency Pandemic: Approaches for Diagnosis, Treatment and Prevention. *Rev Endocrine Metab Disord* (2017) 18:153–65. doi: 10.1007/s11154-017-9424-1
242. Reid IR. Vitamin D Effect on Bone Mineral Density and Fractures. *Endocrinol Metab Clinics North America* (2017) 46:935–45. doi: 10.1016/j.ecl.2017.07.005
243. Bischoff-Ferrari HA. Influence of Vitamin D on Fracture Reduction Among Older Adults: A Discussion of Recent Meta-Analysis Findings. *Osteologie* (2019) 28(2):136–9. doi: 10.1055/a-0861-2813
244. Munns CF, Shaw N, Kiely M, Specker BL, Thacher TD, Ozono K, et al. Global Consensus Recommendations on Prevention and Management of Nutritional Rickets. *J Clin Endocrinol Metab* (2016) 101(2):394–415. doi: 10.1210/jc.2015-2175
245. Cherniack EP, Troen BR. Calciotropic Hormones. In: *Osteoporosis in Older Persons: Advances in Pathophysiology and Therapeutic Approaches*, *2nd ed.* Springer International Publishing (2016). p. 43–58.
246. Tiosano D, Hochberg Z. Hypophosphatemia: The Common Denominator of All Rickets. *J Bone Mineral Metab* (2009) 27:392–401. doi: 10.1007/s00774-009-0079-1
247. Cavalier E, Souberbielle JC. Vitamin D and Its Metabolites: From Now and Beyond. *EJIFCC* (2018) 29(2):105–10.
248. Uday S, Högler W. Spot the Silent Sufferers: A Call for Clinical Diagnostic Criteria for Solar and Nutritional Osteomalacia. *J Steroid Biochem Mol Biol* (2019) 188:141–6. doi: 10.1016/j.jsbmb.2019.01.004
249. Seldeen KL, Pang M, Rodríguez-Gonzalez M, Hernandez M, Sheridan Z, Yu P, et al. A Mouse Model of Vitamin D Insufficiency: Is There a Relationship Between 25(OH) Vitamin D Levels and Obesity? *Nutr Metab* (2017) 14 (1):26. doi: 10.1186/s12986-017-0174-6
250. Szulc P, Naylor K, Hoyle NR, Eastell R, Leary ET. Use of CTX-I and PINP as Bone Turnover Markers: National Bone Health Alliance Recommendations to Standardize Sample Handling and Patient Preparation to Reduce Pre-Analytical Variability. *Osteoporos Int* (2017) 28(9):2541–56. doi: 10.1007/s00198-017-4082-4
251. Shaw N, Högler W. Biochemical Markers of Bone Metabolism. In: Glorieux FH, Pettifor JM, Jüppner H. *Pediatric Bone*. Elsevier Inc (2012). p. 361–81. doi: 10.1016/B978-0-12-382040-2.10015-2
252. Guañabens N, Parés A, Alvarez L, De Osaba MJM, Monegal A, Peris P, et al. Collagen-Related Markers of Bone Turnover Reflect the Severity of Liver Fibrosis in Patients With Primary Biliary Cirrhosis. *J Bone Miner Res* (1998) 13(4):731–8. doi: 10.1359/jbmr.1998.13.4.731
253. Delmas PD, Demiaux B, Malaval L, Chapuy MC, Edouard C, Meunier PJ. Serum Bone Gamma Carboxyglutamic Acid-Containing Protein in Primary Hyperparathyroidism and in Malignant Hypercalcemia. Comparison With Bone Histomorphometry. *J Clin Invest* (1986) 77(3):985–91. doi: 10.1172/JCI112400
254. Uebelhart D, Gineyts E, Chapuy M-C, Delmas PD. Urinary Excretion of Pyridinium Crosslinks: A New Marker of Bone Resorption in Metabolic Bone Disease. *Bone Miner* (1990) 8(1):87–96. doi: 10.1016/0169-6009(91)90143-N
255. Eisman JA, Bone HG, Hosking DJ, McClung MR, Reid IR, Rizzoli R, et al. Odanacatib in the Treatment of Postmenopausal Women With Low Bone Mineral Density: Three-Year Continued Therapy and Resolution of Effect. *J Bone Miner Res* (2011) 26(2):242–51. doi: 10.1002/jbmr.212
256. Imel EA, Liu Z, Acton D, Coffman M, Gebregziabher N, Tong Y, et al. Interferon Gamma-1b Does Not Increase Markers of Bone Resorption in Autosomal Dominant Osteopetrosis. *J Bone Miner Res* (2019) 34(8):1436–45. doi: 10.1002/jbmr.3715
257. Vasikaran S, Cooper C, Eastell R, Griesmacher A, Morris HA, Trenti T, et al. International Osteoporosis Foundation and International Federation of Clinical Chemistry and Laboratory Medicine Position on Bone Marker Standards in Osteoporosis. *Clin Chem Lab Med* (2011) 49(8):1271–4. doi: 10.1515/CCLM.2011.602
258. Szulc P, Delmas PD. Biochemical Markers of Bone Turnover in Men. *Calciied Tissue Int* (2001) 69(4):229–34. doi: 10.1007/s00223-001-1059-1
259. Naylor KE, Jacques RM, Paggiosi M, Gossiel F, Peel NFA, McCloskey EV, et al. Response of Bone Turnover Markers to Three Oral Bisphosphonate Therapies in Postmenopausal Osteoporosis: The TRIO Study. *Osteoporos Int* (2016) 27(1):21–31. doi: 10.1007/s00198-015-3145-7
260. Stepan JJ. Prediction of Bone Loss in Postmenopausal Women. *Osteoporosis Int* (2000) 11:S45–54. doi: 10.1007/s001980070005
261. Vilaca T, Gossiel F, Eastell R. Bone Turnover Markers: Use in Fracture Prediction. *J Clin Densitom* (2017) 20(3):346–52. doi: 10.1016/j.jocd.2017.06.020
262. Eastell R, Pigott T, Gossiel F, Naylor KE, Walsh JS, APeel NF. Bone Turnover Markers: Are They Clinically Useful? *Eur J Endocrinol* (2018) 178:R19–31. doi: 10.1530/EJE-17-0585
263. *A Practical Approach to Adolescent Bone Health. A Practical Approach to Adolescent Bone Health*. Springer International Publishing (2018). doi: 10.1007/978-3-319-72880-3
264. Redmond J, Fulford AJ, Jarjou L, Zhou B, Prentice A, Schoenmakers I. Diurnal Rhythms of Bone Turnover Markers in Three Ethnic Groups. *J Clin Endocrinol Metab* (2016) 101(8):3222–30. doi: 10.1210/jc.2016-1183
265. Christgau S, Bitsch-Jensen O, Hanover Bjarnason N, Gamwell Henriksen E, Qvist P, Alexandersen P, et al. Serum CrossLaps for Monitoring the Response in Individuals Undergoing Antiresorptive Therapy. *Bone* (2000) 26(5):505–11. doi: 10.1016/S8756-3282(00)00248-9
266. Rauchenzauner M, Schmid A, Heinz-Erian P, Kapelari K, Falkensammer G, Griesmacher A, et al. Sex- and Age-Specific Reference Curves for Serum Markers of Bone Turnover in Healthy Children From 2 Months to 18 Years. *J Clin Endocrinol Metab* (2007) 92(2):443–9. doi: 10.1210/jc.2006-1706
267. Choi JI, Cho HH. Effects of Di(2-Ethylhexyl)Phthalate on Bone Metabolism in Ovariectomized Mice. *J Bone Metab* (2019) 26(3):169–77. doi: 10.11005/jbm.2019.26.3.169
268. Kim TH, Kim HJ, Lee SH, Kim SY. Potent Inhibitory Effect of Foeniculum Vulgare Miller Extract on Osteoclast Differentiation and Ovariectomy-Induced Bone Loss. *Int J Mol Med* (2012) 29(6):1053–9. doi: 10.3892/ijmm.2012.950
269. Hammond CL, Moro E. Using Transgenic Reporters to Visualize Bone and Cartilage Signaling During Development In Vivo. *Front Endocrinol (Lausanne)* (2012) 3(JUL). doi: 10.3389/fendo.2012.00091
270. Baird DA, Evans DMDS, Kamanu FK, Gregory JS, Saunders FR, Giuraniuc CV, et al. Identification of Novel Loci Associated With Hip Shape: A Meta-Analysis of Genomewide Association Studies. *J Bone Miner Res* (2019) 34 (2):241–51. doi: 10.1002/jbmr.3605
271. Yi L, Guo X, Sun L, Hou B. Structural and Functional Sensing of Bio-Tissues Based on Compressive Sensing Spectral Domain Optical Coherence Tomography. *Sensors* (2019) 19(19):4208. doi: 10.3390/s19194208
272. Du J, Bydder GM. Qualitative and Quantitative Ultrashort-TE MRI of Cortical Bone. *NMR Biomedicine* (2013) 26:489–506. doi: 10.1002/nbm.2906
273. Rad HS, Lam SCB, Magland JF, Ong H, Li C, Song HK, et al. Quantifying Cortical Bone Water *In Vivo* by Three-Dimensional Ultra-Short Echo-Time MRI. *NMR Biomed* (2011) 24(7):855–64. doi: 10.1002/nbm.1631
274. Klinck RJ, Campbell GM, Boyd SK. Radiation Effects on Bone Architecture in Mice and Rats Resulting From *In Vivo* Micro-Computed Tomography Scanning. *Med Eng Phys* (2008) 30(7):888–95. doi: 10.1016/j.medengphy.2007.11.004
275. Solsona CM, Sasser T, Salmon P, Gsell W, Viertl D, Massey JC, et al. Low-Dose Imaging in a New Preclinical Total-Body PET/CT Scanner. *Front Med* (2019) 6(APR). doi: 10.3389/fmed.2019.00088
276. Ferizi U, Honig S, Chang G. Artificial Intelligence, Osteoporosis and Fragility Fractures. *Curr Opin Rheumatol* (2019) 31:368–75. doi: 10.1097/BOR.0000000000000607
277. Olczak J, Fahlberg N, Maki A, Razavian AS, Jilert A, Stark A, et al. Artificial Intelligence for Analyzing Orthopedic Trauma Radiographs: Deep Learning Algorithms—are They on Par With Humans for Diagnosing Fractures? *Acta Orthop* (2017) 88(6):581–6. doi: 10.1080/17453674.2017.1344459
278. Letarouilly JG, Broux O, Clabaut A. New Insights Into the Epigenetics of Osteoporosis. *Genomics* (2019) 111:793–8. doi: 10.1016/j.ygeno.2018.05.001

279. Astleford K, Campbell E, Norton A, Mansky KC. Epigenetic Regulators Involved in Osteoclast Differentiation. *Int J Mol Sci* (2020) 21:1–15. doi: 10.3390/ijms21197080
280. Martinez-Moreno JM, Fontecha-Barriuso M, Martin-Sanchez D, Guerrero-Mauvecin J, Goma-Garces E, Fernandez-Fernandez B, et al. Epigenetic Modifiers as Potential Therapeutic Targets in Diabetic Kidney Disease. *Int J Mol Sci* (2020) 21:1–26. doi: 10.3390/ijms21114113
281. Kwon DH, Ryu J, Kim YK, Kook H. Roles of Histone Acetylation Modifiers and Other Epigenetic Regulators in Vascular Calcification. *Int J Mol Sci* (2020) 21(9):3246. doi: 10.3390/ijms21093246
282. Lin W, Li Y, Chen F, Yin S, Liu Z, Cao W. Klotho Preservation *via* Histone Deacetylase Inhibition Attenuates Chronic Kidney Disease-Associated Bone Injury in Mice. *Sci Rep* (2017) 7(1):46195. doi: 10.1038/srep46195
283. Silva AM, Moura SR, Teixeira JH, Barbosa MA, Santos SG, Almeida MI. Long Noncoding RNAs: A Missing Link in Osteoporosis. *Bone Res* (2019) 7:10. doi: 10.1038/s41413-019-0048-9
284. Srinivasan S, Duval MX, Kaimal V, Cuff C, Clarke SH. Assessment of Methods for Serum Extracellular Vesicle Small RNA Sequencing to Support Biomarker Development. *J Extracell Vesicles* (2019) 8(1):1684425. doi: 10.1080/20013078.2019.1684425
285. Ge XQ, Lin H. Noncoding RNAs in the Regulation of DNA Replication. *Trends Biochem Sci* (2014) 39:341–3. doi: 10.1016/j.tibs.2014.06.003
286. Beroual W, Brilli M, Biondi EG. Non-Coding RNAs Potentially Controlling Cell Cycle in the Model Caulobacter Crescentus: A Bioinformatic Approach. *Front Genet* (2018) 9:164. doi: 10.3389/fgene.2018.00164
287. Pircher A, Gebetsberger J, Polacek N. Ribosome-Associated ncRNAs: An Emerging Class of Translation Regulators. *RNA Biol* (2014) 11(11):1335–9. doi: 10.1080/15476286.2014.996459
288. Will CL, Lührmann R. Spliceosome Structure and Function. *Cold Spring Harb Perspect Biol* (2011) 3(7):1–2. doi: 10.1101/cshperspect.a003707
289. Dykes IM, Emanueli C. Transcriptional and Post-Transcriptional Gene Regulation by Long Non-Coding RNA. *Genomics Proteomics Bioinf* (2017) 15:177–86. doi: 10.1016/j.gpb.2016.12.005
290. Foessl I, Kotzbeck P, Obermayer-Pietsch B. miRNAs as Novel Biomarkers for Bone Related Diseases. *J Lab Precis Med* (2019) 4:2–2. doi: 10.21037/jlpm.2018.12.06
291. Yavropoulou M, Anastasilakis A, Makras P, Grammatiki M, Kotsa K, Yovos J. Circulating microRNAs in Postmenopausal Women With Osteoporosis and Vertebral Fractures. *Bone Abstr* (2016) 5:245. doi: 10.1530/boneabs.5.P245
292. Hassan MQ, Tye CE, Stein GS, Lian JB. Non-Coding RNAs: Epigenetic Regulators of Bone Development and Homeostasis. *Bone* (2015) 81:746–56. doi: 10.1016/j.bone.2015.05.026
293. Hackl M, Heilmeier U, Weilner S, Grillari J. Circulating microRNAs as Novel Biomarkers for Bone Diseases – Complex Signatures for Multifactorial Diseases? *Mol Cell Endocrinol* (2016) 432:83–95. doi: 10.1016/j.mce.2015.10.015
294. Lee YR, Kim G, Tak WY, Jang SY, Kweon YO, Park JG, et al. Circulating Exosomal Noncoding RNAs as Prognostic Biomarkers in Human Hepatocellular Carcinoma. *Int J Cancer* (2019) 144(6):1444–52. doi: 10.1002/ijc.31931
295. Lian JB, Stein GS, van Wijnen AJ, Stein JL, Hassan MQ, Gaur T, et al. MicroRNA Control of Bone Formation and Homeostasis. *Nat Rev Endocrinol* (2012) 8(4):212–27. doi: 10.1038/nrendo.2011.234
296. Masuda T, Mori A, Ito S, Ohtsuki S. Quantitative and Targeted Proteomics-Based Identification and Validation of Drug Efficacy Biomarkers. *Drug Metab* (2021) 36:100361. doi: 10.1016/j.dmpk.2020.09.006
297. Lee JH, Cho JY. Proteomics Approaches for the Studies of Bone Metabolism. *BMB Rep* (2014) 47(3):141–8. doi: 10.5483/BMBRep.2014.47.3.270
298. Nielson CM, Jacobs JM, Orwoll ES. Proteomic Studies of Bone and Skeletal Health Outcomes. *Bone* (2019) 126:18–26. doi: 10.1016/j.bone.2019.03.032
299. Calciolari E, Donos N. Proteomic and Transcriptomic Approaches for Studying Bone Regeneration in Health and Systemically Compromised Conditions. *Proteomics – Clin Appl* (2020) 14(3):1900084. doi: 10.1002/prca.201900084
300. Yang TL, Shen H, Liu A, Dong SS, Zhang L, Deng FY, et al. A Road Map for Understanding Molecular and Genetic Determinants of Osteoporosis. *Nat Rev Endocrinol* (2020) 16:91–103. doi: 10.1038/s41574-019-0282-7
301. Ohlsson C, Sjögren K. Effects of the Gut Microbiota on Bone Mass. *Trends Endocrinol Metab* (2015) 26:69–74. doi: 10.1016/j.tem.2014.11.004
302. Medina-Gomez C. Bone and the Gut Microbiome: A New Dimension. *J Lab Precis Med* (2018) 3:96–6. doi: 10.21037/jlpm.2018.11.03
303. Ohlsson C, Sjögren K. Osteomicrobiology: A New Cross-Disciplinary Research Field. *Calciied Tissue Int* (2018) 102:426–32. doi: 10.1007/s00223-017-0336-6
304. Guss JD, Horsfield MW, Fontenele FF, Sandoval TN, Luna M, Apoorva F, et al. Alterations to the Gut Microbiome Impair Bone Strength and Tissue Material Properties. *J Bone Miner Res* (2017) 32(6):1343–53. doi: 10.1002/jbmr.3114
305. Jansson PA, Curiac D, Lazou Ahrén I, Hansson F, Martinsson Niskanen T, Sjögren K, et al. Probiotic Treatment Using a Mix of Three Lactobacillus Strains for Lumbar Spine Bone Loss in Postmenopausal Women: A Randomised, Double-Blind, Placebo-Controlled, Multicentre Trial. *Lancet Rheumatol* (2019) 1(3):e154–62. doi: 10.1016/S2665-9913(19)30068-2
306. Nilsson AG, Sundh D, Bäckhed F, Lorentzon M. *Lactobacillus Reuteri* Reduces Bone Loss in Older Women With Low Bone Mineral Density: A Randomized, Placebo-Controlled, Double-Blind, Clinical Trial. *J Intern Med* (2018) 284(3):307–17. doi: 10.1111/joim.12805
307. Heale R, Forbes D. Understanding Triangulation in Research. *Evidence-Based Nursing* (2013) 16:98. doi: 10.1136/eb-2013-101494

Conflict of Interest: The authors declare that the research was conducted in the absence of any commercial or financial relationships that could be construed as a potential conflict of interest.

Publisher's Note: All claims expressed in this article are solely those of the authors and do not necessarily represent those of their affiliated organizations, or those of the publisher, the editors and the reviewers. Any product that may be evaluated in this article, or claim that may be made by its manufacturer, is not guaranteed or endorsed by the publisher.

International Journal of
Molecular Sciences

MDPI

Article

miRNAs as Regulators of the Early Local Response to Burn Injuries

Ines Foessl [1,*], Christoph Walter Haudum [1,2], Ivan Vidakovic [3], Ruth Prassl [3], Joakim Franz [1,2], Selma I. Mautner [1,4], Sonja Kainz [4], Elisabeth Hofmann [5], Barbara Obermayer-Pietsch [1], Thomas Birngruber [4] and Petra Kotzbeck [1,5,6]

1 Department of Internal Medicine, Division of Endocrinology and Diabetology, Medical University of Graz, 8036 Graz, Austria; christoph.haudum@medunigraz.at (C.W.H.); joakim.franz@medunigraz.at (J.F.); selma.mautner@medunigraz.at (S.I.M.); barbara.obermayer@medunigraz.at (B.O.-P.); petra.kotzbeck@medunigraz.at (P.K.)
2 CBmed GmbH—Center for Biomarker Research in Medicine, 8010 Graz, Austria
3 Gottfried Schatz Research Center (for Cell Signaling, Metabolism and Aging), Division of Biophysics, Medical University of Graz, 8010 Graz, Austria; ivan.vidakovic@medunigraz.at (I.V.); ruth.prassl@medunigraz.at (R.P.)
4 HEALTH—Institute for Biomedicine and Health Sciences, JOANNEUM RESEARCH Forschungsgesellschaft mbH, 8010 Graz, Austria; sonja.kainz@joanneum.at (S.K.); thomas.birngruber@joanneum.at (T.B.)
5 Department of Surgery, Division of Plastic, Aesthetic and Reconstructive Surgery, Medical University of Graz, 8036 Graz, Austria; elisabeth.hofmann@joanneum.at
6 COREMED—Cooperative Centre for Regenerative Medicine, JOANNEUM RESEARCH Forschungsgesellschaft mbH, 8010 Graz, Austria
* Correspondence: ines.foessl@medunigraz.at; Tel.: +43-316-385-72936

Abstract: In burn injuries, risk factors and limitations to treatment success are difficult to assess clinically. However, local cellular responses are characterized by specific gene-expression patterns. MicroRNAs (miRNAs) are single-stranded, non-coding RNAs that regulate mRNA expression on a posttranscriptional level. Secreted through exosome-like vesicles (ELV), miRNAs are intracellular signalers and epigenetic regulators. To date, their role in the regulation of the early burn response remains unclear. Here, we identified 43 miRNAs as potential regulators of the early burn response through the bioinformatics analysis of an existing dataset. We used an established human ex vivo skin model of a deep partial-thickness burn to characterize ELVs and miRNAs in dermal interstitial fluid (dISF). Moreover, we identified miR-497-5p as stably downregulated in tissue and dISF in the early phase after a burn injury. MiR-218-5p and miR-212-3p were downregulated in dISF, but not in tissue. Target genes of the miRNAs were mainly upregulated in tissue post-burn. The altered levels of miRNAs in dISF of thermally injured skin mark them as new biomarker candidates for burn injuries. To our knowledge, this is the first study to report miRNAs altered in the dISF in the early phase of deep partial-thickness burns.

Keywords: burn; skin; miRNAs; biomarkers; gene regulation; extracellular vesicles

Citation: Foessl, I.; Haudum, C.W.; Vidakovic, I.; Prassl, R.; Franz, J.; Mautner, S.I.; Kainz, S.; Hofmann, E.; Obermayer-Pietsch, B.; Birngruber, T.; et al. miRNAs as Regulators of the Early Local Response to Burn Injuries. *Int. J. Mol. Sci.* **2021**, *22*, 9209. https://doi.org/10.3390/ijms22179209

Academic Editor: Maria Greabu

Received: 30 July 2021
Accepted: 20 August 2021
Published: 26 August 2021

1. Introduction

Burns are complex injuries with a multitude of local and systemic changes that are aggravated in severe and large lesions caused by full-thickness burns. Several local responses have already been described to be triggered by a severe burn injury [1–3], but the determinants of why and when a burn injury is causing the transition from a local to a systemic response are still widely unknown [4]. As a local response, immediately after the burn, the transcription activator nuclear factor-κB (NF-κB) is activated to regulate further inflammatory mediators. In the following pro-inflammatory phase [3], macrophages release mediators, such as interleukin-6 (IL-6), tumor necrosis factor alpha (TNF-α), prostaglandins and reactive nitrogen species [1]. Pro-inflammatory cytokines are released and accompanied by the formation of reactive oxygen species (ROS), and increased apoptosis is, in

part, triggered by TNF-α [2]. The systemic responses to severe burns affect almost every organ system and are referred to as hypermetabolic response. The exact cause of this effect is still unclear, but an increased and prolonged expression of glucocorticoids, glucagon, catecholamines and dopamine, together with increased levels of cytokines, ROS, nitric oxide and several other mediators after a burn injury, lead to the hypermetabolic state in the patient that can last for years [5]. The first 48 h of the systemic response to a severe burn are characterized by a decrease in metabolism, cardiac output and oxygen consumption [6]. Surgical treatment of burn injuries in the early phase within the first 24 h after the burn has shown to improve patients' prognosis in terms of inflammatory and hypermetabolic response [7]. However, the mere clinical assessment regarding depth and severity of such wounds is often imprecise and underestimated [8] and does not allow a prediction of the systemic response. Biomarkers for an evidence-based decision as to whether or not a burn wound should be surgically restored are needed to improve patient outcome. Therefore, an in-depth understanding of how local responses transition into systemic changes is highly relevant.

MicroRNAs (miRNAs) have been reported as reliable biomarkers for multiple disease types, including several skin conditions [9]. Differential expressions of certain miRNAs are described for psoriasis [10–12], atopic dermatitis [13,14] and keloid tissue [15]. In the denatured dermis of patients with full-thickness burns, 66 miRNAs showed differential expression four days after the burn, when compared to unburned skin [16], but to date, no biomarker has been established among these in clinical practice. Most of the biomarker studies for skin conditions have used plasma or serum samples [9,17,18], but local miRNAs might be masked by miRNAs from tissues that are in close contact with the bloodstream, such as blood cells, liver, kidney or lung tissue [19]. Locally, miRNAs have already been found in the dermal interstitial fluid (dISF) of rats and humans [20]. Because of the use of minimally invasive sampling techniques, such as dermal open-flow microperfusion (dOFM) [21], dISF is now more easily accessible [19] and offers the opportunity of measuring miRNA directly at the burned skin site. Reportedly, miRNAs are transported by extracellular vesicles [18], which have also been detected in dISF, where they were shown to mediate crosstalk of keratinocytes and fibroblasts in the context of aging [22]. Little is known about alterations in dermal extracellular vesicles/exosome-like vesicles (ELVs) at the burn injury site, but ELVs derived from human mesenchymal stem cells from the umbilical-chord were shown to accelerate wound healing in the burn wounds of rats [23].

The aim of this study was to identify miRNAs in the dISF that can be used as biomarkers for burn injuries and to assess their interaction with genes of the early burn response. We used a bioinformatics approach [24] to preselect potential miRNA–mRNA interaction partners by analyzing a publicly available microarray dataset [25] for changes in gene expression in the first 3 days after a partial-thickness burn. We used an established ex vivo human skin model [26] to study alterations within 24 h after a deep partial-thickness burn injury. We analyzed ELVs in dISF collected by using dOFM and followed miRNA tracks into the extracellular space. By using real-time PCR (qPCR), we screened burned skin tissue for a subset of both miRNAs and mRNAs.

2. Results

The study concept and workflow is depicted in Figure 1.

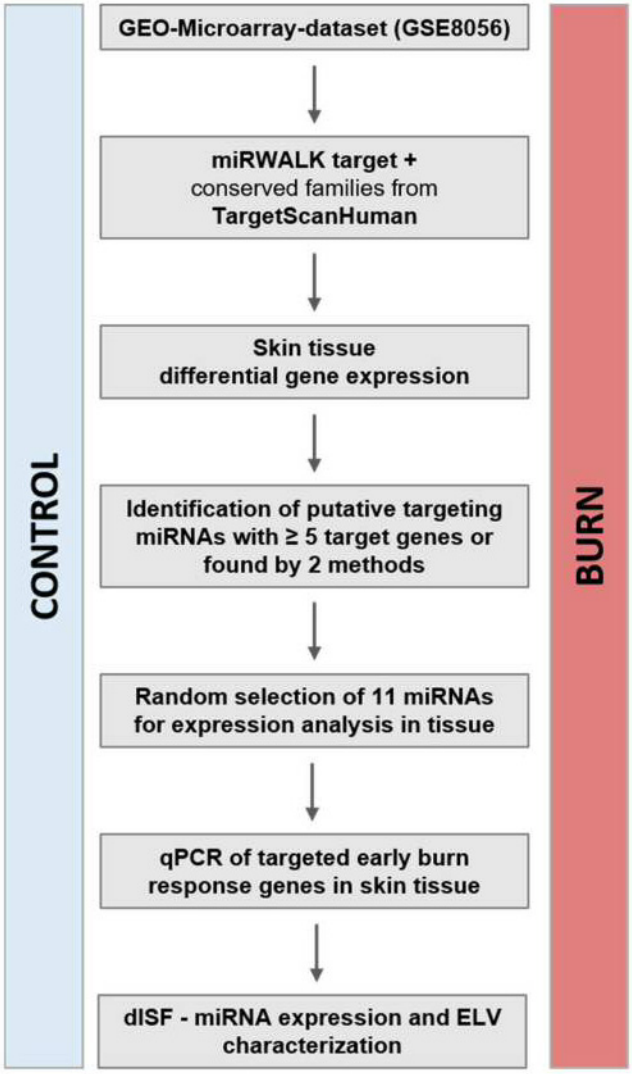

Figure 1. Study concept and workflow. From the publicly available dataset of GSE8056, we compared the groups for control (no burn) and the sample pools of up to 3 days after the burn wound. The genes with a $p_{adj} < 0.001$ were considered the genes of the early burn response. The miRNAs putatively targeting these mRNAs were identified via the bioinformatics approach (miRWalk target, TargetScan-Human). Selected miRNAs and the early burn response genes they target were analyzed in a human skin model for burn injuries. The miRNAs in human dISF were characterized. Abbreviations: GEO, Gene Expression Omnibus; miRNA, microRNA; qPCR, real-time quantitative PCR; p_{adj}, adjusted *p*-value; dISF, dermal interstitial fluid; ELV, exosome-like vesicles.

2.1. In the Early Response to Burn Injuries Putatively Involved miRNAs Are Identified through a Bioinformatics Approach

To identify regulated miRNAs after burn injuries, we set up a bioinformatics approach and analyzed publicly available GEO datasets from transcriptomic studies of biopsies collected from burn patients. To do so, the NCBI-GEO database [27] was screened for expression data in the early phase of partial-thickness burns of human skin biopsies. The GEO-dataset GSE8056 [25] was considered the most suitable at the time of the analysis. It included microarray data of 12 samples, three per group, each consisting of the pooled RNA of five patients. We compared three sample-pools from 0 to 3 days after the burn injury, with the three corresponding control sample-pools. Of the 54,675 annotated genes in the analyzed dataset, 3558 (6.5%) were differentially regulated with an adjusted *p*-value (p_{adj}) of < 0.05, 992 (1.8%) with $p_{adj} < 0.01$ and 114 (0.2%) with $p_{adj} < 0.001$ (Table 1). These highly significant early burn-response genes (differentially regulated genes with

$p_{adj} < 0.001$) (Table 2) were depicted in a heatmap (Figure 2) and considered for further analysis steps. Among these genes of the early burn response were matrix-associated genes, such as matrix metalloproteases (MMP) and collagens (COL); immunomodulatory genes, such as members of the interleukin (IL) and chemokine (c-x-c motif) ligand (CXCL) families; signal cascade transducers that activate various major cellular pathways; and several others. Of the 114 genes, 79 were upregulated in burn samples (70%) and 35 were downregulated (30%) (Table 1). This is also visualized in the volcano plot (Supplementary Materials Figure S1a) and Venn diagram (Supplementary Materials Figure S1b).

Table 1. Results of the GEO2R analysis of the GSE8056 dataset. The groups for control (no burn) and the pooled burn samples 3 days after the burn wounds were compared.

	No.	%
Total genes annotated	54,675	100%
$p_{adj} < 0.05$	3558	6.5%
$p_{adj} < 0.01$	992	1.8%
$p_{adj} < 0.001$	114	0.2%
upregulated	79	70%
downregulated	35	30%

Within these 114 early burn response genes, miRNA target sites in their 3′UTRs were identified by using two platforms:

In TargetScanHuman, mRNAs of the early burn response genes were entered and conserved sites for miRNA families broadly conserved among vertebrates were recorded. In parallel, potential miRNA interaction partners for the early burn response genes were also scanned with miRWalk. We identified 113 miRNAs by TargetScanHuman and 251 miRNAs with miRWalk that potentially regulate the 114 early burn response genes. For further analysis, we selected those miRNAs that showed $\geq$5 interaction partners and/or were found as potential targets by both methods (Supplementary Materials Table S1). Thereby, 43 miRNAs were identified as potential regulators of early burn response genes. For 37 of these miRNAs, gene expression assays for analysis were commercially available (Supplementary Materials Table S2).

Table 2. Selected early burn-response genes, including their rank based on FDR (compare with heatmap Figure 2).

	ID	p_{adj}	*P*	t	B	logFC	Gene Symbol	Gene Title	GSM 198875 0 h	GSM 198876 0 h	GSM 198877 0 h	Mean 0 h	GSM 198866 3 d	GSM 198867 3 d	GSM 198868 3 d	Mean 3 d
14	203434_s_at	0.0001246	3.19×10^{-8}	19.65	9.10	4.28	*MME*	membrane metalloendopeptidase	12.02	11.80	16.98	13.60	211.84	278.65	300.48	263.66
49	238512_at	0.0006066	5.67×10^{-7}	−13.73	6.78	−2.38	*WNT2B*	Wnt family member 2B	190.56	162.10	190.51	181.06	35.37	30.40	38.82	34.87
51	201150_s_at	0.0006066	5.88×10^{-7}	−13.67	6.75	−2.35	*TIMP3*	TIMP metallopeptidase inhibitor 3	2684.61	2025.09	2336.93	2348.88	471.36	471.65	431.15	458.05
56	204745_x_at	0.0006066	6.22×10^{-7}	13.57	6.70	2.62	*MT1G*	metallothionein 1G	642.73	474.11	677.58	598.14	3296.03	3958.74	3704.69	3653.15
62	219908_at	0.000613	7.14×10^{-7}	−13.34	6.58	−3.11	*DKK2*	dickkopf WNT signaling pathway inhibitor 2	210.42	228.11	234.28	224.27	26.20	34.89	18.92	26.67
76	201645_at	0.000613	8.52×10^{-7}	13.04	6.42	3.08	*TNC*	tenascin C	293.96	214.10	190.91	232.99	1506.81	2321.70	2087.41	1971.97
81	205000_at	0.0006873	1.02×10^{-6}	12.75	6.26	4.96	*DDX3Y*	DEAD-box helicase 3. Y-linked	11.08	6.00	10.63	9.24	152.53	371.48	375.00	299.67
87	229947_at	0.0007308	1.16×10^{-6}	12.54	6.14	5.05	*PI15*	peptidase inhibitor 15	18.37	22.90	19.28	20.18	332.87	1159.94	760.88	751.23
101	219181_at	0.0008774	1.62×10^{-6}	12.02	5.83	3.30	*LIPG*	lipase G. endothelial type	16.70	12.60	27.13	18.81	196.16	170.26	164.54	176.99
106	202499_s_at	0.0009022	1.77×10^{-6}	11.89	5.75	3.23	*SLC2A3*	solute carrier family 2 member 3	133.38	70.10	72.10	91.86	785.79	729.58	970.77	828.71
113	238009_at	0.0009914	2.07×10^{-6}	−11.65	5.61	−2.13	*SOX5*	SRY-box 5	92.71	104.10	133.17	109.99	24.77	24.69	24.90	24.79

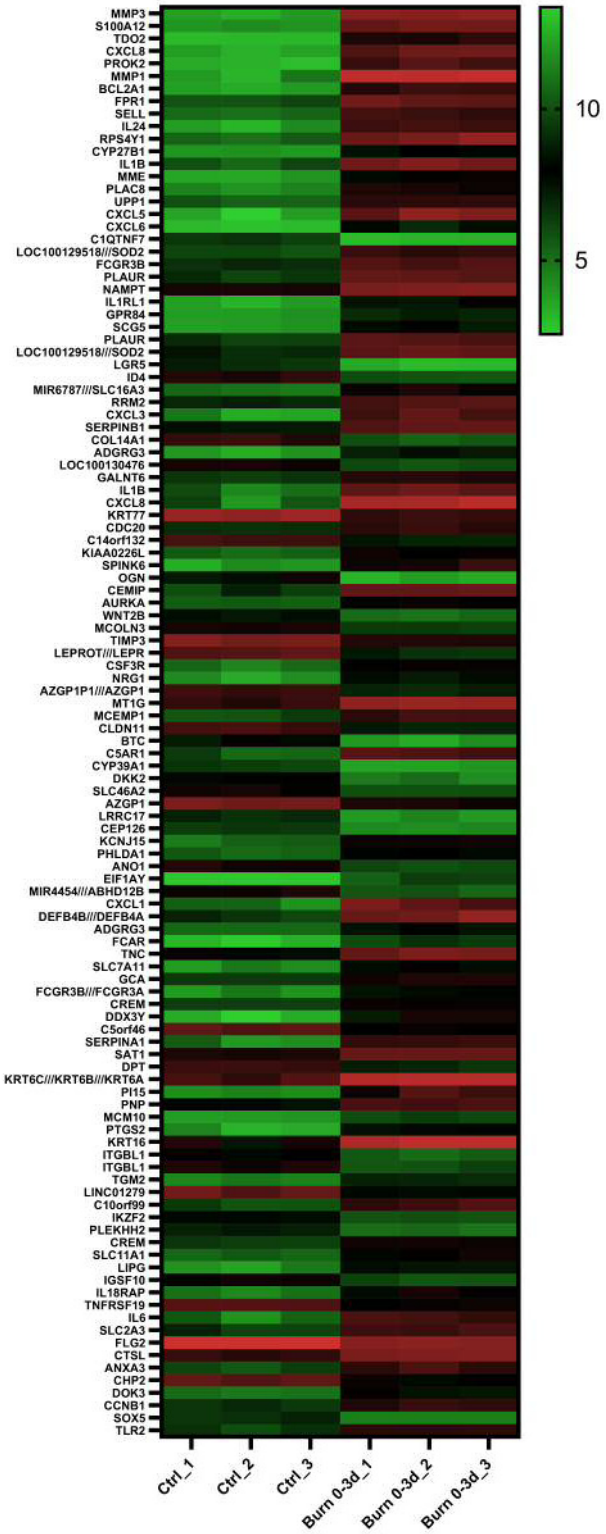

Figure 2. Heatmap displaying 114 early burn response genes that are differentially expressed in the GSE8056 dataset with $p_{adj} < 0.001$. The color indicates the expression, with green being downregulated and red upregulated. Data are displayed as log2 of normalized counts.

2.2. Extracellular Vesicles and Their miRNA Cargo in dISF of Burned Skin Have Been Characterized

To investigate the presence and characteristics of ELVs in the dISF of burn injuries, dOFM was performed as previously described [21,28,29], and ELVs were enriched through centrifugation (Figure 3). To verify the presence of ELVs, the exosomal markers flotillin

and CD9 were detected in ELV-enriched fractions and mixed particle fractions (MPF) of burned skin and control skin (Figure 4a). There were no changes in the CD9 signal in the ELV-enriched fraction. A slight decrease in CD9 was present in the MPF of burned skin. Protein concentrations in the MPF were 0.8 mg/mL in burn samples and 0.5 mg/mL in control samples ($p = 0.06$). There were no changes in protein concentrations in the ELV-enriched fractions of burn sites (Figure 4b). Particle sizes in ELV-enriched fractions were not altered in the dISF of burned skin (Figure 4c and Supplementary Materials Figure S2).

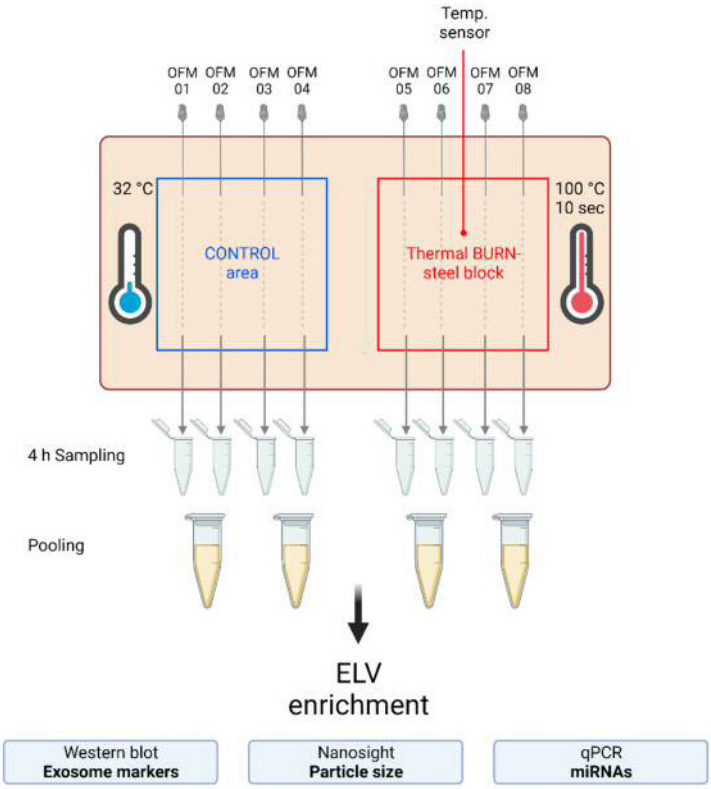

Figure 3. Experimental setup of the dISF sampling with dOFM in an ex vivo human skin model for burn injuries. OFM probes were inserted into ex vivo human skin at the control area (OFM 1–4) and burn area (OFM 5–8), where a steel block of 100 °C was applied for 10 s to provoke a thermal burn. A temperature sensor inserted into the skin enabled the control of temperature at the burn area. OFM was sampled over 4 h. Samples from 2 adjacent probes were pooled. The collected dISF was centrifuged at increasing speeds to enrich ELVs for further experiments.

2.3. After a Burn Injury miR-497-5p Is Downregulated in dISF

Of the 37 miRNAs analyzed as potential regulators of early burn response, 32 were detected by qPCR in the ELV-enriched fractions of dISF, collected within the first 4 h after a burn (Supplementary Materials Figure S3). Five miRNAs could not be detected, namely miR-182-5p, miR-183-5p, miR-302c-3p, miR-367-3p and miR-372-3p. Three miRNAs were altered in ELV-enriched fractions. In tissue and in dISF of burn sites, miRNA-497-5p was downregulated. For miR-218-5p and miR-212-3p, a downregulation was observed in dISF, but not in tissue (Figures 4d and 5).

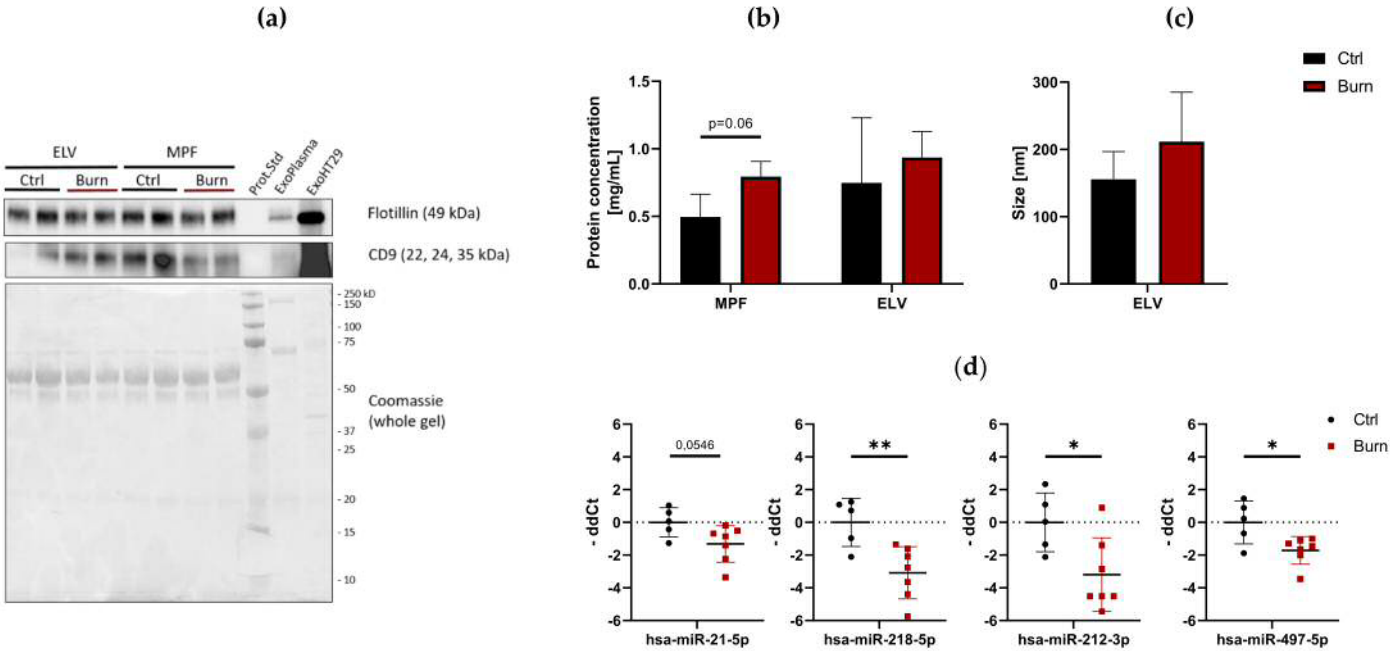

Figure 4. Characterization of dISF in an ex vivo human skin model for burn injuries. (**a**) Western blot for expression of exosomal markers flotillin and CD9. Coomassie staining of the whole gel is displayed as loading control. (**b**) Protein concentration in MPF and ELV and (**c**) mean size (nm) of particles in the ELV. (**d**) MiRNAs differentially expressed in dISF sampled with dOFM. Data are derived from 3 independent experiments and presented as individual values of -ddCt, normalized to an interplate calibrator and expressed relative to controls, with means (line) and standard deviation (whiskers). Significance was tested with Student´s *t*-test, followed by Bonferroni correction; *p*-values <0.05 were considered as statistically significant, with *, ** indicating $p < 0.05$, $p < 0.01$.

We created a potential interaction network (Supplementary Materials Figure S4) of miRNAs in dISF (black and red) with the selected mRNA target genes (blue). The miRNAs found to be differentially regulated in dISF are displayed in red and highlighted by their name next to the interaction point. The miRNAs that showed differential expression were tightly embedded within the network and they were potential regulators of several genes that are differentially regulated in early burn response. For miR-497-5p, five interaction points were recorded; miR-218-5p showed six network interactions; miR-21-5p interacted with four partners; and miR-212-5p had one interaction.

2.4. A Subset of miRNAs and Genes Is Differentially Expressed within the First 24 h in Burned Tissue

The early burn-response genes that we identified through bioinformatics were only available from a mixed pool from biopsies derived from burn injuries from 1 up to 3 days post-burn. We were interested in identifying genes that were deregulated in the first 24 h after burn injury. To study the regulation within the first 24 h after a burn injury, we analyzed a new set of skin biopsies by using an established ex vivo human skin model. Healthy human skin explants from abdominoplastic surgeries were inflicted with a contact burn injury by using a heated steel block [26]. At time points 1, 4 and 24 h after burn injury, skin biopsies were collected, and expression of selected miRNAs (Table 3 and Supplementary Materials Table S2) and mRNAs (Table 3 and Supplementary Materials Table S3) were compared to control samples taken at the same time points.

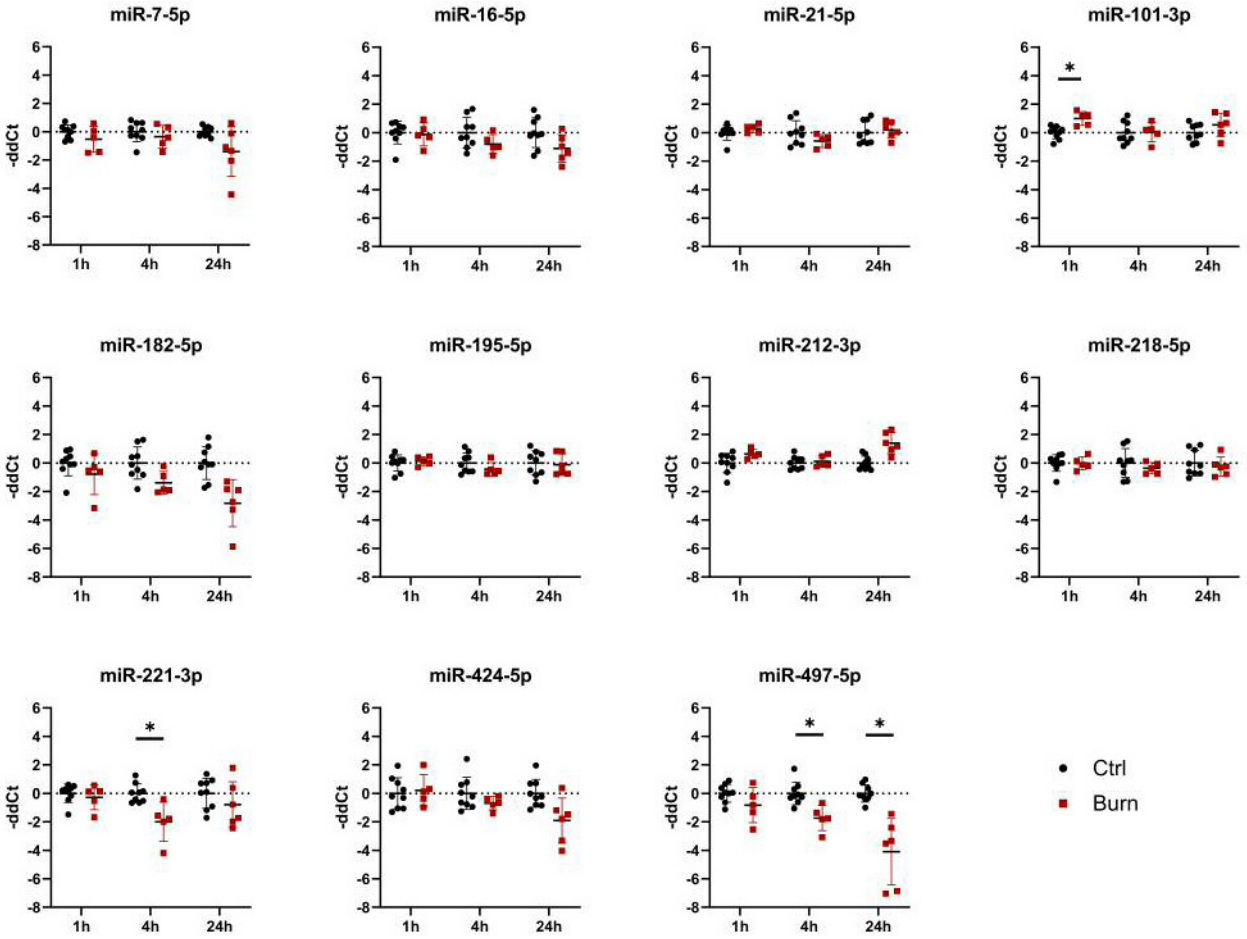

Figure 5. Expression of 11 selected miRNAs in skin biopsies putatively targeting early burn-response genes. Data are derived from 3 independent experiments and presented as individual values of –ddCt, normalized to SNORD 48 and U6 and expressed relative to control, with means (line) and standard deviation (whiskers). Significance was tested with Student´s *t*-test, followed by Bonferroni correction; *p*-values < 0.05 were considered as statistically significant, with * indicating $p < 0.05$.

Table 3. Putative interactions between the analyzed miRNAs and mRNAs. The interactions are based on the TargetScan Human 7.2 search for conserved sites.

	WNT2B	TIMP3	PI15	SOX5	MME	DKK2	TNC	LIPG	MT1G	DDX3Y	SLC2A3
miR-7-5p	x										
miR-16-5p	x			x					x	x	x
miR-21-5p	x	x	x	x							
miR-101-3p										x	
miR-182-5p	x			x		x		x			
miR-195-5p	x			x					x	x	x
miR-212-3p				x							
miR-218-5p	x			x	x	x	x	x			
miR-221-3p		x				x					
miR-424-5p	x			x					x	x	x
miR-497-5p	x			x					x	x	x

In tissue, we analyzed 11 miRNAs out of the 43 miRNAs identified. We analyzed miR-7-5p, miR-16-5p, miR-21-5p, miR-101-3p, miR-182-5p, miR-195-5p, miR-212-3p, miR-

218-5p, miR-221-3p, miR-424-5p and miR-497-5p in tissue biopsies (see Figure 5 and Table 3). We found that all 11 analyzed miRNAs were expressed in skin biopsies, with three of them differentially expressed in a time-dependent manner (Figure 5). Of the 11 analyzed early burn response genes, eight showed differential expression at least at one time point (Figure 6). DEAD-box helicase 3 Y-linked (DDX3Y), peptidase inhibitor 15 (PI15) and endothelial lipase (LIPG) showed upregulation in burned tissue after 1 h. TIMP Metallopeptidase Inhibitor 3 (TIMP3), Dickkopf-related protein 2 (DKK2), membrane metalloendopeptidase (MME), tenascin C (TNC) and solute carrier family 2 member 3 (SLC2A3) showed an increase in expression at 24 h. There were no differences observed for the expressions of WNT2B, a member of the wingless-type MMTV integration site (WNT) family, SRY-Box transcription factor 5 (SOX5) and metallothionein-1G (MT1G) within the first 24 h post-burn (Figure 6).

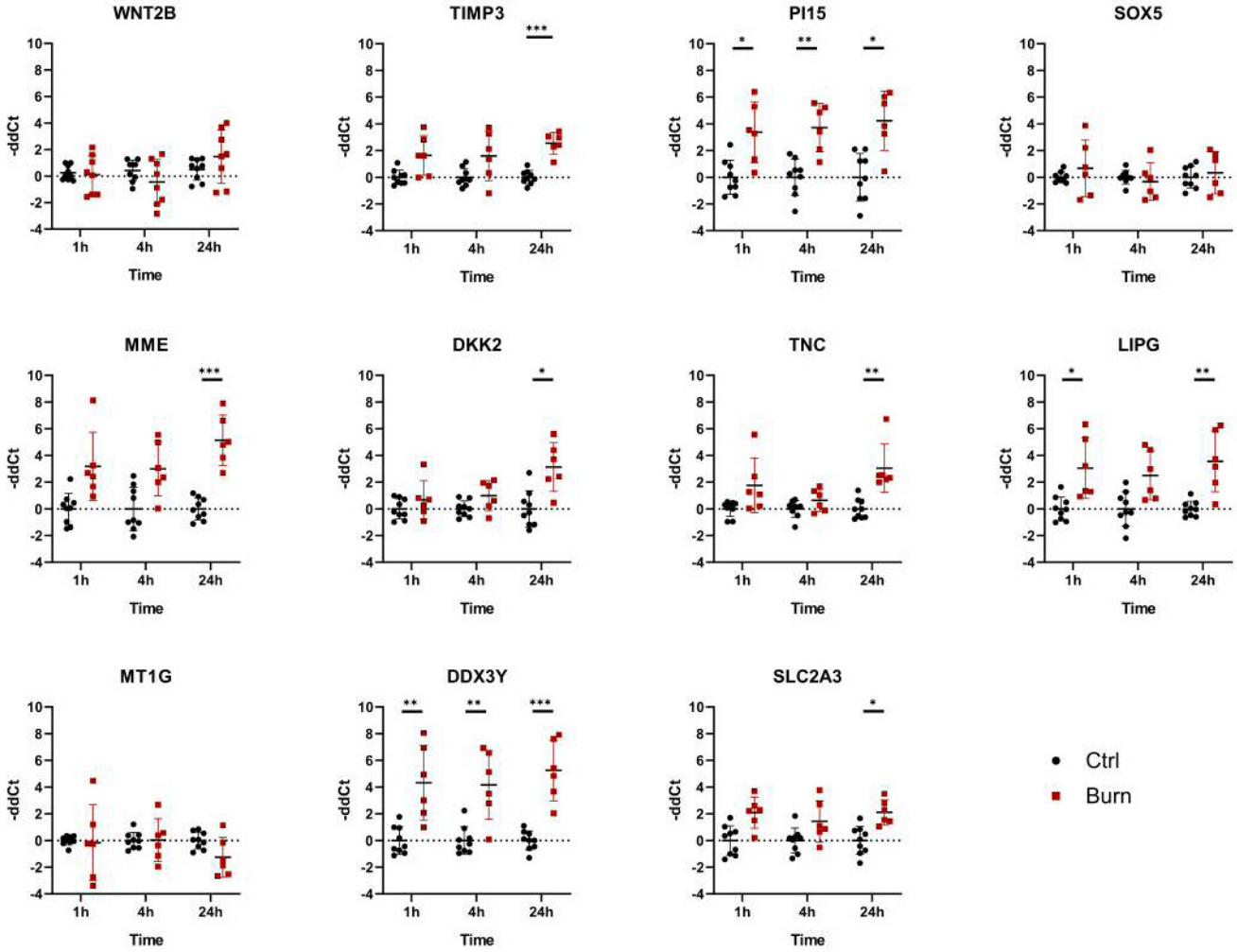

Figure 6. mRNA differential expression in biopsies from burned skin. Data are derived from 3 independent experiments and presented as individual values of –ddCt, normalized to TBP, RPLP0 and GAPDH and displayed relative to control samples, with means (line) and standard deviation (whiskers). Significance was tested with Student´s *t*-test, followed by Bonferroni correction; *p*-values < 0.05 were considered as statistically significant, with *, ** and *** indicating $p < 0.05$, $p < 0.01$ and $p < 0.001$.

2.5. In Burned Skin Tissue miRNAs and Their Potential Targets Are Regulated in a Time-Dependent Manner

In tissue, miR-101-3p was upregulated in the early phase 1 h after the burn stimulus, and its expression declined to control levels at later time points. DDX3Y is one of the genes putatively interacting with miR-101-3p (Table 3). DDX3Y was upregulated in skin biopsies

of burn injuries at 1, 4 and 24 h post-burn (Figure 6). The expression of miR-497-5p, another interaction partner of DDX3Y, was decreasing over time post-burn. Downregulation 4 h after the burn was shown for miR-221-3p, and this was followed by an upregulation of its interaction partners TIMP3 and DKK2 at 24 h after the burn injury. MiR-497-5p was downregulated in tissue 4 h post-burn. Its interaction partners were WNT2B, SOX5, MT1G, DDX3Y and SLC2A3. Among them, DDX3Y was upregulated at all time points, and SLC2A3 was upregulated 24 h post-burn.

3. Discussion

In this study, we analyzed miRNAs and gene expression of the early burn response in human skin tissue after a deep partial-thickness burn. Gaining insight into local tissue alterations in the early phase of skin burns could identify biomarkers for evidence-based treatment options. To overcome the struggle of clinical sample collection in vivo, we used an established ex vivo human skin model for burn injuries. This allowed us to study the early phase after a burn in a time-dependent manner. In order to screen for biomarkers in the skin without having to take invasive tissue samples, we focused on dISF, a fluid that is accessible with the minimally invasive dOFM method. We chose dISF instead of other body fluids, such as plasma, due to the close contact of dISF with the skin cells which enables a better representation of local conditions.

In our model, miR-497-5p was continuously downregulated in the tissue 1, 4 and 24 h post-burn, and this downregulation was reflected in dISF. Of note, miR-497-5p has been reported as a regulator of fibroblast viability. Recent work showed that miR-497-5p was upregulated in hypertrophic scars [30], which often occur after burn injuries [31]. In malignant melanoma tissues, miR-497-5p was found significantly downregulated [32]. Various cancer studies reported miR-497-5p as a tumor regulator [32–34], potentially through its regulatory effects on NF-κB [35] and FGF-2 signaling [36]. Hofmann et. al. were able to show that FGF2 was upregulated to a similar extent, while miR-497-5p was downregulated in our study [26]. Effective downregulation of miR-497-5p may therefore be an indicator for the regeneration capacity of a burn injury.

We found miR-21-5p downregulated in dISF of partial-thickness burns, but not in skin biopsies. A potential source of miR-21 might be mesenchymal stem cells, since miR-21 is known to regulate adipogenic differentiation through TGF-β signaling [37]. In healthy skin, miR-21 was found highly expressed in adipocytes and sebaceous glands, but not in the epidermis of mice. In the same study, during wound healing of full-thickness skin excisions, miR-21 was found highly expressed in the epidermis around the wound, especially at the sites where epithelial cells were migrating. In granulation tissue, miR-21 was also found upregulated in mesenchymal cells. Furthermore, miR-21-antagomir was shown to inhibit wound healing in mice by inhibiting collagen deposition [38]. MiR-21 is also reportedly upregulated in many cancer types [39,40]. This might indicate a contribution of miR-21-5p to the wound healing of burns. The skin cells might take up part of the surrounding miR-21-3p to support cell growth and migration.

We found miR-218-5p downregulated in dISF of burn injuries. MiR-218-5p was reported to enhance apoptosis by targeting secreted frizzled-related protein 2 (SFRP2), which, in turn, is an activator of the Wnt signaling pathway [41]. We did not observe alterations in WNT2B expression in the skin tissue within the first 24 h post-burn in our study. MiR-218 increased apoptotic cell death in the context of lung cancer [42]. Local downregulation of miR-218-5p could decrease apoptosis in the skin, thereby acting as a protection mechanism against cell death.

In our study of deep partial-thickness burns, we found miR-221-3p downregulated in tissue 4 h post-burn. This resembles the findings of Liang et al. in denatured dermal tissue of deep burn patients, where a profile of 66 miRNAs was found altered, including a downregulation of miR-221 [16] at day four post-burn. MiR-221-3p is reportedly downregulated in human skin fibroblasts exposed to bacterial lipopolysaccharides (LPS), a model for infected skin wounds, and overexpression of miR-221-3p reduced the negative effect of

LPS on cell growth [43]. In the serum of psoriatic patients, miR-221-3p was upregulated, and lower expression inhibited cell growth in culture [44]. Therefore, miR-221-3p might be a regulator of fibroblast regeneration. This is supported by the fact that miR-221 was found downregulated in keloid skin tissue [15]. The control of miR-221-3p levels may be beneficial for the recovery of skin from inflammatory processes. Our data show that miR-221-3p was downregulated 4 h post-burn, and the levels were restored to control levels at 24 h, which is controversial to the findings of Liang et al. which showed its downregulation in burned skin after 4 days in denatured dermis of deep burn wounds. We thus speculate that miR-221-3p might be a candidate marker for the severity of burns. To clarify that, further experiments are needed to elucidate the expression of miR-221-3p over time in different degrees of burn wounds.

In another study, one in which human dermal fibroblasts were heat-shocked and their altered miRNA-expression was determined, neither the expression of miR-221-3p nor miR-497-5p was altered [45], indicating that other cells in human skin might be the source of these two miRNAs. Extracellular miR-497-3p could derive from Langerhans-cells, dendritic cells, or T-cells in the skin [46] as paracrine signal to the tissue.

In the tissue, 1 h after the burn stimulus, miR-101-3p was upregulated, and its expression declined to control levels at later time points. MiR-101-3p might thus be an early response regulator of skin burns, potentially by fine-tuning the upregulation of its interaction partner DDX3Y in the first hour after a burn.

Little is known about miRNA expression in the early phase after a partial-thickness burn injury. Guided by a bioinformatics approach, we identified potential miRNA–mRNA interaction partners of the early burn response. We are aware that this biased approach holds its limitations. However, we chose it to identify miRNAs that might specifically target genes of the early burn response, allowing for the exclusion of genetic noise that is a great struggle with unbiased methods, such as miRNA sequencing [47]. A combination of target prediction tools in order to minimize false-positive findings by in silico approaches has previously been described [48].

In line with the observation of a general upregulation of genes in burned skin in the here-analyzed GEO dataset and in the literature [49], we found most miRNAs in our analysis downregulated. Whether this downregulation of miRNAs is an active regulatory mechanism or a secondary effect needs further investigation. In our study, TIMP3, DKK2, MME, TNC and SLC2A3 showed an increase in expression only at 24 h, indicating that there is a time dependency in the onset of the upregulation of certain genes. That might also explain why we could not find differences in the expressions of WNT2B, SOX5 and MT1G while there was a difference in the GEO-dataset analyzed. Since the timeframes of sampling are different for the two analyses, namely 3 days for the GEO-dataset and 24 h for the skin burn model, these latter genes might only be upregulated at time points later than 1 day.

MiRNAs can act as intercellular messengers [50,51] and are packed in ELVs for that purpose [52]. Those ELVs are then released into the extracellular fluid [18]. Therefore, we claim that dISF is the ideal fluid to examine such intercellular communication via miRNAs, in the context of signaling from skin injuries. Motivated by the growing interest of the scientific community in minimally invasive sampling, we analyzed the feasibility of dOFM as a tool for the sampling of miRNAs and their further analysis. MiRNAs in extracellular body fluids are found to be surprisingly well protected from RNase degradation. They are packed into exosomes and protected by carrier proteins [34]. Exosomes and their miRNA cargo have been reported to impair wound healing and epidermal differentiation in mouse models [53]. Furthermore, they are mediators in the cellular crosstalk between fibroblasts and keratinocytes in skin aging [22]. However, little is known about their function in the early burn response. As carriers of miRNAs, they might play pivotal roles in the local cellular response to a burn stimulus and could serve as potential biomarkers.

We were able to show the presence of ELVs in dISF of burned skin. The dilution of the dISF as a result of the sampling method led to low concentrations in the final samples; thus,

isolation methods should be further improved. Both fractions with possible ELV content stained positive for the exosomal markers flotillin and CD9 and showed a characteristic size pattern, as determined by nanoparticle tracking analysis. We did not find any major differences in ELV size and count but we observed a tendency towards an increase in protein concentration in the MVP fraction post-burn. This might be caused by an increased secretion of proteins and ELVs from the heat-stressed tissue [54]. However, further research is needed to investigate the contribution of ELVs in detail in the context of burn injuries.

In this work, we showed the presence of miRNAs in dISF and suggest miRNA-497-5p as a potential biomarker for the early burn response. We are aware that this study holds general limitations. One limiting factor is the small sample size in the bioinformatics analysis, as well as the limited amount of ex vivo skin model samples. The stringent inclusion criteria of $p_{adj} < 0.001$ for the selection of the early burn response genes was chosen to reliably identify targeting miRNAs. Based on our data presented in this manuscript, a follow-up study with skin samples collected at days 0–3 post-burn should be conducted to sequence mRNA, as well as miRNA from tissue, dISF and serum miRNAs from the same patients in order to elucidate the feasibility of miR-497-5p and other miRNAs as biomarkers for the early burn response.

To conclude, this study has identified miRNAs that are potentially involved in the early burn-response gene regulation. We found miRNA-497-5p, a known regulator of skin cell regeneration, downregulated in tissue and dISF of burned skin. Therefore, we propose the further examination of miR-497-5p as a biomarker for the severity of burn wounds, potentially through signaling via ELVs.

4. Materials and Methods

4.1. Tissue Samples

Fresh abdominal human skin explants from adult Caucasian donors were obtained from 10 donors, with a mean age of 36 (range = 51–25; 8 females and 2 males) undergoing abdominoplasty or circumferential body-lift surgery at the Division of Plastic, Aesthetic and Reconstructive Surgery, Department of Surgery, Medical University of Graz, Austria. The subcutaneous lipid layer and skin integrity of the skin explants were kept intact to ensure maximum resemblance to the in vivo situation.

Study approval was given by the Ethical Committee of the Medical University of Graz, Austria (EK: 28-151 ex 15/16; approval extended until 22 December 2020). All subjects gave written informed consent. The tissue transport and pseudonymization was carried out by Biobank Graz (Medical University of Graz, Austria). The study was carried out in accordance with the principles of the Declaration of Helsinki.

4.2. Human Skin-Burn Injury Ex Vivo Model and Dermal Open Flow Microperfusion (dOFM)

For a detailed description of the previously described method, please refer to References [26,55]. Shortly, fresh skin explants were cleaned by using gauze and water and immobilized with cannulas on a plastic-wrapped polystyrene plate. Then dOFM implantation sites were marked by using a stencil and a permanent marker. After that, dOFM probes were inserted with the help of guide cannulas. To monitor the dermal temperature, a temperature sensor was inserted and connected to a temperature data logger. Implantation sites were sealed with cyanoacrylate adhesive. The dOFM probes were connected to the tubing, the filled perfusate bags and the peristaltic pumps. Between the outlet of the dOFM probe and the pull tubing, a sampling tube was connected. At the run-in phase, dOFM probes were flushed with a flow rate of 10 µL/min for a maximum of 5 min. Afterwards, the flow rate was reduced to 1 µL/min. After 30 min, the run-in samples were discarded, and the regular sampling tubes were attached. For the burn stimulus, a preheated (100 °C) stainless-steel block of 5 × 5 cm, 1.9 kg (Zultner Metall GmbH, Graz, Austria), was placed on the skin for 10 s, without additional pressure. Sampling was performed for 4 h. At 1, 4 and 24 h, biopsies were taken from the burned sites and from the control areas. Biopsy material was snap-frozen on dry ice and stored at −80 °C until further processing.

4.3. Gene-Expression Data Analysis and Selection of miRNA-Targets

Data freely available on the GEO gene expression omnibus database [27] were screened for miRNA expression in the early phase, preferably within the first days, of deep partial-thickness skin burns. Since such miRNA expression data were absent, our search was extended to RNA expression. The most suitable dataset found was "Gene Expression Profiles in Thermally Injured Human Skin: A Temporal Microarray Analysis" with the accession number GSE8056 from Greco et al. (2010) [25], who analyzed it in silico. From the total of 12 samples in the microarray dataset, the 3 datasets "normal human skin, pooled replicate #1–3 of normal (no thermal injury) skin control" with accessions GSM198875, GSP198876 and GSM198877 were selected as controls. These were compared to the samples "burn wound margin of human skin, replicate #1–3 of pooled time group 0–3 days post-thermal injury" with accessions GSM198866, GSM198867 and GSM198868. Differential expressions between control and burn samples were determined with GEO2R with log-transformed data, calculating false discovery rate (Benjamini–Hochberg adjusted *p*-values, p_{adj}). Significance level cutoff was set at 0.001. Visualization of the GEO2R analysis is depicted in Supplementary Materials Figure S1. The genes with an adjusted *p*-value of <0.001 were analyzed with TargetScanHuman 7.2 [24] for conserved sites for miRNA families broadly conserved among vertebrates and with miRWalk 2.0 [56]. The interactive interaction network (Supplementary Materials Figure S4) was created with RStudio (2020, Integrated Development for R. RStudio, PBC, Boston, MA, USA) and the networkD3 package.

4.4. RNA Extraction and qPCR

Homogenization of skin biopsies was performed in Qiazol, using MagNa Lyser Beads and the MagNA Lyser instrument (Roche, Basel, Switzerland). RNA was isolated with RNAeasy Lipid Tissue Mini Kit (Qiagen, Hilden, Germany) immediately after homogenization, according to the manufacturer's instructions. RNA concentration was determined on a NanoDrop microvolume spectrophotometer (Thermo Fisher Scientific, MA, USA). For cDNA synthesis (iScript gDNA clear kit, Biorad, CA, USA) 0.5–1 µg of total RNA was used. Predesigned TaqMan assays for the genes of interest and the endogenous control genes (Supplementary Materials Table S3) and the TaqMan Gene Expression Master Mix were purchased from Thermo Fisher Scientific, MA, USA. For miRNA expression from tissue, RNA was extracted with RNeasy Mini Kit including Spike-In controls, and cDNA synthesis was performed with miRCURY LNA RT Kit and miRCURY LNA SYBR Green PCR Kit was used with predesigned miRCURY LNA miRNA PCR Assays (Supplementary Materials Table S2) (all from Qiagen, Hilden, Germany).

MiRNA extraction from ELV fractions was performed with an miRNeasy Serum/Plasma Advanced Kit, according to manufacturer's protocol, including Spike-In controls (UniSp2, UniSp4 and UniSp5), followed by cDNA synthesis with miRCURY LNA RT Kit (including Spike-Ins UniSp6 and cel-miR-39-5p). For qPCR, the miRCURY LNA SYBR Green PCR Kit was used with miRCURY LNA miRNA PCR Assays (all from Qiagen, Hilden, Germany) (Supplementary Materials Table S2), according to the manufacturer's instructions.

4.5. qPCR Analysis

Relative gene expression was calculated by using the minus delta–delta Ct (-ddCt) method [57]. For gene expression in tissue, target gene expression was normalized to the averaged Cq of the three endogenous control genes (TPB, RPLP0 and GAPDH). For miRNA expression in tissue, the averages of SNORD48 and U6 were used for normalization. For miRNAs in dISF, samples were calibrated with an interplate calibrator. Spike-ins were used to determine the quality and homogeneity of RNA extraction and cDNA preparation.

Expression levels were determined as duplicates from samples of at least three independent experiments. Individual values were calibrated to the average of the control samples and are presented as individual -ddCt values with mean (line) and standard devi-

ation (whiskers). All qPCR experiments were run on a CFX384 cycler (Bio-Rad, Hercules, CA, USA), using standard conditions, according to the manufacturer's instructions.

4.6. Sample Processing and ELV Enrichment

After 4 h of dOFM sampling from ex vivo skin explants, perfusates were stored at 4 °C and processed immediately. A perfusate volume of approximately 60 µL/probe/hour was collected. ISF was pooled from 2 adjacent probes in order to get a sufficient sample amount for further processing. Occasional blood smears were not aspirated, and hemolytic samples were carefully recorded by visual assessment. To remove debris, ISF was centrifuged at 500× *g* for 30 min. All centrifugation steps were performed at 4 °C. To remove apoptotic bodies (ApoBD) and cell fragments, supernatant was transferred to a fresh tube and centrifuged at 2000× *g* for 20 min. To pellet microvesicles, the supernatant was transferred to a fresh tube. Then 50 µL was removed as mixed particle fraction (MPF), and the remaining supernatant was centrifuged at 20,000× *g* for 70 min. The non-visible pellets from each centrifugation step (except the debris) were resuspended in 50 µL sterile-filtered PBS and stored at 4 °C overnight for nanoparticle tracking. For RNA extraction, the samples were frozen at −20 °C for short-term storage.

4.7. Nanoparticle Tracking Analysis

For nanoparticle tracking, dISF samples collected by OFM were stored at 4 °C overnight and measured the next day. MVP and ELV fractions were diluted with filtered deionized water (Whatman Anotop® 25 Plus syringe filter, pore size 20 nm) 1:10 or 1:20 (v/v), depending on particle concentration. Samples were measured with the NanoSight LM10 (Malvern Panalytical Ltd., Kassel, Germany) with a 532 nm (green) laser at 25 °C, with the following settings: camera level 14, slide shutter at 1239, slider gain 366, number of frames 1499 and script SOP standard measurement. Five independent measurements were taken and analyzed for average particle properties in terms of size and numbers.

4.8. Protein Concentration and Immunoblot Analysis

Protein concentration was determined with Bio-Rad Protein Assay Dye Reagent (Bio-Rad Laboratories GmbH, Vienna, Austria), according to manufacturer's protocol. Then 13.5 µg of protein was separated by SDS–PAGE and transferred to a PVDF membrane (Bio-Rad Laboratories GmbH, Vienna, Austria). Protein detection was performed with monoclonal antibodies for CD9 ((D8O1A) Rabbit mAb #13174) and flotillin-1 ((D2V7J) XP Rabbit mAb #18634) (Cell Signalling Technology, Boston, MA, USA). Specific antibodies were detected by an HRP-conjugated goat anti-rabbit antibody (Anti-rabbit IgG, HRP-linked Antibody #7074, Cell Signalling Technology, Boston, MA, USA). For loading control, Coomassie Blue staining of the membrane was performed. Bands were visualized by ChemiDoc™system with Clarity™ substrate (Bio-Rad Laboratories GmbH, Vienna, Austria).

4.9. Statistical Analysis

Statistical analysis was performed by using the software GraphPad Prism (version 8.0, San Diego, CA, USA). Data are presented as mean +/− SD. Two-sided Student's *t*-test, followed by Bonferroni correction, was used to compare the data. A $p < 0.05$ was considered statistically significant, with *, ** and *** indicating $p < 0.05$, $p < 0.01$ and $p < 0.001$ in the graphs.

Supplementary Materials: The following are available online at https://www.mdpi.com/article/10.3390/ijms22179209/s1. Figure S1: Visualization of the GEO2R analysis performed in the GSE8056 microarray-dataset for control vs. burn with significance level cut-off at $p_{adj} < 0.001$. Figure S2: Size distribution of particles in dISF of an ex vivo skin model for burn injuries. Figure S3: Characterization of miRNAs in dISF in an ex vivo human skin model for burn injuries—all analysed miRNAs. Figure S4: Interaction network of miRNAs (black and red) with the selected mRNA target genes

(blue). Table S1: miRNAs with the number of interactions based on 2 different tools that were considered as putative early burn response regulators. Table S2: Selected miRNAs for gene expression analysis. Table S3: TaqMan assays used for gene expression analysis with qPCR.

Author Contributions: Conceptualization, I.F., E.H., B.O.-P., T.B. and P.K.; data curation, I.F., C.W.H., J.F. and S.K.; formal analysis, I.F., C.W.H., I.V. and J.F.; investigation, I.F.; methodology, I.F., I.V., R.P., S.I.M., S.K., E.H. and P.K.; project administration, B.O.-P. and P.K.; resources, R.P., B.O.-P., T.B. and P.K.; software, C.W.H.; supervision, R.P., S.I.M., B.O.-P., T.B. and P.K.; visualization, C.W.H.; writing—original draft, I.F.; writing—review and editing, I.F.,C.W.H., I.V., R.P., J.F., S.I.M., S.K., E.H., B.O.-P., T.B. and P.K. All authors have read and agreed to the published version of the manuscript.

Funding: This work was supported by the Austrian Science Fund FWF (DK MOLIN-W1241).

Institutional Review Board Statement: The study was conducted according to the guidelines of the Declaration of Helsinki and approved by the Ethical Committee of the Medical University of Graz, Austria (EK: 28-151 ex 15/16; approval extended until 22 December 2020).

Informed Consent Statement: Informed consent was obtained from all subjects involved in the study.

Data Availability Statement: Data freely available on the GEO gene expression omnibus database [27] on "Gene Expression Profiles in Thermally Injured Human Skin: A Temporal Microarray Analysis" with the accession number GSE8056 from Greco et al. (2010) [25] were analyzed in silico.

Acknowledgments: We thank K. Bounab for technical support and J. van de Peppel and V. Francic for advice and discussions. Figure 3 was created with biorender.com.

Conflicts of Interest: The authors declare no conflict of interest.

References

1. Schwacha, M.G. Macrophages and post-burn immune dysfunction. *Burns* **2003**, *29*, 1–14. [CrossRef]
2. Plackett, T.P.; Colantoni, A.; Heinrich, S.A.; Messingham, K.A.N.; Gamelli, R.L.; Kovacs, E.J. The early acute phase response after burn injury in mice. *J. Burn Care Res.* **2007**, *28*, 167–172. [CrossRef]
3. Nielson, C.B.; Duethman, N.C.; Howard, J.M.; Moncure, M.; Wood, J.G. Burns: Pathophysiology of Systemic Complications and Current Management. *J. Burn Care Res.* **2017**, *38*, e469–e481. [CrossRef]
4. Kallinen, O.; Maisniemi, K.; Böhling, T.; Tukiainen, E.; Koljonen, V. Multiple organ failure as a cause of death in patients with severe burns. *J. Burn Care Res.* **2012**, *33*, 206–211. [CrossRef] [PubMed]
5. Jeschke, M.G. Postburn hypermetabolism: Past, present, and future. *J. Burn Care Res.* **2016**, *37*, 86–96. [CrossRef] [PubMed]
6. Auger, C.; Samadi, O.; Jeschke, M.G. The biochemical alterations underlying post-burn hypermetabolism. *Biochim. Biophys. Acta-Mol. Basis Dis.* **2017**, *1863*, 2633–2644. [CrossRef]
7. Barret, J.P.; Herndon, D.N. Modulation of inflammatory and catabolic responses in severely burned children by early burn wound excision in the first 24 hours. *Arch. Surg.* **2003**, *138*, 127–132. [CrossRef] [PubMed]
8. Hoeksema, H.; Van de Sijpe, K.; Tondu, T.; Hamdi, M.; Van Landuyt, K.; Blondeel, P.; Monstrey, S. Accuracy of early burn depth assessment by laser Doppler imaging on different days post burn. *Burns* **2009**, *35*, 36–45. [CrossRef] [PubMed]
9. Condrat, C.E.; Thompson, D.C.; Barbu, M.G.; Bugnar, O.L.; Boboc, A.; Cretoiu, D.; Suciu, N.; Cretoiu, S.M.; Voinea, S.C. miRNAs as Biomarkers in Disease: Latest Findings Regarding Their Role in Diagnosis and Prognosis. *Cells* **2020**, *9*, 276. [CrossRef]
10. Solvin, Å.Ø.; Chawla, K.; Olsen, L.C.; Danielsen, K.; Jenssen, M.; Furberg, A.S.; Saunes, M.; Hveem, K.; Sætrom, P.; Løset, M. RNA sequencing of a large number of psoriatic patients identifies 131 novel miRNAs and 11 miRNAs associated with disease severity. *medRxiv* **2021**. [CrossRef]
11. Srivastava, A.; Meisgen, F.; Pasquali, L.; Munkhammar, S.; Xia, P.; Ståhle, M.; Landén, N.X.; Pivarcsi, A.; Sonkoly, E. Next-Generation Sequencing Identifies the Keratinocyte-Specific miRNA Signature of Psoriasis. *J. Investig. Dermatol.* **2019**, *139*, 2547–2550.e12. [CrossRef]
12. Lerman, G.; Avivi, C.; Mardoukh, C.; Barzilai, A.; Tessone, A.; Gradus, B.; Pavlotsky, F.; Barshack, I.; Polak-Charcon, S.; Orenstein, A.; et al. MiRNA expression in psoriatic skin: Reciprocal regulation of hsa-miR-99a and IGF-1R. *PLoS ONE* **2011**, *6*, e20916. [CrossRef]
13. Suárez-Fariñas, M.; Ungar, B.; Correa Da Rosa, J.; Ewald, D.A.; Rozenblit, M.; Gonzalez, J.; Xu, H.; Zheng, X.; Peng, X.; Estrada, Y.D.; et al. RNA sequencing atopic dermatitis transcriptome profiling provides insights into novel disease mechanisms with potential therapeutic implications. *J. Allergy Clin. Immunol.* **2015**, *135*, 1218–1227. [CrossRef]
14. Polak, M.E. Early life regulation of inflammation in atopic dermatitis by microRNA. *Br. J. Dermatol.* **2021**, *184*, 391–392. [CrossRef] [PubMed]
15. Liu, Y.; Yang, D.; Xiao, Z.; Zhang, M. MiRNA expression profiles in keloid tissue and corresponding normal skin tissue. *Aesthetic Plast. Surg.* **2012**, *36*, 193–201. [CrossRef] [PubMed]

16. Liang, P.; Lv, C.; Jiang, B.; Long, X.; Zhang, P.; Zhang, M.; Xie, T.; Huang, X. MicroRNA profiling in denatured dermis of deep burn patients. *Burns* **2012**, *38*, 534–540. [CrossRef] [PubMed]
17. Singhvi, G.; Manchanda, P.; Krishna Rapalli, V.; Kumar Dubey, S.; Gupta, G.; Dua, K. MicroRNAs as biological regulators in skin disorders. *Biomed. Pharmacother.* **2018**, *108*, 996–1004. [CrossRef]
18. Mori, M.A.; Ludwig, R.G.; Garcia-Martin, R.; Brandão, B.B.; Kahn, C.R. Extracellular miRNAs: From Biomarkers to Mediators of Physiology and Disease. *Cell Metab.* **2019**, *30*, 656–673. [CrossRef] [PubMed]
19. Turchinovich, A.; Weiz, L.; Langheinz, A.; Burwinkel, B. Characterization of extracellular circulating microRNA. *Nucleic Acids Res.* **2011**, *39*, 7223–7233. [CrossRef] [PubMed]
20. Miller, P.R.; Taylor, R.M.; Tran, B.Q.; Boyd, G.; Glaros, T.; Chavez, V.H.; Krishnakumar, R.; Sinha, A.; Poorey, K.; Williams, K.P.; et al. Extraction and biomolecular analysis of dermal interstitial fluid collected with hollow microneedles. *Commun. Biol.* **2018**, *1*, 173. [CrossRef]
21. Bodenlenz, M.; Aigner, B.; Dragatin, C.; Liebenberger, L.; Zahiragic, S.; Höfferer, C.; Birngruber, T.; Priedl, J.; Feichtner, F.; Schaupp, L.; et al. Clinical applicability of dOFM devices for dermal sampling. *Ski. Res. Technol.* **2013**, *19*, 474–483. [CrossRef] [PubMed]
22. Terlecki-Zaniewicz, L.; Pils, V.; Bobbili, M.R.; Lämmermann, I.; Perrotta, I.; Grillenberger, T.; Schwestka, J.; Weiß, K.; Pum, D.; Arcalis, E.; et al. Extracellular Vesicles in Human Skin: Cross-Talk from Senescent Fibroblasts to Keratinocytes by miRNAs. *J. Investig. Dermatol.* **2019**, *139*, 2425–2436.e5. [CrossRef] [PubMed]
23. Liu, J.; Yan, Z.; Yang, F.; Huang, Y.; Yu, Y.; Zhou, L.; Sun, Z.; Cui, D.; Yan, Y. Exosomes Derived from Human Umbilical Cord Mesenchymal Stem Cells Accelerate Cutaneous Wound Healing by Enhancing Angiogenesis through Delivering Angiopoietin-2. *Stem Cell Rev. Rep.* **2021**, *17*, 305–317. [CrossRef] [PubMed]
24. Agarwal, V.; Bell, G.W.; Nam, J.W.; Bartel, D.P. Predicting effective microRNA target sites in mammalian mRNAs. *Elife* **2015**, *4*. [CrossRef] [PubMed]
25. Greco, J.A.; Pollins, A.C.; Boone, B.E.; Levy, S.E.; Nanney, L.B. A microarray analysis of temporal gene expression profiles in thermally injured human skin. *Burns* **2010**, *36*, 192–204. [CrossRef]
26. Hofmann, E.; Fink, J.; Eberl, A.; Prugger, E.M.; Kolb, D.; Luze, H.; Schwingenschuh, S.; Birngruber, T.; Magnes, C.; Mautner, S.I.; et al. A novel human ex vivo skin model to study early local responses to burn injuries. *Sci. Rep.* **2021**, *11*, 364. [CrossRef]
27. Barrett, T.; Wilhite, S.E.; Ledoux, P.; Evangelista, C.; Kim, I.F.; Tomashevsky, M.; Marshall, K.A.; Phillippy, K.H.; Sherman, P.M.; Holko, M.; et al. NCBI GEO: Archive for functional genomics data sets—Update. *Nucleic Acids Res.* **2013**, *41*, D991–D995. [CrossRef]
28. Kolbinger, F.; Loesche, C.; Valentin, M.A.; Jiang, X.; Cheng, Y.; Jarvis, P.; Peters, T.; Calonder, C.; Bruin, G.; Polus, F.; et al. β-Defensin 2 is a responsive biomarker of IL-17A–driven skin pathology in patients with psoriasis. *J. Allergy Clin. Immunol.* **2017**, *139*, 923–932.e8. [CrossRef]
29. Bodenlenz, M.; Tiffner, K.I.; Raml, R.; Augustin, T.; Dragatin, C.; Birngruber, T.; Schimek, D.; Schwagerle, G.; Pieber, T.R.; Raney, S.G.; et al. Open Flow Microperfusion as a Dermal Pharmacokinetic Approach to Evaluate Topical Bioequivalence. *Clin. Pharmacokinet.* **2017**, *56*, 91–98. [CrossRef]
30. Li, Z.; Wang, P.; Zhang, J.; Zhao, D. MicroRNA-497-5p downregulation inhibits cell viability, reduces extracellular matrix deposition and induces apoptosis in human hyperplastic scar fibroblasts by regulating Smad7. *Exp. Ther. Med.* **2021**, *21*, 1–8. [CrossRef]
31. Finnerty, C.C.; Jeschke, M.G.; Branski, L.K.; Barret, J.P.; Dziewulski, P.; Herndon, D.N. Hypertrophic scarring: The greatest unmet challenge after burn injury. *Lancet* **2016**, *388*, 1427–1436. [CrossRef]
32. Chai, L.; Kang, X.J.; Sun, Z.Z.; Zeng, M.F.; Yu, S.R.; Ding, Y.; Liang, J.Q.; Li, T.T.; Zhao, J. MiR-497-5p, miR-195-5p and miR-455-3p function as tumor suppressors by targeting hTERT in melanoma A375 cells. *Cancer Manag. Res.* **2018**, *10*, 989–1003. [CrossRef] [PubMed]
33. Huang, C.; Ma, R.; Yue, J.; Li, N.; Li, Z.; Qi, D. MiR-497 suppresses YAP1 and inhibits tumor growth in non-small cell lung cancer. *Cell. Physiol. Biochem.* **2015**, *37*, 342–352. [CrossRef] [PubMed]
34. Yang, G.; Xiong, G.; Cao, Z.; Zheng, S.; You, L.; Zhang, T.; Zhao, Y. miR-497 expression, function and clinical application in cancer. *Oncotarget* **2016**, *7*, 55900–55911. [CrossRef] [PubMed]
35. Wei, W.; Zhang, W.Y.; Bai, J.B.; Zhang, H.X.; Zhao, Y.Y.; Li, X.Y.; Zhao, S.H. The NF-κB-modulated microRNAs miR-195 and miR-497 inhibit myoblast proliferation by targeting Igf1r, Insr and cyclin genes. *J. Cell Sci.* **2016**, *129*, 39–50. [CrossRef] [PubMed]
36. Huang, X.; Wang, L.E.I.; Liu, W.E.I.; Li, F.E.I. MicroRNA-497-5p inhibits proliferation and invasion of non-small cell lung cancer by regulating FGF2. *Oncol. Lett.* **2019**, *17*, 3425–3431. [CrossRef]
37. Jeong Kim, Y.; Jin Hwang, S.; Chan Bae, Y.; Sup Jung, J. MiR-21 regulates adipogenic differentiation through the modulation of TGF-β signaling in mesenchymal stem cells derived from human adipose tissue. *Stem Cells* **2009**, *27*, 3093–3102. [CrossRef]
38. Wang, T.; Feng, Y.; Sun, H.; Zhang, L.; Hao, L.; Shi, C.; Wang, J.; Li, R.; Ran, X.; Su, Y.; et al. MiR-21 regulates skin wound healing by targeting multiple aspects of the healing process. *Am. J. Pathol.* **2012**, *181*, 1911–1920. [CrossRef]
39. Wu, Y.; Song, Y.; Xiong, Y.; Wang, X.; Xu, K.; Han, B.; Bai, Y.; Li, L.; Zhang, Y.; Zhou, L. MicroRNA-21 (Mir-21) Promotes Cell Growth and Invasion by Repressing Tumor Suppressor PTEN in Colorectal Cancer. *Cell. Physiol. Biochem.* **2017**, *43*, 945–958. [CrossRef]

40. Ourô, S.; Mourato, C.; Velho, S.; Cardador, A.; Ferreira, M.P.; Albergaria, D.; Castro, R.E.; Maio, R.; Rodrigues, C.M.P. Potential of miR-21 to Predict Incomplete Response to Chemoradiotherapy in Rectal Adenocarcinoma. *Front. Oncol.* **2020**, *10*, 2212. [CrossRef]
41. Zhao, B.; Chen, Y.; Yang, N.; Chen, Q.; Bao, Z.; Liu, M.; Hu, S.; Li, J.; Wu, X. miR-218-5p regulates skin and hair follicle development through Wnt/β-catenin signaling pathway by targeting SFRP2. *J. Cell. Physiol.* **2019**, *234*, 20329–20341. [CrossRef]
42. Shi, Z.M.; Wang, L.; Shen, H.; Jiang, C.F.; Ge, X.; Li, D.M.; Wen, Y.Y.; Sun, H.R.; Pan, M.H.; Li, W.; et al. Downregulation of miR-218 contributes to epithelial-mesenchymal transition and tumor metastasis in lung cancer by targeting Slug/ZEB2 signaling. *Oncogene* **2017**, *36*, 2577–2588. [CrossRef] [PubMed]
43. Wang, Y.; Wang, C. microRNA-211-3p has a Role in the Effects of Lipopolysaccharide on Endoplasmic Reticulum Stress in Cultured Human Skin Fibroblasts. *Med. Sci. Monit. Basic Res.* **2019**, *25*, 164–168. [CrossRef] [PubMed]
44. Meng, Z.; Qiu, J.; Zhang, H. MiR-221-3p as a Potential Biomarker for Patients with Psoriasis and Its Role in Inflammatory Responses in Keratinocytes. *Skin Pharmacol. Physiol.* **2021**, 1–7. [CrossRef]
45. Wilmink, G.J.; Roth, C.L.; Ibey, B.L.; Ketchum, N.; Bernhard, J.; Cerna, C.Z.; Roach, W.P. Identification of microRNAs associated with hyperthermia-induced cellular stress response. *Cell Stress Chaperones* **2010**, *15*, 1027–1038. [CrossRef]
46. Mueller, S.N.; Zaid, A.; Carbone, F.R. Tissue-Resident T Cells: Dynamic Players in Skin Immunity. *Front. Immunol.* **2014**, *5*, 332. [CrossRef]
47. Bianchi, F.; Nicassio, F.; Di Fiore, P.P. Unbiased vs. biased approaches to the identification of cancer signatures: The case of lung cancer. *Cell Cycle* **2008**, *7*, 729–734. [CrossRef]
48. Rooda, I.; Hensen, K.; Kaselt, B.; Kasvandik, S.; Pook, M.; Kurg, A.; Salumets, A.; Velthut-Meikas, A. Target prediction and validation of microRNAs expressed from FSHR and aromatase genes in human ovarian granulosa cells. *Sci. Rep.* **2020**, *10*, 1–13. [CrossRef]
49. Spies, M.; Dasu, M.R.K.; Svrakic, N.; Nesic, O.; Barrow, R.E.; Perez-Polo, J.R.; Herndon, D.N. Gene expression analysis in burn wounds of rats. *Am. J. Physiol.-Regul. Integr. Comp. Physiol.* **2002**, *283*. [CrossRef] [PubMed]
50. Vickers, K.C.; Palmisano, B.T.; Shoucri, B.M.; Shamburek, R.D.; Remaley, A.T. MicroRNAs are transported in plasma and delivered to recipient cells by high-density lipoproteins. *Nat. Cell Biol.* **2011**, *13*, 423–435. [CrossRef]
51. Valadi, H.; Ekström, K.; Bossios, A.; Sjöstrand, M.; Lee, J.J.; Lötvall, J.O. Exosome-mediated transfer of mRNAs and microRNAs is a novel mechanism of genetic exchange between cells. *Nat. Cell Biol.* **2007**, *9*, 654–659. [CrossRef]
52. Thomou, T.; Mori, M.A.; Dreyfuss, J.M.; Konishi, M.; Sakaguchi, M.; Wolfrum, C.; Rao, T.N.; Winnay, J.N.; Garcia-Martin, R.; Grinspoon, S.K.; et al. Adipose-derived circulating miRNAs regulate gene expression in other tissues. *Nature* **2017**, *542*, 450–455. [CrossRef]
53. Szabowski, A.; Maas-Szabowski, N.; Andrecht, S.; Kolbus, A.; Schorpp-Kistner, M.; Fusenig, N.E.; Angel, P. c-Jun and JunB antagonistically control cytokine-regulated mesenchymal-epidermal interaction in skin. *Cell* **2000**, *103*, 745–755. [CrossRef]
54. Liu, L.; Awoyemi, A.A.; Fahy, K.E.; Thapa, P.; Borchers, C.; Wu, B.Y.; McGlone, C.L.; Schmeusser, B.; Sattouf, Z.; Rohan, C.A.; et al. Keratinocyte-derived microvesicle particles mediate ultraviolet B radiation–induced systemic immunosuppression. *J. Clin. Investig.* **2021**, *131*. [CrossRef] [PubMed]
55. Holmgaard, R.; Benfeldt, E.; Nielsen, J.B.; Gatschelhofer, C.; Sorensen, J.A.; Höfferer, C.; Bodenlenz, M.; Pieber, T.R.; Sinner, F. Comparison of open-flow microperfusion and microdialysis methodologies when sampling topically applied fentanyl and benzoic acid in human dermis ex vivo. *Pharm. Res.* **2012**, *29*, 1808–1820. [CrossRef]
56. Dweep, H.; Gretz, N. MiRWalk2.0: A comprehensive atlas of microRNA-target interactions. *Nat. Methods* **2015**, *12*, 697. [CrossRef]
57. Livak, K.J.; Schmittgen, T.D. Analysis of relative gene expression data using real-time quantitative PCR and the 2-ΔΔCT method. *Methods* **2001**, *25*, 402–408. [CrossRef] [PubMed]

genes

MDPI

Article

Expression Profiles of miR-22-5p and miR-142-3p Indicate Hashimoto's Disease and Are related to Thyroid Antibodies

Olivia Trummer [1,*,†], Ines Foessl [1,†], Natascha Schweighofer [1,2], Edi Arifi [1], Christoph W. Haudum [1,2], Sharmaine Reintar [1,2], Stefan Pilz [1], Verena Theiler-Schwetz [1], Christian Trummer [1], Andreas Zirlik [3], Albrecht Schmidt [3], Caterina Colantonio [3], Ewald Kolesnik [3], Nicolas Verheyen [3], Thomas R. Pieber [1,2] and Barbara Obermayer-Pietsch [1]

[1] Division of Endocrinology and Diabetology, Department of Internal Medicine, Medical University of Graz, 8036 Graz, Austria; ines.foessl@medunigraz.at (I.F.); natascha.schweighofer@medunigraz.at (N.S.); edi.arifi@stud.medunigraz.at (E.A.); christoph.haudum@medunigraz.at (C.W.H.); sharmaine.reintar@medunigraz.at (S.R.); stefan.pilz@medunigraz.at (S.P.); verena.schwetz@medunigraz.at (V.T.-S.); christian.trummer@medunigraz.at (C.T.); thomas.pieber@medunigraz.at (T.R.P.); barbara.obermayer@medunigraz.at (B.O.-P.)
[2] Center for Biomarker Research in Medicine, CBmed, 8010 Graz, Austria
[3] Division of Cardiology, Department of Cardiology, University Heart Center Graz, Medical University of Graz, 8036 Graz, Austria; andreas.zirlik@medunigraz.at (A.Z.); albrecht.schmidt@medunigraz.at (A.S.); caterina.colantonio@medunigraz.at (C.C.); ewald.kolesnik@medunigraz.at (E.K.); nicolas.verheyen@medunigraz.at (N.V.)
* Correspondence: olivia.trummer@medunigraz.at
† These authors contributed equally to this study.

check for updates

Citation: Trummer, O.; Foessl, I.; Schweighofer, N.; Arifi, E.; Haudum, C.W.; Reintar, S.; Pilz, S.; Theiler-Schwetz, V.; Trummer, C.; Zirlik, A.; et al. Expression Profiles of miR-22-5p and miR-142-3p Indicate Hashimoto's Disease and Are related to Thyroid Antibodies. *Genes* **2022**, *13*, 171. https://doi.org/10.3390/genes13020171

Academic Editor: Paula Soares

Received: 22 December 2021
Accepted: 15 January 2022
Published: 19 January 2022

Abstract: Hashimoto's thyroiditis (HT) is the most prevalent autoimmune disorder of the thyroid (AITD) and characterized by the presence of circulating autoantibodies evoked by a, to date, not fully understood dysregulation of the immune system. Autoreactive lymphocytes and inflammatory processes in the thyroid gland can impair or enhance thyroid hormone secretion. MicroRNAs (miRNAs) are small noncoding RNAs, which can play a pivotal role in immune functions and the development of autoimmunity. The aim of the present study was to evaluate whether the expression of 9 selected miRNAs related to immunological functions differ in patients with HT compared to healthy controls. MiRNA profiles were analysed using quantitative reverse transcription polymerase chain reaction (qRT-PCR) in 24 patients with HT and 17 healthy controls. Systemic expressions of miR-21-5p, miR-22-3p, miR-22-5p, miR-142-3p, miR-146a-5p, miR-301-3p and miR-451 were significantly upregulated in patients with HT ($p \leq 0.01$) and were suitable to discriminate between HT and healthy controls in AUC analysis. Altered expressions of miR-22-5p and miR-142-3p were associated with higher levels of thyroid antibodies, suggesting their contribution to the pathogenesis of HT.

Keywords: miRNA; autoimmune thyroid disease; AITD; Hashimoto's thyroiditis

1. Introduction

Autoimmune thyroid diseases (AITDs) are the most common autoimmune diseases, affecting 2–5% of the population in high-income countries [1]. Hashimoto's thyroiditis (HT), the most frequent AITD, is the leading cause of hypothyroidism in iodine-sufficient areas of the world. Although exact mechanisms of aetiology and pathogenesis of HT are not completely understood, a strong genetic susceptibility to the disease has been confirmed by studies carried out within families and twins [2]. As in other autoimmune disorders, humoral and cellular immune mechanisms are closely related and cross-linked in AITDs. Disturbed self-tolerance accompanied by an increased antigen presentation is a precondition for their manifestation, based also on the interaction of thyroid, antigen presenting and T cells. Secreted cytokines provoke predominantly a T-helper type 1 (Th1)

as well as a Th17 response, which has been described [3]. Impaired thyroxin production and hypothyroidism as well as, more rarely, hyperthyroidism, are the consequences.

Early diagnosis and intervention may help to prevent the development of HT and abnormal thyroid function. The final diagnosis of HT depends on lymphocytic infiltration of the thyroid gland by fine-needle aspiration biopsy (FNAB) and further histopathological examination which is invasive and sometimes unfeasible [4]. Serum thyroid antibodies and ultrasonography are now used for diagnosis. At an early stage, HT is asymptomatic, easily leading to misdiagnosis [5]. Therefore, more biological markers need to be discovered to assist in early and accurate diagnosis of HT.

Micro RNAs (miRNAs) are small, noncoding, highly conserved ribonucleic acids (RNAs) that regulate gene expression by binding to messenger RNA (mRNA), thus modifying transcriptional processes. A single miRNA can regulate the expression of multiple genes and their encoded proteins [6]. In total, over 30% of human mRNAs are regulated by miRNAs [7]. Many miRNAs have been found to be important for the survival, development, differentiation, and function of T cells, B cells, dendritic cells, macrophages and other immune cell types [8,9]. Accordingly, differential miRNA expression profiles have been reported in autoimmunological disorders such as rheumatoid arthritis, systemic lupus erythematosus and psoriasis, [10–14] as well as in AITDs [15–19]. The aim of the study was to examine a panel of nine selected miRNAs to evaluate whether there is a difference in serum expressions of patients with HT and to investigate possible relations to thyroid antibodies. Candidate miRNAs for the present investigation have been selected according to their presence in serum as well as to previously described associations of humoral and/or cellular immune mechanisms involved in AITDs (Table 1).

Table 1. MiRNAs, mature sequence and source of reference of each selected miRNA.

micro RNAs	Sequence	Reference
hsa-miR-21-5p	5′UAGCUUAUCAGACUGAUGUUGA	[15]
hsa-miR-22-3p	5′AAGCUGCCAGUUGAAGAACUGU	[16]
hsa-miR-22-5p	5′AGUUCUUCAGUGGCAAGCUUUA	[16]
hsa-miR-96-5p	5′UUUGGCACUAGCACAUUUUUGCU	[15]
hsa-miR-142-3p	5′UGUAGUGUUUCCUACUUUAUGGA	[15]
hsa-miR-146a-5p	5′UGAGAACUGAAUUCCAUGGGUU	[15]
hsa-miR-301-3p	5′CAGUGCAAUAGUAUUGUCAAAGC	[15]
hsa-miR-375	5′UUUGUUCGUUCGGCUCGCGUGA	[16]
hsa-miR-451	5′AAACCGUUACCAUUACUGAGUU	[16]

hsa, homo sapiens; miRNA, micro RNA.

2. Materials and Methods

2.1. Study Populations

Data of the present investigation were obtained from the BioPersMed cohort ("Biomarkers of Personalized Medicine"), an ongoing single-centre, prospective, observational study to evaluate novel biomarkers for the assessment of cardiovascular and common metabolic diseases and their related complications. This observational trial was initiated in the year 2010 and the study population consists of 1022 asymptomatic subjects without diagnosed cardiovascular disease (CVD) with at least one classical risk factor for CVD, such as family history of CVD, hypertension or dyslipidaemia. Extensive anthropometric and clinical data were carefully recorded, including comorbidities such as previously diagnosed HT. Patients presenting with severe illnesses independent of aetiology, or who were expected not to be able to complete study specific examinations, have been excluded from participation. Moreover, persons with serious co-morbidities or mental health problems have also been excluded. Written informed consent from each participant was obtained after the study approval by the institutional review board of the Medical University of Graz (EC Nr. 24-224 ex 11-12). The BioPersMed study is conducted in compliance with Good Clinical Practice Guidelines Procedures (GCP) and carried out according to the principles of the Declaration of Helsinki.

For the present observational investigation, we screened the BioPersMed cohort for previously diagnosed HT patients (n = 27) as well as age and sex matched participants suitable as healthy controls (n = 22). HT patients have been diagnosed based on the commonly used diagnostic tools such as clinical manifestations, ultrasound and measurement of thyroid stimulating hormone (TSH), free triiodothyronine (fT3), free thyroxine (fT4), thyroglobulin autoantibody (TgAb) and thyroid peroxidase autoantibody (TPOAb) by their general practitioner or any other medical facilities. Exclusion criteria for HT patients were comorbidities such as acute (e.g., pancreatitis) or chronic inflammations (e.g., rheumatoid arthritis, polymyalgia, diabetes mellitus), endocrine disturbances in need of treatment (other than HT), history of myocardial infarction as well as history of cancers (e.g., bladder cancer, acoustic neuroma). Participants in the healthy control group showed at least one classical risk factor for CVD, but no serious comorbidities after a clinical validation by an experienced clinician. Serum samples were excluded if haemolysis was visually detected. We therefore excluded 3 samples of the HT group and 5 samples of the control group. In total, we investigated 24 HT patients compared to 17 healthy controls. A study flow chart is given in Figure 1.

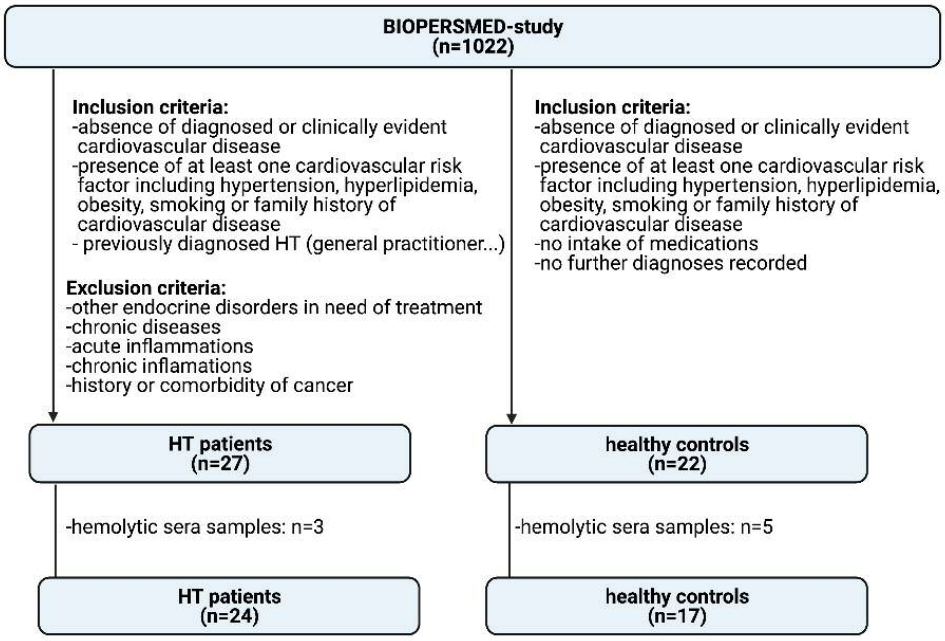

Figure 1. Study flow chart.

2.2. Patient Visit

Anthropometric data were measured in all participants. Baseline blood samples for laboratory analyses were collected between 7.00 and 9.00 a.m. after an overnight fast. Biobanking of blood samples was performed by freezing and storing the samples at −80 °C until analysis. To evaluate thyroid function and common autoantibodies, serum levels of TSH, fT3, fT4, TPOAb and TgAb were determined by luminescence immunoassay (Siemens, Erlangen, Germany) with intra- and inter-assay coefficients of variation (CV) of: TSH, 5.0% and 6.0%; FT3, 2.4% and 2.9%; FT4, 2.2% and 2.3%; TPO Ab, 5.2% and 6.1%, as well as Tg Ab, 5.0% and 4.6%, respectively. Body mass index (BMI) was calculated as body weight in kilograms (kg) divided by height in meters squared (m^2).

2.3. Selection of miRNAs

Based on previous studies [15,16], we selected 9 miRNAs that have been related to relevant immunological functions as candidates for the present investigation. These miRNAs are listed in Table 1.

2.4. miRNA Isolation and qPCR

MiRNA was isolated using the miRNeasy Serum/Plasma Advanced Kit (Qiagen, Hilden, Germany) according to the manufacturer's instructions. RNA was eluted from the columns by addition of 20 µL RNase-free water, followed by centrifugation. The isolated miRNAs were short-term stored at −80 °C. Complementary DNA (cDNA) was generated using miRCURY LNA RT synthesis kit (Qiagen, Hilden, Germany), and subsequent quantitative real-time PCR (qPCR) was performed in duplicates using miRCURY LNA SYBR Green PCR Kit and specific miRCURY LNA miRNA PCR Assays (both from Qiagen, Hilden, Germany) with the CFX384 Touch Real-Time PCR Detection System (Bio-Rad, Hercules, CA, USA). Exogenous oligonucleotides have been added as spike-in controls (UniSp2, UniSp4, UniSp5, UniSp6 and cel-miR-39-3p) and were used to estimate the efficiency of RNA extraction, reverse transcription reaction and qPCR amplification (RNA Spike in Kit for RT, Qiagen, Hilden, Germany). All qPCRs were performed with interplate calibration, a maximum of 40 cycles were performed in duplicates and the average of cycle threshold (Ct) values were calculated. Only those miRNAs with a Ct < 37 were considered for further analysis. The relative expression levels of all investigated miRNAs were calculated as fold change [20]. For that, average Ct values have been normalized to spike-in controls to calculate ΔCt values. Fold change was calculated as $2^{-\Delta\Delta Ct}$ where ΔΔCt was ΔCt of HT patients minus ΔCt of controls. Quantitative qPCR data are reported as mean ± standard deviation (SD).

2.5. Functional Annotation of miRNAs

MiRWalk was used to identify potential target genes of differentially expressed miRNAs [21]. Matched binding sites have been evaluated in genes reportedly involved in the development of AITDs [22].

2.6. Statistical Analysis

Statistical analysis was performed using SPSS statistics version 25.0 (IBM SPSS Statistics GmbH, Ehringen, Germany). Patient characteristics and biomarker results are reported as mean ± SD unless otherwise stated. Distribution of data was analysed by descriptive statistics and Kolmogorov–Smirnov test, as well as by evaluation of quantile-quantile plots. Normally distributed quantitative data were compared using unpaired Student's *t*-test and unequally distributed data by applying Kruskal–Wallis tests for non-parametric samples. Changes of miRNA in the HT group are displayed as relative change compared to miRNA levels of healthy controls as reference. The diagnostic value for discriminating between HT patients and the control group was assessed by calculating the area under the curve (AUC). Receiver-operator characteristic (ROC) curves were generated by plotting sensitivity vs. (1-specificity). A *p*-value of ≤ 0.05 was considered as statistically significant. Adjustment for multiple testing has been performed by Bonferroni correction.

3. Results

3.1. General Results

We included a total of 41 participants, 33 women (81%), and 8 men (19%) in our analysis. Of these, 24 subjects (59%) were patients with previously diagnosed HT (22 women (92%) and 2 men (8%)). 17 subjects (41%) were classified as healthy (11 women (65%) and 6 men (35%)) (Figure 1).

In the HT patients group, 13% (n = 3) showed TgAb > 60 U/mL and 54% (n = 13) showed TPOAb > 60 U/mL. In total, 4 patients had both TgAb as well as TPOAb > 60 U/mL, respectively.

Of the HT patients, 29% (n = 7) were treated with levothyroxine. Control group participants did not take any recorded medication. Demographic data of the study population are given in Table 2.

Table 2. Demographic data of patients with Hashimoto's thyroiditis and healthy subjects. Frequency data are presented as number, (percentage), continuous data as mean ± standard deviation. HT, Hashimoto's thyroiditis; n, number; BMI, body mass index; FT3, free triiodothyronine; FT4, free thyroxine; TSH, Thyroid stimulating hormone; TPOAb, thyroid peroxidase autoantibody; TgAb, thyroglobulin autoantibody. Normal ranges of fT3, 3.0–6.3 pmol/L; fT4, 9.5–24 pmol/L; TSH, 0.10–4.0 µU/mL; TgAb; 0–60 IU/mL; TPOAb, 0–60 IU/mL.

	Patients with HT	Healthy Subjects
n	24	17
Sex female (*n*)	22 (91.7%)	11 (64.7%)
Age (yr)	57.9 ± 7.4	61.1 ± 5.8
BMI (kg/m^2)	25.2 ± 4.2	23.7 ± 2.34
fT3 (pmol/L)	4.4 ± 0.5	4.8 ± 0.4
fT4 (pmol/L)	15.9 ± 2.3	16.3 ± 2.0
TSH (µU/mL)	1.60 ± 0.87	1.83 ± 0.73
TgAb (IU/mL)	213.8 ± 365.6	
TPOAb (IU/mL)	212.2 ± 199.1	
Levothyroxine treatment	7 (29%)	

3.2. miRNA Expression Is Altered in Patients with HT

Systemic expression of miR-21-5p, miR-22-3p, miR-22-5p, miR-96-5p, miR-142-3p, miR-146a-5p, miR-301a-5p, and miR-451 was significantly upregulated in patients with HT. Associations of miR-21-5p, miR-22-3p, miR-142-3p, miR-146a-5p, miR-301-3p as well as miRNA-451 remained stable after Bonferroni correction. In contrast, miRNA-22-5p and miRNA-96-5p lost the level of significance after adjustment for multiple testing. Out of the nine selected miRNAs, miR-375 was the only candidate that was not upregulated in serum of HT patients. (Table 3). ΔCt values per group were normally distributed. Respective scatter plots are given in Figure 2. An annotation in miRWalk provided information on binding sites of the potential miRNAs.

Table 3. MiRNA ΔCt values according to the selected miRNAs of patients with Hashimoto's thyroiditis and healthy subjects. Data are shown as mean ± standard deviation.

hsa-miRNA	Patients with HT (*n* = 24)	Healthy Subjects (*n* = 17)	*p*-Value
miR-21-5p	−0.43 ± 0.54	0.68 ± 0.58	<0.001 *
miR-22-3p	1.58 ± 0.85	2.98 ± 0.80	<0.001 *
miR-22-5p	6.42 ± 0.95	7.22 ± 0.91	0.010
miR-96-5p	8.40 ± 1.21	9.22 ± 1.22	0.040
miR-142-3p	−0.84 ± 0.58	1.03 ± 0.60	<0.001 *
miR-146a-5p	2.71 ± 0.63	3.69 ± 0.65	<0.001 *
miR-301-3p	6.09 ± 1.01	7.21 ± 0.82	0.001 *
miR-375	8.52 ± 1.67	8.21 ± 1.10	0.503
miR-451	−2.60 ± 1.00	2.82 ± 1.35	<0.001 *

* indicates significant *p*-values after Bonferroni correction.

3.3. miR-22-5p and miR-142-3p Are Altered in HT Patients with Higher Levels of Thyroid Antibodies

Subgroup analyses within HT patients showed significantly higher miRNA expression for miR-22-5p in HT patients with higher thyroid antibody levels (TgAb and/or TPOAb > 60 U/mL, *n* = 13), 5.97 ± 0.74, as compared to HT patients with lower thyroid antibody levels (TgAb and/or TPOAb < 60 U/mL, *n* = 11) 6.95 ± 0.90; *p* = 0.008.

MiR-142-3p was also found to be significantly different (*p* = 0.05) in HT patients with higher levels of thyroid antibodies −0.25 ± 0.57 as compared to HT patients with thyroid antibody levels < 60 U/mL, 0.21 ± 0.51. In our regression analysis miR-22-5p and miR-142-3p expressions did not correlate with TPOAb levels (Figure 3).

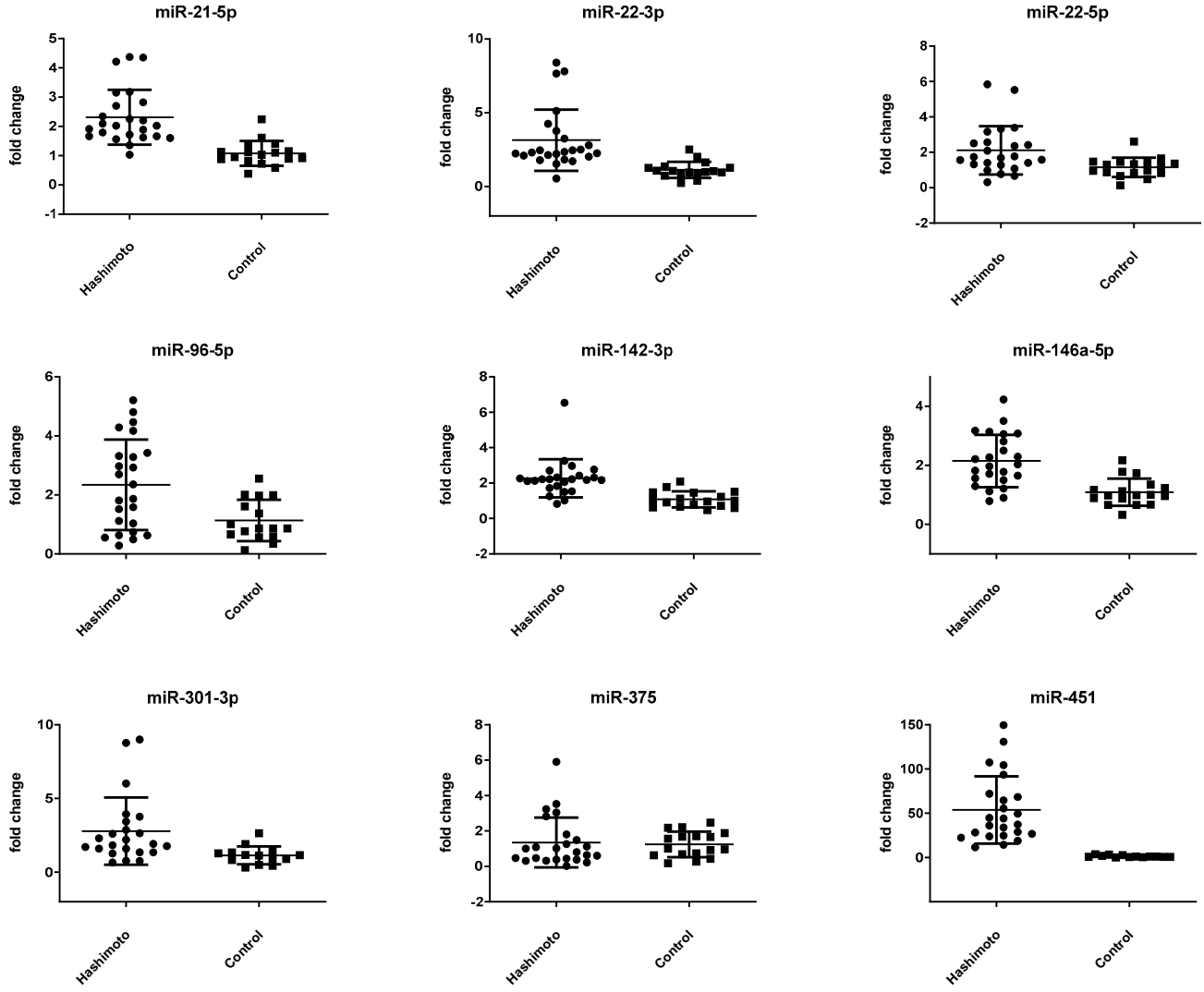

Figure 2. Expression of 9 miRNAs in serum of samples of HT patients and healthy controls. Data are displayed as scatter plots, where each dot represents the fold change as $2^{-\Delta\Delta ct}$-value of one study sample. Significance was tested by unpaired Student's *t*-test.

3.4. Potential Binding Site Targets

A functional annotation of these differentially expressed miRNAs revealed potential binding sites in genes of important immune mediators such as interleukins (IL), interferons (IFN), transforming growth factors (TGF), and granulocyte-macrophage colony-stimulating factor (GM-CSF). A scheme on how these miRNAs may interact in the development of AITD is given in Figure 4. Higher numbers of predicted miRNA binding sites were determined for miR-22-5p (n = 6) and for miR-142-3p (n = 4) compared to the mean number of binding sites for all miRNAs of 3.3 $\pm$ 2.0 (SD). MiR-21-5p showed potential interactions with IL-5, IFN-γ and IL-12. MiR-22-3p potentially interacts with IL-2, IL-5, IL-12, IL-17, IL-23, IFN-γ and TGF-β. MiR-22-5p potentially interacts with IL-1, IL-12, IL-13, IL-17 and IL-23 and IFN-γ. MiR-96-5p potentially interacts with IL-5, IL-13 and IL-23. MiR-142-3p potentially interacts with IL-1, TGFβ, IFN-γ and GM-CSF. MiR-146a-5p potentially interacts with IL-12, IL-5 and IL-17. MiR-301-3p potentially interacts with IL-7 and IL-17. MiR-451 potentially interacts with IL-1 and IL-12.

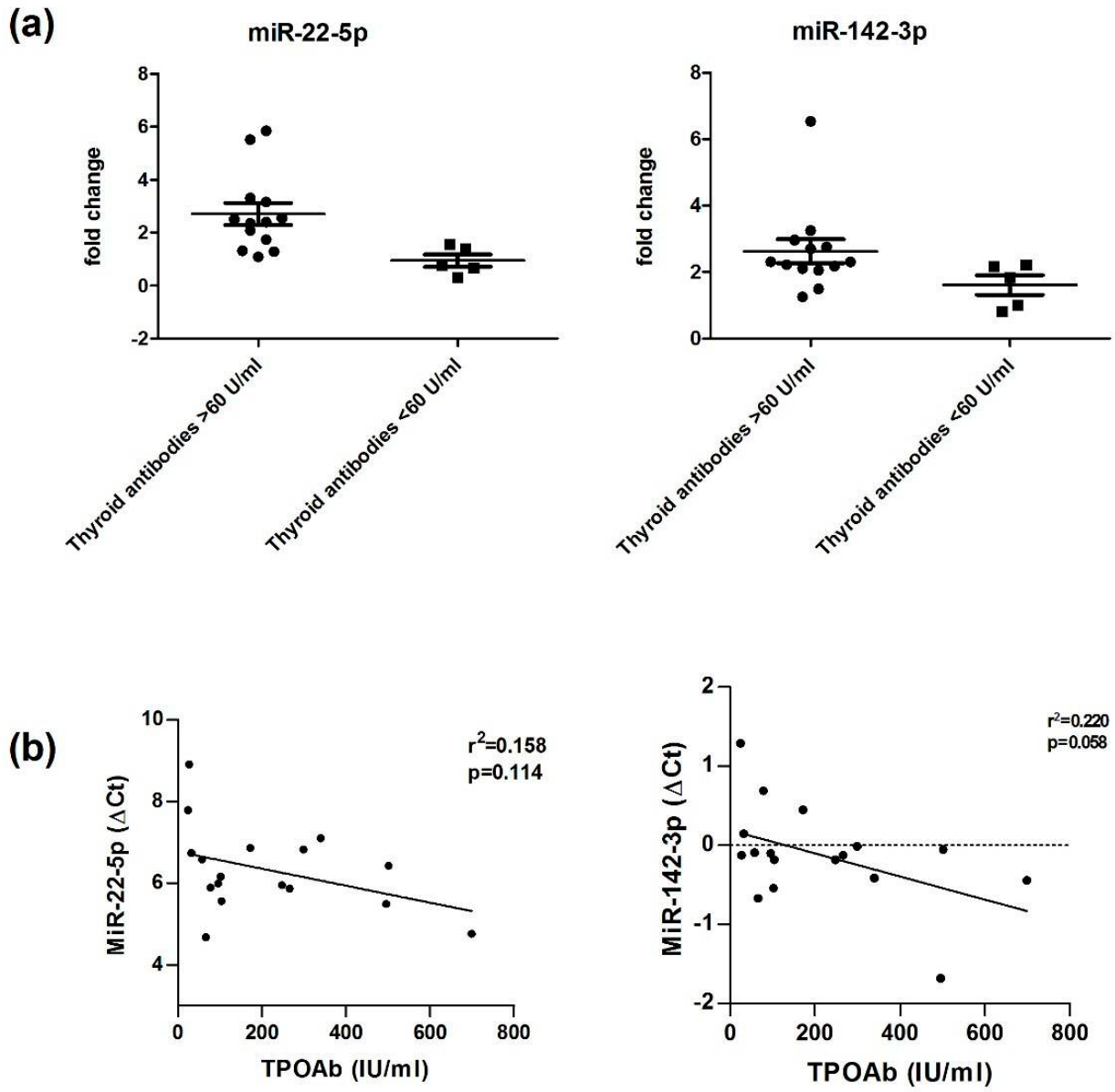

Figure 3. (**a**) Altered Expressions of miR-22-5p and miR-142-3p in serum of HT patients with higher levels of thyroid antibodies compared to HT patients with thyroid antibody levels <60 U/mL. Data are displayed as scatter plots, where each dot represents the ΔCt value of one HT patient. Significance was tested by unpaired Student's *t*-test. (**b**)Thyroid Antibodies (TPOAb) did not correlate with higher expressions of miR-22-5p and miR-142-3p (ΔCt values). TgAb, thyroglobulin autoantibody; TPOAb, thyroid peroxidase autoantibody; ΔCt, delta Cycle threshold.

3.5. miRNAs as Discriminators for HT Status in ROC Analysis

To evaluate the discriminatory potential of the differentially expressed miRNAs, we performed receiver-operating characteristic (ROC) analysis and calculated area under the curve (AUC) values. With the exception of miR-96-5p, differentially expressed miRNAs are "fair" (miRNA 22-5p: AUC = 0.76; 95% CI, 0.61–0.91; $p = 0.006$), "good" (miR-301-3p: AUC = 0.82; 95% CI, 0.68–0.96; $p = 0.001$ and miR-146a-5p: AUC = 0.86; 95% CI, 0.75–0.97; $p < 0.001$) or "excellent" (miR-21-5p: AUC = 0.99; 95% CI, 0.85–1; $p < 0.001$; miR-22-3p: AUC = 0.92; 95% CI, 0.82–1.00; $p < 0.001$; miR-142-3p: AUC = 0.92; 95% CI, 0.84–1.00; $p < 0.001$ and miR-451: AUC = 1.00; 95% CI, 1.00–1.00; $p < 0.001$) predictors [23] (Figure 5).

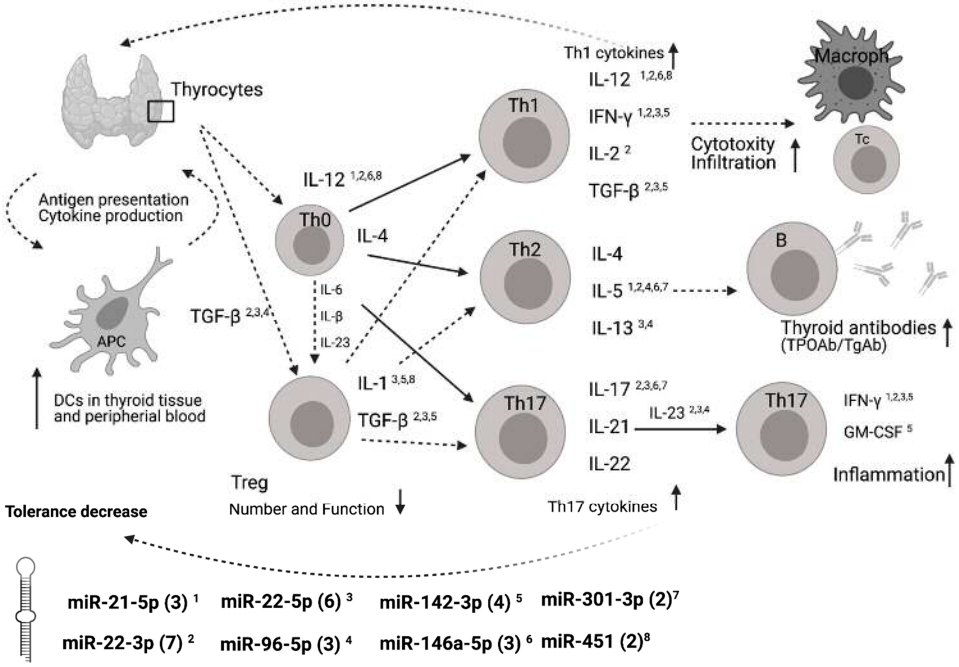

Figure 4. Summary of the main mechanisms related to autoimmunity of HT and potential interaction sites with differentially expressed miRNAs. Schematic representation of T cells differentiating into specific T cell subsets depending on the cytokines to which they are exposed and their main effects. MiRNA binding site predictions have been annotated by miRWalk database. Number of predicted binding sites are shown in brackets for each miRNA. Predicted binding sites of genes of HT immune-related molecules and/or their receptors are marked by superscript numbers. Adapted from [22]. APC, antigen presenting cell; Th, T helper cell; Macroph, macrophage; DC, dentritic cell; Treg, T-regulatory cells; TPOAb; peroxidase autoantibody; TgAb, thyroglobulin autoantibody, IL, interleukin; IFN-γ, interferon-γ; TGF-β, transforming growth factor β; GM-CSF, granulocyte-macrophage colony-stimulating factor; miR, miRNA.

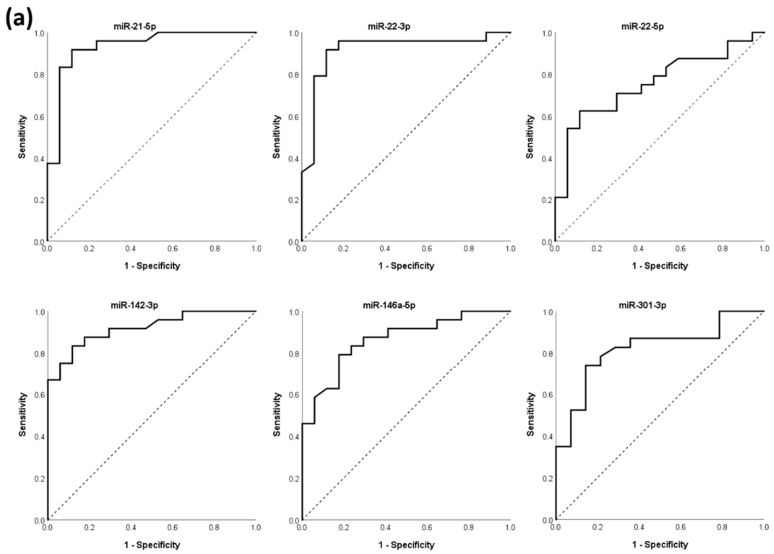

miRNA	AUC	95%CI	*p*-value
miR-21-5p	0.93	0.85-1.00	<0.001
miR-22-3p	0.92	0.82-1.00	<0.001
miR-22-5p	0.76	0.61-0.91	0.006
miR-96-5p	0.68	0.51-0.85	0.055
miR-142-3p	0.92	0.84-1.00	<0.001
miR-146a-5p	0.86	0.75-0.97	<0.001
miR-301-3p	0.82	0.68-0.96	0.001
miR-375	0.45	0.27-0.63	0.560
miR-451	1.00	1.00-1.00	<0.001

Figure 5. The potential of differentially expressed miRNAs to discriminate between HT status and healthy controls, shown in ROC curves. (**a**) ROC curves of selected differently expressed miRNAs. (**b**) Calculated AUC values, 95% CI and *p*-values of each investigated miRNA. ROC, receiver-operating characteristic; DE, differentially expressed; AUC, area under the curve; CI, confidence interval.

4. Discussion

In the present observational study, eight out of nine observed miRNAs were differentially expressed in the serum of HT patients compared to healthy controls. In a subgroup analysis, HT patients with thyroid antibodies (TPOAb and/or TgAb) showed significantly higher expression levels for miR-22-5p and miR-142-3p but not for the other 7 miRNAs (Figure 3). To evaluate the accuracy of these differentially expressed miRNAs in predicting HT, we conducted a ROC analysis. AUC of these miRNAs were at least >0.76, indicating a "fair" test with enough balance between sensitivity and specificity for discriminating accurately between HT patients and healthy controls [24], (Figure 5).

The general tendency to overexpression detectable for all investigated miRNAs might be due to either active secretion as a consequence of increased inflammation in HT patients or derivation from autoimmune-related cell death. Independent from their cells of origin, miRNAs can function as endocrine signallers and are taken up by target cells [25].

We detected an increased expression of miR-22-5p and miRNA-142-3p, both associated with higher levels of serum antibodies (TgAb and/or TPOAb > 60 U/mL) in patients with HT. This corresponds with data of our ROC analysis. Both miRNAs are suitable to discriminate between HT patients and healthy controls. We could not confirm the association between antibody level group and altered expression by correlation analysis. Thyroid antibodies did not correlate with expression levels of miR-22-5p and miR-142-3p (Figure 3). Furthermore, and this counts for all of our analyses, we cannot estimate how the investigated miRNAs vary in their expressions before, during or after development of HT since this study was observational after development of HT.

Our results are in context with previously published data. Zhu et al. reported positive associations of TgAb levels and miR-142-5p but not for miR-142-3p [26], which is in line with our thyroid antibody analysis. Data of ROC curves are corresponding with ROC curves of Martínez-Hernández et al. with the exception of miR-96-5p. According to their analysis this miRNA is an "excellent" predictor (AUC = 0.91, 95% CI, 0.84–0.98) whereas our data failed the level of significance barely ($p = 0.055$) [24].

Our data of overexpression profiles in HT are in accordance with Martínez-Hernández et al. [15] as well as Yamada et al. [16], who both studied miRNA expressions in patients with AITD. The only non-concordant exception is miR-375, which was not differentially expressed in our cohort in contrast to Yamada's study. That in turn is in line with Zhao et al. who showed upregulated plasma levels of miR-375 and miR-451 in a four times larger study cohort than Yamada [5]. We are aware that caution must be taken when comparing miRNA data generated from different types of biofluids [27], since serum and plasma differ in their content of miRNA derived from different blood cells [28,29]. One of the potential reasons for the partly conflicting results of studies on miRNA expression in HT patients may be the interethnic expression differences between Asian (Yamada et al., Zhu et al.) and Caucasian (present study) cohorts [30]. In both investigations, serum miRNA profiling was performed by reverse transcription qPCR, the gold standard for sensitive and specific quantification of miRNAs in cell free biofluids. However, as frequently encountered, the quality of results varies in general strongly with the preanalytical steps such as blood drawing and serum/plasma preparation. The very low amounts of miRNAs, potentially high levels of inhibitors, biological variances of the individuals themselves (diet, exercise, age) as well as normalization strategies contribute to the variance in the results of different miRNA studies [31–33].

As confirmed by our in silico analysis, several T cell differentiation cytokines related to autoimmunity are potential targets of our overexpressed miRNA patterns (Figure 4).

MiR-22-3p binds 7 autoimmune-related cytokines, miR-22-5p has 6 binding partners and miR-142-3p has 4 binding partners. This may suggest a contribution of these miRNAs to differentiation of T cells into specific T cell subsets. MiR-22-5p regulates mainly cytokines involved in the differentiation of Th17 cells, promoting therefore the inflammatory response. Our focus was on miRNA targets related to autoimmunity of HT. We are aware that such

stringent criteria potentially excluded other regulatory interactions that might also play a role in the development of HT.

In our investigation miR-22-3p is associated with HT but not to serum thyroid antibodies. MiR-22-3p mainly targets genes of Th1 cytokines (IL-12, IFN-γ, IL-2 and TGF-β) but is binding partner of fewer TH2 cytokine genes (IL5) (Figure 4). This might suggest that miR-22-3p rather regulates the autoimmune related cytotoxicity and infiltration than changes in the development of thyroid antibodies. These theoretical assumptions are based on our in silico analysis. Whether cytokine levels are affected by the changed miRNA profile remains to be elucidated. This study was focussing on the biomarker aspect of the miRNA pattern. Nevertheless, our data showed serum overexpression of miR-22-5p and miR-142-3p related to the occurrence of thyroid antibodies.

Some further limitations of the study should be taken into account. There is still a debate on how and if normalization should be performed on qPCR results of serum miRNAs [34]. We decided to use exogenous controls (spike-ins) for normalization, excluding a potential bias by normalization on endogenous reference genes [33]. We cannot rule out a certain selection bias by choosing HT patients based on their previous medical history and not their prospective enrolment into the study. Further, cytokine levels were not determined in the BioPersMed cohort at the time of the patients' visits.

It should be kept in mind that published data, including the present study, lack long-term outcome data regarding disease activity and prognostic expectations. In this study, we present 2 miRNA candidates associated with higher occurrence of thyroid antibodies that possibly could be suitable to allow assumptions on whether HT patients are likely to develop higher titers of thyroid antibodies (TPOAb and or TgAb < 60 U/mL).

In conclusion, miRNA profiles of miR-21-5p, miR-22,3p, miR-22-5p, miR-142-3p, miR-146a-5p, miR-301-3p and miR-451 are upregulated in HT patients and suitable to discriminate between HT and healthy controls. Additionally, altered expressions of miR-22-5p and miR-142-3p are associated with higher levels of thyroid antibodies, suggesting important roles in the pathogenesis of HT.

Author Contributions: Conceptualization, O.T. and I.F.; methodology, O.T., I.F. and S.R. software, C.W.H.; validation, O.T. and I.F.; formal analysis, O.T.; investigation, S.P., V.T.-S. and C.T.; resources, B.O.-P. and T.R.P.; data curation, C.W.H.; writing—original draft preparation, O.T. and I.F.; writing—review and editing, I.F., A.Z., A.S. and C.C., visualization, E.K. and N.V.; supervision, B.O.-P.; project administration, E.A. and N.S.; funding acquisition, E.A. All authors have read and agreed to the published version of the manuscript.

Funding: This study was funded by the BioPersMed COMET K (project ID: 825329) and by a research grant of the MEFO Graz health 3000 (project ID: 9670) (https://mefograz.at/; last accessed on 7 January 2022).

Institutional Review Board Statement: The study was conducted in accordance with the Declaration of Helsinki, and approved by the Ethics Committee of the Medical University of Graz (EC Nr. 24-224 ex 11-12).

Informed Consent Statement: Informed consent was obtained from all subjects involved in the study.

Acknowledgments: We thank Roswitha Gumpold for assistance with the patients, Cornelia Missbrenner and Dorrit Münzer-Ornik for continuous lab support, the team of the Endocrinology Lab Platform and all our participants in the study. Figures 1 and 4 were created with BioRender (www.biorender.com).

Conflicts of Interest: The authors declare no conflict of interest. The funders had no role in the design of the study; in the collection, analyses, or interpretation of data; in the writing of the manuscript, or in the decision to publish the results.

References

1. Rapoport, B.; McLachlan, S.M. Thyroid autoimmunity. *J. Clin. Investig.* **2001**, *108*, 1253–1259. [CrossRef]
2. Marwaha, R.K.; Sen, S.; Tandon, N.; Sahoo, M.; Walia, R.P.; Singh, S.; Ganguly, S.K.; Jain, S.K. Familial aggregation of autoimmune thyroiditis in first-degree relatives of patients with juvenile autoimmune thyroid disease. *Thyroid* **2003**, *13*, 297–300. [CrossRef]
3. Zaletel, K.; Gaberščček, S. Hashimoto's Thyroiditis: From Genes to the Disease. *Curr. Genom.* **2011**, *12*, 576–588. [CrossRef]
4. Baloch, Z.W.; LiVolsi, V.A. Fine-needle aspiration of the thyroid: Today and tomorrow. *Best Pract. Res. Clin. Endocrinol. Metab.* **2008**, *22*, 929–939. [CrossRef]
5. Zhao, L.; Zhou, X.; Shan, X.; Qi, L.W.; Wang, T.; Zhu, J.; Zhu, D.; Huang, Z.; Zhang, L.; Zhang, H.; et al. Differential expression levels of plasma microRNA in Hashimoto's disease. *Gene* **2018**, *642*, 152–158. [CrossRef]
6. Gracias, D.T.; Katsikis, P.D. MicroRNAs: Key components of immune regulation. *Adv. Exp. Med. Biol.* **2011**, *780*, 15–26. [CrossRef] [PubMed]
7. Bartel, D.P. MicroRNAs: Genomics, biogenesis, mechanism, and function. *Cell* **2004**, *116*, 281–297. [CrossRef]
8. Liu, R.; Ma, X.; Xu, L.; Wang, D.; Jiang, X.; Zhu, W.; Cui, B.; Ning, G.; Lin, D.; Wang, S. Differential microRNA expression in peripheral blood mononuclear cells from Graves' disease patients. *J. Clin. Endocrinol. Metab.* **2012**, *97*, E968–E972. [CrossRef] [PubMed]
9. O'Connell, R.M.; Rao, D.S.; Chaudhuri, A.A.; Baltimore, D. Physiological and pathological roles for microRNAs in the immune system. *Nat. Rev. Immunol.* **2010**, *10*, 111–122. [CrossRef]
10. Heegaard, N.H.H.; Carlsen, A.L.; Skovgaard, K.; Heegaard, P.M.H. Circulating extracellular microRNA in systemic autoimmunity. *EXS* **2015**, *106*, 171–195. [PubMed]
11. Nakamachi, Y.; Kawano, S.; Takenokuchi, M.; Nishimura, K.; Sakai, Y.; Chin, T.; Saura, R.; Kurosaka, M.; Kumagai, S. MicroRNA-124a is a key regulator of proliferation and monocyte chemoattractant protein 1 secretion in fibroblast-like synoviocytes from patientswith rheumatoid arthritis. *Arthritis Rheum.* **2009**, *60*, 1294–1304. [CrossRef]
12. Wang, H.; Peng, W.; Ouyang, X.; Li, W.; Dai, Y. Circulating microRNAs as candidate biomarkers in patients with systemic lupus erythematosus. *Transl. Res.* **2012**, *160*, 198–206. [CrossRef]
13. Tang, Y.; Luo, X.; Cui, H.; Ni, X.; Yuan, M.; Guo, Y.; Huang, X.; Zhou, H.; de Vries, N.; Tak, P.P.; et al. MicroRNA-146A contributes to abnormal activation of the type I interferon pathway in human lupus by targeting the key signaling proteins. *Arthritis Rheum.* **2009**, *60*, 1065–1075. [CrossRef]
14. Xia, P.; Fang, X.; Zhang, Z.H.; Huang, Q.; Yan, K.X.; Kang, K.F.; Han, L.; Zheng, Z.Z. Dysregulation of miRNA146a versus IRAK1 induces IL-17 persistence in the psoriatic skin lesions. *Immunol. Lett.* **2012**, *148*, 151–162. [CrossRef]
15. Martínez-Hernández, R.; Sampedro-Núñez, M.; Serrano-Somavilla, A.; Ramos-Leví, A.M.; de la Fuente, H.; Triviño, J.C.; Sanz-García, A.; Sánchez-Madrid, F.; Marazuela, M. A MicroRNA Signature for Evaluation of Risk and Severity of Autoimmune Thyroid Diseases. *J. Clin. Endocrinol. Metab.* **2018**, *103*, 1139–1150. [CrossRef]
16. Yamada, H.; Itoh, M.; Hiratsuka, I.; Hashimoto, S. Circulating microRNAs in autoimmune thyroid diseases. *Clin. Endocrinol.* **2014**, *81*, 276–281. [CrossRef] [PubMed]
17. Ajjan, R.A.; Weetman, A.P. The Pathogenesis of Hashimoto's Thyroiditis: Further Developments in our Understanding. *Horm. Metab. Res.* **2015**, *47*, 702–710. [CrossRef] [PubMed]
18. Bernecker, C.; Lenz, L.; Ostapczuk, M.S.; Schinner, S.; Willenberg, H.; Ehlers, M.; Vordenbaumen, S.; Feldkamp, J.; Schott, M. MicroRNAs miR-146a1, miR-155_2, and miR-200a1 are regulated in autoimmune thyroid diseases. *Thyroid* **2012**, *22*, 1294–1295. [CrossRef] [PubMed]
19. Peng, H.; Liu, Y.; Tian, J.; Ma, J.; Tang, X.; Yang, J.; Rui, K.; Zhang, Y.; Mao, C.; Lu, L.; et al. Decreased expression of microRNA-125a-3p upregulates interleukin-23 receptor in patients with Hashimoto's thyroiditis. *Immunol. Res.* **2015**, *62*, 129–136. [CrossRef]
20. Livak, K.J.; Schmittgen, T.D. Analysis of relative gene expression data using real-time quantitative PCR and the 2(−Delta Delta C(T)) Method. *Methods* **2001**, *25*, 402–408. [CrossRef]
21. Sticht, C.; De La Torre, C.; Parveen, A.; Gretz, N. miRWalk: An online resource for prediction of microRNA binding sites. *PLoS ONE* **2018**, *13*, e0206239. [CrossRef]
22. Ramos-Leví, A.M.; Marazuela, M. Pathogenesis of thyroid autoimmune disease: The role of cellular mechanisms. *Endocrinol. Nutr.* **2016**, *63*, 421–429. [CrossRef]
23. Li, F.; He, H. Assessing the Accuracy of Diagnostic Tests. *Shanghai Arch. Psychiatry* **2018**, *30*, 207–212. [CrossRef] [PubMed]
24. Mandrekar, J.N. Receiver operating characteristic curve in diagnostic test assessment. *J. Thorac. Oncol.* **2010**, *5*, 1315–1316. [CrossRef]
25. Mori, M.A.; Ludwig, R.G.; Garcia-Martin, R.; Brandão, B.B.; Kahn, C.R. Extracellular miRNAs: From Biomarkers to Mediators of Physiology and Disease. *Cell Metab.* **2019**, *30*, 656–673. [CrossRef]
26. Zhu, J.; Zhang, Y.; Zhang, W.; Zhang, W.; Fan, L.; Wang, L.; Liu, Y.; Liu, S.; Guo, Y.; Wang, Y.; et al. MicroRNA-142-5p contributes to Hashimoto's thyroiditis by targeting CLDN1. *J. Transl. Med.* **2016**, *14*, 166. [CrossRef]
27. Wang, K.; Yuan, Y.; Cho, J.H.; McClarty, S.; Baxter, D.; Galas, D.J. Comparing the MicroRNA spectrum between serum and plasma. *PLoS ONE* **2012**, *7*, e41561. [CrossRef]
28. Sunderland, N.; Skroblin, P.; Barwari, T.; Huntley, R.P.; Lu, R.; Joshi, A.; Lovering, R.C.; Mayr, M. MicroRNA Biomarkers and Platelet Reactivity: The Clot Thickens. *Circ. Res.* **2017**, *120*, 418–435. [CrossRef] [PubMed]

29. Mussbacher, M.; Schrottmaier, W.C.; Salzmann, M.; Brostjan, C.; Schmid, J.A.; Starlinger, P.; Assinger, A. Optimized plasma preparation is essential to monitor platelet-stored molecules in humans. *PLoS ONE* **2017**, *12*, e0188921. [CrossRef] [PubMed]
30. Fan, H.P.; Di Liao, C.; Fu, B.Y.; Lam, L.C.; Tang, N.L. Interindividual and interethnic variation in genomewide gene expression: Insights into the biological variation of gene expression and clinical implications. *Clin. Chem.* **2009**, *55*, 774–785. [CrossRef]
31. Wu j Cai, H.; Xiang, Y.-B.; Matthews, C.E.; Ye, F.; Zheng, W.; Cai, Q.; Shu, X.-O. Intra-individual variation of miRNA expression levels in human plasma samples. *Biomarkers* **2018**, *23*, 339–346. [CrossRef]
32. Khan, J.; Lieberman, J.A.; Lockwood, C.M. Variability in, variability out: Best practice recommendations to standardize pre-analytical variables in the detection of circulating and tissue microRNAs. *Clin. Chem. Lab Med.* **2017**, *55*, 608–621. [CrossRef] [PubMed]
33. Faraldi, M.; Gomarasca, M.; Sansoni, V.; Perego, S.; Banfi, G.; Lombardi, G. Normalization strategies differently affect circulating miRNA profile associated with the training status. *Sci. Rep.* **2019**, *9*, 1584. [CrossRef] [PubMed]
34. Schwarzenbach, H.; Machado da Silva, A.; Calin, G.; Pantel, K. Data Normalization Strategies for MicroRNA Quantification. *Clin. Chem.* **2015**, *61*, 1333–1342. [CrossRef] [PubMed]